SODIUM CHANNELS ARE REQUIRED FOR CARDIAC CELL-FATE SPECIFICATION VIA A NOVEL, NON-ELECTROGENIC MECHANISM IN ZEBRAFISH

By

Sameer Chopra

Dissertation

Submitted to the Faculty of the

Graduate School of Vanderbilt University

in partial fulfillment of the requirements

for the degree of

DOCTOR OF PHILOSOPHY

in

Pharmacology

December, 2008

Nashville, Tennessee

Approved:

Dan Roden, M.D.

Tao Zhong, Ph.D.

Al George, M.D.

Joey Barnett, Ph.D.

Ron Emeson, Ph.D.

Bruce Appel, Ph.D.

To my parents, Om and Kawal Chopra, for providing me with the tools to learn and the spirit to discover.

ACKNOWLEDGEMENTS

Perhaps more commonly than in the last century, meaningful scientific advancement is made by the collective motivation, skills, and ideas of teams of people, not single individuals. In this spirit, the work reported here has resulted from the contributions of numerous individuals with whom I interacted over the course of my dissertation research. Foremost, I credit my dissertation mentors, Dr. Dan Roden and Dr. Tao Zhong, for investing in my development as a scientist. The act of being a mentor is unselfish and uncompromising and required that each of them believe that I could be trained to become a competent scientist. I am indebted to them for both supporting me and for allowing me to engage in such a remarkable learning experience.

Dan Roden introduced me to the elegant world of ion channels, drawing on both medicine and science interchangeably to help me think critically about how the heart functions normally and in disease. He is a terrific mentor, friend, and role model for how to be a successful and effective physician-scientist. Dan taught me to never forget the "big picture" but also to never overlook each and every tiny detail. His enthusiasm, encouragement, and curiosity motivated me to move forward into an area of science where neither of us had previously ventured, because we suspected that nature was about to reveal to us something new about a protein that once seemed so familiar. Having participated in this precious intellectual experience, where a number of my assumptions were challenged and overturned by empirical data, I am now confident that I well-prepared to embark on my career as a scientist. For all of Dan's contributions and his generosity, I am extremely thankful.

As a co-mentor for this project, Dr. Tao Zhong introduced me to the fields of organogenesis and development in the zebrafish model system. Tao has made numerous contributions to my training as a scientist, teaching me how to be critical about my research and how to distinguish important data from artifact. He consistently motivated me to realize my potential as a graduate student, encouraging me to always do my best and to never be satisfied with mediocre effort and results. Tao taught me that persistence and committment, particularly at times of great difficulty, are important requisites for success in science. For these contributions, I

am extremely thankful. I hope that one day in the future, we can again work together as colleagues.

I would be remiss here if I did not also give special thanks to the chair of my thesis committee, Dr. Al George, who was a consistent source of sound advice, support, mentoring, and camaraderie throughout this project. I am privileged to have interacted so frequently with Dr. George, as I have greatly benefited from his wealth of knowledge and experience. As a successful physician-scientist, Dr. George has also served as an important role model for my future career.

I would next like to thank the other members of my thesis committee including Dr. Bruce Appel, Dr. Ron Emeson, and Dr. Joey Barnett for their diverse perspectives, support, and expert guidance at every stage of this project. Without their contributions and attentiveness, it is unlikely that I would have been able to complete this dissertation work. I give a special thanks to Joey, who in addition to serving as a member of my dissertation committee, holds the post of Director of Graduate Studies (DGS) in Pharmacology where he acts as an advocate for both me and other students in the department. I would also like to thank Dr. Terry Dermody for all of his mentoring throughout the PhD phase of Vanderbilt's Medical Scientist Training Program (MSTP).

In the Roden lab, I would like to thank Hiroshi Watanabe, with whom I collaborated for a number of the electrophysiological analyses presented here. I would also like to thank Dina Stroud, Tao Yang and Justine Stassun for their constant guidance, support, and encouragement. In the Zhong lab, I would like to thank John Guan, whose expert care and dedication to the zebrafish facility was essential for the success of this project. I would also like to thank both current (Haiyan Wan, Haibo Jia) and past post-docs (Feng Liu, Hyunju Ro) for their expert assistance.

Through my research, I am also fortunate to have interacted with a number of exceptionally talented scientists outside of the Roden and Zhong laboratories. These included: Sam Wells, who helped us launch our initiatives in confocal imaging; Jerod Denton, who courageously accepted the difficult task of isolating early cardiac progenitors from zebrafish and surveying the currents of different ion channels by electrophysiology; Lorene Batts and H. Scott

Baldwin, who readily agreed to assist us in studying the expression pattern of *scn5a* in mouse embryos; Chunyue Yin, Xin-xin Zheng and Lila Solnica-Krezel, who provided us with initial instruction in the technique of transplantation.

In my personal life, there is no one who more deserves more credit for this work than my wife, Sharmila. My dissertation research would not have been possible without her support at every step of the way. For both her encouragement and understanding, I am indebted to her.

I would also like to give my thanks to my family and friends. My parents have been supportive of my goals from day one – though they never failed to ask me when I was going to be done with school and get a job. My younger brother continues to laugh at me for not going to business school. In earnest, however, I owe my family for the gift of their support, and for encouraging me to do whatever I chose with my life as long as I put my heart into it.

I am also grateful for the support and encouragement of my extended family, including Dr. Uma Sharma, Drs. Harsh and Jeet Gupta, Dr. N.S. Ramamurthy and Mrs. Sharon Oliver-Murthy, Drs. Inder and Arun Perkash, and Dr. Kamlesh Sahney.

Last but not least, I would to thank those who financially supported my work, including the chancellor's academic venture capital fund and Public Health Service award T32 GM07347 from the National Institute of General Medical Studies for the Vanderbilt Medical-Scientist Training Program.

TABLE OF CONTENTS

PAGE

LIST OF TABLES

TABLE **PAGE**

LIST OF FIGURES

FIGURE **PAGE**

CHAPTER I

INTRODUCTION TO VOLTAGE-GATED SODUM CHANNELS

Overview

Electrical signaling events are required for every human thought, feeling, and perception, the movement of our limbs, and each beat of our hearts. Not surprisingly, the fundamental contribution of electrical signals to so many defining human qualities has lured several generations of accomplished scientists to study the basis of membrane excitability. In this chapter, a brief history of the milestones that culminated in an ion theory for membrane excitability is presented. Although unknown until relatively recently in this history, the remarkable ion channel proteins that mediate electrical signals in response to changes in membrane potential are introduced. As the initiators of action potentials in excitable tissues, voltage-gated sodium channels play significant roles in both normal and pathological signaling events. In the heart, the opening of sodium channels initiates the cardiac cycle and culminates in contraction. Not surprisingly, mutations in the gene encoding the cardiac sodium channel have been linked to multiple distinct disorders of heart rhythm. Although it is increasingly well-appreciated that sodium channels exist in the membrane as macromolecular complexes, the functions of channel-associated proteins are not well understood. In Chapter 1, I propose that zebrafish, a tractable vertebrate model amenable to reverse genetics and with numerous additional experimental advantages, could serve as a valuable *in vivo* platform to test hypotheses regarding the role of sodium channel subunits and associated proteins in the regulation of heart rhythm. In chapters 2 and 4, I discuss the identification, cloning, and evolution of zebrafish cardiac-type α and β subunit genes. In chapter 3, I describe the unexpected discovery of a role for sodium channels in early heart development, prior to their role in modulating heart rhythm.

Voltage-gated sodium channels

Coordinated electrical signals in the metazoan nervous system, heart, and skeletal muscle depend on the generation of action potentials, rapid changes in membrane potential mediated by the passage of ions through voltage-gated ion channels (1). The initial upstroke or phase 0 of the action potential in most excitable cells is determined by sodium channels (Figure 1.1), membrane proteins characterized by rapid activation and inactivation and high ionic conductance (1-3). Unlike evolutionarily-ancient, tetrameric potassium channel complexes, sodium channels consist of four homologous domains with 6 membrane-spanning segments each, which are encoded by a single polypeptide (1-3). Sodium channels are suspected to have evolved from structurally-similar calcium channels, which in turn likely arose following reduplication of potassium channel genes (1-3). The use of sodium as a conducting ion rather than calcium is thought to have permitted rapid conduction and high-frequency electrical signaling in the rudimentary nervous systems of early multicellular animals, without the numerous additional intracellular effects mediated by calcium's role as a second messenger (1;4).

In mammals, members of the Na_v1 family of voltage-gated sodium channels are multi-protein complexes that include a pore-forming α subunit and 1 or more modulatory β subunits (5-9). Whereas sodium channel α subunits are ~260kDa proteins with 24 membrane-spanning domains, β subunits are smaller 30-40kDa proteins with a single transmembrane domain and an extracellular V-type immunoglobulin-like domain (10-14). Ten distinct α subunit genes (*SCNxA*) and 4 β subunit genes (*SCN1B-4B*) have been cloned from mammals, and their protein products have been functionally expressed with the exception of *SCN7A* (2;3;15). Using tetrodotoxin (TTX), a pufferfish toxin that blocks the external vestibule of the sodium channel pore, all functionally-expressed mammalian sodium channels have historically been classified as "TTX-sensitive" ($Na_v1.1$/SCN1A, $Na_v1.2$/SCN2A, $Na_v1.3$/SCN3A, $Na_v1.4$/SCN4A, $Na_v1.6$/SCN8A, $Na_v1.7$/SCN9A) or "TTX-resistant" ($Na_v1.5$/SCN5A, $Na_v1.8$/SCN10A, $Na_v1.9$/SCN11A) based on whether they exhibit sensitivity to nanomolar or micromolar concentrations of this potent toxin (15). While heterologous expression of α subunit genes alone can reconstitute key properties of voltage-gated sodium channels observed in native tissues, including sensitivity to TTX, co-expression

with β subunit genes modifies channel gating and increases channel cell surface expression (10-13;16). Studies of mice with targeted ablation of either *scn1b* or *scn2b* genes corroborated these roles for β subunits *in vivo* and revealed an additional function for β subunits in α subunit localization (17;18). Moreover, the unique expression profiles of each β subunit gene and their variable effects on α subunit function, expression, and localization suggest that different subunit combinations in heart, brain, and muscle may contribute to diversity and specialization in electrical signaling (19;20).

The ion theory for membrane excitation

Although it is now well-appreciated that action potentials are self-propagating electrical signals generated by transient, selective changes in the permeability of various ions through protein channels in the membrane (Figure 1.1), this basic understanding has resulted from nearly two centuries of investigation into the basis of membrane excitability (1). One of the first reported observations of an electrical potential in resting muscle was the *injury current* observed by Matteuchi in 1840, when dissection of a frog leg muscle was found to produce a measurable outward current flow from the interior of the tissue to the undamaged surface (21;22). Upon stimulating a frog nerve, du Bois-Reymond noted a transient decrease in the outward, injury current, which he named *negative variation* (21;22). In 1868, Julius Bernstein developed the first device ("differential rheotome") that enabled accurate measurement of this negative variation and demonstrated that when induced by strong stimuli, its amplitude exceeded that of the "injury current" (21-23). For his device and his measurements, Bernstein is widely credited for the first quantitative description of the action potential in nerve and muscle.

In the late nineteenth century, it became increasingly well-appreciated that ions in solutions surrounding excitable tissues were essential for electrical signaling and function. In a series of studies of frogs, Sidney Ringer and colleagues made a number of salient observations regarding the basis of function of excitable tissues: 1. potassium salts induced sensory loss and motor paralysis when locally applied to the leg (24;25); 2. systemic injection of potassium and sodium salts produced markedly different effects on motor and nerve function (26); 3. application

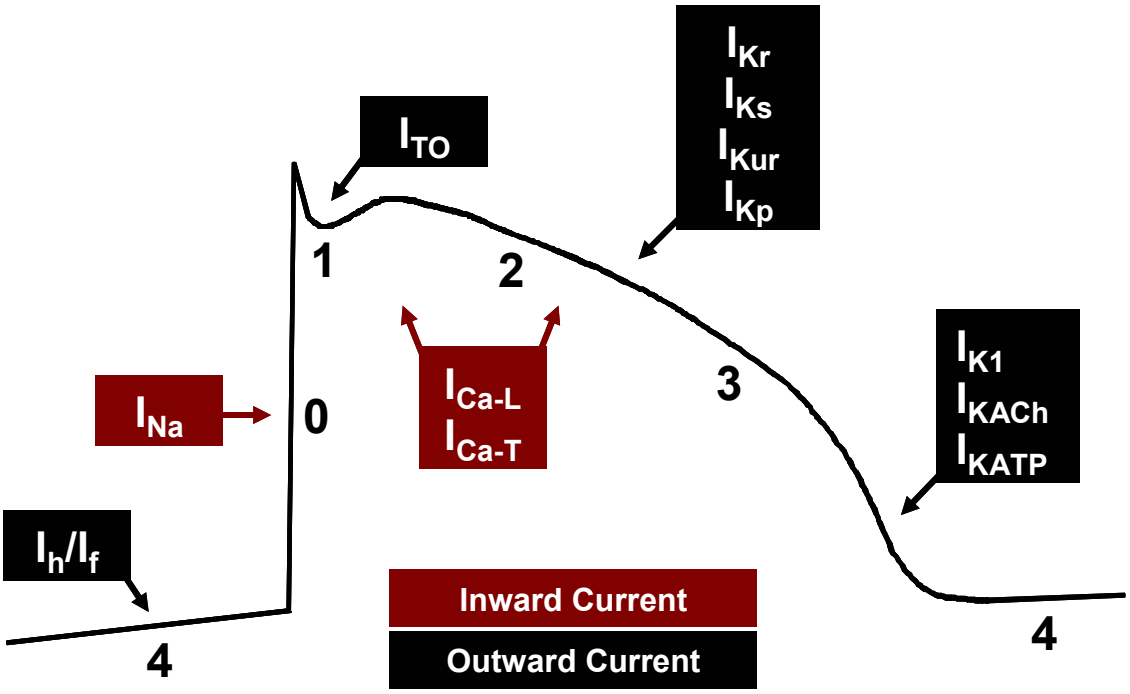

Figure 1.1: Currents contributing to the cardiac action potential. Cardiac action potentials exhibit four phases. Phase 4 is the resting membrane potential, typically between -85 and -90mV, which is primarily determined by the equilibrium potential for potassium. Nodal cells exhibit pacemaker currents (Ih/If) that result in spontaneous depolarization of the membrane. Phase 0 is the upstroke, a rapid membrane depolarization mediated by sodium influx (I_{Na}) through voltage-gated sodium channels. Phase 1 is the notch and results from the inactivation of sodium channels and the activation of transient outward potassium currents (I_{TO}). Phase 2 is the plateau and represents the balancing of inward currents primarily through L-type calcium channels and outward currents through delayed rectifier potassium channels. Phase 3 is characterized by the closing of calcium channels, continued activation of delayed rectifier potassium channels, and the activation of inward rectifier potassium channels that return the membrane potential to baseline.

of potassium salts directly to the heart arrested its function (27); and 4. normal, continuous function of the beating heart required perfusion with solutions containing small quantities of sodium, potassium, and calcium, whereas absence of any of these ions from the perfusate perturbed heart function (28-30). The experimental findings of Ringer demonstrated that perturbation of the normal ionic gradients required for establishing the resting potential and generating action potentials adversely affected the function of excitable tissues.

Building on the ideas of Nernst and Ostwalt, who earlier had developed theories to describe the basis of electrical potentials resulting from the movement of ions through semi-permeable barriers in solution, Bernstein formulated his famous *membrane theory* for electrical signaling in cells of living organisms (1;21;23;31;32). His theory represented a conceptual milestone in ion channel biology and inspired the efforts of a number of biophysicists in the twentieth century, including the Nobel laureates Hodgkin and Huxley (33;34). Bernstein posited that all excitable cells were surrounded by membranes with selective permeability towards certain ions, particularly K^+, and with limited permeability to other larger, negatively-charged ions within the cell such as phosphates. In his view, the measurable, negative resting potential of a nerve cell thus resulted from the "leak" of potassium ions from the inside of a cell to the outside, following the concentration gradient for potassium. Electrical signals, Bernstein argued, were then generated by a breakdown of the membrane that temporarily eliminated this selective permeability for potassium and made it permeable to other ions. His theory predicted that electrical signals traveling through nerve fibers represented the transient elimination of the negative resting potential. Although later studies revealed that Bernstein had accurately conceptualized the basis of membrane resting potential, however, he did not account for the action potential *overshoot* which he had measured in his own recordings. The overshoot made action potentials greater in amplitude than the resting potential of excitable cells, and could not be explained by a breakdown of the membrane that transiently eliminated the resting membrane potential. It was in fact Charles Overton who first predicted than an exchange of Na^+ and K^+ ions were required for the signals measured by Bernstein (35).

Studies into the molecular basis of electrical signaling were accelerated in the 1930s by the discovery that axonal processes of squid neurons were of large enough size to permit direct electrical recording (1;36;37). The squid giant axon thus facilitated the first intracellular recordings of the neuronal resting membrane potential and action potential. Working with this system, Alan Hodgkin and Bernard Katz directly tested Bernstein's membrane theory. Among their earliest contributions was confirmation of significant differences between the magnitudes of the resting potential and the action potential (38), and the recognition that Bernstein's theory could not adequately explain for the transient reversal of membrane potentials they routinely observed in squid giant axons. Hypothesizing that action potentials resulted from a transient increase in the permeability of an ion other than potassium (39), Hodgkin and Katz conclusively demonstrated that the rate of rise and the amplitude of neuronal action potentials depended on the concentration of extracellular sodium ions (40). By modifying methods developed by Cole and Marmont to clamp voltage across the giant axon membrane (41;42), Hodgkin and Huxley analyzed the changes in current through the nerve membrane at different potentials and were thus able to model the time- and voltage-dependence of Na^+ and K^+ components of the action potential (43). These experiments led them to theorize the existence of membrane *channels* that mediated the selective permeability of sodium and potassium ions in response to changes in membrane potential. Although they had no means of observing the function of single ion channels, the studies of Hodgkin and Huxley remarkably led them to predict many of the fundamental properties of voltage-gated ion channels that have since been observed and earned them the Nobel Prize in 1963. Many experimentalists have contributed further results that have gained wide acceptance for the ion channel hypothesis for membrane excitability, most notably the Nobel laureates Neher and Sakmann, who developed electrophysiological methods for resolving the behavior of single channels in patches of excitable membranes (1;44-46).

Physiology of voltage-gated sodium channels

Voltage-gated sodium channel proteins undergo conformational changes in response to changes in membrane potential (1). Once triggered to open, sodium channels act similarly to

other ion channels in that they are passive conduits for the flow of ions. The number of ions that flow through a single open channel is dependent upon an intrinsic property of the channel protein referred to as *conductance*, which is expressed as charge per second per volt (1;36;47). Mathematically, conductance is the reciprocal of resistance, and is represented as:

$$\mathbf{G = i/V}$$

where **i** represents the current through the channel and **V** represents the voltage that acts as a driving force for the flow of ions (1;36;47). Sodium channels have extremely high conductance for sodium, permitting a large influx of these ions to enter the cell during a very brief period of opening during depolarization (approximately 10ms) (1;36).

Although intrinsic properties of a channel determine the number of ions that can travel across the membrane, the direction of ion movement is determined by extrinsic properties of the membranous environment including the concentration gradient of ion on each side of the membrane and the prevailing electrical potential established by the permeability of all other ions across the membrane (1). Excitable cells bear large energetic costs (up to 30% of total energy expenditure) to fuel the Na^+-K^+ ATPase transporters that concentrate sodium ions extracellularly and potassium ions intracellularly (47). The potential energy stored within these gradients drives the depolarizing influx of Na^+ ions that follows the opening of sodium channels and the repolarizing efflux of K^+ ions that follows the opening of potassium channels. Without gradients of ions across the membrane, the driving force behind their movement would be lost.

In excitable membranes, electrical forces normally act to balance the driving force established by a concentration gradient for any particular ion. For example, as any particular ion moves through its channel across the membrane driven by its concentration gradient, the accumulation of charge on the other side of the membrane alters the prevailing membrane potential in a manner that acts to oppose the further movement of ion. Without considering the intrinsic time-dependent properties of ion channel closing here (for simplicity), the flow of charged particles would be self-limiting as chemical and electrical forces come into balance. The

equilibrium potential for any ion across an excitable membrane describes the voltage at which electrical and chemical forces across the membrane are equal and there is no net movement of charge. For any single ion species, this value can be predicted by the Nernst equation (1;36):

$$\mathbf{E_x = (RT/zF) * \ln[X_2]/[X_1]}$$

where E_x = equilibrium potential for any ion "X"; R = gas constant; T = temperature in Kelvin; z = valence of the permeant ion; F = Faraday constant (amount of charge of 1 mole of a monovalent ion); X = ion concentration on each side of a membrane. In mammalian skeletal muscle, for example, where the extracellular sodium concentration is typically 145mM and the intracellular sodium concentration is 12mM, the equilibrium potential for sodium is +67mV (1). Therefore, a membrane potential of +67mV would be required to oppose the driving force for sodium influx that is established by the concentration gradient of sodium across the myocyte membrane. If sodium channels exclusively open under such conditions, sodium ions will move into the cell until the membrane potential nears the equilibrium potential or this ion. If multiple permeant ions are unequally distributed across an excitable membrane, consideration must be given to the permeability of each respective ion. As predicted by Bernstein over 100 years ago, the resting potential of a cell (approximately -70mV) thus most closely resembles the equilibrium potential of the ion with the greatest resting permeability (potassium, approximately -98mV). In summary, the movement of any ion across the membrane at a particular point in time through an open channel is thus largely determined by the three key factors: 1. the conductance of an ion through its channel; 2. the ion concentration on each side of the membrane; 3. the prevailing membrane potential. The forces that determine when a channel opens and closes are briefly described below.

Sodium channel "gating"

In their seminal work, Hodgkin and Huxley made the important observation that kinetic processes termed *activation* and *inactivation* also controlled the permeability of specific ions such as sodium across the membrane, because depolarization induced a rapid rise in current that was

inevitably followed by a slower decay (43;48). In fact, ion channels in excitable tissues have intrinsic *gates* that represent conducting and non-conducting conformational states of the protein. Voltage-gated sodium channels, for example, are dynamic proteins that move between *open*, *closed*, and *inactivated* states that are co-dependent on the prevailing membrane potential and on time. As whole-cell and single-channel electrophysiological approaches have directly revealed for sodium channels, for example, a prolonged depolarizing pulse does not lead to individual sodium channels staying open throughout the pulse. Rather, channels open for a brief period of time before inactivating. Once inactive, they have entered into a state from which the channel opening cannot be achieved with further depolarization. Sodium channel inactivation is a time- and voltage-dependent process, and only recovery from this state will permit the channel to subsequently reopen.

Sodium channel structure-function relationships

Similar to voltage-gated calcium channels, the secondary structure of a typical Na_v1 family member includes 4 homologous domains (DI-DIV) that are each comprised of 6 membrane-spanning segments (S1-S6) (Figure 1.2) (49-51). The pore of the channel is comprised predominantly of residues in the S5-S6 linkers or *pore loops* and S6 segments in each of four domains. Deep within the extracellular pore, the residues “D” (DI), “E” (DII), “K” (DIII), and “A” (DIV) come together to form the channel’s *selectivity filter*. The intracellular linker connecting domains III and IV acts as the *fast inactivation gate*, which plugs the ion permeation pathway during repolarization. The opening of the channel in response to depolarization is suspected to be mediated by the outward movement of the S4 transmembrane segments of each domain, which have charged residues (arginine or lysine) at every third position.

Sodium channel subunits in human disease

As integral components of action potential generation, voltage-gated sodium channels have been implicated in a number of heritable disorders of membrane excitability including arrhythmia, epilepsy, and myotonia (50;52). The cloning and functional expression of sodium

channel genes harboring mutations identified in human patients have revealed that a number of distinct biophysical abnormalities of sodium channel function may result in disease (50). Moreover, these studies have contributed to our appreciation that even subtle changes in sodium channel function can act a substrate for severe, paroxysmal phenotypes. To date, mutations in 6 α subunit genes (*SCN1A*, *SCN2A*, *SCN4A*, *SCN5A*, *SCN8A*, *SCN9A*) have been linked to human disease (53-59). Mutations in *SCN1A* (encoding the neuronal sodium channel $Na_v1.1$) were first linked to an autosomal dominant epilepsy syndrome termed generalized epilepsy with febrile seizures plus type 2 (GEFS+2) and have more recently been associated with severe myoclonic epilepsy of infancy (SMEI), intractable childhood epilepsy with generalized tonic-clonic seizures (ICEGTC), familial hemiplegic migraine-3, and familial febrile convulsions-3 (53;60-65). Mutations in *SCN2A* (encoding the neuronal sodium channel $Na_v1.2$) are most commonly associated with another autosomal dominant seizure disorder, benign familial neonatal-infantile seizures (BFNISs), and in one case, have been linked to febrile seizures associated with afebrile seizures (54;66;67). *SCN1A* and *SCN2A* mutations may also be associated with familial autism (55). Mutations in *SCN4A* (encoding $Na_v1.4$) have been associated with multiple disorders of skeletal muscle, including paramyotonia congenita, hyperkalemic periodic paralysis, hypokalemic periodic paralysis, and potassium-aggravated myotonia (56;68-73). In a single case, a mutation in *SCN8A* (encoding $Na_v1.6$) was associated with mental retardation, pan-cerebellar atrophy, and ataxia (58). Mutations in *SCN9A* (encoding $Na_v1.7$) underlie primary erythermalgia, paroxysmal extreme pain disorder (PEPD), and a recently-identified, autosomal recessive condition known as channeolopathy-associated insensitivity to pain (59;74;75). There is an extensive literature associating variants in *SCN5A* (encoding $Na_v1.5$) with cardiac disease, notably the type 3 variant of the long QT syndrome (LQT3) and Brugada syndrome, as will be discussed further.

Given their important modulatory effects on the expression and function of sodium channel α subunits, β subunits are also important candidate genes for human diseases related to sodium channel dysfunction. β1 subunit gene mutations are a cause of generalized epilepsy with febrile seizures plus (GEFS+), and variants in sodium channel α subunits that disrupt their

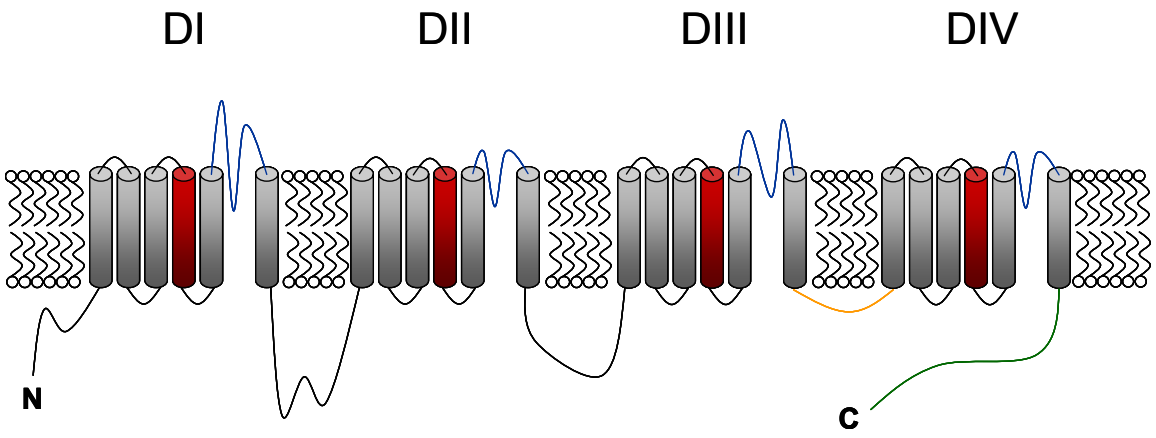

Figure 1.2: Secondary structure of a typical voltage-gated sodium channel. Voltage-gated sodium channels are comprised of 4 homologous domains, each with 6 membrane-spanning segments. Among the functionally-important regions of the channel are the S4 voltage sensors (**red**), which have basic residues at every third position and act to transduce changes in membrane potential into movement of the channel; the pore loops (**blue**), comprised of the linkers connecting the S5 and S6 transmembrane segments within each domain and which contain the channel's selectivity filter (D-E-K-A) and TTX binding site; the fast inactivation gate (**orange**), which is the intracellular linker connecting domains III and IV that acts to plug the ion permeation pathway after depolarization; and the C-terminus (**green**), which has calcium-binding EF hand structures and motifs for interaction with diverse proteins including calmodulin, FHF1b, syntrophin, and Nedd4-2 ubiquitinase.

interaction with β subunits may be pathological in the heart (76-80). A recent report has implicated a mutation in the β4 subunit gene as a cause of the long QT syndrome (81).

Murine models of sodium channel loss-of-function

Although not yet available for every mammalian sodium channel gene, loss-of-function mouse models have further enhanced our understanding of the consequences of reduced sodium channel expression in excitable tissues. In the mammalian central nervous system, the expression of multiple sodium channel genes (*SCN1A*, *SCN2A*, *SCN3A*, and *SCN8A*) suggests either functional redundancy or specialization of neuronal sodium channel proteins. To begin to explore these possibilities, Planells-cases et al. targeted exon 1 of the *scn2a* locus on mouse chromosome 2 (82). *Scn2a*$^{-/-}$ mice displayed significantly reduced levels of *scn2a* transcripts in the brainstem, cortex, and hippocampus and died within two days of birth from severe hypoxia, suggesting a specific, non-redundant role for *scn2a* in brainstem neurons (82). These findings were consistent with the results of ^{3}H-saxitoxin binding assays, which demonstrated a significant reduction of activity in the brainstem of *scn2a*$^{-/-}$ mice compared to wild-type mice (82). Despite the absence of gross anatomical or histological abnormalities in the brains of *scn2a*$^{-/-}$ mice, assays for cell death revealed significantly increased neuronal apoptosis in the brainstem and neocortex (82). Although the authors could not rule out that apoptosis was secondary to hypoxia, they hypothesized that decreased neuronal electrical activity in these regions may have directly initiated programmed cell death (82).

Murine *scn6a* (*SCN7A* in humans) encodes the atypical sodium channel Na_x. Although phylogenetically classified as a member of the Na_v1 sodium channel family, neither *scn6a* nor *SCN7A* have ever been shown to encode a functional voltage-gated sodium channel by heterologous expression. To better understand the function of this gene, Watanabe and colleagues targeted the *scn6a* locus in mice (83). *Scn6a*$^{-/-}$ mice were born healthy and were fertile but displayed abnormalities of salt consumption (83). As lacZ knocked into the *scn6a* locus revealed expression of this gene in regions of the brain that are normally involved in body-fluid homeostasis, these data suggested that *scn6a* may have evolved a role in regulating salt intake

behavior (83). Since *scn6a* was also found to be expressed in the lung and the heart, future studies of these mice may seek to investigate the role of *scn6a* in these tissues.

Although the gene *scn8a* has not been directly targeted by homologous recombination, several mutant alleles have provided insight into the function of $Na_v1.6$ in mice. The motor endplate disease (*med*) mutant mouse resulted from the random insertion of a transgene that produced a 5-10kb deletion within the *scn8a* locus, eliminating expression of this gene and resulting in hindlimb paralysis, perturbed development of the neuromuscular junction, muscular atrophy, and degeneration of Purkinje cells in the cerebellum (84). Moreover, *med* mutant mice died as juveniles. Four additional mutant alleles of *scn8a* induced by ENU or by spontaneous mutation resulted in similar spectrum of defects including sustained dystonic postures, hindlimb paralysis, cerebellar ataxia and juvenile lethality (85).

The gene *scn9a*, which was found to be highly expressed in dorsal root ganglia and the adrenal and thyroid glands, was deleted from mice both globally as well as specifically in nociceptor neurons using Cre-loxP technology (86). Global s*cn9a*$^{-/-}$ mice died shortly after birth because of a failure to feed (86). Deletion of *scn9a* specifically in nociceptive neurons, however, resulted in mice that displayed increased pain thresholds in response to mechanical, thermal, or inflammatory stimuli (86). The gene *scn10a* also appears to have evolved non-redundant functions in nociception. Mice lacking *scn10a* were healthy and viable, but displayed profound resistance to pain induced by mechanical stimuli, and attenuated responses to pain induced by both thermal and inflammatory stimuli (87). A recent study also revealed that *scn10a* has evolved a specific role in pain transmission at cold temperatures (88).

Finally, the gene *scn5a* has also been targeted in mice, resulting in phenotypes that will be discussed below.

Cardiac sodium channels

In the mature mammalian heart, the opening of sodium channels initiates the cardiac cycle (Figure 1.1) (89). Inward, depolarizing sodium current underlies the upstroke or phase 0 of the cardiac action potential in all areas of the heart except for the sinoatrial (SA) and

atrioventricular (AV) nodes, where inward calcium currents underlie depolarization (90). The wave of depolarization mediated by sodium channels results in the activation of myocardial L-type calcium channels at the myocyte plasma membrane ("sarcolemma"), which then act to provide the calcium spark that triggers the opening of large, calcium-release channels on the sarcoplasmic reticulum (SR) known as ryanodine receptors (91;92). During systole, the opening of ryanodine receptors permits the release of calcium stores from the SR, resulting in the elevation of cytosolic calcium levels nearly 100-fold (from approximately 10^{-7} to 10^{-5}M) (91;92). Elevated cytosolic calcium regulates the activity of troponin-C, which then permits the interaction of actin and myosin filaments, cross-bridge formation and contraction. To initiate diastole, cytosolic calcium levels are normalized by the re-sequestration of calcium into the SR by the intracellular SR membrane pump SERCA, and by calcium extrusion extracellularly via the Na^+/Ca^{2+} ATPase transporter. Meanwhile, at the depolarized sarcolemma, a number of voltage-dependent potassium channels open to permit the efflux of K^+ ions and repolarization of the membrane to values near the myocyte resting potential (-70mV) (Figure 1.1). Every heartbeat is thus the result of two distinct biophysical processes: excitability, which is localized at the sarcolemma and results in the activation of L-type calcium channels; and contraction, which occurs intracellularly and results from transient elevations in cytosolic calcium that permit functional interactions between cardiac actin and myosin. For these reasons, the term "excitation-contraction coupling" is commonly used to describe the physiology whereby electrical activity generates and regulates contractile function of the heart (93;94).

SCN5A: the cardiac isoform of the voltage-gated sodium channel

In humans and other mammals, *SCN5A* is most highly expressed sodium channel gene in the mature myocardium and the function of $Na_v1.5$, the protein encoded by this gene, is required for imitating cardiac excitation-contraction coupling (89). At the genomic level, *SCN5A* is comprised of 28 exons that span approximately 80kb (95). Prior to the sequencing of the human genome, *SCN5A* was mapped to 3p21 by fluorescence *in situ* hybridization (96). *SCN5A* resides

alongside the genes *SCN10A* and *SCN11A*, supporting the idea that these three genes arose following the tandem duplication of a common ancestral sodium channel gene (97;98).

Roles for other Na_v1 sodium channel isoforms in the heart

Although *SCN5A* is the most highly expressed sodium channel in mammalian cardiac tissue, emerging evidence suggests that additional sodium channel isoforms are also expressed in the heart (albeit at lower levels) where they may act to perform more specialized roles. By immunohistochemistry, Maier and colleagues detected expression of the TTX-sensitive "brain-type" channels $Na_v1.1$ (*scn1a*), $Na_v1.3$ (*scn3a*), and $Na_v1.6$ (*scn8a*) in murine ventricular myocytes (99-101). While $Na_v1.5$ appeared to localize at the intercalated disks, other Na_v1 sodium channel isoforms were expressed in the transverse tubules, specialized invaginations of myocyte sarcolemma where L-type calcium channels are closely apposed to ryanodine receptors (99). This expression pattern and functional studies demonstrating reduced cardiac contractility in the presence of nanomolar concentrations of TTX suggested that brain-type sodium channels play a specialized role in transmitting excitation on the sarcolemma to the cell's interior, in order to permit the more efficient EC coupling (99). Similarly, isoform-specific antibodies detected expression of $Na_v1.1$ and $Na_v1.3$, but not $Na_v1.5$, in the mouse SA node (102). Exposure of the mouse heart to nanomolar quantities of TTX elicited bradycardia and heart rate variability in a Langendorff preparation (102). A subsequent study, however, detected expression of both $Na_v1.1$ and $Na_v1.5$ in the SA node and demonstrated that both channels are likely to be important for pacemaking (101). Some evidence suggests that *SCN4A* ($Na_v1.4$) is also expressed in the heart, but the importance of $Na_v1.4$ to cardiac function has not been thoroughly investigated (103;104). Similarly, the gene *SCN7A* is also expressed in cardiac tissue, but with unknown functions (105;106).

Sodium channels in human heart disease

Sudden cardiac death (SCD) due to ventricular fibrillation is a leading cause of mortality in the United States, contributing to over 300,000 deaths in 1998 (107). The risk for this fatal

cardiac arrhythmia is heightened by rare mutations, including those in *SCN5A* found to cause the Brugada and long QT syndromes (90;108), by drugs that either intentionally or inappropriately bind to ion channels (antiarrhythmic agents, I_{Kr} blockers) (89) (109), and more commonly, by pathological cardiovascular states such as myocardial ischemia, cardiomyopathy, and heart failure (107;110). The pharmacological management of abnormalities of cardiac rhythm is suboptimal and patient outcomes are highly variable (107;111). Existing antiarrhythmic agents – which primarily target and block cardiac ion channels – are often inefficacious, unsafe, and may even contribute to patient mortality (111-114). As a result, implantable devices such as pacemakers and defibrillators constitute the current standard of care for the prevention of many arrhythmias (111;115).

Although rare, mutations in *SCN5A* have been associated with a number of distinct disorders of cardiac rhythm including the long QT syndrome (type 3), Brugada syndrome, progressive cardiac conduction system (Lenègre's) disease, congenital sick sinus syndrome, atrial standstill, and sudden infant death syndrome (SIDS) (50;52). As demonstrated by *SCN5A* mutations that cause the Brugada and long QT syndromes, the human heart is highly sensitive to even slight perturbations of sodium channel expression or function (116;117). The Brugada syndrome is characterized by right bundle branch block, persistent ST segment elevation in ECG leads V1-V3, and predisposition to ventricular fibrillation in patients with structurally normal hearts (118). *SCN5A* mutations associated with this condition appear to result in a loss of channel function through one of multiple mechanisms, including perturbations of gating that reduce sodium channel availability and reduced trafficking of mutant channels to the cell membrane (119-122). The long QT syndrome (LQTS) is characterized by QT interval prolongation, recurrent syncope, and sudden death due to a polymorphic tachycardia called *torsades de pointes* (123), is linked to inherited defects in multiple cardiac ion channel subunits in addition to *SCN5A* (57;124;125), as well as occasionally in other genes thought to regulate ion channel function (126;127). When studied in heterologous expression systems, sodium channels with LQTS mutations do not appear to normally inactivate, leading to sustained inward depolarizing current during the plateau phase of the action potential (128-130). Although mutations in *SCN5A* have

contributed to our understanding of the molecular determinants of arrhythmia susceptibility, nearly 80% of patients with the Brugada syndrome do not appear to have variants in the coding regions of this gene (116;131). Likewise, the etiology of disease in approximately 35% of patients with the LQT syndrome remains unknown (124).

Mouse models of $Na_v1.5$ dysfunction/loss-of-function have further solidified our mechanistic understanding of the relationship between sodium channel dysfunction and arrhythmia. Mice heterozygous for a knock-in long QT syndrome mutation (ΔKPQ) developed both spontaneous and triggered polymorphic ventricular arrhythmias (132). Similarly, mice heterozygous for *scn5a* by targeted deletion displayed slow conduction, increased refractoriness, sinus node dysfunction and pacing-induced ventricular tachycardia (133;134). Notably, both $scn5a^{\Delta/\Delta}$ and $scn5a^{-/-}$ mice were reported to be embryo-lethal, suggesting an important role for sodium current in the embryonic heart (132;133).

Finally, the importance of sodium channels in the heart has been supported by data from patients demonstrating that $Na_v1.5$-blocking antiarrhythmic agents paradoxically induce lethal arrhythmias, a phenomenon referred to as *proarrhythmia*. The Cardiac Arrhythmia Suppression Trial (CAST) reported that suppression of ventricular ectopic beats with the sodium-channel blocking agents flecainide and encainide led to a 3-fold increase in mortality in patients convalescing from myocardial infarction (135). Although the use of many sodium channel blocking agents to suppress arrhythmias has since fallen out of favor, the phenomenon of sodium channel blocker-induced proarrhythmia has been extensively studied. Existing evidence suggests that conditions that reduce sodium current such as *SCN5A* mutations or acute ischemia may in turn increase the risk of sodium channel blocker-related proarrhythmia (136-140).

The sodium channel "complex"

It has become increasingly well-appreciated that voltage-gated sodium channel pore-forming α subunits do not exist alone at the membrane but form macromolecular complexes with a number of ancillary proteins. Despite clear evidence implicating the perturbed function or expression of $Na_v1.5$ in multiple disorders of heart rhythm, however, little is known about the

potential role of altered protein-protein interactions as a substrate for arrhythmia. Literature demonstrating the functional importance of sodium channel-interacting proteins is expanding rapidly (141), and presents the intriguing possibility that the study of $Na_v1.5$ protein partners may help to further clarify the molecular determinants of the risk for arrhythmia.

Sodium channel β subunits: modulators of $Na_v1.5$ expression and function

Ancillary sodium channel β subunits are small, single membrane-spanning proteins with extracellular immunoglobulin-like domains and short intracellular C-terminal tails. These proteins were first identified over 2 decades ago during the biochemical purification of much larger pore-forming α subunit proteins from rat brain and skeletal muscle (5-7;142-145). Since that time, numerous studies have demonstrated that mammalian sodium channel β subunits proteins are integral components of the channel complex in excitable tissues, modulators of the expression and function of the larger pore-forming α subunits, and genes that underlie clinical disorders linked to perturbed membrane excitability such as epilepsy and arrhythmia (19;76;146-150). In mammals, four sodium channel ancillary β subunits (β1-4) have been identified, encoded by the genes *SCN1B-4B*. Primarily through evidence derived from heterologous systems, sodium channel β subunits have been shown to influence the expression and function of $Na_v1.5$ as well as its affinity for antiarrhythmic medications (19;151).

Sodium channel β subunits in the heart

Although β1 was originally cloned from the human brain, mRNA transcripts for this subunit have since been identified in the rat heart by northern blotting and in the human heart by RT-PCR (152-154). The functional importance of β1 in the heart is not well-understood. While two studies reported that co-expression of SCN1B and SCN5A resulted in enhanced channel expression with no effect on channel function (154;155), two additional studies reported that β1 affected both sodium current density and channel gating (156;157). The β1 subunit has also been implicated as a modifier of *SCN5A* mutations that cause the Brugada syndrome and idiopathic ventricular fibrillation (IVF) (158). Moreover, it was suggested that the long QT

syndrome may be caused by mutations in *SCN5A* that specifically affect α-β subunit interactions (78). Finally, some evidence suggests that β1 modulates the sensitivity of $Na_v1.5$ to antiarrhythmic drugs such as lidocaine, reducing the rest affinity for the drug (159;160). Taken together, the available data strongly suggest that β1 increases the amplitude and may influence the gating of sodium currents conveyed by $Na_v1.5$.

Although *scn1b* has been targeted in mice, analysis of the resulting phenotype has heretofore been limited to the nervous system (17;18). However, the deficits seen in this model may provide clues to the types of functions this gene may have in the heart. Loss of β1 resulted in mice with an ataxic gait and spontaneous seizure activity (17). At the cellular level, these *scn1b*$^{-/-}$ mice displayed slow conduction (as measured in optic nerve fibers), defects in the architecture of nodes of Ranvier, and changes in the expression of $Na_v1.1$ and $Na_v1.3$ in a subset of hippocampal neurons (17). Despite the evidence that β1 affects sodium channel expression and localization in vivo, analysis of the cardiac phenotype of these mice has not yet been reported.

Less is known about the roles of β2 (*SCN2B*), β3 (*SCN3B*), and β4 (*SCN4B*) subunits in cardiac tissue. Unlike β1, β2 is suspected to form covalent linkages pore-forming α subunits via disulfide bonds (11). Since co-expression of *SCN2B* and *SCN5A* was not demonstrated to modulate the function of $Na_v1.5$ *in vitro*, it has been hypothesized that β2 may be more important for cell-adhesion, a property that has been attributed to all 4 subunits because of their extracellular IG domains (161;162). *SCN3B* expression has been detected in the rat and human heart by RT-PCR (12;163). Northern and Western blots of sheep heart extracts also demonstrated that *SCN3B* is highly expressed in both the endocardium and epicardium of the ventricles as well as in the Purkinje fibers, but is absent from the atrium (164). Co-expression of *SCN3B* and *SCN5A* resulted in a threefold increase in peak sodium current amplitude, faster recovery from inactivation, and a significant depolarizing shift in the half-voltage ($V_{1/2}$) of steady-state inactivation (164). *SCN4B* encodes the more recently-discovered fourth β subunit of voltage-gated sodium channels (13). Although *SCN4B* expression in the rat heart was detected by RT-PCR, co-expression of *SCN4B* and *SCN5A* in tsA-201 cells did not appear to alter channel

function (13). However, a mutation in *SCN4B* was recently described in a single patient with the congenital long QT syndrome (165). Although no significant differences were observed in the amplitude and time course of whole cell sodium currents when either wild type or mutant β4 was expressed in a line of HEK 293 cells that stably expressed $Na_v1.5$, the mutant subunit affected the voltage-dependence of inactivation of the channel resulting in a significant increase in late sodium current (166).

Immunohistochemistry of β subunits in the heart

To resolve discrepancies regarding the expression and subunit composition of sodium channels in the heart, detailed immunohistochemical analyses of α and β subunits have been recently been performed. Using subunit-specific antibodies, Malhotra et al. demonstrated expression of both β1 and β2 proteins in mouse and rat ventricular myocytes, where they appeared to co-localize with $Na_v1.1$ and $Na_v1.5$ in the transverse tubules (161). Maier et al. subsequently analyzed the expression of all four β subunit proteins in murine ventricular myocytes (100). In this report, $Na_v1.5$ was found exclusively at the intercalated disks, the junctional complex connecting adjacent cardiomyocytes (100). Moreover, $Na_v1.5$ was found to co-localize with the β2 and β4 subunits in all cells analyzed, and with the β1 subunit in a fraction of cells (100). Interestingly, β1 and β3 were found to primarily co-localize with the "brain-type" sodium channels $Na_v1.1$, $Na_v1.3$, and $Na_v1.6$ in the transverse tubules (100). These studies revealed that all 4 sodium channel β subunits are expressed in the heart and suggested that the stoichiometry of subunits in cardiac sodium channel complexes is likely to be similar to that of channels found in the central nervous system (1:1:1, $\alpha:\beta_x:\beta_y$).

Limits of traditional approaches to studying subunit-subunit interactions

Although β subunits are logical candidate genes for human disease, the functional importance of this gene family *in vivo* is still not well understood. Although *in vitro* studies have clearly advanced our understanding of the role of β subunits in modulating membrane excitability, heterologous expression systems may not accurately recapitulate complex *in vivo* mechanisms.

The observed effects of α-β subunit interactions in cells are variable, for example, and may depend on the cell-type in which these genes are co-expressed (154;155;157;167). This implies that the intracellular milieu and its specific complement of endogenously-expressed proteins influence the functional interactions that occur between transfected α and β subunits. Numerous studies have demonstrated that the functional properties of a sodium channel complex *in vitro* may be modulated by a diverse array of proteins including cell-adhesion molecules, calcium binding proteins, and components of the extracellular matrix and cytoskeleton that are capable of functionally interacting with either α or β subunits (19;168). The expression of any of these modulatory factors may differ among the cell lines currently employed for *in vitro* biophysical studies. Moreover, both the purification of neuronal sodium channel subunits and the immunohistochemical analyses of these proteins in native cardiac tissues described above suggested that sodium channel complexes are likely to exist as heterotrimeric structures comprised of one α subunit and two different β subunits (9;169). For these reasons, it may be difficult to accurately model *in vivo* interactions by the transient transfection of single α and β subunits in heterologous cell systems. Additional studies using the intact hearts of animal models are clearly needed to both confirm and expand upon the results of *in vitro* experiments.

Zebrafish: a genetically-tractable vertebrate model system

Large-scale forward genetic screens conducted in the mid-1990s demonstrated that zebrafish could facilitate the identification of novel genes that regulate the development and function of the vertebrate cardiovascular system (170;171). From these initial efforts, a number of mutant fish lines were recovered that displayed arrhythmias including fibrillation, AV block, and bradycardia, demonstrating that the simple two-chambered heart of a young fish embryo could manifest physiologically-meaningful rhythm phenotypes and be useful as a model to study the molecular determinants of cardiac impulse propagation (172;173). Moreover, initial electrophysiological studies of cultured embryonic zebrafish cardiomyocytes revealed currents typical of the multiple families of cardiac ion channels found in the mammalian heart (174). For these reasons, we surmised that zebrafish could serve as a valuable experimental platform for

clarifying the role of sodium channel-associated proteins such as ancillary β subunits in the regulation of heart rhythm.

Compared to mammals such as mice and dogs, zebrafish appeared to be an attractive model system for a number of key experimental advantages. First, zebrafish embryos are amenable to efficient reverse genetic manipulation using morpholino-modified antisense oligonucleotides, facilitating the rapid knockdown of genes individually or in combination (e.g. genes encoding two different β subunits). Second, the zebrafish cardiovascular system develops quickly, permitting one study the rhythm of the embryonic heart as early as 1-2 days following the formation of the beating heart tube and basic circulatory loop at approximately 24 hours post fertilization. Third, large clutch sizes facilitate the simultaneous study of dozens of embryos, improving the validity of experimental findings. Fourth, zebrafish embryos are optically transparent and develop externally, allowing one to study cardiovascular physiology at any stage of development without surgical or other manipulation. Fifth, zebrafish embryos do not require circulation for survival during the first several days of development, enabling one to study defects in cardiovascular function (induced by gene knockdown or mutagenesis) that would be embryo lethal in other model organisms. Sixth, zebrafish embryos are permeable to most pharmacological compounds placed in their surrounding medium, an important tool for confirming the effects of gene knockdown and for studying phenotypes elicited by drug challenge. Seventh, gene overexpression phenotypes can be readily characterized following the injection of sense RNA into early embryos. Finally, a draft zebrafish genome sequence was available to help identify and clone genes of interest.

Experimental objective(s)

Because of the exquisite sensitivity of the heart to perturbations of sodium current, we hypothesized that sodium channel-interacting proteins including ancillary β subunits would be important regulators of heart rhythm *in vivo*. **The specific aim of our studies was thus to create and characterize a loss of function model for the cardiac sodium channel $Na_v1.5$ in zebrafish embryos.** This model would be a useful benchmark for parallel studies of sodium

channel-interacting proteins, or serve as the background in which gain- or loss-of-function studies of such ancillary molecules could be performed. Our larger goal was to establish a new *in vivo* platform for investigating the function of various components of the cardiac voltage-gated sodium channel complex, with the aim of being able to rapidly test hypotheses regarding novel candidate genes as they emerged from studies in our laboratory or from the literature. In chapters 2 and 4 of this dissertation, I discuss the identification, cloning, and evolution of zebrafish cardiac-type α and β subunit genes. In chapter 3, I describe the unexpected discovery of a role for sodium channels in early heart development, prior to their role in modulating heart rhythm.

CHAPTER II

EVOLUTION AND FUNCTION OF CARDIAC SODIUM CHANNELS

Overview

Mammals (class Mammalia) and ray-finned fish (class Actinopterygii) are distantly-related vertebrate lineages whose nearest common ancestor is suspected to have lived over 400 million years ago (Figure 2.1). Although humans and zebrafish share enough similarity to make the fish a popular model system for genetic studies, many gene families have undergone significant evolutionary change and diversification across vertebrate lineages. The extension of our studies of cardiac sodium channels in humans and mice to a non-mammalian vertebrate model system thus warranted special consideration of the evolutionary history of the Na_v1 family of sodium channel genes in vertebrates. To identify cardiac sodium channels in zebrafish, we used both *in silico* and *in vitro* approaches. While mammals have 10 Na_v1 channel genes, we identified 8 conserved sodium channel genes in zebrafish. Although 2 of these 8 genes were putative homologs to *scn5a* by sequence, expression of only 1 gene was detected in the adult atrium and ventricle. The cloning, sequence analysis, assembly, and functional expression of this gene revealed a probable functional ortholog to mammalian *scn5a*. As a recent study revealed expression of the second *scn5a* homolog in the embryonic heart, we have pursued studies of both putative zebrafish *scn5a* genes in parallel. To be consistent with recent literature, we have adopted the nomenclature *scn5Laa* and *scn5Lab* (*SCN5A*-like gene isoforms A and B) and $zNa_v1.5a$ and $zNa_v1.5b$ to describe the genes and the channels they encode, respectively. The significance of duplicate zebrafish *scn5a*-like genes is discussed. Functional studies of both genes are described in Chapter 3.

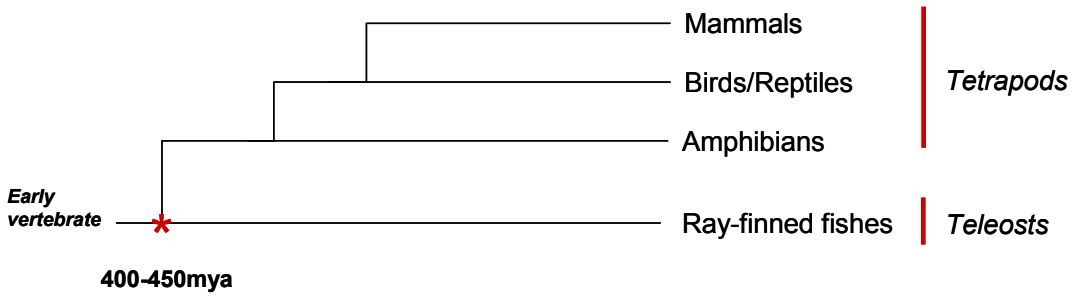

Figure 2.1: Teleosts and tetrapods diverged 400-450 million years ago. Fish and mammals share a common vertebrate ancestor that is suspected to have lived 400-450 million years ago.

Abstract

Although gene duplication is widely suspected to underlie the evolution of novel protein function, the mechanisms that determine the fate of genes following duplication events are not well understood. Na_v1 voltage-gated sodium channels are highly conserved proteins that act to initiate action potentials in excitable tissues. Mammalian sodium channels are encoded by 10 distinct but homologous genes, suggesting that the duplication of ancestral sodium channel genes played an important role in the expansion of this gene family. Since successful heterologous expression of 9 of 10 Na_v1 channels has revealed conserved function among these proteins, however, it is unclear why many Na_v1 genes have been retained in mammalian genomes. To address this question, we investigated the evolution of cardiac-type sodium channel genes in two divergent vertebrate clades, mammals and teleosts. In mammals, the genes *scn5a*, *scn10a*, and *scn11a* are phylogenetically related and occupy adjacent positions in the genome but have evolved divergent roles in cardiac excitation (*scn5a*) and peripheral nociception (*scn10a*, *scn11a*). In zebrafish, we also observed divergence of the expression of *scn5a*-like genes. *In silico* and *in vitro* approaches first identified 8 distinct zebrafish Na_v1 sodium channel genes. Phylogenetic analysis implicated two putative homologs to *scn5a* (*scn5Laa, scn5Lab*), one of which was found to be expressed in both the adult and developing heart, as well as in the central nervous system (*scn5Lab*). Like *scn10a* and *scn11a*, however, the expression of *scn5Laa* was not detected in the adult heart but only in nervous tissue. Despite its absence from mature heart tissue, *scn5Laa* transcripts were amplified from the developing myocardium. Cloning, assembly, and functional expression of *scn5Lab* in CHO cells demonstrated typical sodium current with gating kinetics that are similar to mammalian $Na_v1.5$. Our results demonstrate the independent duplication of an ancestral vertebrate *scn5a*-like gene in mammals (3 genes) and fish (2 genes). The expression of both zebrafish *scn5a*-like genes in cardiac tissue suggests that $Na_v1.5$-like sodium channels have played a conserved role in cardiac excitation at least since the split of tetrapods and teleosts over 400 million years ago. The expression of *scn5a*, *scn10a*, *scn11a*, *scn5Laa* and *scn5Lab* in nervous tissue indicates, however, that the ancestral vertebrate *scn5a*-like gene may have also played an important role in neuronal

excitability. We thus propose that the divergence of vertebrate *scn5a*-like genes following duplication reflects a partitioning of the role of the ancestral vertebrate gene (*subfunctionalization*), rather than the evolution of completely novel function (*neofunctionalization*).

Introduction

The Na_v1 family of sodium channel genes in mammals is comprised of 9 highly-homologous isoforms and a 10th member that has diverged in sequence (2;15). The unique expression patterns and physiological roles of sodium channels suggest that the expansion of this gene family may have been an adaptation that permitted their diversification and specialization in excitable tissues (1;175;176). Although the cloning and heterologous expression of mammalian sodium channel genes have revealed many functional similarities among Na_v1 isoforms *in vitro*, loss-of-function studies in vertebrate animal models suggest that extant sodium channel isoforms are not likely to be functionally redundant in vivo (82-84;133).

Origin of mammalian sodium channel gene isoforms

The relatively large number of distinct mammalian sodium channel α subunit isoforms has generated interest in the evolution of this gene family, particularly because invertebrate genomes often contain only 1-2 conserved Na_v1 sodium channel genes (98;177-179). The physical linkage of voltage-gated sodium channel genes to the 4 homeobox (HOX) gene clusters (HOXA-D) strongly suggests that as for HOX genes, a large-scale expansion of the vertebrate genome through polyploidization may have contributed to the emergence of 4 ancestral Na_v1 sodium channel genes in early vertebrates (97;98). Phylogenetic analyses of cloned human, mouse, and rat sodium channel gene sequences in turn support the informal classification of extant Na_v1 sodium channel genes into 1 of 4 groups: group 1 includes the genes *SCN1A*, *SCN2A*, *SCN3A*, *SCN7A*, and *SCN9A*; group 2 includes the genes *SCN5A*, *SCN10A*, and *SCN11A*; group 3 includes the gene *SCN8A*; and group 4 includes the gene *SCN4A* (3;15;97;98). The classification of Na_v1 channels in this manner is further supported by the physical proximity of closely-related sodium channel genes in mammalian genomes. For example, *SCN1A*, *SCN2A*, *SCN3A*, *SCN7A*, and *SCN9A* all occupy adjacent positions on chromosome 2, whereas *SCN5A*, *SCN10A*, and *SCN11A* all localize to the same region of chromosome 3. Taken together, these findings are consistent with an evolutionary model where 4 ancestral vertebrate sodium channel genes first arose by polyploidization from 1-2 invertebrate precursors, followed by the tandem

duplication of a subset of these ancestral genes to produce the 10 Na_v1 sodium channel genes that exist today (97;98).

An explicit test of this proposed model required the cloning and phylogenetic analysis of all Na_v1 sodium channel genes from an appropriate non-mammalian vertebrate outgroup. Lopreato and colleagues investigated the Na_v1 family of genes in the weakly electric fish *Sternopygus macrurus* and found evidence for 6 distinct Na_v1 sodium channel genes (180). The cloning of partial sequences (domains II and III) of all of these genes permitted phylogenetic analysis with the equivalent regions of previously cloned mammalian sodium channel genes. As the prevailing evolutionary model for vertebrate Na_v1 sodium channels predicted, all 6 of *Sternopygus* sodium channel genes occupied positions on 1 of 4 phylogenetic branches with their mammalian counterparts (180). These findings strongly support the concept that extant vertebrate sodium channel genes have arisen from 4 ancestral Na_v1 genes.

One unanticipated finding of Lopreato et al. was that fish and mammals possess different numbers of sodium channel isoforms. The duplication of ancestral vertebrate sodium channel genes thus appears to have proceeded independently in teleost and tetrapod lineages, and the expansion of the Na_v1 sodium channel gene family in mammals (from 4 to 10 genes) is likely to have occurred after the divergence of teleosts and tetrapods over 400 million years ago (180). Additional information about the timing of these duplications cannot be gleaned from available sodium channel sequences. It is thus unknown whether all tetrapod lineages including mammals, reptiles, birds, and amphibians share the same complement of sodium channel genes (e.g. gene duplications occurred prior to the split of these lineages) or whether sodium channel genes independently duplicated in some or all of these vertebrate classes. This particular question may be resolved by cloning and analyzing the full complement of Na_v1 sodium channel genes in a non-mammalian tetrapod.

The fate of duplicate genes

Gene duplication is suspected to be an important evolutionary mechanism underlying the emergence of proteins with new functions (176;181-183). As evolutionary forces may act both on

coding and regulatory sequences of gene duplicates simultaneously (184-186), a number of models that account for both types of changes have addressed the mechanisms that promote the retention and evolution of genes following duplication.

The classical *neofunctionalization* or *mutation during non-functionality* (MDN) model posits that duplicate genes freed of the functional role of their parent gene are no longer subject to purifying selection and begin to acquire random mutations (176;181;187;188). While most mutations lead to a degeneration of function and the emergence of pseudogenes, a duplicate gene may on rare occasions evolve useful functions that lead to the retention of its expression. Since the sequencing of genomes of many organisms has revealed the preservation of many more genes for longer periods of evolutionary time than this model would predict (189;190), other models for the retention and evolution of duplicate genes have been proposed.

The model of s*ubfunctionalization* or the *duplication-degeneration-complementation* (DDC) suggests that the functional redundancy resulting from gene duplication is resolved by degenerative mutations that change the spatial or temporal expression of the duplicate, such that the function of the original gene is subdivided among its progeny (189;190). This has also been referred to as *gene sharing*, which implies that the parent gene already plays two distinct roles, facilitating the functional specialization of each duplicate gene for one of those roles (176;182). In these models, the complementary role of each duplicate thus leads to their preservation in the genome. While evidence suggests that DDC robustly explains the origin of certain multi-gene families, recent studies of the homeobox (HOX) gene clusters have demonstrated that adaptive modification through positive selection appeared to be operative rather than the passive process of degeneration (191;192). Some have referred to this as an *immediate model*, where positive Darwinian selection acts immediately on a gene after duplication (181).

Other models for the retention and subsequent evolution of duplicate genes include *epigenetic complementation*, where the position of the duplicate in the genome may affect its temporal or spatial expression due to epigenetic changes (193). *Dosage compensation* refers to the idea that increased protein levels may intrinsically be adaptive, leading the preservation of duplication genes (185). In other cases, such as been observed in *C. elegans*, the evolution of

novel protein function may arise when the duplication events do not result in two exact copies of a gene but include genomic DNA from adjacent loci (194). The theory of *protein subcellular relocalization* suggests that duplicate genes can evolve new functions with changes in their subcellular localization within cells that result in a new metabolic environment (188). Finally, there are numerous instances where duplicate genes have been retained in genomes for *functional redundancy* (186).

In the absence of data addressing the expression and function of sodium channel genes in multiple vertebrates, it is difficult to predict which model best explains the evolution of Na_v1 channel genes in mammals. The distinct and often complex patterns of expression among closely-related mammalian Na_v1 sodium channel genes strongly suggest, however, that both changes in the regulatory and coding sequences of sodium channel duplicate genes may have been an important factor contributing to the retention of 10 distinct gene isoforms. Although the clusters of sodium channel genes on chromosomes 2 and 3 are each suspected to have arisen from common ancestors, for example, the expression patterns of these genes have significantly diverged. While *SCN1A-3A* display temporally and spatially distinct expression domains primarily within the central nervous system, for example, *SCN9A* is expressed in the peripheral nervous system, adrenal glands, and thyroid tissue (195-204). Moreover, the atypical sodium channel gene *SCN7A* is expressed in a number of tissues including the heart, uterus, lung, and fetal skeletal muscle, as well as in restricted areas of both the central and peripheral nervous systems (205;206). Of genes belonging to the group on chromosome 3, *SCN5A* is expressed primarily in cardiac tissue whereas *SCN10A* is expressed selectively in sensory and nociceptive neurons of the peripheral nervous system (87;207-212). Expression of the third member of this group, *SCN11A*, is also detected in peripheral nervous system but can additionally be found throughout the central nervous system and in diverse tissues such as the spleen and placenta (213;214). For the remaining channels, *SCN8A* and *SCN4A*, there has been no evidence of gene duplication in mammals. *SCN8A* is highly expressed in the brain, spinal cord, peripheral nervous system, and neuromuscular junction (201;202;215-217). *SCN4A* is the primary sodium channel isoform of

skeletal muscle (218-220). The expression patterns of *SCN8A* and *SCN4A* may be similar to those of the ancestral genes from which they have descended.

Adaptive functions of duplicate sodium channel genes

The evolutionary significance of an expansion in the number of Na_v1 genes has been well-delineated by studies characterizing the expression and function of mammalian sodium channels. In humans, rats, and mice, extra sodium channel genes appear to have provided the genetic building blocks for increasingly complex and specialized electrical signaling mechanisms in the central and peripheral nervous systems, heart, and other excitable tissues. In mammals, for example, the expression of no less than 5 distinct sodium channel genes in neurons (including *SCN5A*) supports the idea that duplicate Na_v1 channels may have facilitated the emergence of increasingly complex central nervous systems in early vertebrates (1). Although *SCN5A* is the most highly expressed isoform in the mammalian heart, *SCN1A*, *SCN3A*, and *SCN8A* are also expressed to varying degrees in cardiac tissue where they may contribute to pacemaking and excitation-contraction coupling, among other functions (99;100;102;221). The atypical sodium channel Na_x, encoded by the gene *SCN7A*, may have evolved specialized functions essential to regulating salt homeostasis (83). *SCN9A* is highly expressed in sensory neurons of the dorsal route ganglia where the channel it encodes ($Na_v1.7$) plays a non-redundant role in nociception: in humans, loss of function of this gene resulted in a congenital loss of pain experience without other detectable neurological deficits (74;222;223). Similarly, $Na_v1.8$ (*SCN10A*) is selectively expressed in nociceptive neurons where it has evolved functions essential to the transmission of pain at cold temperatures (88). Given the energetic costs associated with retaining or expressing non-functional genes, multiple Na_v1 channel genes are likely to have been retained in mammals because they have evolved specialized and adaptive roles that contribute to genetic fitness.

Zebrafish sodium channel genes

Despite the popularity of zebrafish embryo as a model system, the family of zebrafish Na_v1 sodium channel genes has only recently attracted attention in this model system. The few

reports available at the outset of this work suggested that zebrafish Na_v1 sodium channel genes are likely to be conserved in sequence, expression and function (174;224-226). However, the complex evolutionary history of Na_v1 genes in vertebrates, as well as strong evidence for lineage-specific whole-genome expansion in teleosts via polyploidization, suggested that the zebrafish genome may not possess easily identifiable, single orthologs for each of the 10 mammalian sodium channel genes (227;228). Moreover, even in mammalian models, the expression of Na_v1 sodium channel genes during embryogenesis has not been well documented. A single report describing the sequence and embryonic expression pattern of a conserved zebrafish homolog of the mammalian gene *scn8a*, however, supported the idea that this model may prove useful for *in vivo* studies of Na_v1 sodium channel function (225).

To use the zebrafish embryo as a model system to study the function of sodium channel subunits in the heart, we first attempted to understand the evolution of this gene family, particularly of the phylogenetic group that includes *scn5a*, *scn10a*, and *scn11a*. In zebrafish, our *in silico* and *in vitro* strategies produced evidence for 8 conserved Na_v1 channel genes, 2 of which appeared to be putative sequence homologs of the mammalian gene *scn5a*. The expression of only one of these genes in the adult zebrafish atrium and ventricle ("*scn5Lab*"), however, suggested the presence of a single functional ortholog of mammalian *scn5a* in fish. Despite only 63% identity to human $Na_v1.5$ in amino acid sequence and significant phylogenetic distance, this zebrafish $Na_v1.5$ channel conserves many of the important structural features found in its human counterpart. Moreover, heterologous expression of this zebrafish channel in CHO cells revealed typical sodium currents with biophysical properties that are similar to mammalian sodium channels. Expression of this gene was also detected in the developing heart, suggesting that the sodium channel it encodes may contribute to cardiac excitation and function from the early stages through adulthood.

Another laboratory recently reported expression of the second zebrafish *scn5a* gene homolog ("*scn5Laa*") in the embryonic myocardium (229). Accordingly, we confirmed this expression and initiated studies of *scn5Laa* including the independent cloning and assembly of a full-length expression vector (see Chapter 5, Future Directions). To distinguish between the 2

zebrafish *scn5a* homologs, we have adopted names suggested by the literature (*scn5Laa* and *scn5Lab* for *SCN5A*-like gene isoforms A and B) that indicate the phylogenetic relationship of these genes to the group of HOXA-linked, mammalian Na_v1 channel genes that include *SCN5A*, *SCN10A*, and *SCN11A* (230).

Our results demonstrate the independent duplication of an ancestral vertebrate *scn5a*-like gene in mammals (3 genes) and fish (2 genes). The expression of both zebrafish *scn5a*-like genes in cardiac tissue suggests that $Na_v1.5$-like sodium channels have played a conserved role in cardiac excitation at least since the split of tetrapods and teleosts over 400 million years ago. The expression of *scn5a*, *scn10a*, *scn11a*, *scn5Laa* and *scn5Lab* in nervous tissue indicates, however, that the ancestral vertebrate *scn5a*-like gene may have also played an important role in neuronal excitability. We thus propose that the divergence of vertebrate *scn5a*-like genes following duplication reflects a partitioning of the role of the ancestral vertebrate gene (*subfunctionalization*), rather than the evolution of completely novel function (*neofunctionalization*). The functional characterization of both *scn5Laa* and *scn5Lab in vivo* will be described in Chapter 3.

Methods

Identification and cloning of a putative zebrafish scn5a ("scn5Lab") gene homolog

BLAST searches of the draft zebrafish genome cDNA database (ensembl Zv2, Zv3) were performed using full-length cDNA sequences and individual exons of the genes encoding the mammalian voltage-gated sodium channels $Na_v1.1$-1.9. Manual searches of unmapped contig hits and alignments of protein sequences predicted by the top 60 hits subsequently identified 15 highly-conserved, predicted zebrafish sodium channel cDNAs of varying lengths whose sequences were used to generate PCR primers. Primers directed against two of the 15 predicted cDNAs consistently produced single amplicons of the anticipated size from an adult zebrafish heart cDNA library (Stratagene) which were gel purified, subcloned, and sequenced in their entirety to confirm their specificity. The larger RT-PCR amplicon, whose deduced translation product corresponded to the terminal exon and 3'UTR of a sodium channel, was used to generate reverse primers that were used in conjunction with forward primers directed against vector-specific promoter sites (T7, SP6) to isolate 3 additional, overlapping sections of the *zscn5a* cDNA from the adult zebrafish heart library. 5' and 3' RLM-RACE (Ambion) was used to complete the preliminary full-length cDNA sequence and extend sequences corresponding to 5' and 3' untranslated regions (UTRs). All amplicons were subcloned directly into the pGEM-Teasy vector (Invitrogen), transformed into DH5α competent cells, and sequenced in their entirety. In the process of cloning *zscn5a*, it was determined that both partial cDNAs expressed in the zebrafish heart library represented upstream and downstream regions of a single cDNA. The preliminary, full-length *zscn5a* cDNA sequence was confirmed by using new primer pairs to amplify the entire channel in 6 overlapping sections (A>F) from total D2 embryonic RNA using one-step Titan RT-PCR (Roche). The PCR primers used to amplify these sections are reported in Table 1. These 6 sections also provided the template for assembling a full-length cDNA construct for heterologous expression (see "Assembly of full-length *$zNa_v1.5$* expression construct," below). The final *zscn5a* cDNA consensus sequence was determined after aligning the forward and reverse sequences of

8-10 clones of each of the 6 overlapping channel sections and was deposited in GenBank (DQ837300).

Zebrafish Na_v1 gene expression screen

Using *in silico* and *in vitro* approaches, the entire complement of zebrafish Na_v1 channel genes was identified and assayed for expression in different excitable tissues. This was achieved by using sequences of the distinctive, conserved terminal two-most exons of mammalian voltage-gated sodium channel genes in BLAST searches of updated versions of the draft zebrafish genome (ensembl Zv4, Zv5) to identify *in silico* predicted "sequence tags" of all non-redundant Na_v1 genes. Eight unique zebrafish sodium channel genes were identified using this strategy. These *in silico* Na_v1 sequence tags were then used to design primers that spanned the intervening intron, and RT-PCR was performed to both validate these sequences and determine their pattern of expression in RNA extracted from various zebrafish tissues. Primer pairs used for this experiment are listed in Table 2. Tissues were freshly dissected from wild type adult zebrafish (strain TuAB, 12-16 months old) and flash frozen on dry ice in ethanol. Tissue-specific total RNA was isolated RNA using Trizol (GIBCO), digested with RQ1 DNase (Promega), and purified with the RNeasy Mini Kit (Qiagen). First strand cDNA synthesis was performed using 1µg of RNA from each tissue, random hexamer primers, and Transcriptor reverse transcriptase enzyme (Roche). 2µl of first strand cDNA was used in 25µl PCR reactions with Expand High Fidelity DNA polymerase (Roche). Amplicons were analyzed on a 1-2% agarose gel made with 1x Tris-Acetate-EDTA (TAE) buffer. All amplicons were subcloned directly into the pGEM-TEasy vector (Promega) and sequenced in their entirety in both sense and antisense directions.

Identification of additional Na_v1 gene sequences

The entry for a putative zebrafish homolog to mammalian *scn8a* was the only sodium channel sequence available in GenBank (NM_131628) at the outset of this work (225). Therefore, to facilitate reconstruction of the phylogeny of sodium channel genes in zebrafish, we additionally determined the complete full-length sequence of a zebrafish brain-type Na_v1 sodium channel

gene. Predicted exons spanning 90% of the coding region for a putative *zscn2a* homolog were identified in the draft zebrafish genome sequence (ensembl Zv4) during the expression screen described above. These predictions were used to design primers that successfully amplified overlapping sections of a near-complete, full-length cDNA from D2 total embryonic RNA by Titan one-step RT-PCR (Roche). 5'/3' RLM-RACE PCR (Ambion) was used to complete the ends of this cDNA. The final putative *zscn2a* cDNA consensus sequence was determined after aligning forward and reverse sequences of 6-8 clones of each overlapping section. During our efforts to clone additional full-length zebrafish sodium channel genes for phylogenetic analysis, two new zebrafish Na_v1 sequences appeared in public databases encoding putative zebrafish homologs of the skeletal-muscle type mammalian sodium channel *scn4a* (DQ221253, DQ221254) (231). The collection of our zebrafish clones (*zscn5a*, *zscn2a*) and publicly available sequences (*zscn8a*, *zscn4aa*, *zscn4ab*) spanned the 4 phylogenetic groups of related sodium channel genes proposed in the evolutionary literature (97;98;180): (1. *scn5a/10a/11a* – heart/DRG – HOXA; 2. brain – *scn8a* – HOXB; 3. skeletal muscle – *scn4a* – HOXC; 4. brain – *scn1a/2a/3a/7a/9a* – HOXD). We reasoned that these five sequences would thus be sufficient to reconstruct the phylogeny of zebrafish sodium channels (and confirm the identity of our clone), even without access to the remaining 3 (and possibly other) full-length sodium channel gene sequences.

Phylogenetic analysis of zebrafish Na_v1 Sequences

To estimate phylogeny, nucleotide and amino acid sequences of human voltage-gated sodium channels (*SCN1A-11A*) were each aligned with cloned zebrafish sequences using CLUSTALX (v1.83). Phylogenetic trees were reconstructed using the neighbor-joining method of Saitou and Nei (232) and viewed with NJplot software. Alignment gaps were excluded in the analysis, and the Kimura correction was made for multiple substitutions. The robustness of each node in the phylogenetic tree was tested with bootstrap analysis (n=1000). Trees were rooted with sodium channel sequences from invertebrate species (98).

Assembly of full-length zNa$_v$1.5 expression construct

Overlapping sections (A-F) of the putative z*scn5a* gene spanning the entire coding region and a small portion of the 5' and 3' UTR were amplified from Day 2 total zebrafish embryonic RNA using one-step Titan RT-PCR (Roche), using the primers listed in Table 1. PCR amplicons for sections B and C and sections E and F were then used as templates in a second PCR reaction to produce the fusion products BC and EF. PCR products for A, BC, D, and EF were subcloned directly into the pGEM-Teasy vector (Invitrogen) and transformed into DH5α competent cells. Multiple clones of each segment were fully sequenced and aligned to identify single clones that matched the consensus the sequence (A*, BC*, D*, and EF*). All 4 sections were designed to overlap at unique restriction enzyme sites and the full-length channel clone was assembled in pGEM-Teasy by a series of digests and ligations as summarized in figure 2.9. The entire 5.9kb *zscn5a* insert was then removed from the pGEM-Teasy cloning vector using *NheI* and *KpnI* restriction sites that had been initially appended to the primers used to amplify sections A and F, and subcloned into a pBK-CMV mammalian expression vector to produce pBK-CMV-*zscn5a*. The full-length channel construct was propagated in DH5α cells under standard conditions.

Transient transfection and electrophysiology

Cultured Chinese Hamster Ovary (CHO) cells were transiently transfected with the pBK-CMV-*zscn5a* construct using FuGENE6 (Roche). Cells were grown for 48 hours after transfection prior to electrophysiology. Whole-cell voltage clamp was performed at room temperature with 2MΩ patch microelectrodes and an Axopatch 200A amplifier. To minimize the capacitive transients, we compensated for approximately 70% to 80% of the cell capacitance and series resistance (233). Cells exhibiting very large currents (>6 nA) were also excluded from further analysis. Cells were also excluded if voltage control was compromised. The extracellular bath solution contained (in mmol/L) NaCl 145, KCl 4.0, $MgCl_2$ 1.0, $CaCl_2$ 1.8, glucose 10, and HEPES 10; the pH was 7.4, adjusted with NaOH. The pipette (intracellular) solution contained (in mmol/L) NaF 10, CsF 110, CsCl 20, EGTA 10, and HEPES 10; the pH was 7.4, adjusted with

CsOH. Cells were held at -120 mV, and activating currents were elicited with depolarizing pulses from -100 to +50 mV in 10 mV increments. Specific clamp protocols are indicated with the data. Data were acquired by pClamp8.0 (Axon Instruments Inc), sampled at 50 kHz, and low-pass filtered at 5 kHz. All currents were normalized to the cell capacitance calculated by Membrane Test (OUT O) in pClamp8.0.

Results

Identification and cloning of a putative zebrafish scn5a gene homolog

In humans, *SCN5A* is a large gene comprised of 28 exons spanning nearly 80kb of genomic DNA. Initial BLAST searches of the draft zebrafish genome (Zv2) using the full-length human *SCN5A* cDNA sequence (approximately 6kb) and smaller regions of the gene that are highly conserved among mammalian species (human, mouse, rat, and cow) but which distinguish *SCN5A* from other sodium channel isoforms (cytoplasmic interdomain linkers) yielded hundreds of unique, partial hits of varying size with e-values ranging form 10^{-05} to 10^{-276}. These sequences represented genes encoding sodium channels, calcium channels, and an array of non-ion channel genes. Zebrafish contigs containing the top 30 hits were individually analyzed with MIT *Genscan* software to predict exons, and the resulting partial cDNAs and their translated protein products were aligned against the known sequences of all 10 human voltage-gated sodium channels. However, this approach did not identify any convincing zebrafish homologs to mammalian *scn5a*.

Given the extensive number of non-specific hits in our initial screen, subsequent *in silico* strategies focused on first identifying all conserved zebrafish Na_v1 genes. BLAST searches of updated versions of the draft zebrafish genome cDNA database (ensemble Zv3) were performed using both full-length cDNA sequences and individual exons of the genes encoding the mammalian voltage-gated sodium channels $Na_v1.1$-1.9. As before, this approach yielded >100 hits of putative sodium channel and calcium channel genes of various lengths, scattered across unmapped contigs of zebrafish genomic DNA. Manual searches, exon prediction, and alignments of cDNA and protein sequences predicted by the top 60 hits subsequently identified 16 highly-conserved, predicted zebrafish Na_v1 cDNAs of varying lengths (Figure 2.2). As one of these genes represented a previously-cloned putative zebrafish homolog to *scn8a*, we tentatively named the remaining sequences *zscn1-zscn15*.

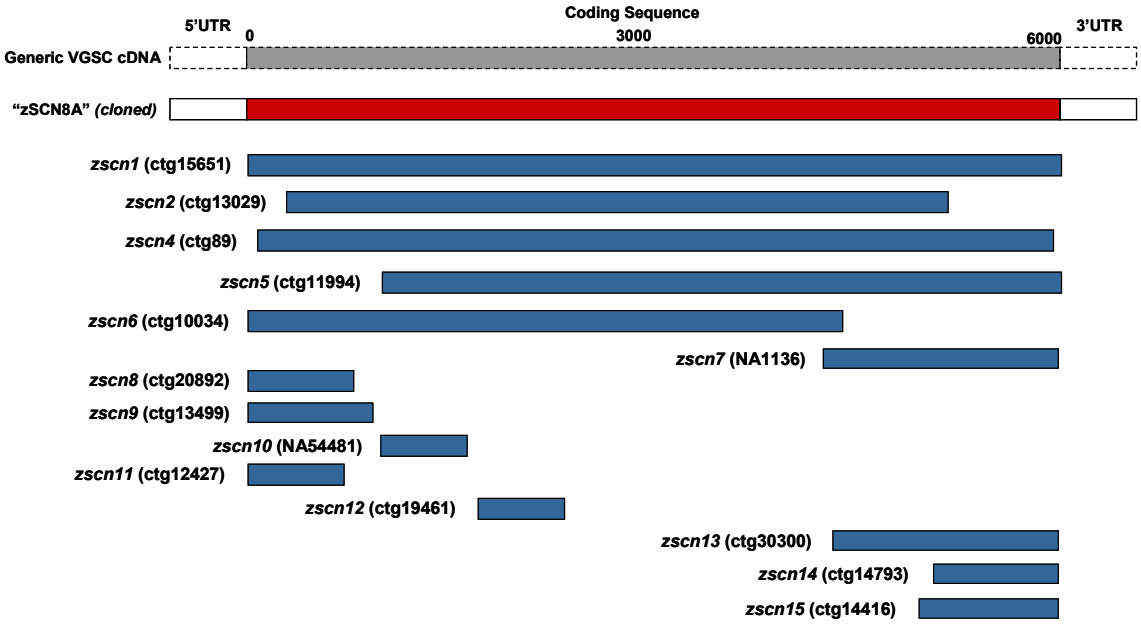

Figure 2.2: Top candidates for conserved zebrafish Na_v1 sodium channel genes. Sequences encoding both full-length cDNAs and individual exons of the mammalian voltage-gated sodium channel genes *scn1A*, *scn4A*, *scn5A*, *scn8A*, and *scn10A* were used in BLAST searches of the draft zebrafish genome (Zv3, 2003) to identify conserved zebrafish Na_v1 voltage-gated sodium channel loci. The results above represent the top 15 candidates of over 60 gene sequences manually searched and analyzed by alignment with mammalian homologs. These putative Na_v1 genes were named *zscn1-zscn15*. Zv3 contig numbers are provided in parentheses. Additional details for these these predicted genes are displayed in Figure 2-3.

Gene	Contig	Chromosome	# predicted exons	length of translated product (aa)	corresponding channel domain	closest human homolog (by alignment)	% identity (aa)	predicted TTX sensitivity
zscn1	*cloned*	11	*26 (actual)*	1949	whole channel *(cloned)*	*SCN8A*	81.7%	sensitive
zscn2	ctg15651	6	30	1999	whole channel	*SCN2A*	72.5%	sensitive
zscn3	ctg13029	6	24	1456	N terminus >> DIV, S3	*SCN8A*	71.5%	sensitive
zscn4	ctg89	11	31	1856	whole channel	*SCN4A*	61.8%	sensitive
zscn5	ctg11994	7	21	1590	D1 (S5-6 linker) >> C-terminus	*SCN2A*	62.2%	n/a
zscn6	ctg10034	3	25	1242	N terminus >> DIII (S5-6 linker)	*SCN4A*	49.2%	sensitive
zscn7	NA1136	unmapped	6	724	DIII (S3) >> C-terminus	*SCN5A*	70.5%	n/a
zscn8	ctg20892	unmapped	6	324	N terminus >> DI (S5-6 linker)	*SCN2A*	60.0%	n/a
zscn9	ctg13499	8	9	381	N terminus >> DI (S5-6 linker)	*SCN3A*	59.9%	sensitive
zscn10	NA54481	unmapped	5	265	D1(S6) >> D1-2 linker	*SCN5A*	33.8%	n/a
zscn11	ctg12427	11	5	307	N terminus >> D1 (S5-6 linker)	*SCN8A*	53.7%	n/a
zscn12	ctg19461	unmapped	4	272	DI-II linker >> DII-III linker	*SCN3A*	40.9%	n/a
zscn13	ctg30300	unmapped	6	698	DIII (S4-5 linker) >> C terminus	*SCN5A*	71.5%	n/a
zscn14	ctg14793	10	1	384	DIV (S3-4 linker) >> C terminus	*SCN8A*	85.4%	n/a
zscn15	ctg14416	3	1	411	DIV (S3-4 linker) >> C terminus	*SCN4A*	68.0%	n/a

Figure 2.3: Details of predicted Na_v1 sodium channel genes identified in an early version of the draft zebrafish genome (Zv3, 2003).

As several of these gene fragments displayed homology to mammalian *scn5a* (Figure 2.3), all predicted sequences were used to generate primers for RT-PCR. Primers directed against 2 of the 15 predicted Na_v1 cDNAs (*zscn7*, *zscn10*) consistently produced single amplicons of the anticipated size from an adult zebrafish heart cDNA library (data not shown). After sequencing, it was determined that the deduced translation product of the larger RT-PCR amplicon (*zscn7*) product aligned with homology to amino acids 1445-2002 of *SCN5A* (74.7% identity, 84.0% similarity). As the remainder of the genomic DNA sequence was missing from the draft zebrafish genome database (Zv3), this partial clone used as a starting point to identify additional overlapping clones of the putative *zscn5a* cDNA from the zebrafish heart library (Figure 2.4). 5'/3' RNA ligase-mediated rapid amplification of cDNA ends (RLM-RACE) was used to complete the preliminary full-length coding *zscn5a* cDNA sequence and extend it into regions corresponding to 5' and 3' untranslated regions (UTRs) (Figure 2.4). In the process of cloning *zscn5a*, it was determined that both partial cDNAs initially detected in the zebrafish heart library (*zscn7* and *zscn10*) represented upstream and downstream regions of a single cDNA. The preliminary, full-length *zscn5a* cDNA sequence was confirmed by using new primer pairs (Table 1) to amplify the entire channel in 6 overlapping sections from total day 2 embryonic RNA. The final *zscn5a* cDNA consensus sequence was determined after aligning the forward and reverse sequences of 8-10 clones of each of the 6 overlapping channel sections and was subsequently deposited in GenBank (DQ837300).

Conserved features of zebrafish and human $Na_v1.5$

The full-length cloned *zscn5a* cDNA sequence spans 6,541 nucleotides, with an open reading frame of 5,865 nucleotides that encodes a sodium channel protein of 1954 amino acids (Figure 2.5). The reduced predicted protein size compared to human $Na_v1.5$ (2016 amino acids) was accounted for primarily by the loss of a single 162 nucleotide exon in the zebrafish cDNA that encodes for a portion of the cytoplasmic linker connecting domains II and III, a region known to

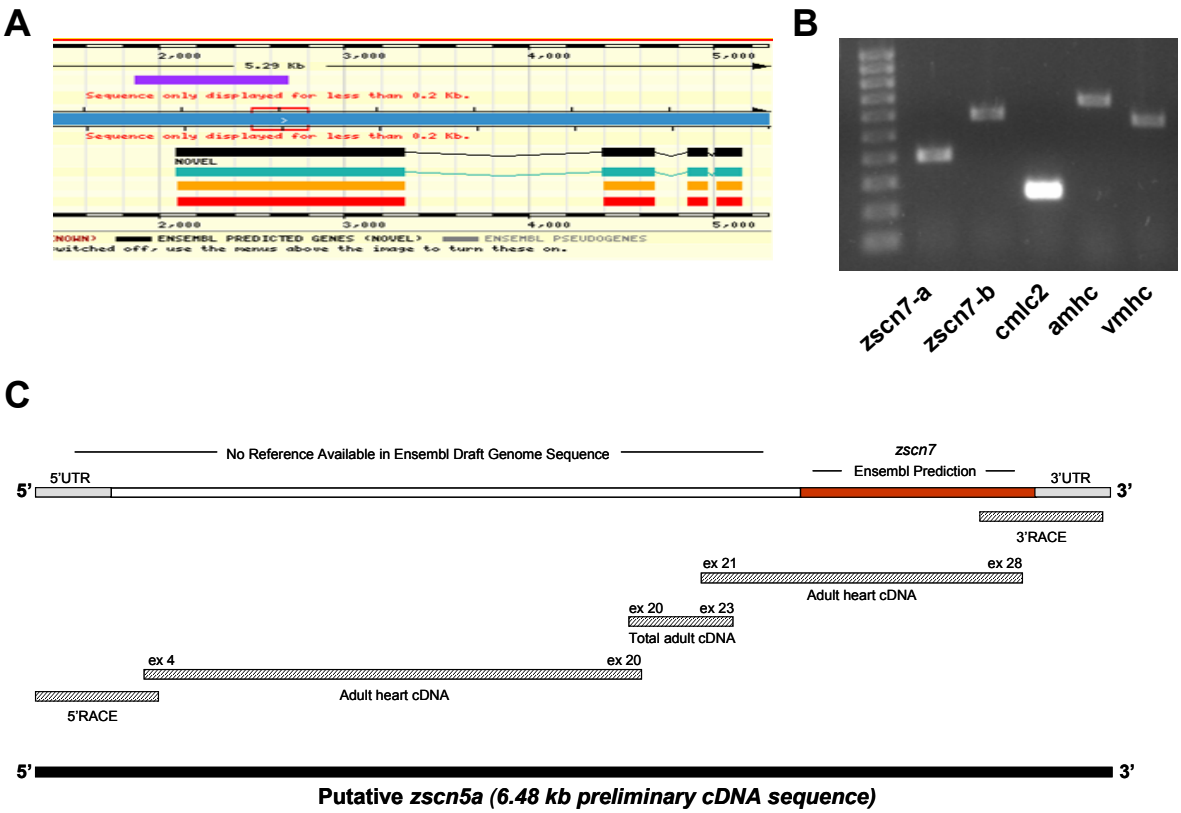

Figure 2.4: Identification and cloning of the predicted sodium channel gene *zscn7* (putative *zscn5a)* from an adult zebrafish heart cDNA library. (A) Mining of the draft zebrafish genome (ensembl Zv3) using human and mouse Na_v1 cDNA sequences identified numerous partial predicted Na_v1 cDNAs on unmapped contigs that were distinct from the previously cloned sequence of *zscn8a* (Tsai et al., 2001). These included a cDNA fragment encoding the 4 terminal-most exons of a predicted zebrafish sodium channel gene (*zscn7*, NA1136). The translated product of this partial cDNA (negative strand) aligned with high homology to amino acids 1445-2002 of the human SCN5A protein (75% identity, 84% similarity). Purple bar = EST. Black, green, orange, and red bars indicate exons predicted by computer algorithms and/or homology (ensembl, MIT Genscan; Unigene, etc.). **(B)** *zscn7* transcripts were detected in an adult zebrafish heart cDNA library (Stratagene) using two distinct primer pairs (zscn7-a, zscn7-b) directed against predicted exons. Positive controls include cardiac myosin light chain 2 (*cmlc2*), atrial myosin heavy chain (*amhc*), and ventricular myosin heavy chain (*vmhc*). Although *zscn7* amplicons were of the expected product size, the bands were gel purified, subcloned, and sequenced to ensure specificity. **(C)** Identification of the full-length *zscn7* cDNA sequence required isolation of 3 overlapping pieces from two different adult zebrafish cDNA libraries (heart cDNA, total cDNA). 5' and 3' RNA ligase-mediated rapid amplification of cDNA ends (RLM-RACE) were used to complete the full-length putative *zscn5a* cDNA sequence at 5' and 3' ends, respectively.

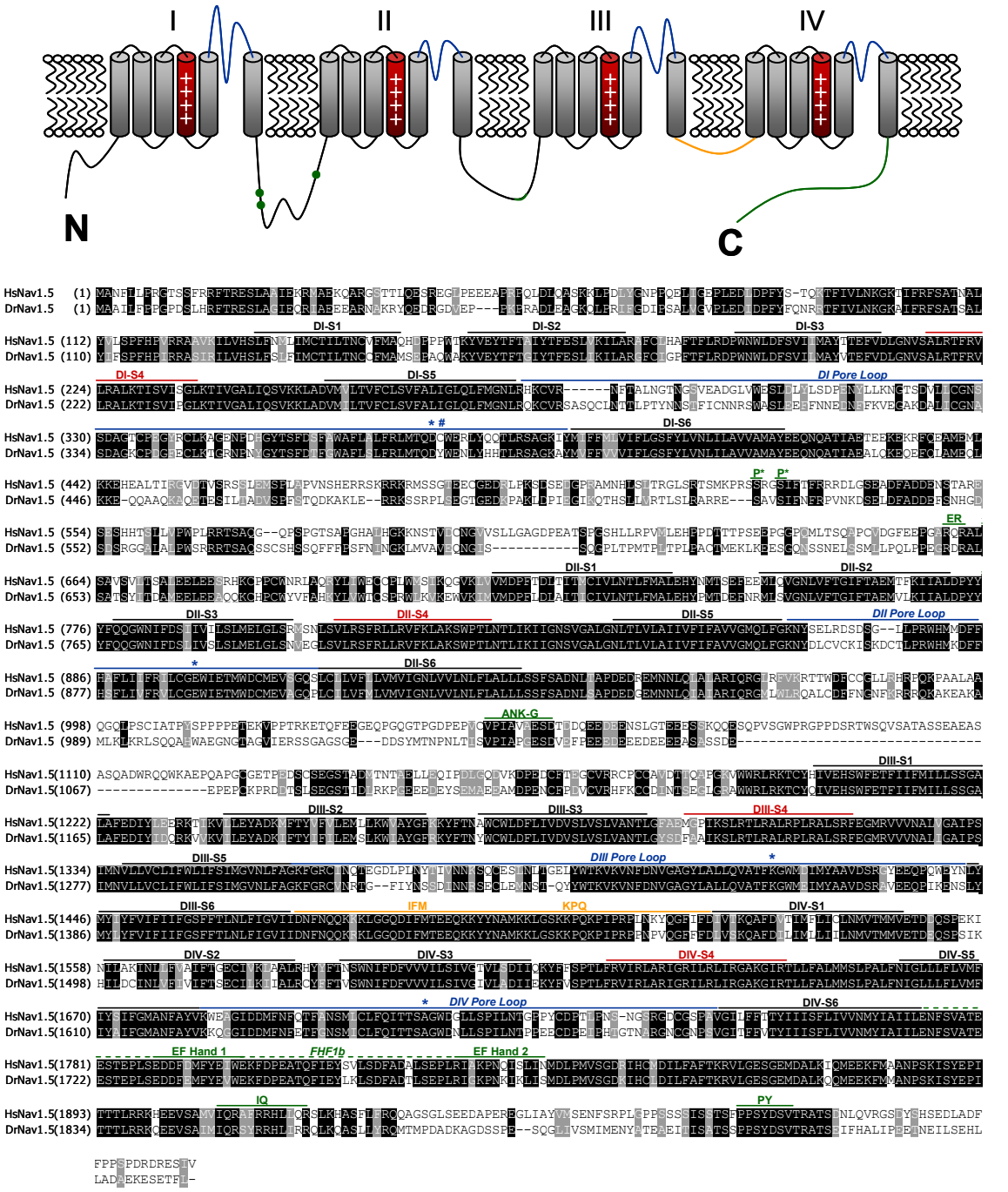

Figure 2.5: Annotated alignment of the putative zNa$_v$1.5 (*zscn5a*) with human Na$_v$1.5 (*SCN5A*). Top = schematic of Na$_v$1.5 with important functional domains highlighted in color. Bottom = annotated amino acid alignment (top = human, bottom = zebrafish). Color coding: **Pore loops** = S5-6 linkers, domains I-IV); * = D-E-K-A residues that constitute the ion selectivity filter; # = single cysteine residue in Na$_v$1.5 that confers TTX resistance. **Voltage "sensors"** = S4 membrane-spanning segments. **Inactivation gate** = intracellular DIII-IV linker. **Sites of predicted protein-protein interaction/Ca2+ regulation**: **P*** = PKA phosphorylation site; **ER** = endoplasmic reticulum retention motif; **ANK-G** = ankyrin-G interaction motif; **EF hand** = Ca+ binding motif; ***FHF1b*** = fibroblast growth factor homologous factor 1b interacting domain; **IQ** = calmodulin binding domain; **PY** = interaction motif for Nedd4-like E3 ubiquitin-protein ligases.

vary among sodium channel isoforms in humans (Figure 2.6). Analysis of the genomic structure otherwise revealed homology to *SCN5A*, including a first exon that is entirely non-coding (Figure 2.6). Alignment of the deduced protein sequence of zNa_v1.5 with its human counterpart demonstrated 63.4% identity and 71.9% similarity between the two proteins. Unexpectedly, these initial assessments revealed significantly greater sequence divergence between the two Na_v1.5 homologs than was previously demonstrated for human and zebrafish homologs of Na_v1.6 (*scn8a*), which share 82% identity in amino acid sequence (225). As indicated by a full-protein alignment, most of the divergence between human and zebrafish Na_v1.5 is found in the cytoplasmic linker regions connecting domains I-II and domains II-III, as well as at distal N- and C-termini (Figure 2.5). Nonetheless, annotation of the aligned Na_v1.5 protein sequences revealed conservation of important functional domains in both proteins. These regions included the S5-6 linkers or *pore loops* of domains I-IV, which contribute to the external pore of the channel and display the highly conserved D-E-K-A residues that constitute the Na_v1 ion selectivity filter (calcium channels have E-E-E-E residues); the S4 membrane-spanning segments in each domain that act as the channel's *voltage sensors* and display the expected basic amino acid residues (arginine, lysine) at every third position within the 4 amphipathic alpha helices; the intracellular DIII-IV linker, which functions as the channel's *fast inactivation gate* and plugs the ion permeation pathway after depolarization; and finally, sites of demonstrated, functional protein-protein interactions including an ankyrin-G interaction motif (234;235); a fibroblast growth factor homologous factor 1b (*FHF1b*) interacting domain (236); an IQ domain associated with calmodulin binding (237-240), and a PY motif that permits interaction with Nedd4-like E3 ubiquitin-protein ligases (141;241). Moreover, putative Ca+ binding EF hand structures also appear to be conserved in the C-terminus of zebrafish Na_v1.5 (240;242). We did not, however, observe conservation of a PDZ binding domain at the distal tip of the channel ("SIV") (243). In other regions of the channel, we noted conservation of an endoplasmic reticulum (ER) retention motif and putative PKA phosphorylation sites (122;244;245).

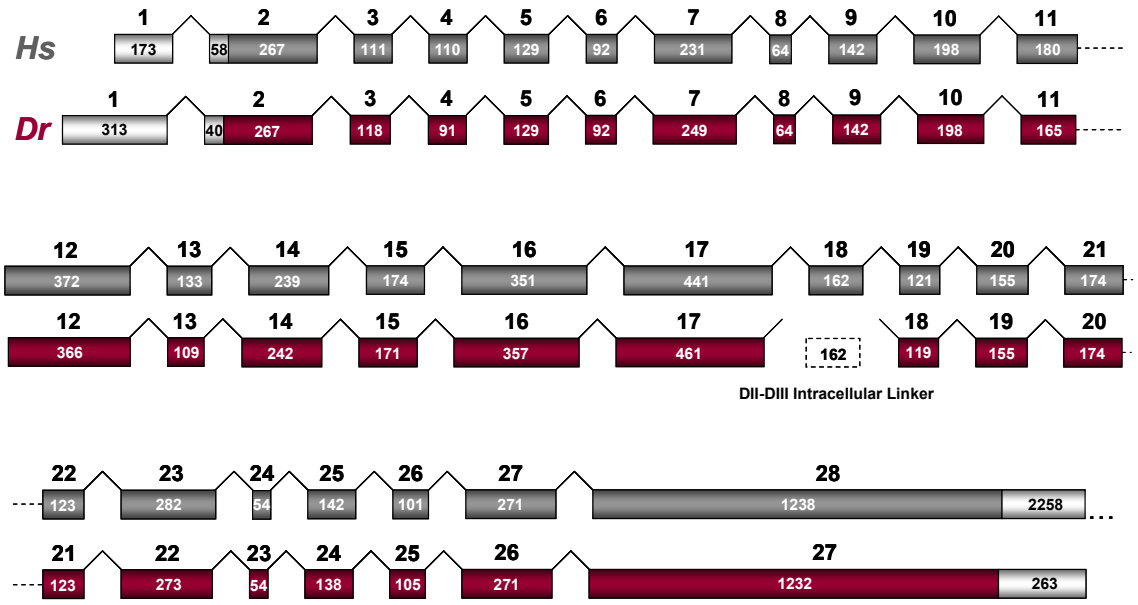

Figure 2.6: The genomic structure of human (Hs) *SCN5A* and zebrafish (Dr) *zscn5a* differ by a single exon. The genomic structure of the zebrafish *scn5a* gene was solved by comparing our cloned cDNA sequence to recently-released contigs of genomic DNA in updated versions of the zebrafish genome (ensembl Zv5-Zv6). The genomic structure of *zscn5a* is completely conserved with human SCN5A with the exception of a single exon in the II-III linker.

Cardiac expression of zscn5a

Cloning of the full-length cDNA of *zscn5a* permitted a preliminary assessment of the gene's 5' regulatory regions *in silico* (Figure 2.7). Both human and zebrafish *scn5a* genes have untranslated initial exons and large intervening introns between exons 1 and 2. Alignment of 2000 nucleotides flanking the transcriptional start site (TSS) of *SCN5A* and *zscn5a* revealed moderate levels of conservation between putative regulatory elements for the two genes (Y-axis = 0-90%; each peak represents a window size of 10 nucleotides). Using the program MatInspector, binding sites for cardiac transcription factors including *MEF2*, *SRF*, and *Nkx2.5* were predicted in this putative regulatory region of *zscn5a*. To examine the cardiac expression of *zscn5a in vitro*, three independent primer pairs (a, b, c) corresponding to different regions of the cloned *zscn5a* cDNA were designed. By RT-PCR, *zscn5a* transcripts were detected in total RNA isolated from the adult atrium and ventricle (panel A) and the embryonic heart (panel B) (Figure 2.8). These findings reinforced the putative identity of this cloned channel as an ortholog to mammalian *scn5a*.

Functional expression of zscn5a (zNa$_v$1.5)

To study the biophysical properties of zNa$_v$1.5 *in vitro*, a full-length, 10.5kb expression construct was assembled as detailed in Methods and Figure 2.9. Successful heterologous expression of *zscn5a* in CHO cells demonstrated that zNa$_v$1.5 functions as a typical voltage-gated sodium channel (Figure 2.10A), with biophysical properties comparable to those observed for mammalian sodium channels expressed in heterologous systems (Table 3). Current-voltage (I-V) analysis, for example, indicated peak inward sodium current density at membrane potentials between -40 and -30mV (Figure 2.10B). Analysis of steady state activation and inactivation properties revealed $V_{1/2}$ values of -42.2±1.1 and -85.3±0.8, respectively. Finally, analysis of the time-dependence of recovery from inactivation, which can be resolved into two components T_1 and T_2) indicated values of 9.1±1.4ms and 144.8±15.1ms, respectively.

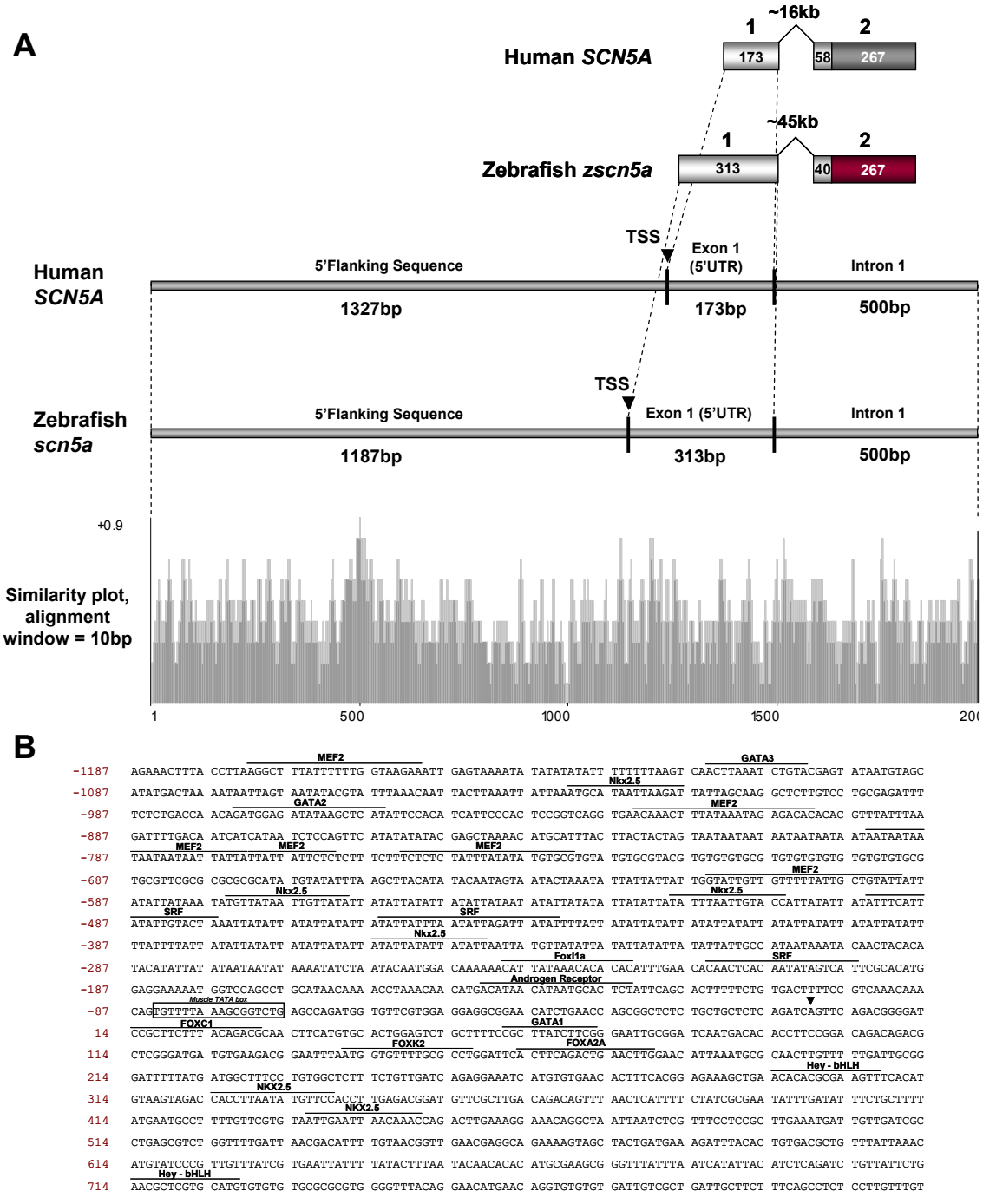

Figure 2.7: *In silico* analysis of putative 5' regulatory regions of human *SCN5A* and zebrafish *scn5a*. **(A)** Comparison of putative 5' regulatory regions of the human *SCN5A* and zebrafish *scn5a* genomic loci. Both genes have untranslated initial exons and large intervening introns between exons 1 and 2. Alignment of 2000 nucleotides flanking the transcriptional start site (TSS) of *SCN5A* and *zscn5a* revealed moderate levels of conservation between putative regulatory elements for the two genes (Y-axis = 0-90%; each peak represents a window size of 10 nucleotides). Position 1 is 1327bp upstream of the TSS for *SCN5A* and 1187bp upstream of the TSS for *zscn5a,* as indicated. **(B)** Using the program MatInspector, predicted binding sites for cardiac transcription factors including *MEF2*, *SRF*, and *Nkx2.5* were identified in this region of *zscn5a*.

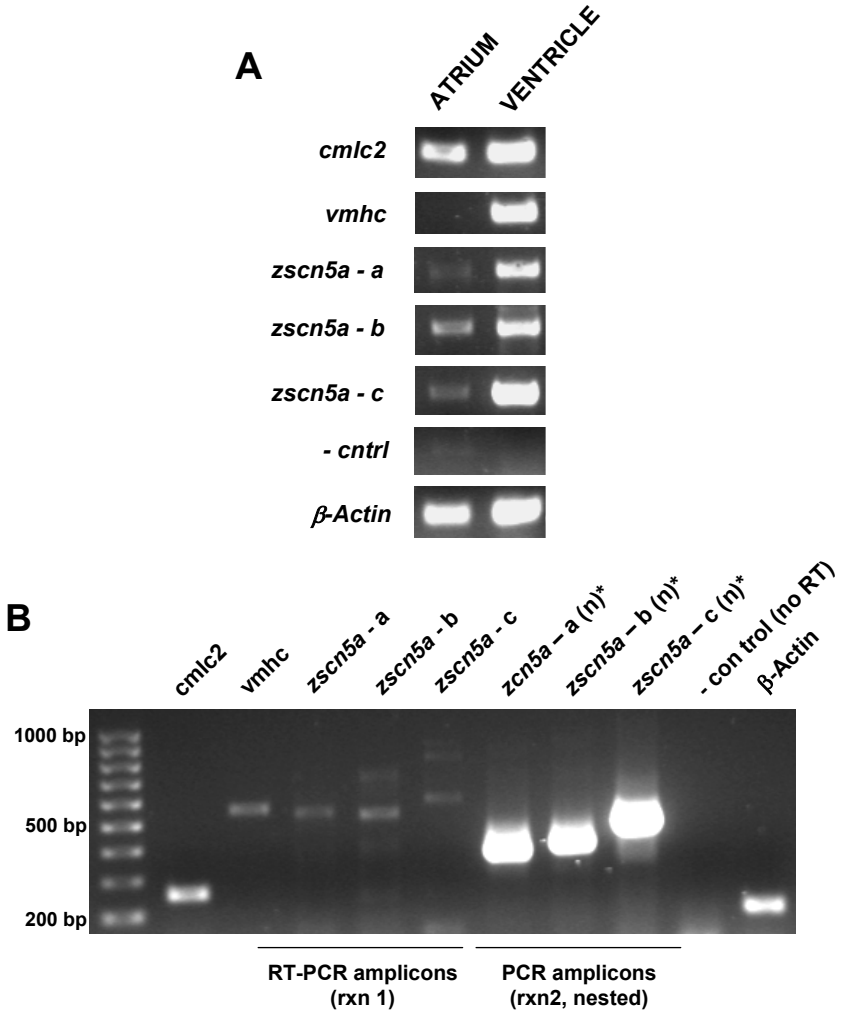

Figure 2.8: RT-PCR was used to assay for expression of *zscn5a* in the adult atrium and ventricle and in the day 3 embryo heart. Three primer pairs (a, b, c) corresponding to different regions of the cloned *zscn5a* cDNA were used to assay for expression in total RNA isolated from the adult atrium and ventricle **(A)** and the embryonic heart **(B)**. To avoid amplification of genomic DNA, RNA templates were DNAse treated and primers were located in different exons with large intervening introns. *cmlc2* is a positive control for cardiac RNA. *vmhc* is a positive control for ventricular RNA and a negative control for atrial RNA. *β-Actin* transcripts were amplified as an additional positive control. Negative control reaction included primers for *cmlc2* and DNA polymerase but no reverse transcriptase. (n)* indicates a nested PCR reaction that used 1µl of amplicon from the initial RT-PCR reaction as a template for the second reaction. In **(B)**, *cmlc2:eGFP5* transgenic zebrafish embryos were used to facilitate the microdissection of day 3 hearts.

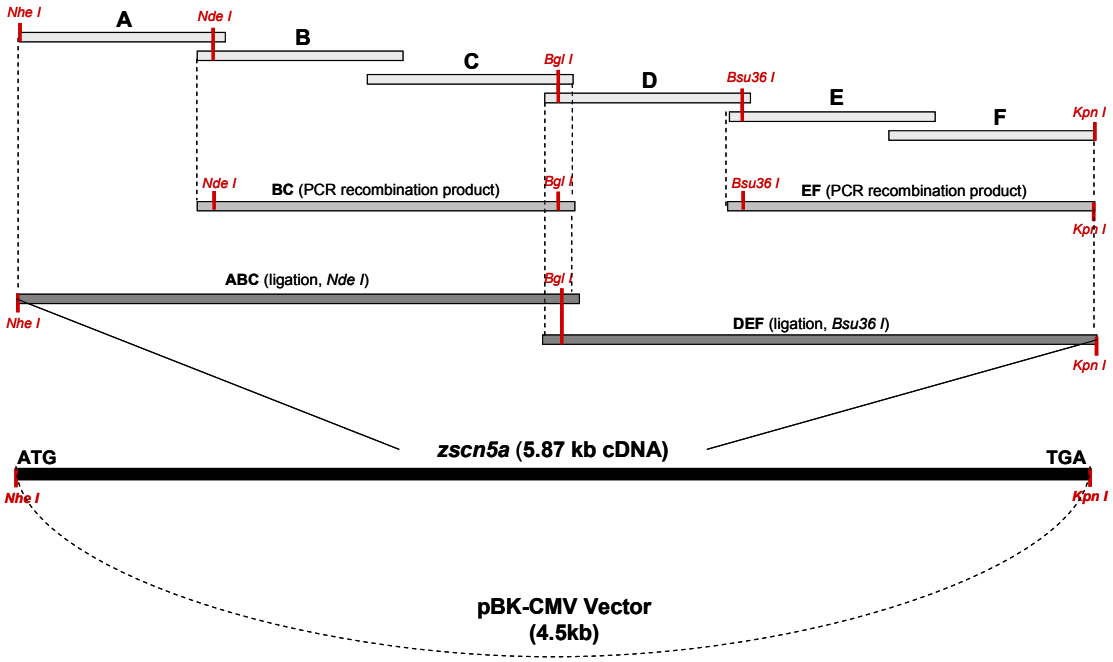

Figure 2.9: Assembly of a full-length mammalian expression vector for *zscn5a* (zNa$_v$1.5). See methods for details of amplification, ligation, and assembly.

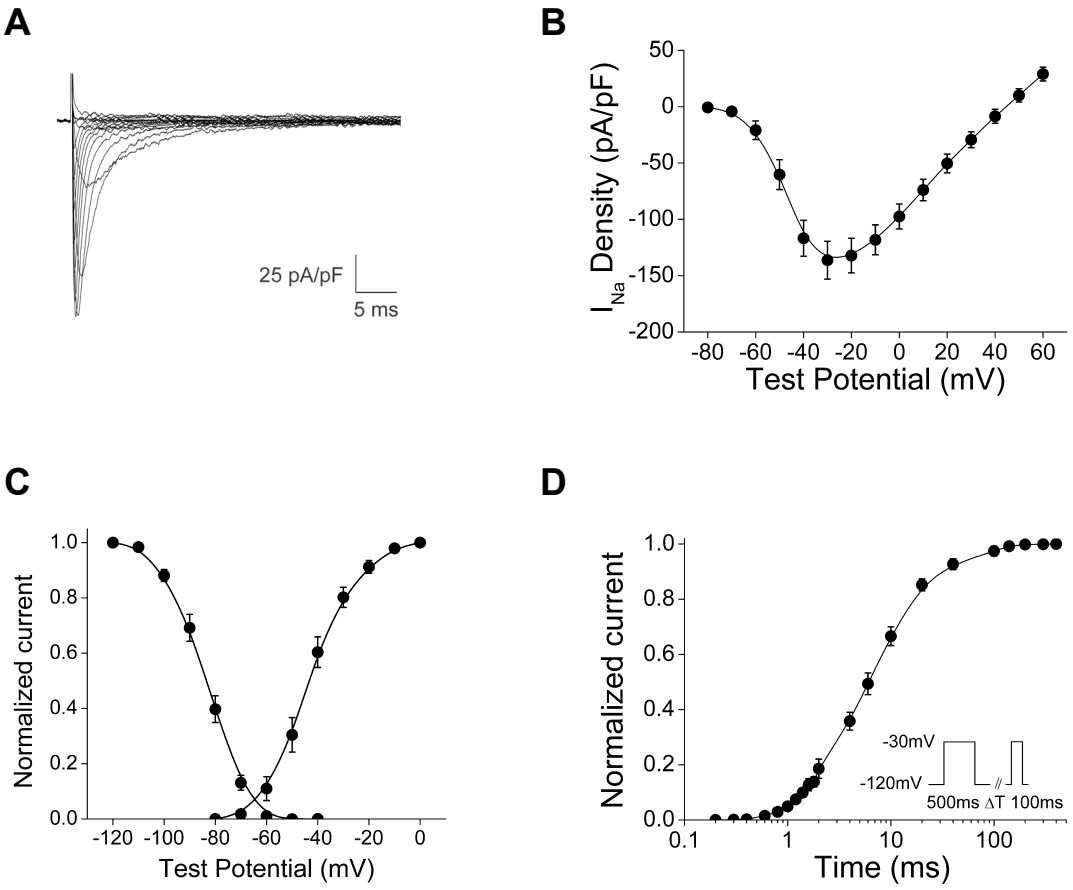

Figure 2.10: Heterologous expression of *zscn5a* (zNa$_v$1.5) in CHO cells. *zscn5a* encodes a typical voltage-gated sodium channel. **(A)** Whole cell sodium current trace. **(B)** Current-voltage (I-V) relationship. **(C)** Voltage-dependent activation and inactivation properties. **(D)** Time-dependent recovery from inactivation. See methods for details on electrophysiology protocols.

Key differences between zNa$_v$1.5 (zscn5a) and mammalian Na$_v$1.5 (scn5a)

Despite preliminary evidence supporting the identity of zebrafish *scn7* as an ortholog to mammalian *scn5a*, the large number of homologous Na$_v$1 sodium channel genes in other species and the moderate level of amino acid identity with human Na$_v$1.5 (63%) prompted us to further scrutinize the putative zNa$_v$1.5 sequence by direct, domain-by-domain comparison to all other mammalian sodium channel amino acid sequences (Figure 2.11). In this analysis, each domain of the putative zebrafish Na$_v$1.5 (*zscn7*) protein was aligned with equivalent regions of human Na$_v$1 channels to determine percent identity and similarity. Domains were identified based on the secondary structure predicted by the amino acid sequence of each channel. Similar comparisons were performed for the pore loop sequences (S5-6 linkers) which represent subdomains of domains I, II, III, and IV that contribute to the sodium channel pore (Figure 2.11). Despite conserved features of the amino acid sequence identified by direct alignment (Figure 2.5) and significant similarity to mammalian Na$_v$1.5 in domains III and IV and the C-terminus (Figure 2.3), this follow-up analysis unexpectedly revealed homology of the putative zNa$_v$1.5 to several different mammalian Na$_v$1 channels across multiple domains. The DI-II and DII-III linker regions displayed the lowest overall levels of similarity. Notably, these are known to be regions of divergence among sodium channels both with and between species.

As another means of investigating the identity of our cloned channel, we examined its sequence for the specific determinants of toxin sensitivity. Historically, sodium channels have been classified by their sensitivity to the pufferfish toxin TTX, which blocks sodium permeation through Na$_v$1 channels by binding to residues in the outer vestibule of the pore (1;15). While most cloned sodium channels are sensitive to nanomolar concentrations of TTX, all mammalian Na$_v$1.5 channels are blocked by micromolar concentrations of toxin and are thus considered prototypical TTX-resistant channels. The basis of this resistance to TTX, which is also displayed by other members of the HOXA-linked Na$_v$1 channel group in mammals including Na$_v$1.8 (*SCN10A*) and Na$_v$1.9 (*SCN11A*), was determined to result from the loss of an aromatic amino acid in the domain I pore loop (Y>C in Na$_v$1.5 and Y>S in both Na$_v$1.8 and Na$_v$1.9) (246). To predict whether zNa$_v$1.5 (like mammalian Na$_v$1.5) is likely to be resistant to TTX, we aligned the

Human Channel	Total		N-terminus		DI		I-II linker		DII		II-III linker		DIII		III-IV linker		DIV		C-terminus	
	ID	*SIM*	*ID*	*SIM*	*ID*	*SIM*	*ID*	*SIM*	*ID*	*SIM*	*ID*	*SIM*	*ID*	*SIM*	*ID*	*SIM*	*ID*	*SIM*	*ID*	*SIM*
$Na_v1.1$ (*SCN1A*)	63.10%	72.10%	60	74.4	71.5	79.1	27.1	36.6	86.6	92.6	35.9	49.4	80	86.3	86.8	88.7	78.8	88.8	55.4	66.5
$Na_v1.2$ (*SCN2A*)	63.80%	72.50%	61.6	74.4	71.9	78.9	27.4	37.2	88.3	93	36.5	50.9	78.1	83	86.8	88.7	79.6	89.6	59.5	70.2
$Na_v1.3$ (*SCN3A*)	63.10%	72.10%	57.6	75.2	73.9	81.2	26.4	36.2	89.1	94.3	33.9	49.3	80.1	84.3	86.8	88.7	76.8	88	57	66.9
$Na_v1.4$ (*SCN4A*)	60.10%	69.10%	56.2	72.3	68.8	77.9	25.8	34.4	85.6	93.9	32.2	44.3	77.3	84.4	84.9	90.6	78.8	88	55.8	64.9
$Na_v1.5$ (*SCN5A*)	63.40%	71.90%	55.9	67.7	72.9	81	34.5	44.9	83	88.3	31.4	42.1	81.9	90	90.6	92.5	79.6	86.8	61.9	70.9
Na_x (*SCN7A*)	41.30%	54.70%	35.5	46.8	47.3	62.6	24.8	33.3	61	76.3	22.2	35.6	54.6	68	53.7	66.7	54.6	74.3	45.7	63.4
$Na_v1.6$ (*SCN8A*)	62.00%	70.30%	53.9	66.4	74.6	83.4	23.2	32.1	85.7	91.7	38.8	52	77.9	84.1	86.8	90.6	79.2	87.6	53.3	62
$Na_v1.7$ (*SCN9A*)	62.20%	72.20%	58.1	71	72.5	80.3	24.3	34.8	85.2	93	34.5	48.5	78.5	86.3	88.7	92.5	77.2	87.6	58.3	69.4
$Na_v1.8$ (*SCN10A*)	54.80%	65.90%	44.4	57.1	62.4	72.5	27	38.3	68.8	81.4	30	42	71.2	81.2	90.6	92.5	69	81.7	53.3	64.9
$Na_v1.9$ (*SCN11A*)	45.70%	57.00%	41.9	57.4	49.7	60.7	23	26.5	61.9	74.9	17.1	27.1	62.9	76	86.8	88.7	59.9	75.4	40.1	50

Pore Loops (S5-S6 Linkers)												
	DI (= 119aa)			DII (= 53aa)			DIII (= 81aa)			DIV (= 66aa)		
Human Channel	*size Hs (aa)*	*ID*	*SIM*	*size Hs (aa)*	*ID*	*SIM*	*size Hs (aa)*	*ID*	*SIM*	*size Hs (aa)*	*ID*	*SIM*
$Na_v1.1$ (*SCN1A*)	126	46.8	57.9	54	81.5	83.3	79	58.2	67.1	66	71.2	80.3
$Na_v1.2$ (*SCN2A*)	127	48	58.3	53	86.8	86.8	79	58.2	64.6	66	72.7	83.3
$Na_v1.3$ (*SCN3A*)	127	48	59.8	53	86.8	86.8	82	57.3	59.8	66	71.2	81.8
$Na_v1.4$ (*SCN4A*)	157	50.3	59.9	52	82.7	86.5	84	52.4	63.1	66	69.7	78.8
$Na_v1.5$ (*SCN5A*)	113	50.4	61.9	51	67.9	77.4	84	58.3	63.1	65	68.2	78.8
Na_x (*SCN7A*)	104	42.2	55.2	54	75.9	83.3	86	40.7	51.2	64	56.3	70.3
$Na_v1.6$ (*SCN8A*)	110	57.3	69.1	53	84.9	84.9	86	50	55.8	65	71.2	78.8
$Na_v1.7$ (*SCN9A*)	107	52.3	66.1	53	86.8	86.8	79	48.1	54.4	66	72.7	78.8
$Na_v1.8$ (*SCN10A*)	101	49.5	60.4	54	53.7	59.3	80	48.8	57.5	65	66.7	77.3
$Na_v1.9$ (*SCN11A*)	107	35.5	44.9	60	46.7	53.3	79	54.9	67.1	57	50	62.1

Figure 2.11: Amino acid sequence homology between zebrafish $Na_v1.5$ (*zscn5a*) and human Na_v1 sodium channels. Each domain of the putative zebrafish $Na_v1.5$ (*zscn5a*) protein was aligned with the equivalent regions of all human Na_v1 channels to determine % identity and % similarity (amino acids). The pore loop sequences (S5-6 linkers) are subdomains of Domains I, II, III, and IV that contribute to the sodium channel pore. **Red** = highest match. **Grey** = other matches within top 5%.

pore-loop sequences of this zebrafish channel with several different mammalian $Na_v1.5$ channels, with human $Na_v1.8$ and $Na_v1.9$, and with several TTX-sensitive human Na_v1 channels (Figure 2.12). This analysis revealed that unlike mammalian $Na_v1.5$, zebrafish $Na_v1.5$ possesses the canonical aromatic residue (Y) required for high-affinity TTX binding. The putative zebrafish $Na_v1.5$ channel is thus predicted to be sensitive to nanomolar TTX because it lacks a key structural determinant of toxin binding that is considered to be a distinguishing feature of mammalian $Na_v1.5$ channels. Electrophysiological analysis subsequently confirmed these predictions, demonstrating that zNav1.5 is sensitive to nanomolar quantities of toxin (Chapter 3).

Consideration of additional Na_v1 channels

In the mammalian Na_v1 sodium channel literature, emerging evidence suggests that both TTX-resistant (*scn5a*) and TTX-sensitive (*scn1a*, *scn3a*, *scn8a*) isoforms are expressed to varying degrees in the mammalian heart where they may play diverse functional roles (9;99;101;102). Because of the key differences between our cloned channel and mammalian $Na_v1.5$ channels, we considered the possibility that we had cloned a gene other than the true functional ortholog of mammalian *scn5a*. We also contemplated whether our initial efforts in mining early versions of the draft zebrafish genome had resulted in the identification of all functionally-important cardiac sodium channels. Therefore, in parallel with the initiation of functional studies of the putative $zNa_v1.5$ *in vivo* (Chapter 3), we formulated a plan for: 1. continued evaluation of new and/or more complete Na_v1 gene sequences appearing in subsequent versions of the draft zebrafish genome; and 2. reconstruction of the phylogeny of zebrafish Na_v1 sodium channel genes by the cloning and mapping of each full-length isoform in the genome (long-term, facilitated by improved zebrafish genome resources). Phylogenetic modeling of full-length sodium channel sequences in combination with the analysis of synteny between these genes and various HOX clusters appealed to us as the most direct means of revealing the identity of each sodium channel isoform in the zebrafish genome, particularly in the context of emerging empirical support for a model of the evolution of Na_v1 channels in vertebrates

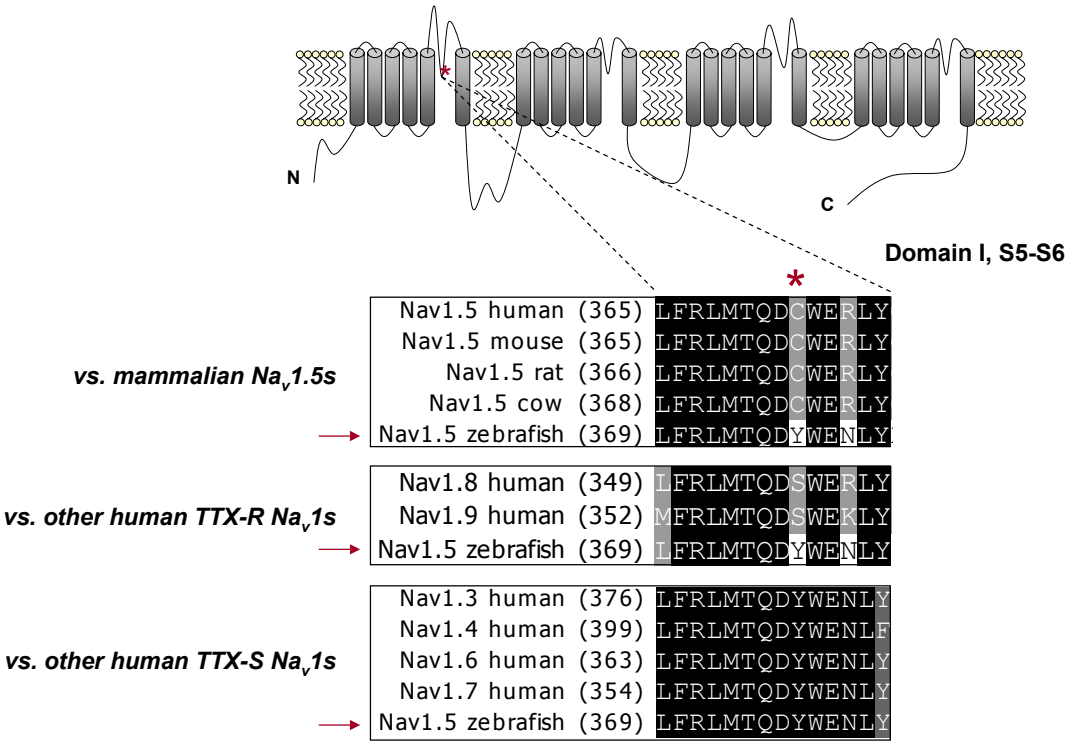

Figure 2.12: Unlike human $Na_v1.5$, zebrafish $Na_v1.5$ is predicted to be sensitive to nanomolar concentrations of the pufferfish toxin TTX. Mammalian sodium channels have evolved resistance to the pufferfish toxin TTX via single amino acid substitutions in the domain I pore (Y > C or S). A cysteine residue in the outer vestibule of the DI pore confers > 100 fold increased resistance to TTX in human $Na_v1.5$ (position marked by **red asterisk**). Alignment of the relevant amino acid sequence of zebrafish $Na_v1.5$ (*zscn5a*) revealed the aromatic residue (Y) required for high-affinity binding in TTX-sensitive channels. Unlike mammalian $Na_v1.5$, zebrafish $Na_v1.5$ (*zscn5a*) is thus predicted to be a TTX sensitive channel. **Red arrow** marks zebrafish $Na_v1.5$.

(97;180). To begin to address these objectives, we devised a simple expression screen to identify the entire complement of zebrafish Na_v1 sodium channels.

Expression screen reveals 8 genes encoding zebrafish Na_v1 channels

We combined *in silico* and *in vitro* approaches to identify all non-redundant Na_v1 sodium channel genes in the zebrafish genome, ascertain their putative phylogenetic identities (based on partial cloned sequences), and subsequently survey their patterns of expression in various excitable tissues from adult zebrafish (Figures 2.13-17). This effort was supported by updated public genome resources (Zv4, Zv5) and by our identification of particular characteristics of the genomic structure of Na_v1 sodium channel genes that would distinguish between them. As illustrated in Figure 2.13, the genes encoding human Na_v1 channels all possess large terminal exons ("TE") that encode nearly all of domain IV and the C-terminus of the protein and preceding exons that encode part of the highly-conserved inactivation gate ("TE_{-1}"). Despite distinct evolutionary origins, we observed that the size of the second to last exon (TE_{-1}) is identical in every human channel (271 nucleotides). Importantly, we determined that the nucleotide sequence of the terminal exon clearly distinguished *SCN5A* from among other isoforms belonging to the three other phylogenetic sodium channel groups (Figure 2.14). Moreover, the large size and sequence of Na_v1 sodium channel terminal exons also differentiated these genes from other related genes in the ion channel superfamily such as those encoding L- and T-type voltage-gated calcium channels (Figure 2.14).

By searching specifically for 3' exons (TE, TE_{-1}) of Na_v1 sodium channels in the draft zebrafish genome (Zv4, Zv5), we identified a total of 8 conserved and non-redundant zebrafish Na_v1 genes. These partial clones most resembled the mammalian genes scn1a, scn2a, scn4a (2 genes), scn5a (2 genes), and scn8a (2 genes), indicating that zebrafish possess 2 genes for each of the four phylogenetic groups and are thus likely to display a different pattern of Na_v1 gene duplication than has occurred in mammals (Figure 2.15). These gene identities were putatively assigned based on phylogenetic relationships (Figure 2.16) and alignment with the nucleotide and amino acid sequences of human sodium channel genes. The identified sequences

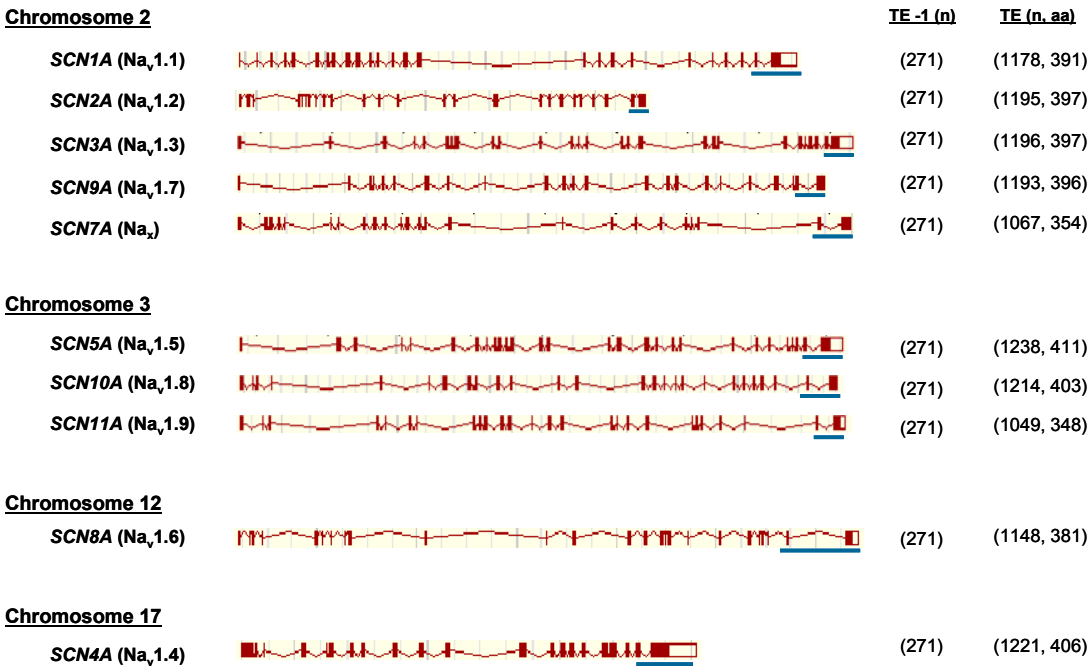

Figure 2.13: Genomic structure of human Na_v1 sodium channel genes. Na_v1 voltage-gated sodium channel genes are distinguished by large, terminal exons that encode nearly all of domain IV of the protein (TE) and preceding exons that encode part of the highly-conserved inactivation gate (TE-1). Shown above are the genomic structures of human sodium channel genes, adapted from the National Cener for Biotechnology Information (NCBI) gene database. **Blue** underline demarcates TE and TE-1. Note that despite distinct evolutionary origins, the size of the second to last exon (TE-1) is identical in every human channel (271 nucleotides). n = nucleotide number; aa = amino acid number.

A

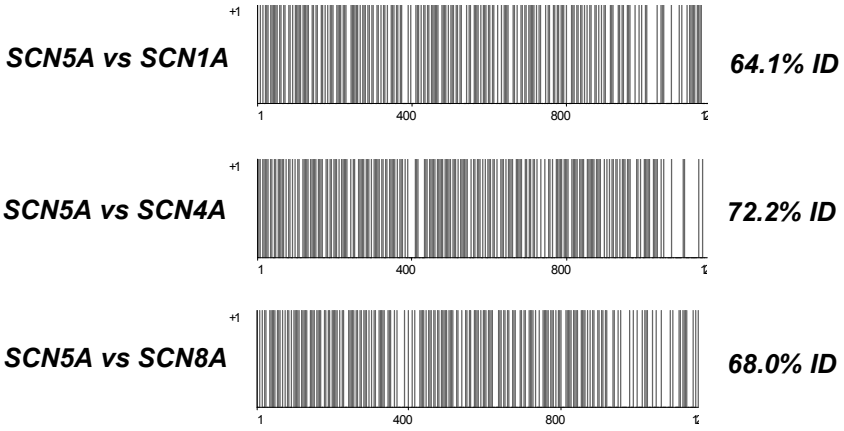

B

Terminal Exon - VGCCs		
gene	*channel*	*exon size*
CACNA1A	L-type	741
CACNA1B	L-type	531
CACNA1C	L-type	300
CACNA1D	L-type	294
CACNA1E	L-type	543
CACNA1F	L-type	231
CACNA1S	L-type	735
CACNA1G	T-type	1014 *
CACNA1H	T-type	645
CACNA1I	T-type	252

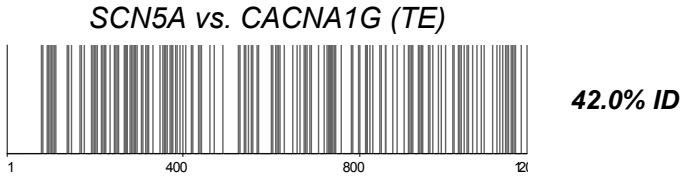

Figure 2.14: Utility of 3' sequences (TE, TE-1) in differentiating sodium channel isoforms from each other and from more distantly-related calcium channel genes. For human Na_v1 sodium channels, the nucleotide sequence of the terminal exon clearly distinguishes individual genes from other homologous isoforms. **(A)** Alignments of the 3' region of *SCN5A* versus analgous regions of channels belonging to the three other phylogenetic sodium channel groups. **(B)** The large size and/or sequence of Na_v1 sodium channel terminal exons also differentiate these genes from other related genes in the ion channel superfamily such as those encoding L- and T-type voltage-gated calcium channels. A **red asterisk** marks the gene *CACNA1G*, which also has a large terminal exon. However, the terminal exon of this gene shares little homology with that of *SCN5A*. For all alignments above, Y-axis = identity (0-1) where the alignment window is 1 nucleotide.

constituted *in silico* predicted "sequence tags" for the genes encoding each zebrafish Na_v1 isoform. Chromosome assignment within the zebrafish genome was based on the reported map positions of contigs that encoded these sequence tags (ensembl).

To validate these Na_v1 sequence tags and determine their pattern of expression in various excitable organs, primers were designed in flanking exons (TE and TE-1) for RT-PCR. As displayed in figure 2.17, primers directed against all 8 predicted Na_v1 sodium channel genes successfully and specifically amplified their targets, as confirmed by direct sequencing of PCR amplicons. Despite two putative *scn5a*-like genes in the zebrafish genome (*zscn6*, *zscn7*), only one Na_v1 gene appeared to be highly-expressed in the adult zebrafish atrium and ventricle (z*scn7*, our cloned Na_v1 gene). Expression of *zscn5* was also detected in the atrium, but at very low levels. These results confirmed that we had cloned the primary sodium channel gene expressed in adult zebrafish heart muscle.

Phylogeny of full-length zebrafish Na_v1 gene sequences

An accurate assessment of the phylogeny and identity of zebrafish Na_v1 channel genes optimally required full-length sequences for each gene. Unfortunately, a putative zebrafish homolog to mammalian *scn8a* was the only sodium channel sequence available in GenBank (NM_131628) at the outset of this work (225). Therefore we sought to ascertain the complete sequences of additional zebrafish sodium channel genes. Initially, we cloned a brain-type Na_v1 sodium channel gene that appeared to be a putative homolog to *zscn2a* (see Methods). During our efforts to clone additional genes, 2 new zebrafish Na_v1 sequences appeared in public databases. These genes encoded putative homologs of the skeletal muscle-type mammalian sodium channel gene *scn4a* (231). The collection of our zebrafish clones (*zscn5a*, *zscn2a*) and publicly available sequences (*zscn8a*, *zscn4aa*, *zscn4ab*) thus spanned the 4 phylogenetic groups of related genes proposed in the sodium channel evolutionary literature (97;98;180): (group 1: *scn5a/10a/11a* – heart/DRG – HOXA; group 2: brain – *scn8a* – HOXB; group 3: skeletal muscle – *scn4a* – HOXC; group 4: brain – *scn1a/2a/3a/7a/9a* – HOXD). We therefore reasoned that these five sequences would be sufficient to reconstruct the phylogeny of zebrafish sodium

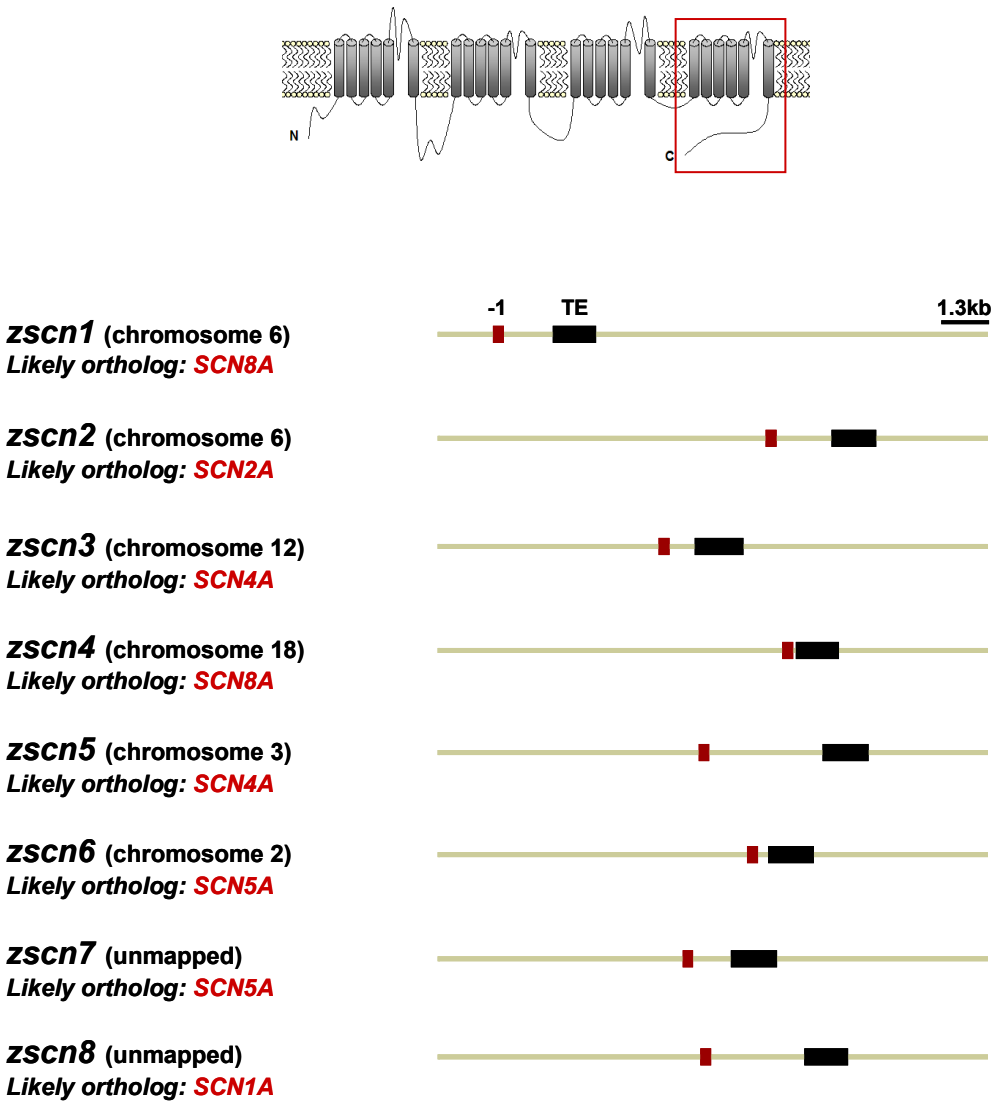

Figure 2.15: *In silico* zebrafish Na_v1 "sequence tags." A bioinformatics strategy using 3' exons (TE, TE-1) of mammalian sodium channel genes that encode all of domain IV identified 8 conserved and non-redundant zebrafish Na_v1 genes in updated versions of the zebrafish genome (Zv4, Zv5). Putative gene identities were assigned based on phylogenetic relationships (Figure 2-16) and alignment with the nucleotide and amino acid sequences of human sodium channel genes. The identified sequences constituted putative *in silico* sodium channel "sequence tags." Chromosome assignment was based on the reported map positions of the relevant contigs within the draft zebrafish genome sequence. Updated map positions are displayed in Figure 2-17. For simplicity, *zscn7* above = the previous *zscn7*.

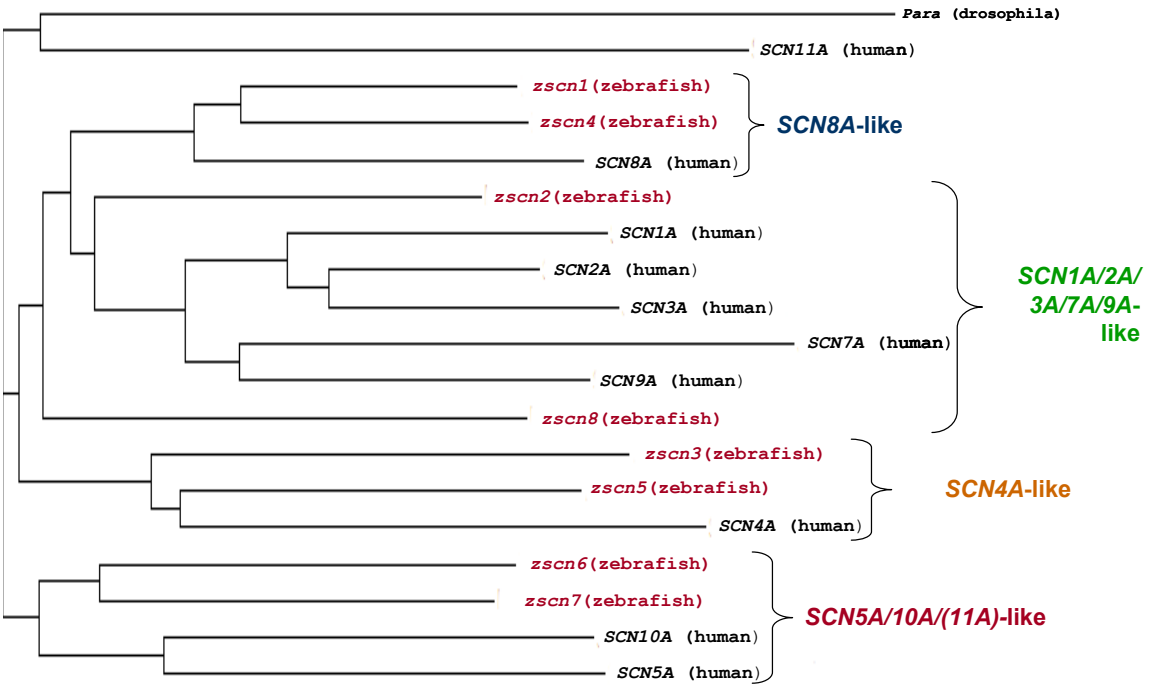

Figure 2.16: Evolutionary relationships of zebrafish Na_v1 sequence tags (TE, TE-1) with human Na_v1 genes. Neighbor-joining phylogenetic tree based on the alignment of zebrafish sequence tags (TE, TE-1) with relevant regions of mammalian sodium channel genes. The *Para* sodium channel gene sequence from *Drosophila* was included as an outgroup. Interestingly, the 3' sequence of the human sodium channel *SCN11A* also aligns as an outgroup, indicating significant divergence from other human sodium channels in regions encoding DIV. Zebrafish Na_v1 channel sequences are marked in **red**.

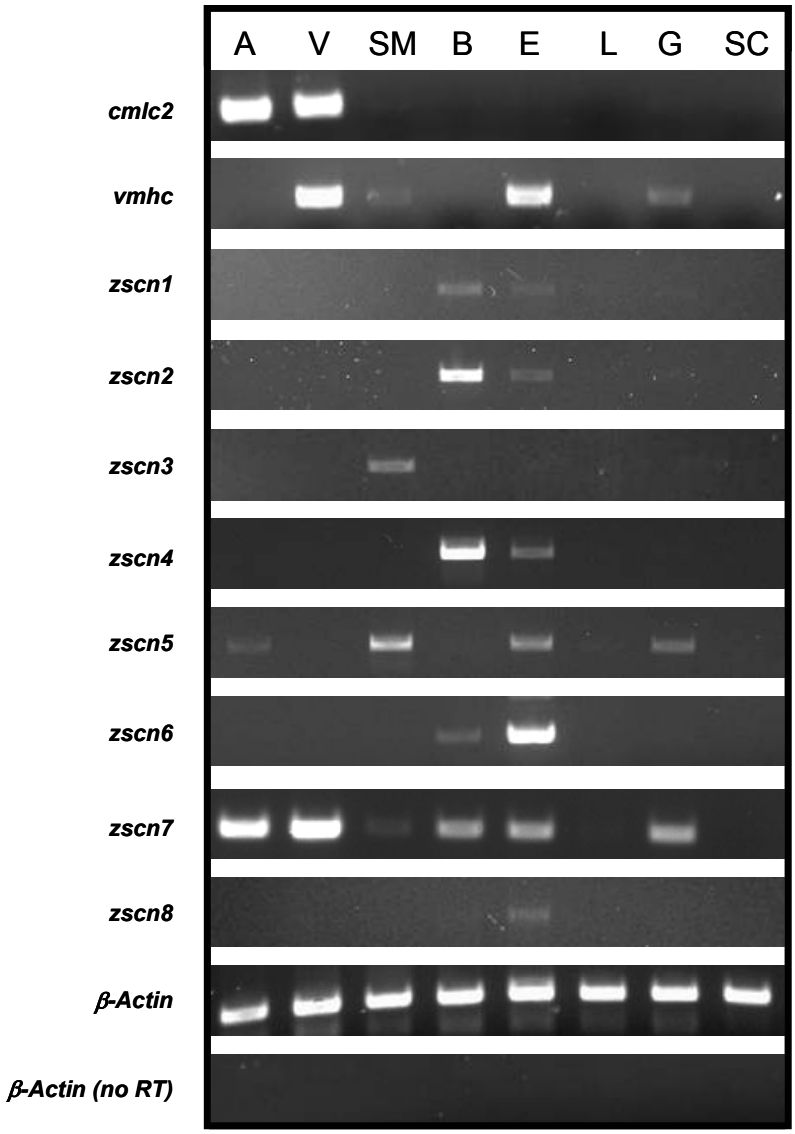

Figure 2.17: Primers directed against *in silico* predicted Na_v1 sequence tags amplify actual sodium channel genes from total RNA. Putative *in silico* sodium channel sequence tags were used to design forward and reverse primers in flanking exons (TE and TE-1) for RT-PCR. Primers directed against all 8 putative Na_v1 sodium channel genes successfully and specifically amplified their targets, as confirmed by direct sequencing. Total RNA was isolated from the following adult zebrafish tissues: A = atrium; V = ventricle; SM = skeletal muscle; B = brain; E = eye and optic nerve; L = liver; G = gill; SC = spinal cord. Despite two putative *scn5a*-like genes in the zebrafish genome, only one Na_v1 gene is highly-expressed in the adult zebrafish atrium and ventricle (z*scn7*). Expression of *zscn5* was also detected in the atrium, but at very low levels.

channels, even without full-length sequences for the remaining 3 (and possibly other) sodium channel genes.

Incorporation of multiple full-length zebrafish sodium channel amino acid sequences in neighbor-joining (distance matrix) phylogenetic model clarified relationships between zebrafish and mammalian channels (Figure 2.18). Moreover, our results supported the model proposed by Lopreato et al., which was based on the analysis of partial sodium channel sequences (encoding domains II and III) from the teleost *Sternopygus macrurus* (180). With the exception of *zscn5a*, all cloned zebrafish channels clearly aligned with mammalian channels on one of 4 branches representing the ancestral vertebrate phylogenetic groups. Although the precise position of zNa_v1.5 (arrow) was somewhat unresolved in our model (suggesting greater evolutionary divergence for the gene encoding this channel than for other isoforms), our analysis provided an initial basis for understanding the evolution of Na_v1 sodium channels in zebrafish. For clarity, human sodium channel sequences were color coded in figure 2.18 both according to their linkage to a particular HOX gene cluster and by their location in the genome.

A comprehensive evolutionary model for vertebrate Na_v1 genes

Many of our preliminary assessments regarding the total number and putative identities of zebrafish Na_v1 channel genes (including 2 *scn5a*-like genes) were confirmed by a recent publication from another laboratory (230). The use of parsimony and likehood methods to reconstruct the phylogeny of cloned vertebrate Na_v1 channel genes, the mapping of each zebrafish sodium channel gene isoform on radiation hybrid panels, and the detailed analysis of synteny of zebrafish Na_v1 channel genes with HOX gene clusters together revealed that different evolutionary mechanisms are likely to have contributed to the evolution of voltage-gated sodium channel genes in mammals and in fish (230). Figure 2.19 displays the location of Na_v1 sodium channel genes relative to HOX gene clusters in human and zebrafish genomes (a second HOXD cluster has been lost in zebrafish), as determined by BLAST searches of mapped contigs and information obtained from published reports (180;227;228;230). As illustrated in figure 2.20, current evidence suggests that the duplication of Na_v1 genes in fish and mammals occurred

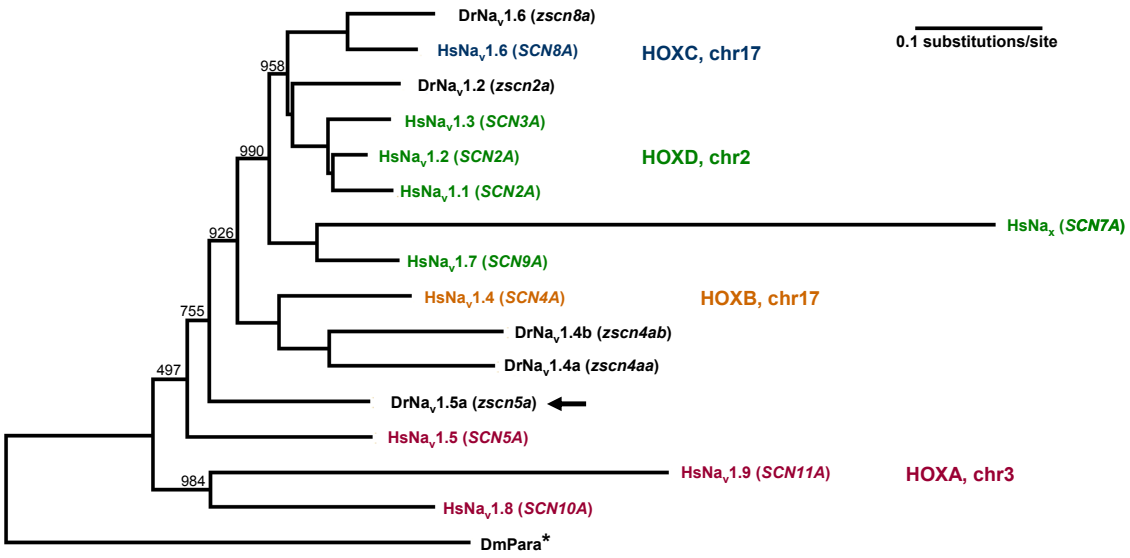

Figure 2.18: Evolutionary relationships of full-length human and zebrafish Na$_v$1 channel amino acid sequences. Incorporation of multiple full-length zebrafish sodium channel amino acid sequences in neighbor-joining phylogenetic model clarified the evolutionary relationships of vertebrate channels and supports the model proposed by Lopreato et al., which used partial sodium channel sequences (representing Domains II and III) from *Sternopygus macrurus*. The phylogenetic position of DrNa$_v$1.5 (arrow) is unresolved, suggesting evolutionary divergence. Dr = *Danio rerio*; Hs = *Homo sapiens*; Dm = *Drosophila melanogaster*; Bootstrapping values (n=1000) for this tree have been included at key nodes; human sodium channel sequences are color coded by their linkage to one of four HOX gene clusters and by their location in the genome; * = *Drosophila* outgroup sequence.

independently. While expansion of the Na_v1 gene family in mammals appears to have occurred by tandem duplication of 4 ancestral vertebrate sodium channel genes, the Na_v1 gene family in fish likely resulted from a whole-genome polyploidization event specific to the teleost lineage that also produced additional HOX gene clusters (97;180;227;228;230).

Consideration of the second scn5a-like gene in zebrafish

To be consistent with this recent literature, we have adopted the nomenclature *scn5Laa* and *scn5Lab* (*SCN5A*-like gene isoforms A and B) and $zNa_v1.5a$ and $zNa_v1.5b$ to describe the genes *zscn6* and *zscn7* and the channels they encode, respectively. Despite our inability to detect expression of *scn5Laa* in mature heart tissue, one recent study reported the amplification of *scn5Laa* transcripts from the developing myocardium (229). We confirmed these findings by designing primers specifically directed against this isoform and used RT-PCR to amplify this gene from and day 2 and 3 embryonic heart total RNA template (data not shown). Moreover, we have independently determined the sequence of *scn5Laa* and have recently initiated efforts to clone and assemble this gene in a full-length vector for heterologous expression (see Chapter 5, Future Directions). Our preliminary sequence analysis suggests that *scn5Laa* encodes a typical voltage gated sodium channel of 1932 amino acids. Zebrafish $Na_v1.5a$ displays 76.1% identity and 82.8% similarity with its counterpart $Na_v1.5b$, and 62.2% identity and 70.5% similarity with human $Na_v1.5$. These data suggest that both *scn5a*-like genes in zebrafish have similarly diverged in sequence from their mammalian counterparts, each displaying approximately 60% amino acid identity to mammalian $Na_v1.5$. However, the divergence between zebrafish $Na_v1.5a$ and $Na_v1.5b$ is far less than that observed among mammalian $Na_v1.5$, $Na_v1.8$, and $Na_v1.9$, suggesting that the duplicate genes in zebrafish may encode channels with similar functions. Notably, zebrafish $Na_v1.5a$ and $Na_v1.5b$ both display significant conservation of residues in important functional domains including the transmembrane segments, voltage-sensors, pore loops, inactivation gate, and C-terminus.

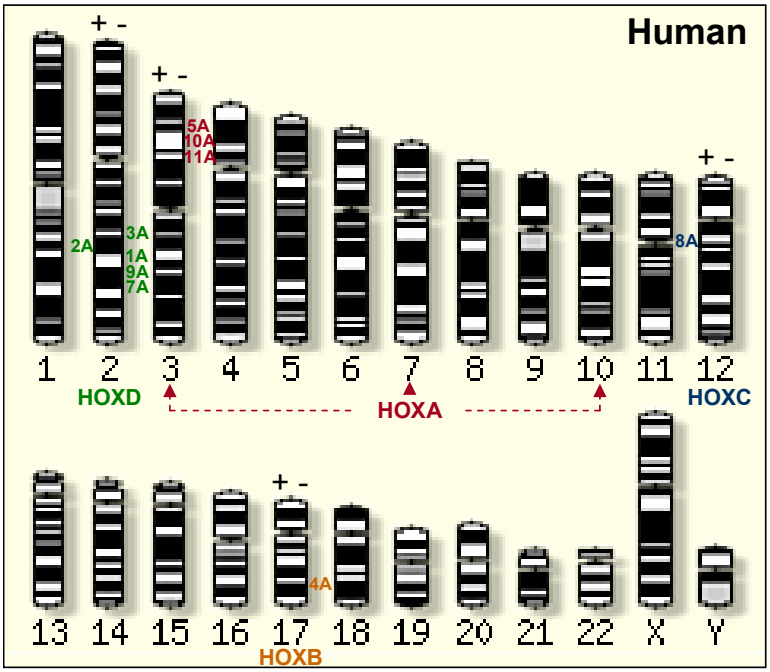

Chromosome 2 (2q24)

SCN1A
SCN2A
SCN3A **HOXD**
SCN7A
SCN9A

Chromosome 3 (3p22)

SCN5A
SCN10A **HOXA**
SCN11A

Chromosome 12 (12q12)

SCN8A **HOXC**

Chromosome 17 (17q23)

SCN4A **HOXB**

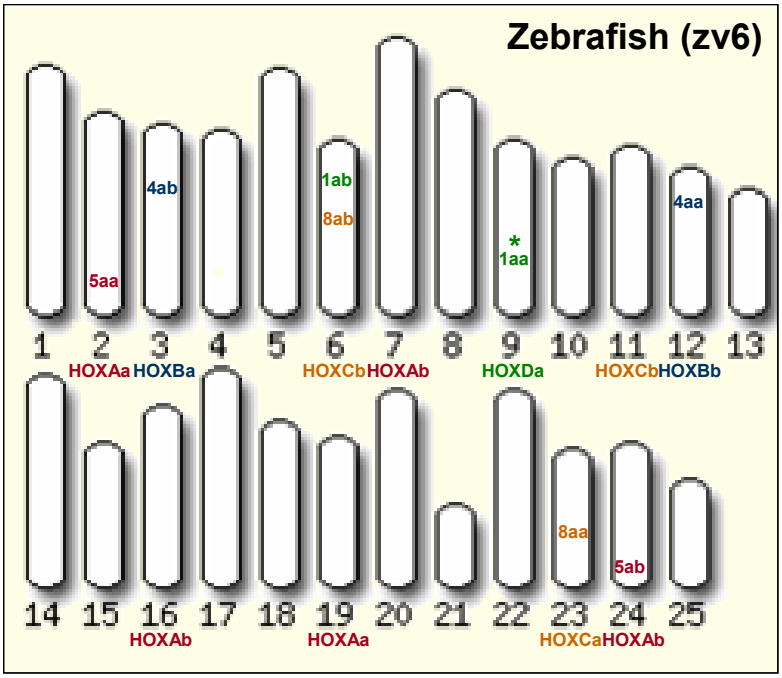

Chromosome 2

scn5Laa **HOXAa**

Chromosome 3

scn4ab **HOXBa**

Chromosome 6

scn8ab **HOXCb**
scn1Lab **~~(HOXDb)~~**

Chromosome 9

*scn1Laa** **HOXDa**

Chromosome 12

scn4aa **HOXBb**

Chromosome 23

scn8aa **HOXCa**

Chromosome 24

scn5Lab **HOXAb**

Figure 2.19: Location of Na_v1 sodium channel genes in the human and zebrafish genomes, as determined by BLAST searches of mapped contigs. Chromosome images adapted from ensembl genome browsers (www.ensembl.org). * indicates location on an unmapped contig; position recently revealed by radiation hybrid mapping (AE Novak, et al., 2006).

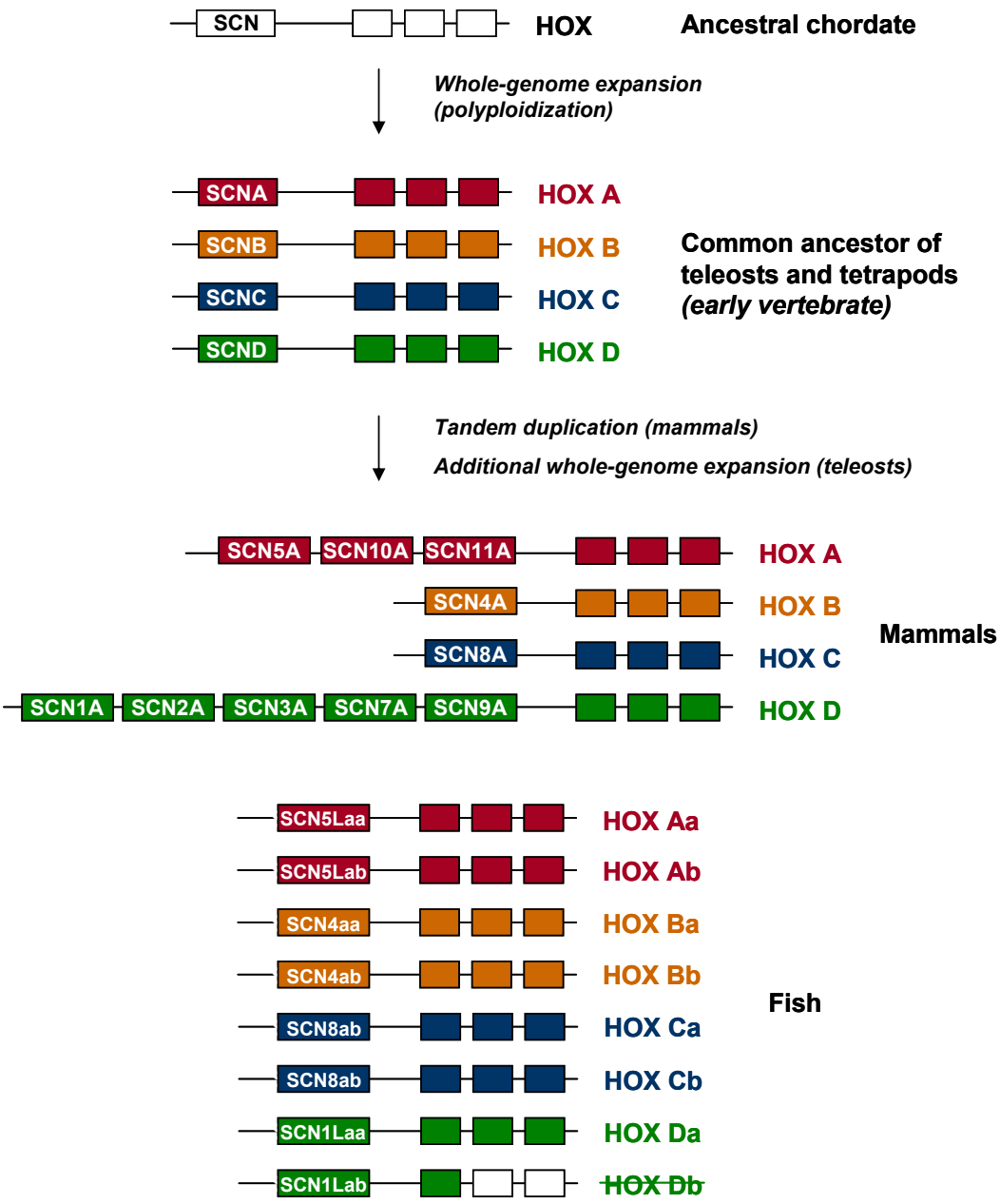

Figure 2.20: Model for the evolution of Na_v1 sodium channel genes in mammals and zebrafish. The family of Na_v1 channel genes in mammals and zebrafish has evolved by different mechanisms. Analyses by Plummer and Meisler (1999), Piontkivska and Hughes (2003), and Lopreato et al. (2001) suggested that all vertebrate sodium channels are derived from 4 ancestral vertebrate Na_v1 genes and that expansion of this gene family in mammals to 10 genes occurred by tandem duplication. Novak et al. (2006) demonstrated that expansion of the Na_v1 family in teleosts to 8 genes likely occurred as part of an additional whole-genome polyploidization event.

Discussion

Deciphering the evolutionary history of Na_v1 sodium channel genes in vertebrates may provide important clues to the function of these proteins in excitable tissues. Tetrapod and teleost genomes both contain multiple, homologous Na_v1 sodium channel genes, with 10 isoforms in mammals and 8 isoforms in fish (230). Despite the similarity in sodium channel function observed among different isoforms, the retention of multiple sodium channel genes in both vertebrate lineages supports the concept that having multiple sodium channel isoforms is an evolutionary advantage. In the context of vertebrate evolution, which has been characterized by increasing structural and functional complexity in the nervous system and other excitable tissues, the availability of multiple sodium channel genes may have provided an important template for the specialization of proteins that regulate membrane excitability (4). Although it has been suggested that the retention of multiple sodium channel isoforms may simply have resulted from the partitioning of these genes into various excitable tissues, the simultaneous expression of different sodium channel genes in single cells may be evidence that even homologous sodium channel proteins play distinct and non-redundant roles that are important for cellular function (4;100;161;247). Moreover, one sodium channel gene in (*SCN7A* in humans, *scn6a* in mice) appears to encode a channel (Na_x) that has evolved entirely new functions in regulating salt homeostasis (83). The gene encoding this channel displays significant divergence in key regions of sodium channel function and has never been shown to act as a voltage-gated sodium channel *in vitro* (206).

The zebrafish genome contains two genes, *zscn5Laa* and *zscn5Lab*, that are evolutionarily related to the HOXA cluster of genes on human chromosome 3 that includes *SCN5A*, *SCN10A*, and *SCN11A* (230). At the protein level, they are approximately 75% identical in sequence. We detected mRNA expression of both *scn5a*-like genes in the central nervous system, one of these genes in the adult atrium and ventricle (*zscn5Lab*), and both genes in the day 3 embryonic heart by RT-PCR (figures 2.8, 2.17, and data not shown). By *in situ* hybridization, both genes are only weakly expressed in the developing zebrafish embryo (229). While expression of *zscn5Laa* was detected diffusely in the brain, *zscn5Lab* expression was

detected in somites, spinal cord and lateral line (229). Expression of neither gene was detected in the embryonic heart by *in situ* hybridization; however, both transcripts were detected in the developing heart by RT-PCR (229).

Our findings regarding the sequence and expression of zebrafish *scn5a*-like genes are consistent with what is known about HOXA-linked Na_v1 channel genes mammals. Although suspected to be derived from a single ancestral vertebrate sodium channel gene, *scn5a*, *scn10a* and *scn11a* display significant differences in sequence and in expression. By direct sequence alignment, for example, we determined that human $Na_v1.5$ shares only 60% identity with $Na_v1.8$ and 47% identity with $Na_v1.9$, whereas $Na_v1.8$ and $Na_v1.9$ share only 48% identity with each other. As in zebrafish, mammalian *scn5a-like* genes are expressed in primarily in the heart and in neurons. While *scn5a* is the primary sodium channel isoform of cardiac muscle, expression of this gene has also been detected in neurons of the peripheral and central nervous systems and in intestinal smooth muscle (248-253). *Scn10a* is selectively expressed in sensory fibers of the peripheral nervous system, particularly in dorsal route ganglia (DRG) (87;211;212). While the gene *scn11a* shares a similar expression pattern with *scn10a* in rats, transcripts of this gene are detectable across the central nervous system in humans (213;214;254).

The expression of both zebrafish *scn5a*-like genes in cardiac tissue suggests that $Na_v1.5$-like sodium channels have played a conserved role in cardiac excitation at least since the split of tetrapods and teleosts over 400 million years ago. The expression of *scn5a*, *scn10a*, *scn11a*, *scn5Laa* and *scn5Lab* in the nervous system indicates, however, that the ancestral vertebrate *scn5a*-like gene may have also played an important role in neuronal excitability. We thus propose that the divergence of vertebrate *scn5a*-like genes following duplication reflects a partitioning of the role of the ancestral vertebrate gene (*subfunctionalization*), rather than the evolution of completely novel function (*neofunctionalization*). However, these processes are not likely to be mutually exclusive, particularly over long periods of evolutionary time. $Na_v1.8$, for example, was recently found to have evolved certain unique biophysical properties that allow it signal during cold temperatures (88). While homology and expression are thus reasonable starting points to estimate the potential functions of $Na_v1.5a$ (*zscn5Laa*) and $Na_v1.5b$ (*zscn5Lab*)

in zebrafish, loss of function studies are required to accurately delineate their roles *in vivo*. These studies are described in Chapter 3.

Table 2.1: Primer sets used to amplify *zscn5a* (*scn5Lab*) in 6 overlapping sections.

Section	Nest*	Forward (5'-3')	Reverse (5'-3')	Length (bp)
A	Outer	CGAAGTTTCACATCTGTGAA	GATGAAAGTGCTGTTGTTGT	950
A	Inner	TCGGACAGAGGCTCAGGATG	TGTCGGTAAGGTGGTGTTGA	901
B	Outer	AGTACACTTTCACTGGCATT	AGAAGAACTGTGAGCTGTGG	1269
B	Inner	TACACGTTCGAGTCGCTGAT	TCTGAGCACTGGTGCGTCTG	1219
C	Outer	AGACAAACCGGCCAAACTGG	ATCACGCCGGCTGTCCCATT	1557
C	Inner	ACCCCATAGAGGGCATTAAGCAA	CGCTTCAGTTTCAGCATGGC	1486
D	Outer	CATGTGGGATTGTATGGAAG	ATAGATGAAACCCGTCCGGT	1264
D	Inner	ACAGCCGCTCTGCATCCTGGTGTT	CGGCCGAACTTTCCAGCGAA	1209
E	Outer	CTTCATTCTGGAGATGAGCT	ATCATCAATGCAAACAGGAG	1200
E	Inner	AAGTGGATCGCCTACGGTTT	CGGATCACGCGGAAGAGAGT	1100
F	Outer	AGAGCAGAAGAAATATTACAACGC	AACACGTTTCCTCAAGAGAA	1469
F	Inner	CATGAAGAAACTGGGCTCCA	CGTCACAGAAAAGTTTCGCT	1377

*Although nesting was not frequently necessary, primers were initially designed for this purpose.

Table 2.2: Primer sets* used to identify all non-redundant zebrafish Na_v1 sodium channel genes.

Gene	Set	Forward (5'-3')	Reverse (5'-3')	Length (bp)
zscn1	1	GAGACAGAGAACATCTTGTATTGG	AGTTTGTTGTTGGCAGGCCT	1133
zscn1	2	TCAGACGAGACAGAGAACAT	TTAACTGTGGTTCCTGGGTT	560
zscn1	3, nest†	AAACTTCGTATTCATCGTGGCC	GTTTGCAGATGAAGCCCCTG	1085
zscn2	1	GACAGAGGATATGGACAATA	CCTTCTTAACTGTTTGTCTT	1118
zscn2	2	GACAGAGGATATGGACAATA	AATCTGGATCTTGCTTGTTC	527
zscn3	1	AGTGCTGAGAAAGAATATGTC	TTGAGAAGATGCCTACGGTA	1100
zscn3	2	AGTGCTGAGAAAGAATATGTC	GAGGGCCACTGTTTAGAATA	520
zscn4	1	CAATCACAGGAGACGGAAAA	ATGAAGCCTTTCCGAATCAG	1112
zscn4	2	ATCACAGGAGACGGAAAACA	GGATTTTCTTTAGTTGGCTC	546
zscn5	1	TGCTGAGATAGAGGAAATATTG	CTTCTCCGGTTGGTTTCTTT	1163
zscn5	2	AAGTGCTGAGATAGAGGAAA	GTAGTTGAACCTGGGTTATC	558
zscn6	1	AATCTGCTCGCATGGAGACC	CCAGGGCGTCTCTTGGTTAA	1160
zscn6	2	ATCCTCAATAACATCAACTTGG	CCACAGTTGCCCTTAGTATT	505
zscn7	1	CGCCCTCCATCAAACACATC	TTTATCAGCGTCCGGCATGG	1160
zscn7	2	GCCCTCCATCAAACACATCC	GCCAGTGTGGGGAATTTCGG	550
zscn8	1	ATTGAAATGACCCGTGCGCT	CCCATTCTGATGCTTGTTTT	1152
zscn8	2	GATTGAAATGACCCGTGCGC	GCCTACGACCGAACTTCCAG	565
zscn8	3, nest†	GTACTGGATCAATGTCATTTTC	TGCGAACTTTCTTCATGCTA	1100

***** To control for amplification of contaminating genomic DNA, all forward and reverse primers are located in different exons (terminal exon and terminal exon -1).

† As indicated for *zscn1* and *zscn8*, additional nested primers were designed to facilitate subcloning because of low gene expression levels and/or low PCR amplification efficiency. For other genes, the following nested primer combinations were used as necessary: *zscn2* (1F/1R>2F/2R); *zscn3* (1F/1R>2F/2R); *zscn4* (1F/1R>2F/2R); *zscn5* (1F/1R>2F/1R); *zscn6* (1F/1R>2F/2R); *zscn7* (1F/1R>2F/2R).

Table 2.3: Biophysical properties of $zNa_v1.5b$ in CHO cells.

	Steady-state activation		Steady-state inactivation		Recovery from inactivation		
	$V_{1/2,}$ mV	*N*	$V_{1/2,}$ mV	*N*	τ_1, ms (%)	τ_2, ms (%)	*N*
$zNa_v1.5b$	-42.2±1.1	18	-85.3±0.8	10	9.1±1.4 (96.2±1.2)	144.8±15.1 (3.8±1.1)	8

Values are shown as mean ± s.e.m.

CHAPTER III

VOLTAGE-GATED SODIUM CHANNELS REGULATE CARDIAC CELL FATE SPECIFICATION VIA A NOVEL, NON-ELECTROGENIC MECHANISM IN ZEBRAFISH

Overview

In prior work, we identified two *scn5a*-like genes in zebrafish, *scn5Laa* and *scn5Lab*, encoding the putative sodium channels zNa_v1.5a and zNa_v1.5b. Transcripts of both genes were detected in the embryonic zebrafish heart. To determine the roles of *scn5Laa* and *scn5Lab* in regulating embryonic zebrafish heart rhythm, we knocked-down their expression using morpholino antisense oligonucleotides. Unexpectedly, reduced expression of either of these genes resulted not only in defects of cardiac function but of cardiac morphogenesis. By confocal imaging of transgenic zebrafish expressing fluorescent proteins in the embryonic heart, we developed methods for quantifying total embryonic heart cell number and discovered a significant reduction in the number of nascent cardiomyocytes in morphant versus wild type embryos. In studying the mechanisms underlying these defects, we found that reduced sodium channel expression disrupted early signaling events in pre-cardiac mesoderm that are required for production of normal numbers of cardiac progenitor cells. Although sodium channels have not previously been implicated to function in undifferentiated tissues, one obvious possibility raised by these findings was that membrane depolarization is required in the gastrulating zebrafish embryo to establish the cardiac cell fate. However, a series of additional studies led us to conclude that channel-mediated electrical activity plays no role in the observed developmental defects. The results of our studies in zebrafish embryos thus suggest that cardiac-type sodium channels have evolved two mechanistically-distinct roles in vertebrates: 1. in differentiated cardiomyocytes, sodium channels depolarize the membrane to initiate action potentials; 2. during development, sodium channels act via a novel, non-electrogenic mechanism to regulate cardiogenesis.

Abstract

Voltage-gated sodium channels initiate action potentials and are required for impulse propagation in excitable tissues. While sodium channel-mediated electrical signaling is critical to the normal development of the nervous system, the role of these channels in the genesis and early function of other excitable tissues is not well understood. Here we report that sodium channels are also required for heart development, but via mechanisms that are independent of electrical signaling. Knockdown of cardiac sodium channel expression in embryonic zebrafish resulted in a failure of chamber morphogenesis and looping, prior to any requirement for these channels in myocardial excitation. These abnormalities were associated with a significant deficit in the production of cardiac progenitor cells and a selective loss of expression of the homeodomain transcription factor *nkx2.5* in early bilateral cardiac primordia. Analysis of mosaic embryos demonstrated that sodium channels are required cell-autonomously in mesoderm for cardiac cell fate determination. However, potent modulators of Na+ influx failed to perturb cardiac lineage specification. Our results indicate that voltage-gated sodium channels have evolved two distinct roles in the vertebrate heart: in addition to acting as the principal orchestrators of heart rhythm, they perform a previously-unappreciated, non-electrogenic function in early cardiogenesis. These findings suggest that other vertebrate sodium channel isoforms may also have important roles in development, via mechanisms that are independent of their role in initiating action potentials.

Introduction

In the adult heart, the voltage-gated sodium channel $Na_v1.5$ initiates the cardiac cycle by permitting a rapid influx of Na+ ions across the sarcolemma in response to changes in membrane potential (89). Mutations in the gene encoding $Na_v1.5$ (*SCN5A*) are associated with the long QT Syndrome (255;256) and a range of other heritable arrhythmia syndromes (257). Moreover, drugs that block the cardiac sodium channel have been demonstrated to be arrhythmogenic in human patients (258). The arrhythmogenic substrate associated with $Na_v1.5$ dysfunction has been recapitulated in mouse models as mice heterozygous for *scn5a* deletion (+/-) displayed increases susceptibility to arrhythmias (133). Similarly, mice heterozygous for a gain-of-function mutation that underlies the long QT Syndrome displayed prolonged action potentials and spontaneous polymorphic ventricular tachycardia (132).

Although coordinated electrical activity is apparent soon after the fusion of cardiac primoridia at the midline in the beating heart tube, evidence from mice, birds, and fish suggest that important electrophysiological changes accompany the dramatic morphological transformation of this tube-like structure to a multi-chambered, looped organ. The genetic and molecular mechanisms that govern excitability during heart development, and the contribution of heart beating itself to normal development, however, are not well understood. We hypothesized that voltage-gated sodium channels, the initiator of action potentials in the mature myocardium, would also have critical roles in regulating the rhythm of developing heart. We first determined whether *scn5a* is expressed in the developing mouse heart. For the ease of access to the embryonic heart at early stages of development, we then used zebrafish embryos to create loss of function models for cardiac sodium channels.

Methods

Zebrafish strains

The zebrafish strains used in this study were raised according to standard procedures. The c*mlc2:eGFP* and *cmlc2*:*dsRed-nuclear* transgenic lines have been described (259;260).

In situ hybridization

In situ hybridization was performed on mouse embryos sectioned at 5μm using P^{33}-labeled antisense and sense probes directed against regions of *scn5a* that have diverged from other sodium channel isoforms. Slides were processed with silver grain emulsion and visualized with dark-field microscopy. For zebrafish, whole embryos at various stages were fixed in 4% paraformaldehyde in PBS overnight at 4ºC. As for mouse *scn5a*, antisense and sense probes were designed against divergent regions of *scn5Laa* and *scn5Lab* transcripts to prevent cross hybridization with other expressed sodium channel genes. *In situ* hybridization was performed under standard conditions using digoxigenin-labeled probes. Antisense probes against the following zebrafish genes were used: *nkx2.5* (NM_131421), *nkx2.7* (NM_131419), *gata4* (NM_131236), *gata5* (NM_131235), *dHand* (NM_131626), *cmlc2* (NM_131692), *vmhc* (AF114427), *amhc* (NM_198823).

Immunohistochemistry

Immunohistochemistry was performed on whole mount zebrafish embryos using the following primary antibodies: S46, MF20 (Developmental Studies Hybridoma Bank, University of Iowa), and monoclonal pan anti-sodium channel, K58/35 clone (Sigma). For S46/MF20 staining, embryos were first fixed for 60 minutes in 1% EM grade formaldehyde in PBS. Embryos were blocked in PBS with 10% (v/v) sheep serum, 2 mg/ml BSA, and 0.2% (w/v) saponin. Primary antibodies were diluted 1:10, and visualized with the appropriate FITC and TRITC-conjugated secondary antibodies (Southern Biotech, 1:100). For sodium channel staining, larve were fixed at room temperature for 30 minutes in freshly-made 4% paraformaldehyde in PBS. Embryos at day

3 and day 6 were permeabilized by washing for 1 hour in PBS with 0.8% Triton X-100 ("PBST"), followed immersion in deionized water for five minutes, immersion in acetone for 7 minutes at -20ºC, and re-immersion in deionized water for an additional five minutes. Embryos were then blocked for at least one hour in 10% goat serum in PBST. Anti-sodium channel primary antibodies were diluted 1:500, and Alexa secondary antibodies (Molecular Probes) were diluted 1:1000. Stained embryos were analyzed with confocal microscopy.

Design and use of antisense-morpholino oligonucleotides

Morpholinos were designed to inhibit translation of mRNAs or perturb splicing of pre-mRNAs. To ensure specificity against specific sodium channel isoforms, all translation blockers were designed using alignments of the identical target regions of all available zebrafish sodium channel sequences. Target specificity was also tested by using putative morpholino sequences in BLAST queries of the zebrafish genome. To identify additional putative target sites for translation inhibiting morpholinos, RNA ligase-mediated rapid amplification of cDNA ends (RLM-RACE) PCR was used to extend 5' untranslated sequence of both *scn5Laa* and *scn5Lab*. For *scn5Laa*, morpholinos with the following sequences targeting the ATG translation initiation site and 5'UTR were used to block translation: *ATG1*: 5'-CCGCTGGTAAGAGCATGGTCGCCAT-3' and *UTR1*: – 5'- CTTTTCATCCTGATCGGCCTGTACT-3.' For *ATG1*, the following 5-mismatch control oligonucleotide was used, where lower case letters represent the substituted nucleotides: 5'-CCcCTGcTAAGAcCATGcTCGCgAT-3'. For *scn5Lab*, the following morpholino was directed against the translation initiation site: *ATG1*: 5'-TGGCTGCCATCTTCTCATCCTGAGC-3'. Optimal splice site targets were identified by examining the pre-mRNA sequence of both *scn5Laa* and *scn5Lab* for exons/introns that were predicted to lead to frameshifts and premature termination of translation if skipped or retained respectively, after splicing. All putative splice-blocking morpholinos were designed by comparing identical intron-exon junction sites between *scn5Laa* and *scn5Lab* to ensure target specificity, when possible. For *scn5Laa*, the following splice site-directed morpholino was used (exon/intron): E3/I3 – 5'-AGGCTGTGGAAGGATATGAATGGAC-3'. A 5-mismatch control morpholino with following sequence was also used: 5'-

AGcCTGTcGAAcGATATcAATGcAC-3'. Splicing of *scn5Lab* was disrupted with the following morpholino oligonucleotide: E24/I24 - 5'-AATTTGTGCTGACCGGTGGTCTGGG -3'; E6/I6- 5'-AGCGGCCTCTCACCTGGGATGACTG-3'. For E6/I6, the following 5-mismatch morpholino was used: 5'-AGCcGCCTgTCAgCTGGcATGAgTG-3'. In all instances where a specific 5-mismatch control morpholino was not mentioned, we used the "standard control" morpholino from Gene Tools. Identical stock and working concentrations of both active and control morpholinos were prepared in Danieu's buffer (58mM NaCl, 0.7mM KCl, 0.4mM $MgSO_4$, 0.6mM $Ca(NO_3)_2$, 5mM HEPES) or water. Solutions were injected into 1-2 cell stage wild type zebrafish embryos at a consistent volume, calculated from the direct measurement of the injectate diameter under a stereomicroscope. To analyze disruptions of splicing, total RNA from morphant, control MO injected, and WT embryos was extracted following phenotyping using the Trizol reagent. 4µg of total RNA was used for first strand cDNA synthesis with the Transcriptor reverse transcriptase enzyme (Roche), and 2µl of cDNA was subsequently used as template for PCR (25µl reaction volume) using Expand Hi-Fidelity polymerase (Roche).

Phenotyping of zebrafish embryos

Morphant embryos were phenotyped at various timepoints after injection as indicated. Heart rate, morphology, and circulation were assessed using a simple dissecting microscope.

Drug and toxin studies

Lidocaine, flecainide, mexiletine, TTX, ATX II, and veratridine were all obtained from Sigma-Aldrich. Nisoldipine was obtained from Bayer. Antiarrhythmic/anesthetic compounds were obtained as salts and were thus directly mixed into embryo medium. To facilitate absorption, the pH of each drug solution was adjusted to values that were above pKA of each compound with 1N NaOH. Control solutions contained no drug but were of the equivalent pH as drug solution. Stock concentrations of toxins were either prepared in water (TTX, ATX II) or ethanol (veratridine) prior to dilution in physiological buffer (Tyrode's). Toxins were pressure injected directly into the yoke sack of early embryos or the trunk circulation or pericardial sack at later stages.

Cell death and proliferation assays

TUNEL staining was performed with the *In Situ* Cell Death Detection KIT, TMR red (Roche), according to the manufacturer's instructions. TUNEL assays were first performed by fixing embryos in 4% paraformaldehyde at 4°C, followed by dehydration in a graded methanol:PBS series (25%:75%, 50%:50%, 75%:25%, 100%:0%) at room temperature. Following dehydration, embryos were incubated in 100% acetone for 10 minutes at -20°C and then washed with PBS. Embryos were then treated with permeabilization solution (0.1% Triton X-100 in 0.1% sodium citrate in 1xPBS) for 15 minutes and washed in PBS. To permit access of the terminal deoxynucleotidyl transferase enzyme (TdT) to the heart, embryos were further treated with 0.25% trypsin-EDTA (Gibco) for 20 minutes before 3 final washes in PBS (5 minutes each). As a negative control, TUNEL staining was performed with all reaction components except for the TdT enzyme. As a positive control, embryos were treated for 15 minutes with 100U/mL DNase I (Promega) in 50mM Tris-HCl, pH7.5, and 1mg/ml BSA, prior to the TUNEL reaction to induce DNA strand breaks. TUNEL-stained embryos were visualized with fluorescence microscopy. *Acridine orange* staining was used to visualize cell death in live embryos. Embryos at the desired stage were incubated for 30 minutes in 10µg/mL acridine orange (Sigma) made from a 100-fold dilution of 1mg/mL stock solution in E3 embryo medium. Acridine orange-labeled embryos were visualized with fluorescence microscopy. Cellular proliferation was assessed by incubating embryos in 10mM BrdU in 15% DMSO/embryo medium on ice for 20 minutes, followed by incubation in BrDU solution at 28.5ºC until the desired age. BrDU labeling was visualized with anti-BrDU antibody (Roche).

Real-time PCR

Transcript levels of *nkx2.5* (NM_131421), *gata4* (NM_131236), *gata5* (NM_131235), and *dHand* (NM_131626) were measured using SYBR green dye (Applied Biosystems). Data were collected on an ABI 7900HT real-time PCR instrument, quantified by the standard curve method, and normalized to zebrafish β-actin levels. No RT and water templates (performed in duplicate) did not yield signal. When possible, real-time PCR primers spanned introns, amplified single

bands by standard RT-PCR, and did not form primer dimers as analyzed by the first derivative of the product melting curve. Standard curves were generated from dilutions of plasmids containing each of the respective targets.

Quantification of cardiomyocyte size and number

For measurement of cell size, *cmlc2:GFP* transgenic embryos were gently flat-mounted between two coverslips. Z-stack images captured for ascertainment of cell number used the same sample preparation. Total embryonic heart cell number was subsequently determined using *cmlc2:dsRED-nuclear* transgenic embryos that were positioned ventral side in a special viewing chamber, stabilized with 1% low melt agarose. Confocal images were captured using a Zeiss LSM 510 Confocal Microscope System equipped with either 40x or 20x objective lenses. Three dimensional projections were constructed using the LSM Browser software (Zeiss), and image analysis was performed using Image J. Cell size was measured as the surface area surrounded by visible cell boundaries. Total embryonic cell number was quantitated using the Pointpicker function of Image J, which permits a single user-defined mark to appear through multiple images in a z-stack. This allowed the tracking of a single cell in subsequent z sections without double counting.

Transplantation

Uninjected or morpholino-injected donor *cmlc2*:*GFP* embryos were labeled by co-injection of 5% tetramethyl rhodamine dextran (MW 10,000, Molecular Probes) in 0.2M KCl and transplanted into uninjected *cmlc2*:*GFP* embryos. Transplantation was performed on blastula stage embryos (oblong) at approximately 4hpf. Mosaic embryos were created by removing a total of 50-75 cells from the margin of each donor embryo and transplanting them to the margin of a wild type host embryo of the equivalent stage. Host embryos were reared in darkness at 28.5º in Danieu buffer supplemented with penicillin/streptomycin. Surviving embryos were examined for rhodamine-labeled beating cells within the green transgenic hearts at days 2 and 3 using both fluorescence and confocal microscopy.

Action potential recordings

The intact, beating heart was exposed in 1 year old TuAB strain zebrafish anesthetized on ice and fixed into a tissue chamber perfused with 95% O_2/5% CO_2 and Tyrode's solution (120mM NaCl, 4mM KCl, 1.8mM $CaCl_2$, 1mM $MgCl_2$, 20mM $NaHCO_3$, 1.2mM NaH_2PO_4, 10mM glucose, 5mM sucrose, pH 7.35 with NaOH) warmed to 37 degrees C. Action potentials were recorded from ventricular muscle using a conventional 3M KCl-filling microelectrode technique. Data were acquired using AcqKnowledge 3.7.3 software (Biopac System, Santa Barbara, CA). Ventricular action potentials were recorded prior to and after perfusion with 50nM TTX prepared in Tyrode's solution.

Transient transfection and electrophysiology

Cultured Chinese Hamster Ovary (CHO) cells were transiently transfected with the pBK-CMV-*zscn5a* construct using FuGENE6 (Roche). Cells were grown for 48 hours after transfection prior to electrophysiology. Whole-cell voltage clamp was performed at room temperature with 2MΩ patch microelectrodes and an Axopatch 200A amplifier. To minimize the capacitive transients, we compensated for approximately 70% to 80% of the cell capacitance and series resistance (233). Cells exhibiting very large currents (>6 nA) were also excluded from further analysis. Cells were also excluded if voltage control was compromised. The extracellular bath solution contained (in mmol/L) NaCl 145, KCl 4.0, $MgCl_2$ 1.0, $CaCl_2$ 1.8, glucose 10, and HEPES 10; the pH was 7.4, adjusted with NaOH. The pipette (intracellular) solution contained (in mmol/L) NaF 10, CsF 110, CsCl 20, EGTA 10, and HEPES 10; the pH was 7.4, adjusted with CsOH. Cells were held at -120 mV, and activating currents were elicited with depolarizing pulses from -100 to +50 mV in 10 mV increments. Specific clamp protocols are indicated with the data. Data were acquired by pClamp8.0 (Axon Instruments Inc), sampled at 50 kHz, and low-pass filtered at 5 kHz. All currents were normalized to the cell capacitance calculated by Membrane Test (OUT O) in pClamp8.0.

Data Analysis

Continuous variables are expressed as means ± SEM and categorical variables are expressed as numbers and percentages. The Student's unpaired *t*-test was used for statistical analysis, when appropriate. $P<0.05$ was considered statistically significant.

Results

Developmental expression of murine scn5a

In mice, differentiating cardiac progenitors from the cardiac crescent fuse at the midline to form a beating heart tube on E8, followed by looping and chamber morphogenesis on E9. To determine whether *scn5a* is expressed during these early stages of development in mammals, we isolated total RNA from mouse embryos starting at E7.5 and embryonic hearts starting at E9.5 to assay for expression of *scn5a* transcripts. Using isoform-specific primers, *scn5a* expression was detected starting at E8.5 in total embryo template and at E9.5 in heart template, suggesting a potential role in the developing heart (Figure 3.1). To resolve the early expression pattern of *scn5a* spatially, we raised two different P^{33}-labeled antisense and sense (control) probes directed against divergent regions of the murine *scn5a* mRNA for section *in situ* hybridization (Figure 3.2). At E9.5 and E10.5, both antisense probes detected expression of *scn5a* transcripts primarily in the developing heart and somites, with weaker expression detected in the forebrain and developing olfactory apparatus (Figure 3.3). In the heart, *scn5a* expression was observed in both the developing myocardium of the common atrial and ventricular chambers, but was absent from the endocardium and the endocardial cushions (Figure 3.3). Sense control probes did not result in specific signals from any of these tissues. These data demonstrate that *scn5a* is expressed during early development of the mammalian heart.

Developmental expression of zebrafish scn5Laa and scn5Lab

We applied similar strategies to assess the expression of *scn5Laa* and *scn5Lab* in zebrafish embryos. In zebrafish, the elongating heart tube commences beating between 22 and 24 hours post fertilization (hpf), and begins to elaborate morphologically distinct atrial and ventricular chambers between 32 and 36hpf coincident with the initiation of looping. During this time period, the initial peristaltic-like activity of the heart tube develops into a more mature pattern of activation with different regions of the heart displaying distinctive patterns of impulse propagation: between 36 and 48hpf, impulses begin to conduct rapidly through the atrial

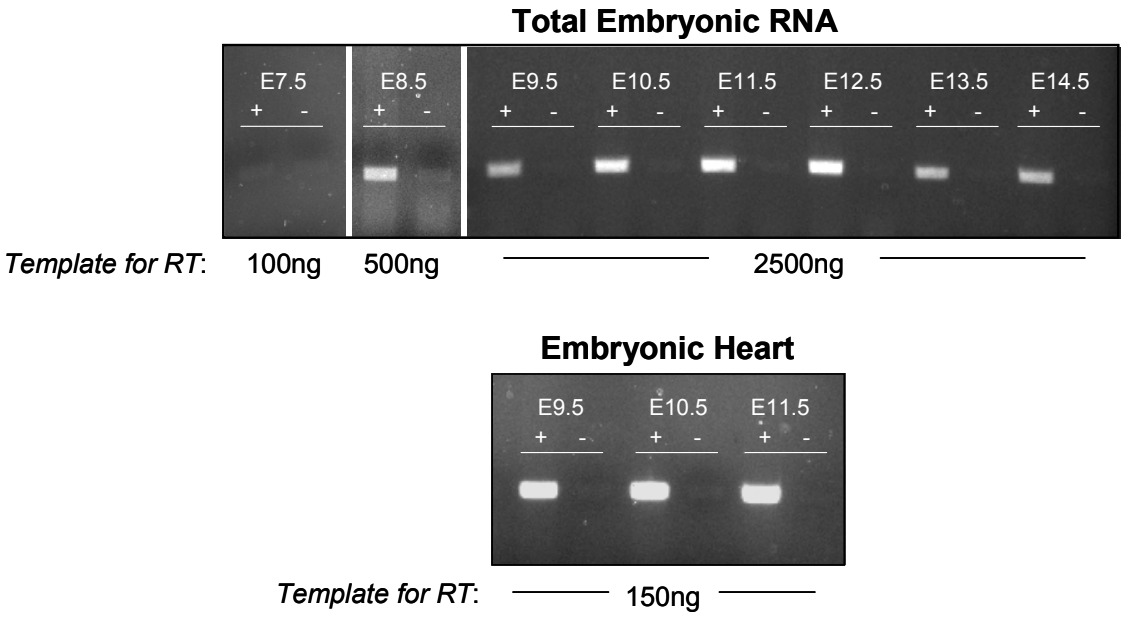

Figure 3.1: Temporal assessment of *scn5a* expression in the developing mouse embryo. Total RNA was isolated from the entire embryo (top) or the embryonic heart (bottom) at different stages of development. The amount of template used for the RT reaction is indicated below each stage. *Scn5a* expression begins between E7.5 and E8.5 where E = embryonic day.

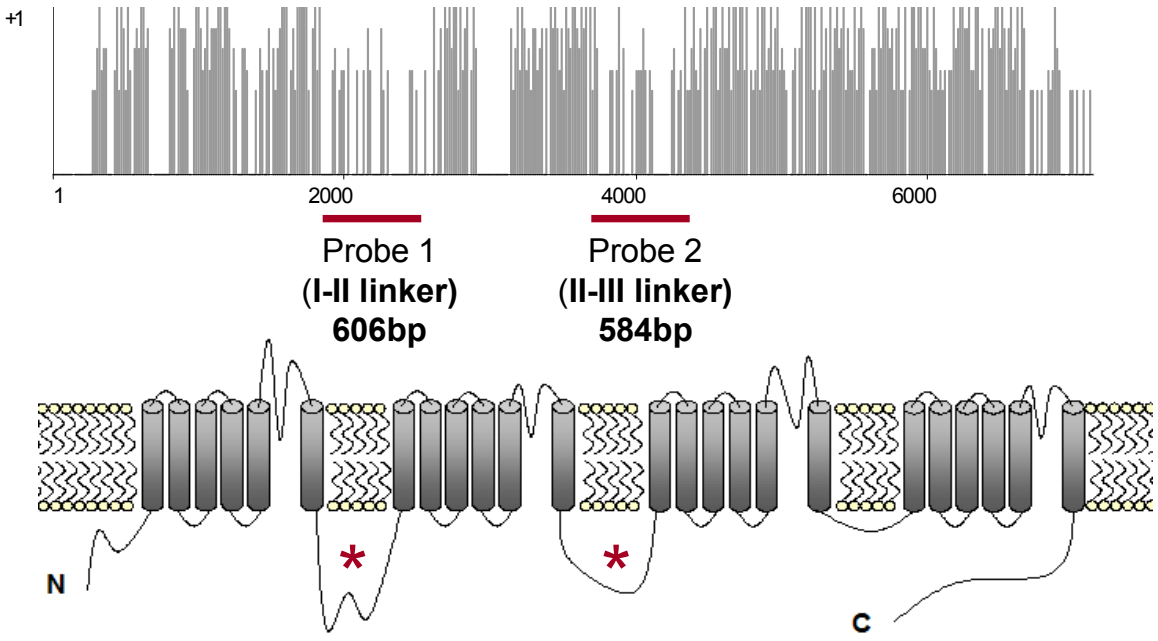

Figure 3.2: Description of probes used for isotopic *in situ* hybridization in mice. (Top) Similarity plot based on alignment of cDNAs of murine voltage-gated sodium channel isoforms (*scn5a* vs. 7 other murine sodium channels). Areas of lowest inter-isoform homology occur at the domain I-II and domain II-III linkers, as indicated by **red asterisks** on the diagram of the predicted channel secondary structure (bottom).

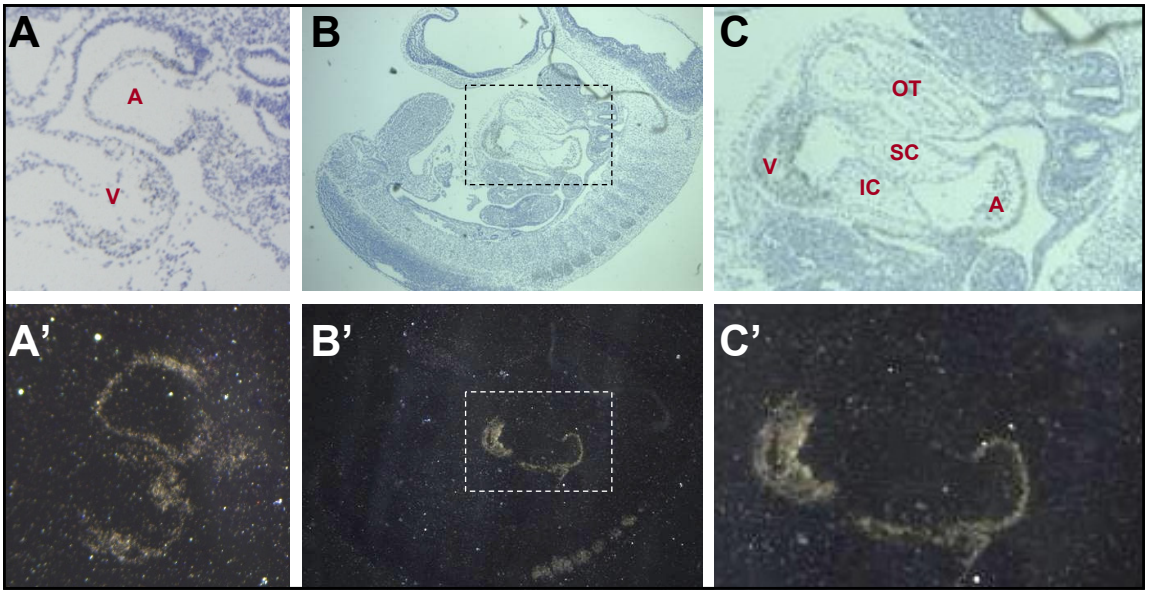

Figure 3.3: Murine section in situ hybridization at E9.5 and E10.5. Representative brightfield (top) and darkfield (bottom) images are presented. (**A, A'**): E9.5 heart. (**B, B'**): E10.5 embryo. (**C, C'**): E10.5 heart at higher magnification, as indicated by dotted box in B, B'. In these sections, specific staining is visible in the heart and somites. A = atrium; V = ventricle; OT = outflow tract; SC = superior endocardial cushion; IC = inferior endocardial cushion.

myocardium, move more slowly in the region constituting the developing atrial-ventricular (AV) node, and then conduct rapidly through the ventricular myocardium (261). During this time period, we detected expression of transcripts of both *zscn5Laa* and *zscn5Lab* in total RNA templates isolated from whole embryos (Figure 3.4). To determine whether *zscn5Laa* and *zscn5Lab* are expressed in the developing myocardium, we microdissected hearts from transgenic zebrafish expressing GFP under the control of the cardiac myosin light chain 2 promoter (Tg[*cmlc2*:gfp]), which specifically drives GFP expression in the developing heart, and assayed expression using gene-specific primers and RT-PCR. As illustrated in figure 3.4, expression of both *zscn5Laa* and *zscn5Lab* was detected in the developing myocardium. To determine the localization of *zscn5Laa* and *zscn5Lab* expression in whole-mount embryos, we generated antisense and sense (control) probes against each gene in selected regions of divergence determined by alignment of the full-length, cloned zebrafish Na_v1 cDNA sequences (Figure 3.5). Although antisense probes against *zscn5Lab* initially detected expression of this gene in the embryo heart at 54hpf, we were unable to consistently reproduce these results by standard methods for *in situ* hybridization. Similar difficulties were encountered using probes directed against different regions of the *zscn5Lab* mRNA sequence that because of high-homology with other Na_v1 sequences, may possibly have detected other isoforms. No *in situ* expression pattern was detected at any stage between day 1 and day 4 using probes directed against *zscn5Laa* mRNA, using standard methods. A survey of the expression of all 8 zebrafish sodium channel genes was recently reported in the literature (229). Antisense probes were directed at similar locations of *zscn5Laa* and *zscn5Lab* mRNA transcripts (229). By *in situ* hybridization, expression of *zscn5Laa* was nearly undetectable at 24 hours post-fertilization (hpf) (229). Between 48hpf and 60hpf, *zscn5Laa* appeared to be weakly and diffusely expressed in the head region, possibly in head muscle or in the central nervous system (229). Expression of the second *scn5a*-like gene, *zscn5Lab*, was detected most clearly in somites at 19hpf using a fluorescent chromogen (229). This expression in somites disappeared and was followed by weak expression in the ventral spinal cord at 30hpf (229). At 60hpf, the expression of *zscn5Lab* was again nearly below the level of detection, but may be expressed in developing lateral line structures (229). Unexpectedly,

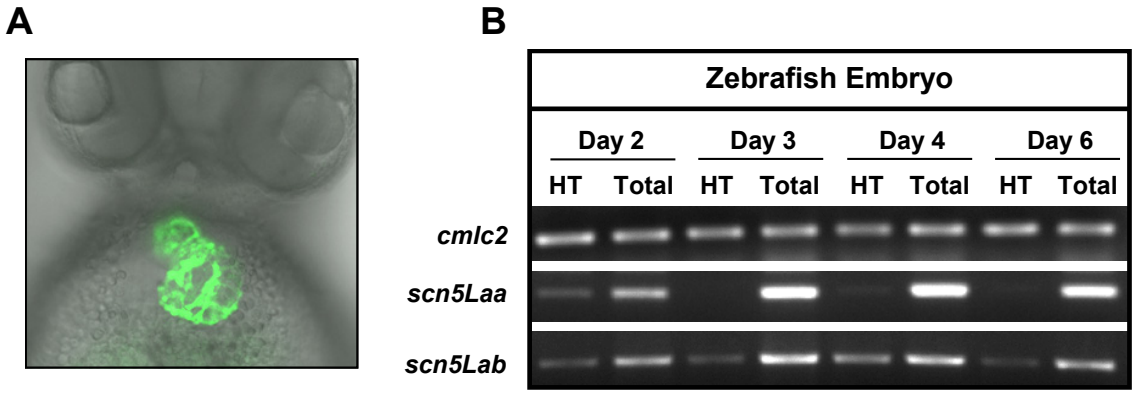

Figure 3.4: Expression of cardiac sodium channels in the zebrafish embryo. (A) Use of *cmlc2*:*GFP* transgenic zebrafish embryos facilitated microdissection of the developing heart. **(B)** Primers were designed to amplify transcripts of *scn5Laa* or *scn5Lab* from the embryonic zebrafish heart (HT) or total embryo at different stages of development. *cmlc2* = cardiac myosin light chain 2.

A

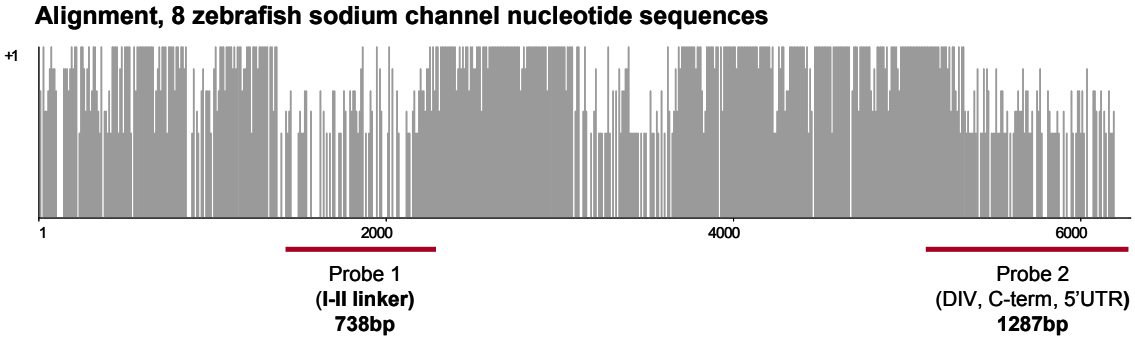

B

Zebrafish Gene	Probe 1 (738bp)	Probe 2 (1287)
scn1aa (DQ149503)	50.1%	65.6%
scn1ab (DQ149504)	50.7%	65.2%
scn4aa (DQ221253)	46.7%	61.5%
scn4ab (DQ221254)	44.7%	63.7%
scn5aa (DQ149507)	99.5%	71.3%
scn5ab (DQ837300)	58.7%	99.5%
scn8aa (NM_131628)	48.9%	62.0%
scn8ab (DQ149509)	48.4%	65.7%

Figure 3.5: Probe design for *in situ* hybridization in zebrafish. **(A)** Similarity plot of the alignment of all 8 zebrafish Na_v1 channel genes. Probes 1 and 2 targeted areas of high divergence. **(B)** Percent homology of *in situ* probes to each full-length Na_v1 sequence.

expression of 0/8 zebrafish sodium channel genes were detected in the developing heart at any stage by *in situ* hybridization (229). The difficulty in detecting sodium channel transcripts in the zebrafish heart by standard *in situ* hybridization may reflect the low abundance of sodium channel transcripts, detectable by only methods that greatly amplify these transcripts such as PCR or isotopic *in situ* hybridization with long exposure times.

Function of sodium channels in the developing heart

The external fertilization of zebrafish embryos, the ease of observing aberrant heart rhythms, and their permeability to small molecules enabled us to survey the putative function of cardiac sodium channels from the earliest stages of heart function using chemicals that target these channels. For their solubility, low cost, and ease of delivery, we tested the effects of the sodium channel blockers lidocaine, mexiletine, and flecainide, as well as the pufferfish toxin TTX, in two strains of wild type zebrafish (EK and TU) at day 2 and day 3. As shown in Figure 3.6, application of lidocaine to the embryo medium resulted in significant, dose-dependent bradycardia in wild-type embryos. Application of mexiletine also resulted in bradycardia, whereas treatment with the more potent drug flecainide elicited 2:1 and 3:1 atrioventricular block. Unexpectedly, TTX in the bath solution did not produce any effects on cardiac rhythm at these stages of development. As embryos immersed in between 10 and 100μM concentrations of TTX continued to display normal muscle and nerve function (e.g. swimming, touch sensitivity), we considered the possibility that the charge and the size of TTX prevented this molecule from freely crossing biological membranes. Similarly, we earlier noted the effects of local anesthetics (which are weak bases) were potentiated by altering the pH of the solution above of the pKa of the drug (e.g. lidocaine pKa ~ 8.2). This suggested that despite the relatively small size of local anesthetics, the charge on these drugs in neutral or acidic solutions was likely to prevent these molecules from freely crossing lipid membranes. Taken together, the results of our chemical studies suggested that sodium channels are likely to be important regulators of beating in the embryonic heart. However, the bradycardia and heart block elicited by sodium channel blockers are not specific for sodium channel perturbation, as similar rhythm abnormalities occur with

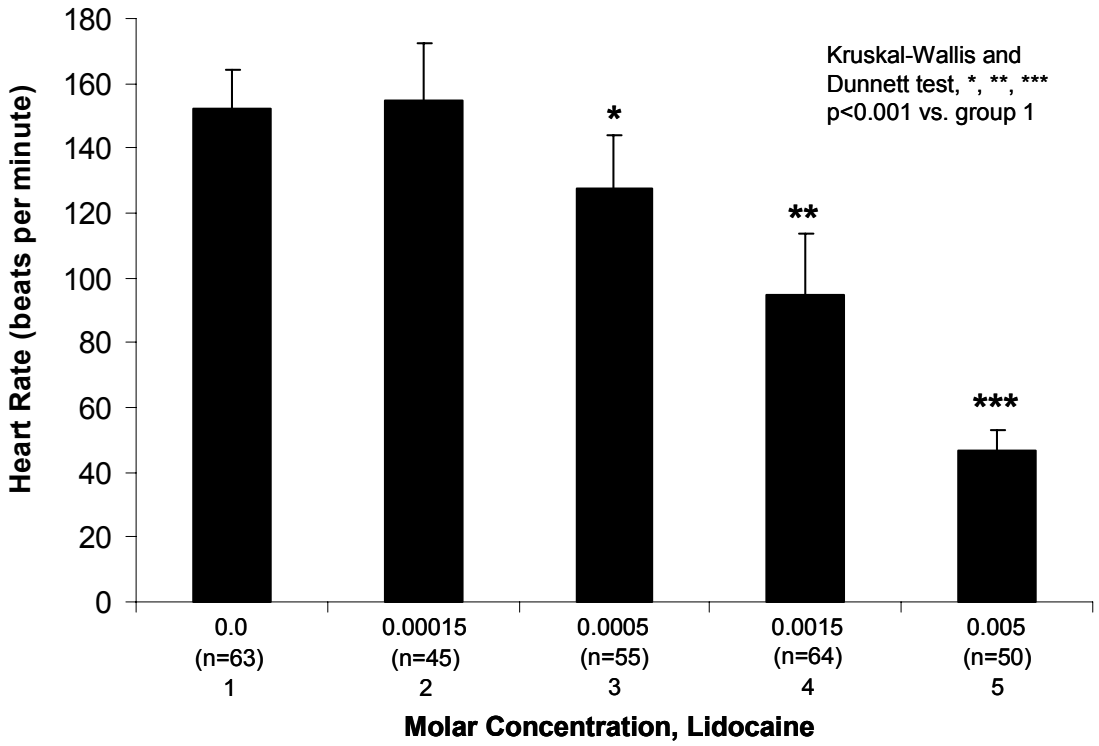

Figure 3.6: Sodium channel blockers such as lidocaine induced bradycardia in the zebrafish heart on day 2 of development. Lidocaine was placed in the bath solution of zebrafish embryos at 48 hours post fertilization and heart rate was assessed. N = number of embryos tested at each drug concentration.

disruption of cardiac potassium channel zERG potassium channel (262). Furthermore, none of the sodium channel blockers used display exquisite specificity for sodium channels, particularly at the doses used to elicit rhythm phenotypes from bath solutions (263-268).

Initial analysis of the function of zNa$_v$1.5Lb (zscn5Lab)

To determine which sodium channel gene(s) were likely to underlie the observed cardiac drug-response phenotypes in the zebrafish embryo heart, we designed experiments to knockdown channel expression using morpholino antisense oligonucleotides. As zNa$_v$1.5Lb was the first cardiac sodium channel we identified, and because of its expression in the embryonic heart and both chambers of the adult heart (Figure 2.8), we first directed morpholino oligonucleotides against transcripts of the gene *zscn5Lab*. Traditionally, antisense morpholino oligonucleotides were designed to recognize the translation start site of processed mRNAs, where they reduced protein expression by acting as steric inhibitors of the ribosome complex. Since morpholinos could penetrate the nucleus, however, it was recognized that they could be directed against intron-exon junctions of pre-mRNAs to perturb splicing, which would in turn knockdown protein expression (269). The latter approach presented certain advantages: in the absence of antibodies against the zebrafish protein target, one could easily track the action of the morpholino oligonucleotide by RT-PCR with priming sites on either side of the splice junction.

As the cloning of *zscn5Lab* proceeded from the 3' end (Figure 2.4), we first analyzed this region of the gene for optimal morpholino target sites and identified the E24/I24 splice junction as a reasonable candidate (see Methods for morpholino design criteria). Injection of low quantities (1-2ng) of E24/I24 morpholino oligonucleotides into 1 cell stage embryos resulted in retention of intron 24 as assayed by RT-PCR across this splice junction (Figure 3.7). This retained intron was predicted to result in a frameshift and likely premature termination of the translation of *zscn5Lab* transcripts prior to domain IV, predicting a loss of approximately 25% of the mature protein (Figure 3-7). As voltage-gated sodium channels are formed from a single polypeptide, we predicted this perturbation would result in complete loss of functional zNa$_v$1.5Lb channels at the membrane. Injection of similar (and greater quantities) of a standard control morpholino that was

not directed against any particular gene did not result in any abnormalities of splicing of *zscn5Lab* transcripts (Figure 3-7).

To determine whether knockdown of $zNa_v1.5Lb$ resulted in abnormalities of heart rhythm, we examined injected embryos at 2 and 3 days post fertilization. As predicted by the drug-response phenotype, knockdown of $zNa_v1.5Lb$ resulted in bradycardia whose severity depended on the amount of morpholino injected (Figure 3.8). At later stages (day 4), a small but significant percentage of morphant embryos also developed more complex arrhythmias such as sinus pauses and AV-block (Figure 3.8). As a simple assay of overall cardiac function, we determined whether morphant hearts could adequately maintain circulation in the embryo. Both by direct observation of circulation through the transparent trunk, as well as by the injection of fluorescent beads into the sinus venosus in a smaller number of embryos, it was revealed that the weakly contractile morphant heart could not sustain circulation (Figure 3.9). Moreover, as revealed by knockdown of $zNa_v1.5b$ in the *flk*:*GFP* transgenic background, morphant circulation was impaired in the absence of defects of development of primary vascular structures (Figure 3.9). Our results indicated that reduced expression of $zNa_v1.5Lb$ significantly compromised heart function in the zebrafish embryo. Most embryos injected with 1.5ng of morpholino died by 5 days post fertilization.

In addition to these functional deficits, however, morphant embryos unexpectedly displayed developmental abnormalities that included reduced body and head size, a slight body curl, and most strikingly, a significant defect in cardiac morphogenesis (Figures 3.10-11). These findings are consistent with the observation that mice homozygous null (-/-) for *scn5a* (but not heterozygote mice) were reported to be embryo-lethal on E10 with significant defects in cardiac morphogenesis, primarily of the developing ventricular myocardium (see Discussion) (133). Zebrafish embryos mutant for the cardiac L-type calcium channel gene *CACNA1C* also displayed significant defects in ventricular morphogenesis at 3 days post-fertilization (270). Moreover, in mouse models and human patients, an array of unexpected myocardial phenotypes have been linked to *SCN5A* mutations and reduced sodium channel expression including dilated cardiomyopathy, left ventricular non-compaction, and age-related cardiac fibrosis (271-276).

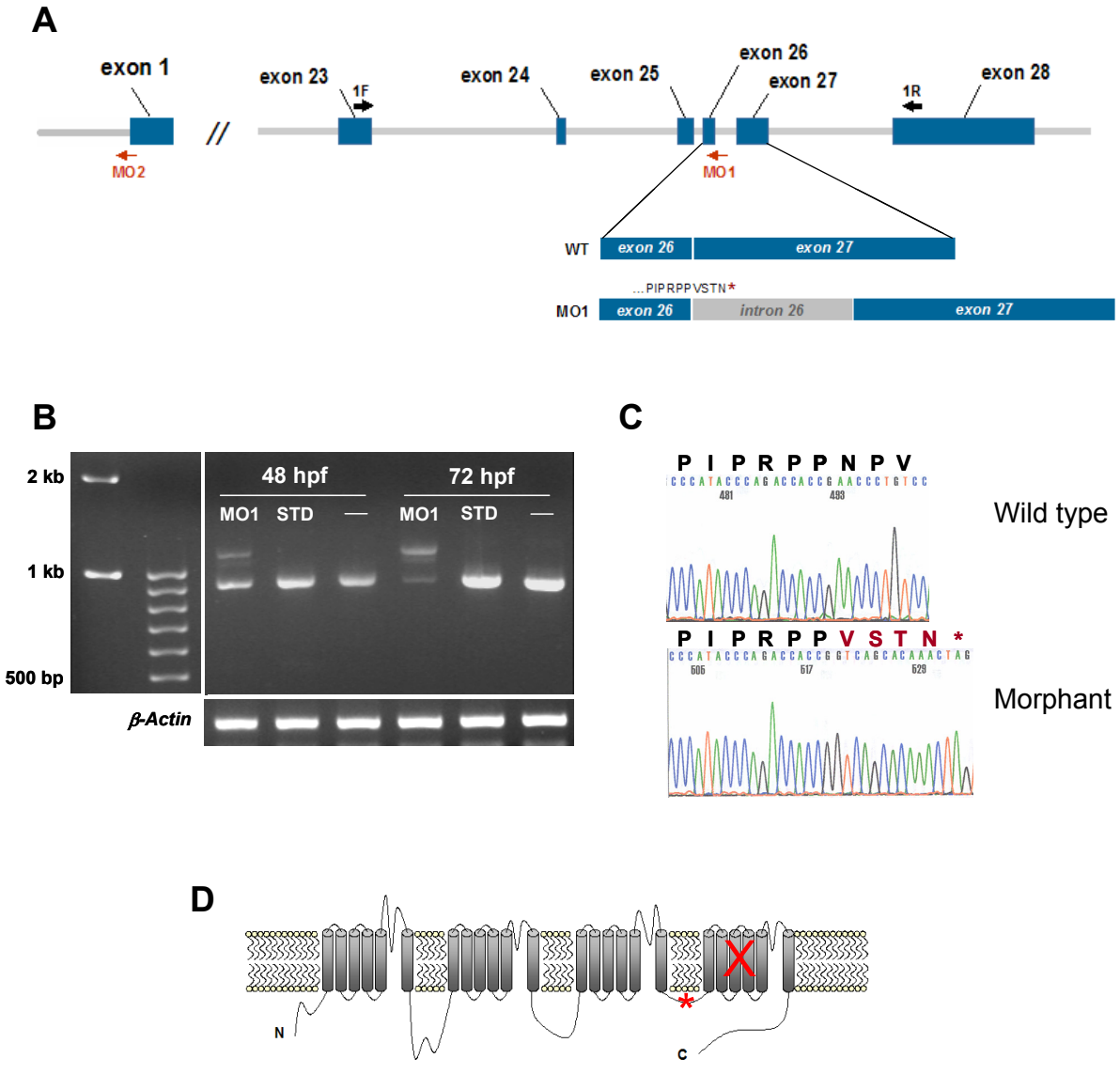

Figure 3.7: E24/I24 antisense oligos ("MO1") effectively reduced wild-type *zscn5Lab* mRNA transcripts. **(A)** Target sites of antisense oligos displayed in reference to *scn5Lab* pre-mRNA. Exon nomenclature above (E26) was based incomplete information while *scn5Lab* was being cloned from its 3' end. **(B)** As determined by RT-PCR across the splice junction and direct sequencing of aberrant splice products **(C)**, the E24/I24 MO induced retention of intron 24, predicting a termination of translation after 4 codons of intronic sequence (VSTN*). Amino acid sequences are listed above the nucleotide sequences in (C). **(D)** The truncated protein is predicted to be 1458 amino acids long and lacks all of domain IV.

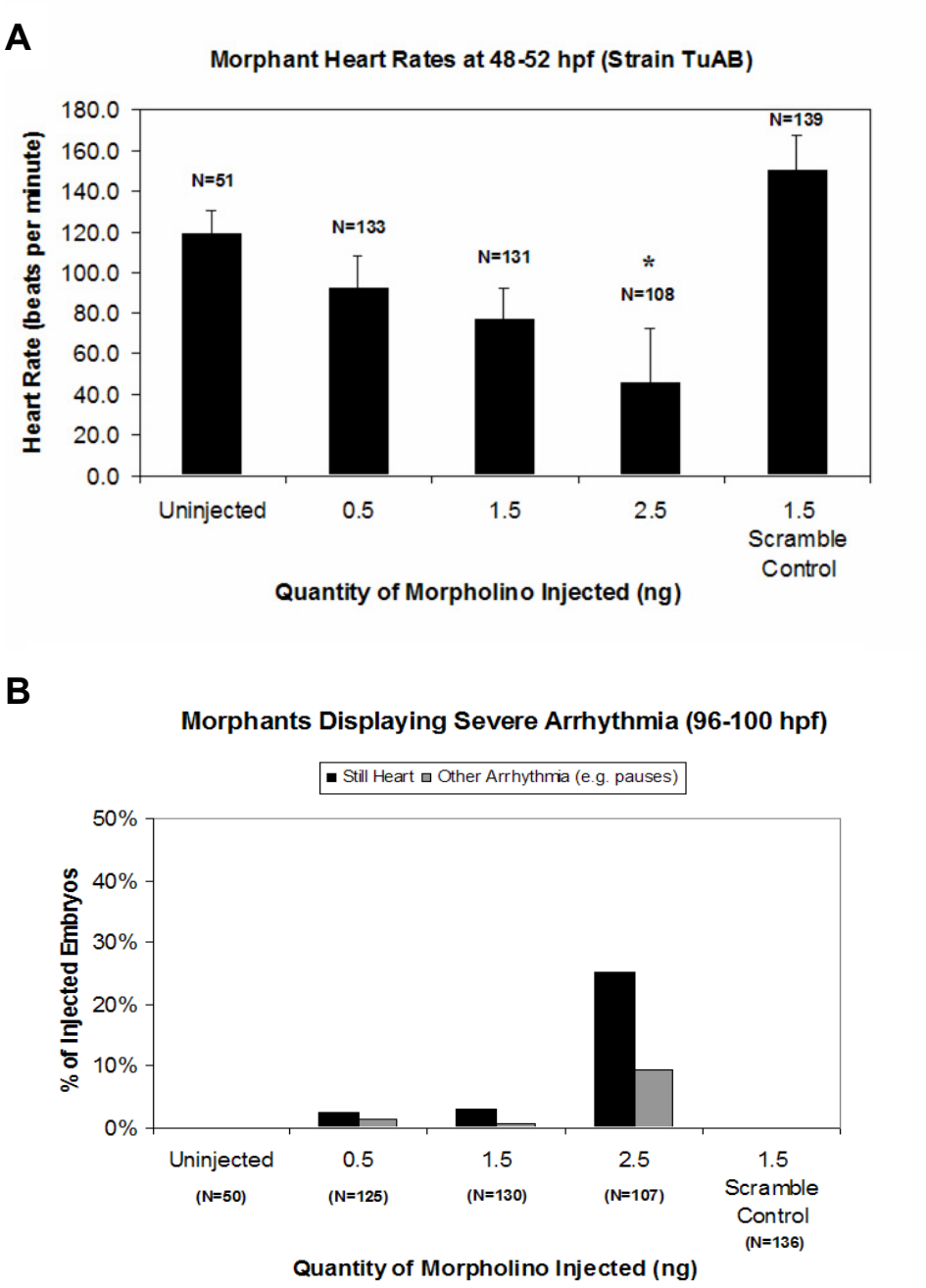

Figure 3.8: Heart rhythm defects at days 2 and 4 following knockdown of $Na_v1.5b$ (*scn5Lab*). **(A)** Morphant embryos display dose-dependent bradycardia at 48-52 hours post-fertilization. **(B)** Morphant embryos display more complex arrhythmias at later stages (96-100 hours post-fertilization).

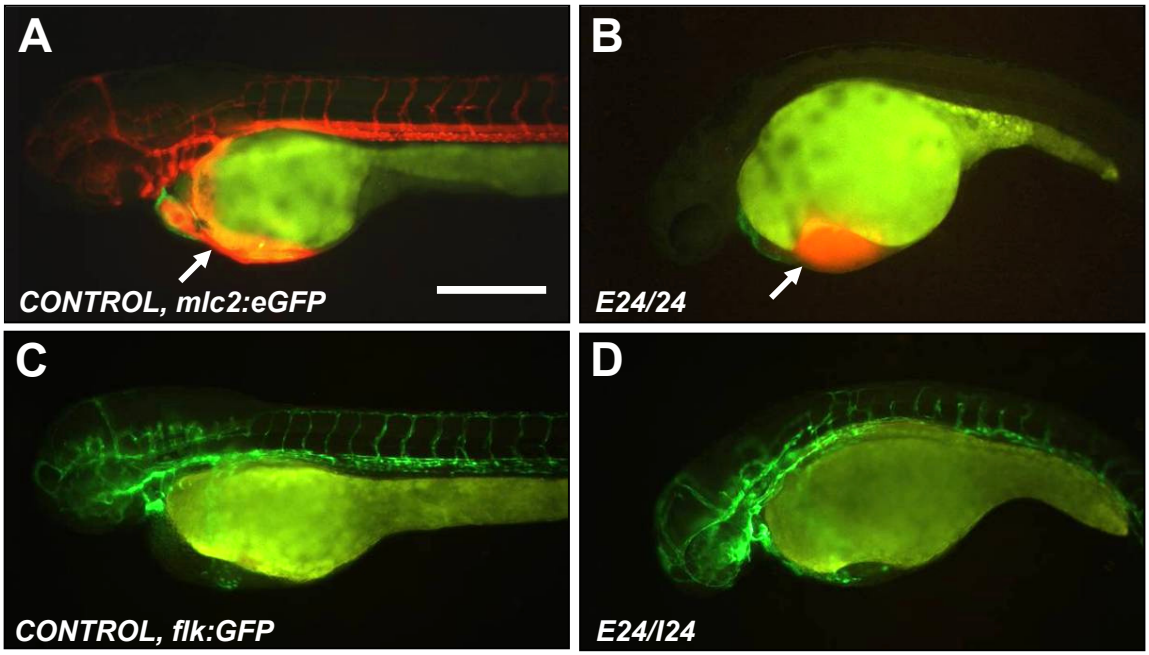

Figure 3.9: zNa$_v$1.5b morphants displayed severe perturbations of heart function that prevented normal circulation. **(A, B)** Fluorescent beads were pressure-injected into the sinus venosus of control and morphant embryos (arrow) to determine whether the heart could adequately maintain systemic circulation. **(C, D)** As assessed by injection of the E24/I24 morpholino into the *flk*:*GFP* transgenic line, zNa$_v$1.5b knockdown perturbed circulation without affecting the development of primary vascular structures.

Since the mechanisms linking ion channel activity to myocardial morphogenesis or maintenance are not well understood, we investigated the morpholino-induced zebrafish cardiac developmental abnormalities in greater detail.

To more easily study cardiac morphogenesis, we used transgenic *cmlc2*:*GFP* zebrafish embryos, where the embryonic heart structures were clearly visible by fluorescence microscopy starting from early stages. At 36 hours, E24/I24 morphant hearts displayed significantly reduced size and GFP intensity and a delay in the initiation of looping (Figure 3.11). Where wild type hearts at 60hpf elaborated morphologically-distinct atrial and ventricular chambers which have looped, morphant hearts remained straight and tube-like, with no evidence of ventricular chamber morphogenesis and compromised atrial formation. At 84hpf, when in wild type embryos the ventricle displayed evidence of concentric thickening and looping had progressed to place the atrium and ventricle into apposition, morphant hearts deteriorated into a stretched, string-like form analogous to those seen in zebrafish mutants of early cardiac transcription factors such as *tbx5* (277). Atrial and ventricular chambers arise from two distinct groups of progenitor cells in the early embryo (278;279). To determine whether the atria and ventricles were patterned properly in morphant hearts, we used double-immunostaining with antibodies that recognize myosin chain epitopes in the atrium and whole heart (S46 and MF20, respectively) (Figure 3.12). These studies revealed normal A-V patterning in morphant hearts, and more clearly demonstrated that both chambers were significantly perturbed following knockdown of zNa_v1.5Lb.

As revealed by zebrafish mutants identified in forward genetic screens, defects in embryonic heart morphogenesis may result from perturbations of genetic pathways that control the number (280), growth (281), movement (282), or patterning (283) of nascent cardiomyocytes. To begin to distinguish between these possibilities in sodium channel morphants, we first sectioned the cardiac chambers of wild type and morphant hearts at 80hpf. Qualitatively, hematoxylin & eosin (H&E) staining revealed that morphant hearts had less cells than wild-type hearts and failed to display the normal concentric thickening of the ventricle (morphant chambers are a single layer) (Figure 3.13). Despite the apparent reduction in cell number, morphant myocytes appeared to be comparable in size to those in wild-type embryos (Figure 3.13).

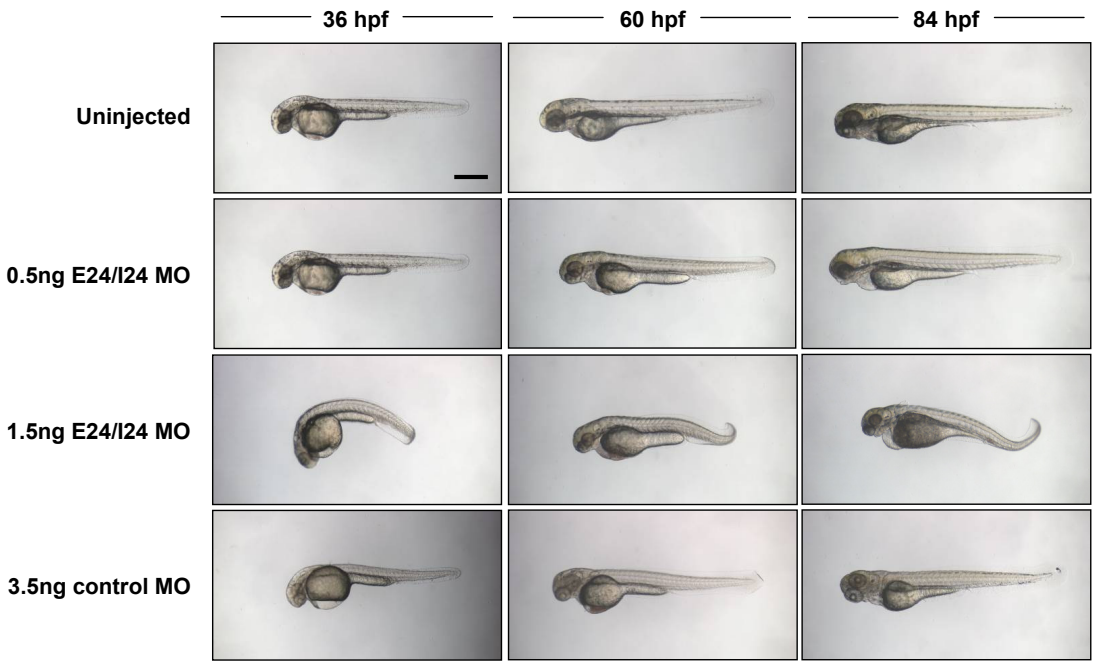

Figure 3.10: Whole-body phenotypes resulting from E24/I24 or control morpholino injections. Embryos were photographed at the designated timepoints using brightfield microscopy. Morphant embryos are shorter in length, have smaller heads, and display abnormal tail curvature.

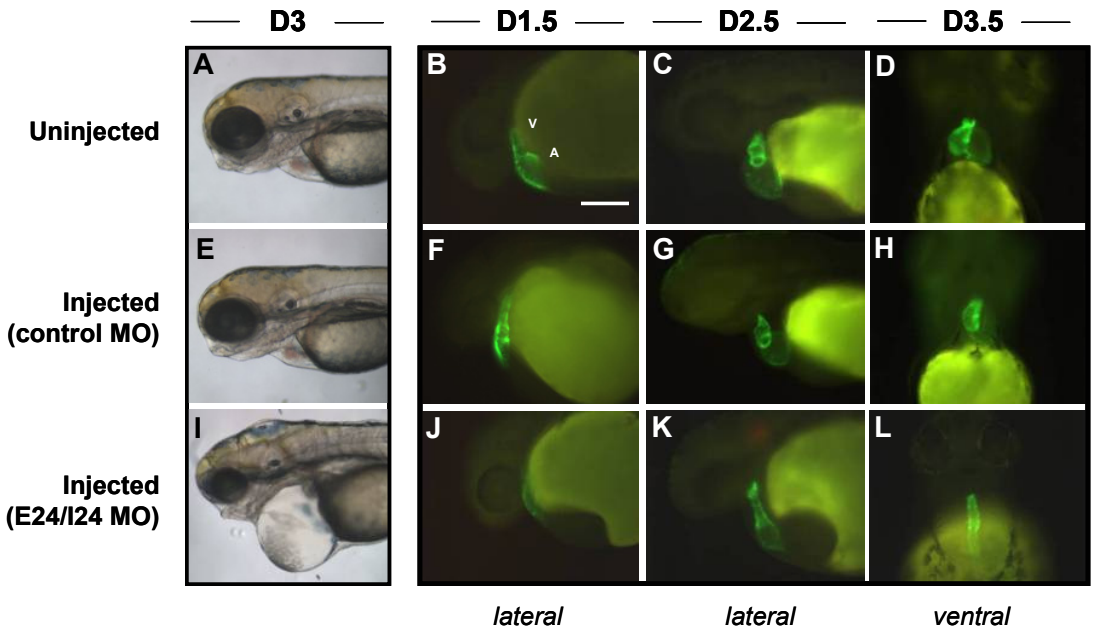

Figure 3.11: Knockdown of zNa$_v$1.5b resulted in defects in cardiac morphogenesis, as assessed in *cmlc2:GFP* transgenic zebrafish embryos. The sodium channel morphant phenotype was visualized in *cmlc2:GFP* embryos. At 1.5 days post fertilization, morphant hearts **(J)** elaborated less myocardial tissue than uninjected **(B)** and control-injected **(F)** embryos. At 2.5 days post-fertilization, morphant chamber morphogenesis and looping were severely perturbed **(K** versus **C, G)**. At 3.5 days post-fertilization, the morphant heart deteriorates while wild-type and control-injected hearts proceed with looping and chamber development **(L** versus **D, H)**.

To quantitate cardiomyocyte growth and number, we developed methods to image the hearts of *cmlc2*:*GFP* transgenic embryos with single-cell resolution using confocal microscopy (Figure 3.13). By gently flat-mounting transgenic embryos, samples could be imaged within the narrow working distances of high magnification confocal lenses (approximately 200μM for 40x/1.3 aperture lens), without damage to individual cardiomyocytes. Cell boundaries were clearly visible at high power in unfixed, unstained embryos (Figure 3.13). Our method of imaging *cmlc2*:*GFP* hearts thus enabled us to use Image J analysis software to measure the surface area (μM^2) of embryonic cardiomyocytes at different stages in both wild-type and mutant embryos. Moreover, by collecting stacks of images that spanned the entire heart in the Z dimension, we were able to use the Pointpicker function of Image J to count the total number of cardiomyocytes across Z sections without double-counting cells. Prior methods of quantifying the total number of cells in the heart relied on the use of serial H&E-stained sections and may have greatly overestimated the true cell number.

To determine whether and to what extent embryonic cardiomyocytes grow in size over the course of early stages of heart development, we first imaged the developing heart at its "cone" stage (22-24 somites), the earliest timepoint at which GFP is expressed in our transgenic embryos and shortly after the fusion of cardiac primorida at the midline, and again after chamber formation on day 3. As prior studies have revealed that differentiating cardiomyocytes already display distinct atrial- and ventricular-specific gene expression patterns prior to heart tube formation, we measured cells in the presumptive ventricle (inner heart cone) at 22-24 somites and compared them to ventricular cells on day 3 for consistency (278;279). Between 24 somites (~20hpf) and day 3 (~76-78hpf), the average size of a wild-type ventricular cardiomyocyte increased from 180±4.1μM^2 (mean±SEM; n = 90 total cells, 4 heart cones) to 250.5±0.69μM^2 (mean±SEM; n = 68 total cells, 4 ventricles). To determine the normal developmental change in cardiac cell number, we counted the number of cells in wild type heart cones (22-24 somites) and in day 2 hearts (54hpf). Our analyses revealed that the total number of embryonic myocardial cells normally increases in number during this time period from 153±7 to 227±16 cells (n=4). While morphant hearts displayed normal cellular growth compared to wild type hearts, they had

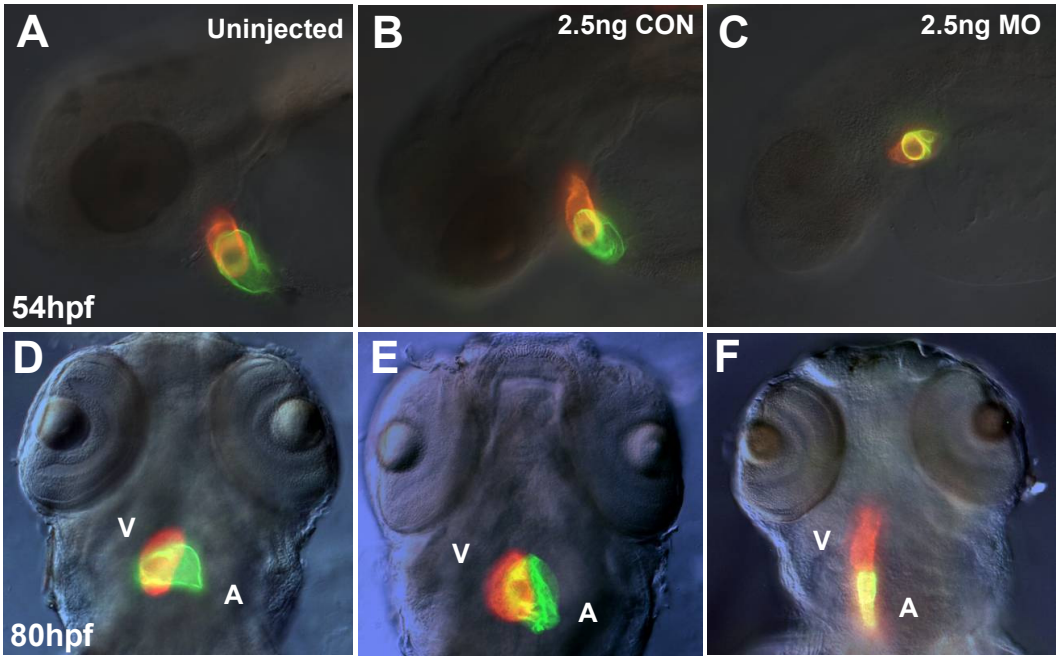

Figure 3.12: Double immunostaining of morphant embryo hearts revealed normal atrial-ventricular patterning. Despite severe defects in morphogenesis, zNa_v1.5b (*scn5Lab*) morphant hearts displayed normal atrial-ventricular patterning as assessed by MF20/S46 double immunostaining. A = atrium (green), V = ventricle (red).

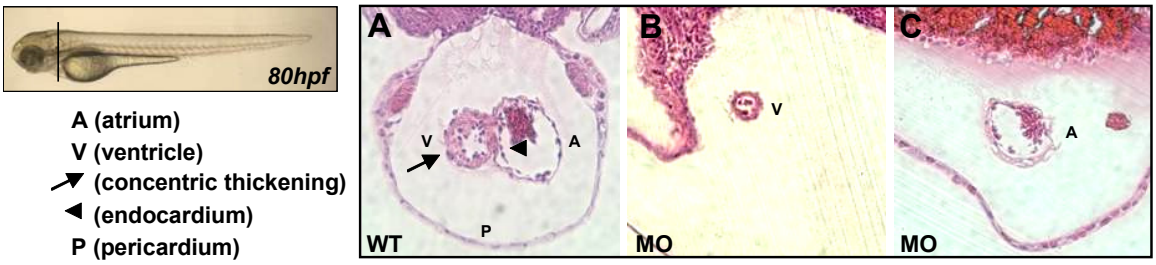

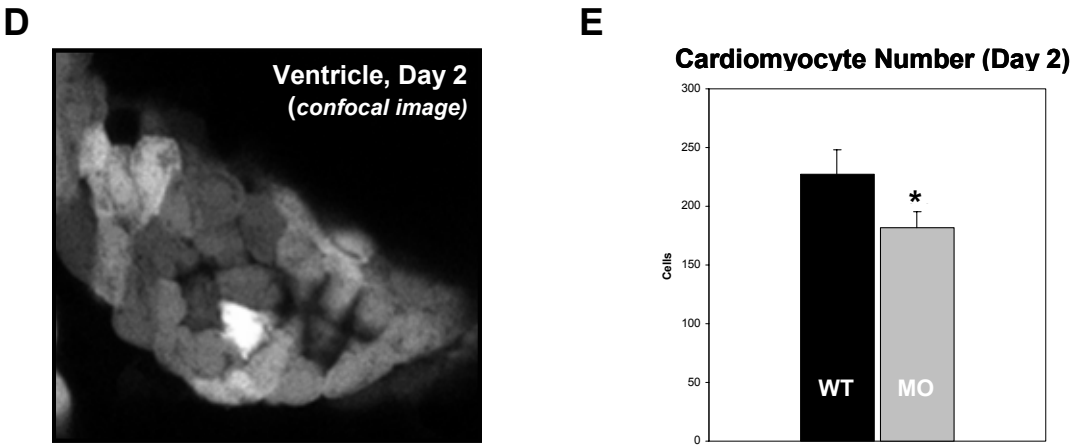

Figure 3.13: Knockdown of zNa$_v$1.5b resulted in a reduced number of embryonic cardiomyocytes. (A-C) Hematoxalin and eosin-stained transverse sections of control and morphant zebrafish hearts on day 3 (80 hours post-fertilization). **(A)** In wild type embryos, chambers were looped and the ventricle displayed concentric thickening. **(B, C)** Morphant hearts lacked concentric thickening of the ventricular wall and displayed abnormal looping as indicated by the appearance of the atrium and ventricle in different sections. The endocardium is also reduced in morphants but intact. Note the massive edema. **(D)** Typical confocal image of a wild type *cmlc2*:*GFP* embryo heart at 2 days post-fertilization, showing single cell resolution and clear cellular boundaries. **(E)** Total cardiomyocyte number is reduced in morphants (wild type: 227±16; morphant: 182±13, mean±SD, $p<0.001$, n=4 hearts each).

significantly fewer cells 182±13 cells (n=4), suggesting a possible cellular mechanism for the observed defects in organ morphogenesis (Figure 3.13).

Is function required for development?

The vertebrate heart begins to beat well before its development is complete. In zebrafish, the simple tube-like heart exhibiting peristaltic-like contractions establishes circulation within the embryo early on day 1. Given the well-established role for sodium channels in initiating the cardiac cycle, we next tested the hypothesis that altered electrical activity resulting from morpholino treatment generated the defects in heart development we observed. As a critical test of this hypothesis, we sought to more clearly establish that voltage-gated sodium channels regulate heart rhythm at early stages (day 1-2) when $zNa_v1.5b$ morphants already displayed significant defects in cardiac morphogenesis. The absence of any effect of micromolar concentrations of TTX in embryo medium suggested the possibility that sodium channels are not required to regulate heart beat in early zebrafish.

To study the functional differentiation of the sodium channel complex in zebrafish, we took several approaches including electrophysiology, *in vivo* administration of channel-specific toxins, and immunohistochemistry of sodium channels in developing excitable tissues. We used three toxins in our studies with distinct binding sites and mechanisms of action on sodium channels: the sodium channel “blocker” tetrodotoxin and the channel “activators” anemone toxin II and veratridine (284;285). As zebrafish sodium channels cDNAs have never been previously functionally expressed and screened for toxin sensitivity, we performed initial experiments *in vitro* to determine the effects of different doses of TTX and ATX II on whole cell sodium currents of $zNa_v1.5b$. In CHO cells, both toxins profoundly affected the function of this zebrafish channel (Figure 3.14). For TTX, 100nM concentrations were sufficient to nearly completely eliminate inward sodium current through the channel (Figure 3.14). Conversely, similar concentrations of ATX II prevented the channel from closing by nearly completely blocking channel inactivation (Figure 3.14). *In vivo*, we successfully recorded action potentials from the adult zebrafish ventricle using the sharp microelectrode technique. To determine whether zebrafish cardiac

Tetrodotoxin (TTX)

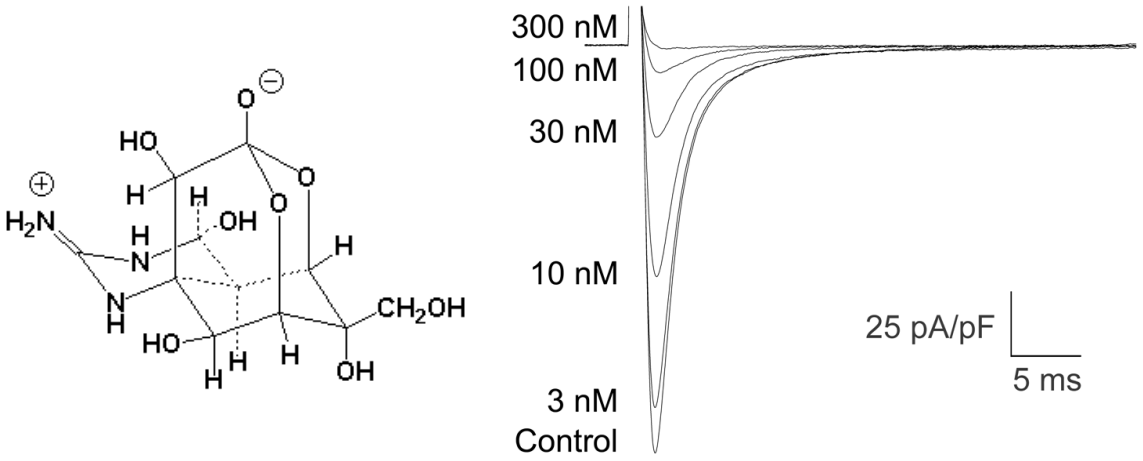

Anemone toxin (ATX II)

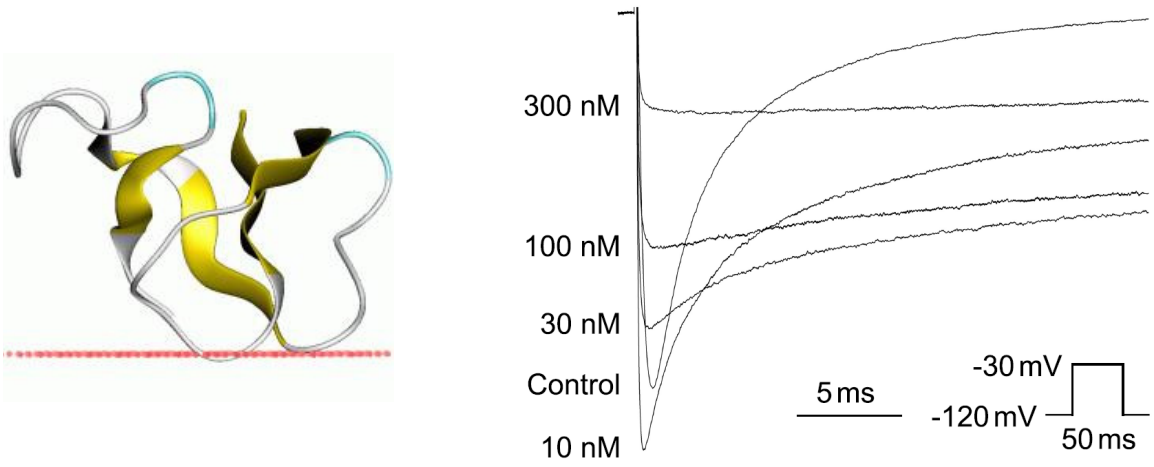

Figure 3.14: Changes in $zNa_v1.5b$ whole cell sodium currents in CHO cells following exposure to TTX and ATX II. Inward sodium currents are downward/negative by convention. Tetrodoxin (TTX) is a heterocyclic guanidinum toxin that binds to "receptor site 1" on the channel from the extraceullar compartment. Since site 1 contributes to the outer vestibule of the sodium channel pore, TTX acts to block the permeation of sodium ions. The 47 amino acid peptide anenome toxin II (ATX II) binds to "receptor site 3," which includes the extracellular linker connecting transmembrane segments S3 and S4 of domain IV. By interfering with the S4 voltage sensor of domain IV, ATX II perturbs movements of the protein that are required for fast inactivation, resulting in channels that do not properly close. The ATX II diagram above was found in the Orientation of Proteins in Membranes (OPM) database, University of Michigan College of Pharmacy: **http://opm.phar.umich.edu/protein.php?pdbid=1atx**

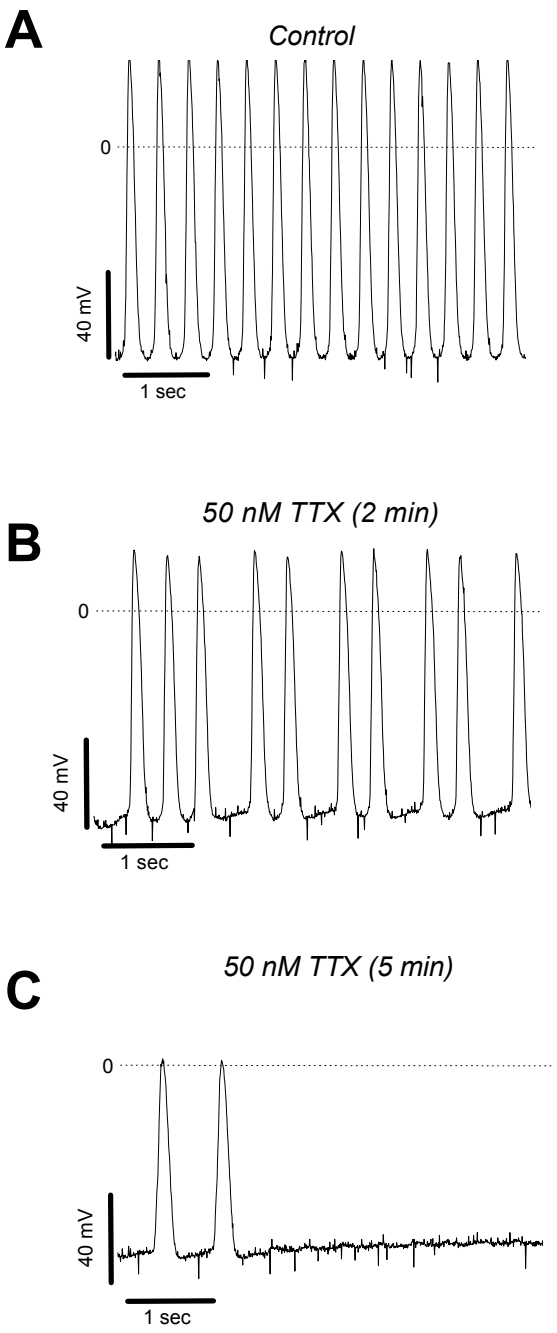

Figure 3.15: Nanomolar concentrations of tetrodotoxin (TTX) suppressed adult zebrafish ventricular action potentials. N = 4; representative traces shown above. **(A)** Action potentials generated by the adult zebrafish ventricular myocardium bathed in Tyrode's solution (physiological control). **(B)** 50nM TTX in physiological solution disrupts the generation of ventricular action potentials. **(C)** At five minutes of TTX exposure, the frequency and amplitude of ventricular action potentials are markedly reduced and the heart stops beating.

action potentials depend on the function of voltage-gated sodium channels, we applied TTX to the bath solution. As shown in Figure 3.15, as little as 50nM TTX completely inhibited the generation of ventricular action potentials (n = 4 hearts), with effects that were nearly completely reversible on washout. As mammalian cardiac channels are blocked only by micromolar doses of TTX, these findings confirmed our prediction of a key difference between zebrafish and mammalian cardiac sodium channels predicted from sequence analysis (Figure 2.12). More importantly, the exquisite sensitivity of the adult zebrafish heart to TTX provided us with a starting point for studying the developmental time-course of sodium channel function in the heart.

On day 1 of development, when the zebrafish embryo heart has just commenced beating, we exposed zebrafish embryos to the sodium channel toxins and examined the effects on the beating heart tube. By this approach, no sodium channel modulators elicited any visible effects on heart beat (Figure 3.16). As a positive control, we immersed embryos in 10-50μM concentrations of the L-type calcium channel blocker nisoldipine, which promptly slowed and then arrested the heartbeat within 20 seconds. Veratridine (150μM) caused hyperkinetic movements of the entire embryo body, followed by tonic contraction of the trunk. However, neither TTX nor ATX II produced any effect, raising the possibility that the compounds were not able to adequately penetrate into the embryo. Therefore, we pressure injected TTX and ATX II directly into the trunk circulation of day 1 embryos. A few seconds after acute delivery into the circulation, 150μM TTX completely inhibited spontaneous movement and the normal “escape response” elicited by stimulation at this stage of development. Conversely, injection of 20μM ATX II by identical methods of delivery promptly resulted in hyperkinetic movements of the embryo for approximately 15-20 seconds, followed by tonic contraction and then complete relaxation. After this initial response, hyperkinetic movements were readily elicited by gentle stimulation, presumably because sodium channels in nerve and muscle needed to be opened before these toxins could exert their effects. Despite the dramatic effects seen on sodium channel-related physiological responses in nerve and muscle, no effect was observed on the beating of the day 1 heart tube. The lack of any effect of high concentrations of any toxin indicated that sodium channels do not play a role in mediating excitability within the early developing heart of zebrafish.

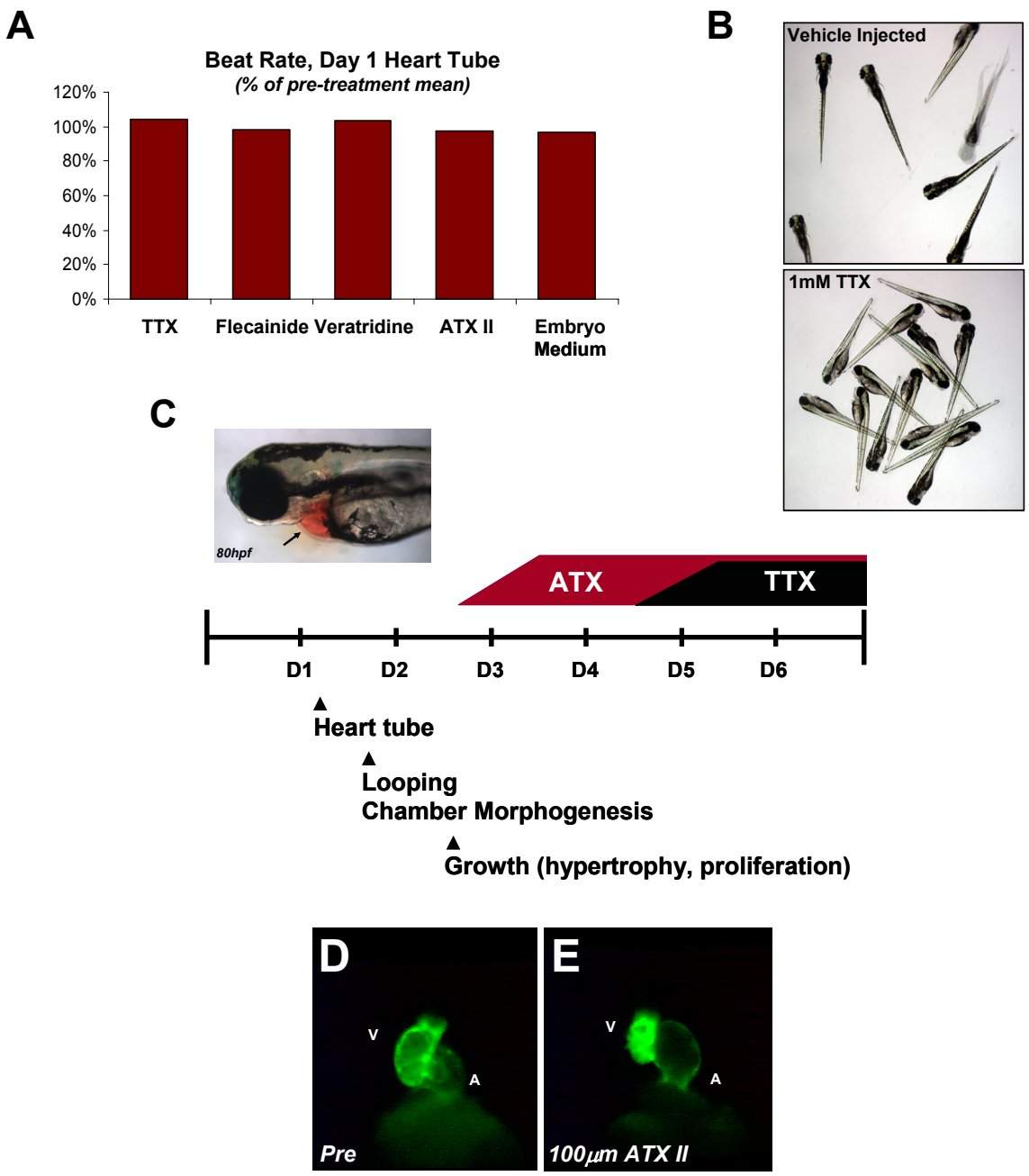

Figure 3.16: Effects of sodium channel modulators on early zebrafish heart function. (A) Sodium channel blockers had little effect on heart beating on day 1, whether delivered by injection or placed in the bath solution. **(B)** 1mM TTX injected into the yoke of 1-2 cell stage embryos resulted in profound paralysis for the first 4-5 days of development, but no change in heart rhythm. **(C)** TTX and ATX II were acutely delivered into the pericardium, as demonstrated by red dye. ATX II caused arrhythmias in a few embryos between days 2 and 3 and in most embryos thereafter. TTX caused arrhythmias in some embryos between days 4 and 5 and in most embryos thereafter. D = days post-fertilization. **(D, E)** ATX II caused tonic ventricular contraction on day 4 when delivered directly into the pericardial sack. Atrial rate and rhythm were unaffected.

Notably, the reliance on sodium channels for excitation was observed to be significantly delayed in the heart compared to other excitable tissues, where sodium channel-mediated effects were readily apparent by the delivery of TTX, ATX II, and veratridine.

To determine when sodium channels become required for function in the embryonic heart, we delivered micromolar doses of TTX in physiological vehicle or vehicle alone directly to the myocardium via microinjection over each of the first 7 days of development. Live embryos were first anesthetized with low doses of tricaine that permitted stabilization of embryos on their lateral aspect in methylcellulose, with no detectable effects on heart rhythm or contractility. Injections were performed with sharp-tipped, borosilicate micropipettes inserted directly from the caudal aspect into the sinus venous, the antechamber where blood collects before traveling into the atrium (day 2), or the pericardial space that surrounds the beating heart (days 3-7) (Figure 3.16). Direct exposure of the myocardium to 150μM TTX caused no adverse effects on heart rhythm until between days 4 and 5 of development, when a small percentage of embryos began to display specific arrhythmias including 2:1, 3:1, and 4:1 AV conduction block and less frequently, atrial and ventricular standstill. By days 5 and 6, a greater percentage of embryos displayed these phenotypes and between days 6 and 7, nearly all embryos tested exhibited these phenotypes. At all stages tested, the zebrafish ventricles appeared to be more adversely effected by application of TTX than the atria, with many atria actually appearing completely unaffected. Unexpectedly, these data suggested that voltage-gated sodium channels are not important contributors to heart rhythm until between days 4 and 5 of development, well after early chamber morphogenesis and looping have occurred, making in unlikely that sodium channel-mediated excitability contributed to the observed defects in cardiac morphogenesis. Moreover, our data also suggested an alternative, yet-unidentified mechanism for depolarization in the early heart, perhaps by voltage-gated calcium channels. Therefore, to directly address whether calcium entry is required for early cardiac development, we reared embryos from early stages in 10μM of the L-type calcium channel blocker nisoldipine. The hearts of embryos reared in nisoldipine were silent at every stage examined, demonstrating that blocking calcium entry through L-type calcium channels was sufficient to eliminate the cyclic cytosolic calcium transients required for contraction

of embryonic zebrafish cardiomyocytes. Surprisingly, blocking calcium entry into the heart did not perturb morphogenesis of the heart through the end of day 2 (Figure 3.17). The cardiac chambers, albeit deflated due to a lack of blood flow, formed relatively normally and initiated normal looping. From these data, we deduced that excitability is not a requirement for early cardiac morphogenesis.

Physiologically "silent" sodium channels

The limited response of the early heart to tetrodotoxin did not preclude the existence of sodium channel protein in developing myocytes. Physiologically "silent" sodium channels were previously identified in the chick embryo heart (286). We therefore hypothesized that physiologically-silent sodium channels may play a role in cardiac development, via a previously-unknown mechanism. To unmask physiologically silent sodium channels in the zebrafish embryo heart, we used ATX II, reasoning that the application of this toxin would stabilize even a few open channels in the open conformation and result in an aberrant heart rhythm. Although injection of ATX II into day 1 embryos resulted in no disturbance of early heart tube contractions (Figure 3.16), a minority of embryos displayed arrhythmias between days 2 and 3 in response to ATX II and nearly all embryos displayed arrhythmia between days 3 and 4. On days 3 and 4, these arrhythmias manifested as tonic ventricular contractions without relaxation or an intermediate phenotype resembling 2:1 or 3:1 AV block with compromised relaxation of the ventricle. The induction of arrhythmias with ATX II primarily on day 3 revealed the presence of at least some competent sodium channels in the membranes of day 3 myocytes, despite the lack of any requirement for these channels in regulating heart rhythm until between days 4 and 5 of development. However, the absence of any effect of ATX II in the majority of embryos on day 2 (54-60hpf) and in younger embryos also suggested that silent but functional sodium channels in the membranes of nascent cardiomyocytes were unlikely to explain the defects in cardiac morphogenesis induced by sodium channel knockdown.

To directly visualize the expression of channel protein, we performed immunohistochemistry using anti-sodium channel antibodies that recognize an epitope in the

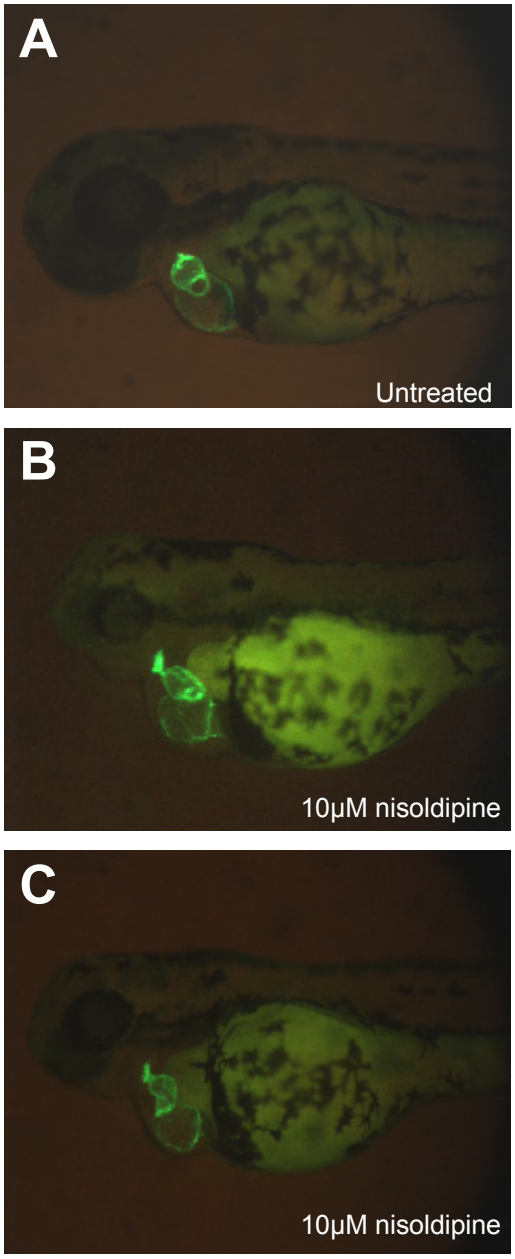

Figure 3.17: Prolonged nisoldipine treatment blocked the heart beat but did not perturb early heart development. Embryos were reared in 10μM nisoldipine from early stages to block L-type calcium currents. At 54 hours post-fertilization, chamber morphogenesis and looping were relatively unperturbed, despite the absence of blood flow, beating, and calcium transients. **B** and **C** depict two different drug-treated embryos.

intracellular domain III-IV linker that is conserved among mammalian and zebrafish sodium channels. We observed both punctuate channel clusters as well as diffuse staining in skeletal muscle, spinal cord, and brain of day 3 embryos (Figure 3.18). In the heart, however, only a small number of channel clusters were observed at this timepoint (Figure 3.19). At day 6, however, we observed an increase in the density of sodium channel clusters per field (Figure 3.19). These results suggested that one possible mechanism underlying the emergence of a physiological role for sodium channels in the heart at day 4 and day 5 might be increased expression of channel protein. Moreover, the severe, early defects in cardiac morphogenesis observed following channel knockdown were in large part unlikely to be related to sodium channel function or expression in the beating embryonic heart.

zNa$_v$1.5b morphants display defects in the production of cardiac progenitor cells

Given these results, we hypothesized that zNa$_v$1.5b may adversely affect the production cardiac progenitor cells, thereby resulting in a reduced number of embryonic cardiomyocytes and perturbation of cardiac morphogenesis. To test this hypothesis, we examined formation of the day 1 heart tube in live *cmlc2*:GFP and *flk*:GFP embryos, which permitted visualization of the myocardial and endocardial layers of the developing heart, respectively (Figure 3.20). In both transgenic lines, we observed a significant reduction in the size of the developing heart tube following knockdown of zNa$_v$1.5b. Moreover, staining for markers of the atrial and ventricular myocardium (*amhc*, *vmhc*) at 30hpf by *in situ* hybridization indicated that both presumptive atrial and ventricular myocyte populations were comparably reduced (Figure 3.21). Taken together, these data suggested that the differentiation of cardiac progenitor cells may be perturbed in morphant embryos. To address this question, we studied the expression of *cmlc2* and *vmhc* at an earlier timepoint during in the developing bilateral cardiac primordia (16 somites). By *in situ* hybridization, both markers were reduced in expression, indicating a deficit in the production of adequate numbers of embryonic cardiomyocytes by differentiation in morphant embryos (Figure 3.22).

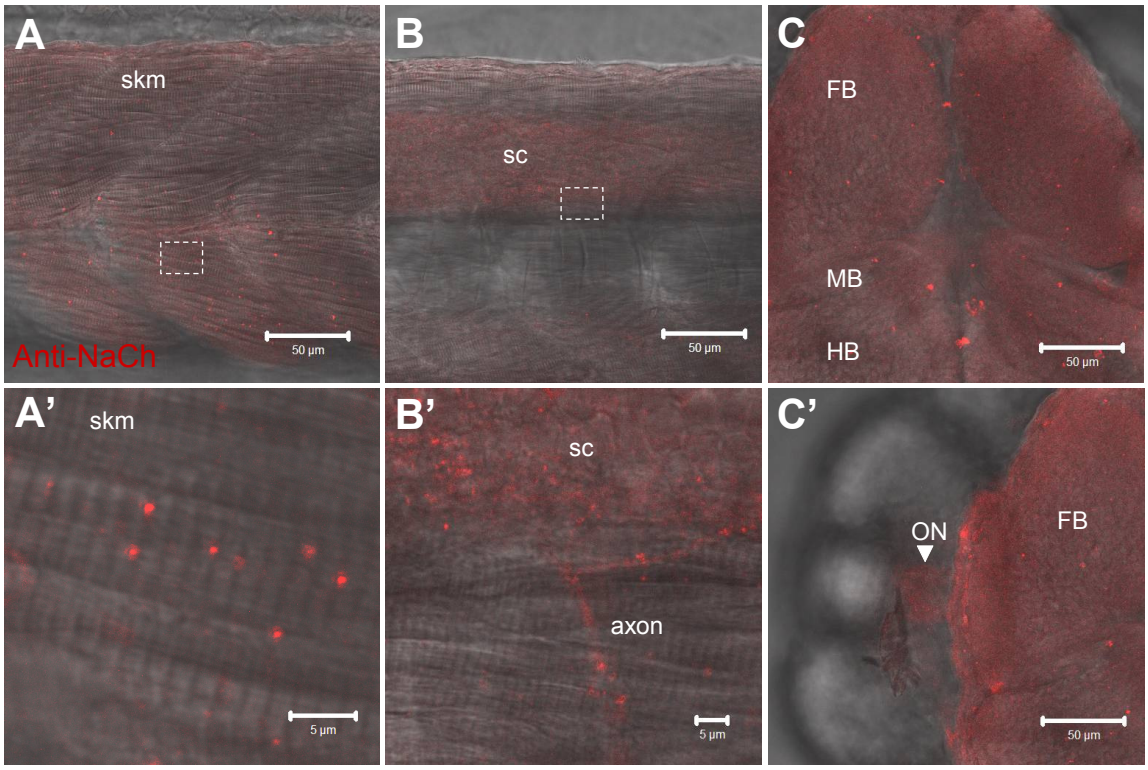

Figure 3.18: Sodium channels are highly expressed in zebrafish muscle and nerve on day 3. Pan anti-sodium channel antibodies detected abundant protein in muscle and in the peripheral and central nervous systems on day 3 (78 hours post-fertilization). Both diffuse and punctate staining of sodium channels are seen in skeletal muscle and in the central and peripheral nervous system. **(A, B, C, C')** Low power (scale = 50 microns). **(A', B')** Magnification of boxed area in A, B (scale = 5 microns). Skm = skeletal muscle; sc = spinal cord; FB/MB/HB = forebrain/midbrain/hindbrain; ON = optic nerve.

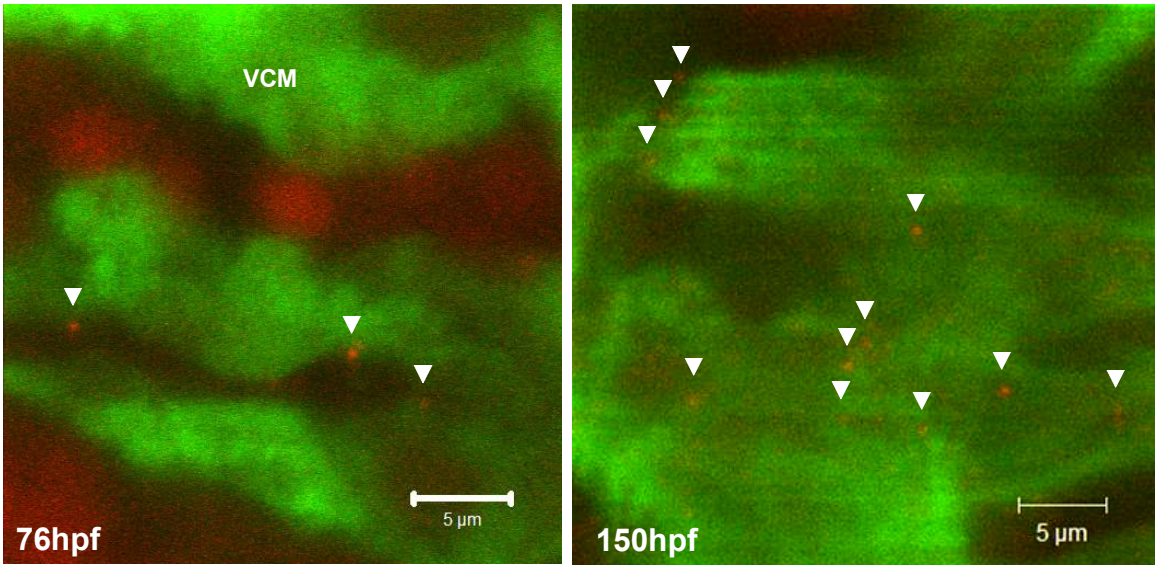

Figure 3.19: Sodium channel protein is upregulated in the heart between days 3 and 6 by immunohistochemistry (*cmlc2*:*GFP* embryos). Pan anti-sodium channel antibodies detected few sodium channel clusters per high powered field on day 3, but greater numbers on day 6. Representative optical sections shown above were 1 micron thick. Arrowheads point to putative sodium channel clusters on the membranes of embryonic cardiomyocytes. Scale bar = 5 microns.

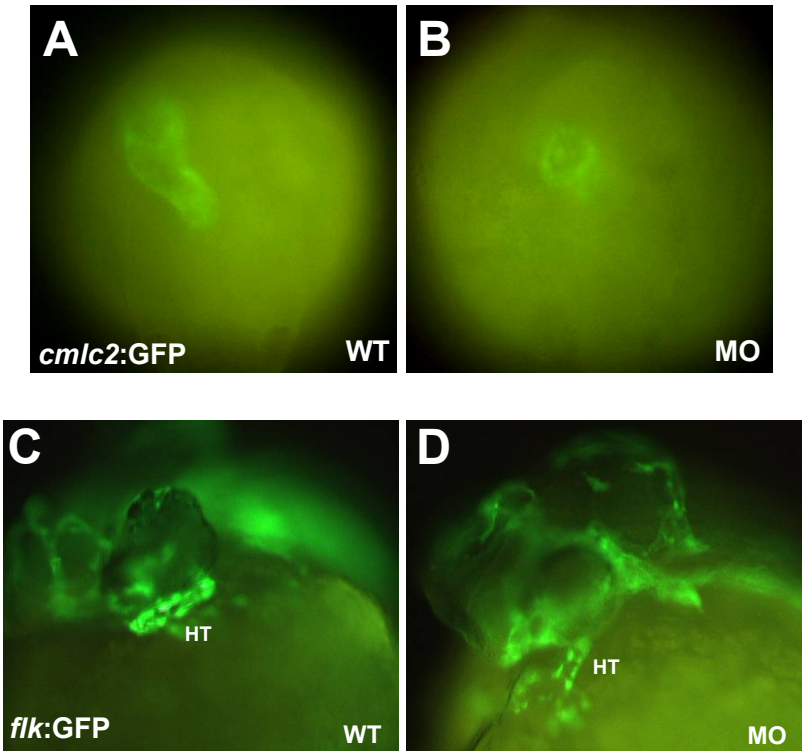

Figure 3.20: zNa$_v$1.5b morphant embryos displayed defects in the formation of the myocardial and endocardial layers of the heart tube at 30 hours post-fertilization. Transgenic zebrafish lines expressing GFP in the myocardium (*cmlc2*) or endocardium (*flk*) were used to study the effects of zNa$_v$1.5 knockdown on heart tube formation at day 1. Both myocardial and endocardial components were reduced in size. WT = wild type, MO = morphant, and HT = heart tube.

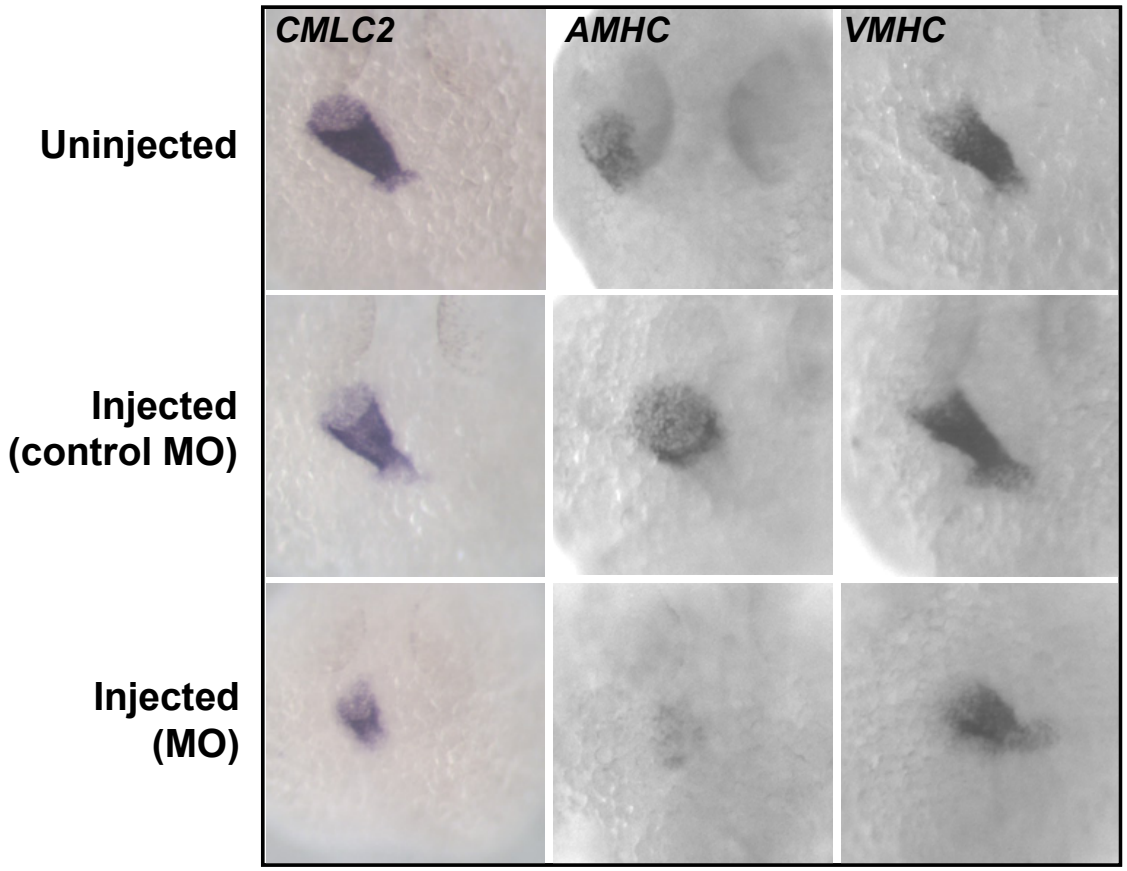

Figure 3.21: Knockdown of zNa$_v$1.5b comparably affected both presumptive atrial and ventricular cells of the developing heart tube at 30 somites. *In situ* hybridization was performed for genes encoding three different markers of the sarcomere, cardiac myosin light chain 2 (*cmlc2*, whole myocardium); atiral myosin heavy chain (*amhc*, atrial myocardium); and ventricular myosin heavy chain (*vmhc*, ventricular myocardium).

Reduced expression of markers of cardiac differentiation suggested one of several possibilities: first, morphant embryos had defects in the specification of cardiac progenitors; second, cardiac progenitors could have been normally specified but then failed to properly differentiate; third, cardiac progenitors could have been normally specified but had defects in proliferation that prevented their normal expansion prior to differentiation. To distinguish among these possibilities, we first stained embryos at 16 somites for expression of the homeodomain transcription factor *nkx2.5*. Since *nkx2.5* is normally expressed starting at 5-6 somites, we reasoned that defects in the field of cells expressing this marker at later stages would suggest and underlying perturbation of the specification of cardiac progenitors from mesoderm. Indeed, by *in situ* hybridization, we found the expression of *nkx2.5* to be dramatically reduced at 16 somites (Figure 3.22). Moreover, by incubating early embryos in the thymidine analog BrDU between 6 and 16 somites to label cycling cells, we found no qualitative difference in the field of proliferating cells with the bilateral stripes of cardiogenic mesoderm (Figure 3.24).

Therefore, we studied whether cardiac progenitors were appropriately specified from mesoderm. Early cardiogenic mesoderm is distinguished by the overlapping expression of a group of highly conserved regulatory genes belonging to the NK2, GATA, MEF2, T-box, and basic helix loop helix (bHLH) families of transcription factors (287-289). These genes act in concert to establish the cardiac cell fate and control different aspects of cardiac morphogenesis, as has been revealed by loss-of-function studies in animal models and mutations identified in human patients with congenital heart disease (288-290). In zebrafish, the expression of *nkx2.5* most specifically marks the pre-cardiac mesoderm in two bilateral stripes (291). The transcription factor *gata4* is expressed in a larger domain of anterior lateral mesoderm, whereas early *dHand* expression marks the anterior lateral mesoderm at early stages (292-295). By *in situ* hybridization at 6 somites, we found that zNa_v1.5b is required for the normal expression of both *nkx2.5* and *gata4* (Figure 3.23). Strikingly, the expression of *nkx2.5* was completely absent whereas *gata4* was reduced. To test whether zNa_v1.5b affected the viability of lateral mesoderm, we used the vital dye acridine orange (AO) to stain live embryos for dying cells. At 6 somites, we

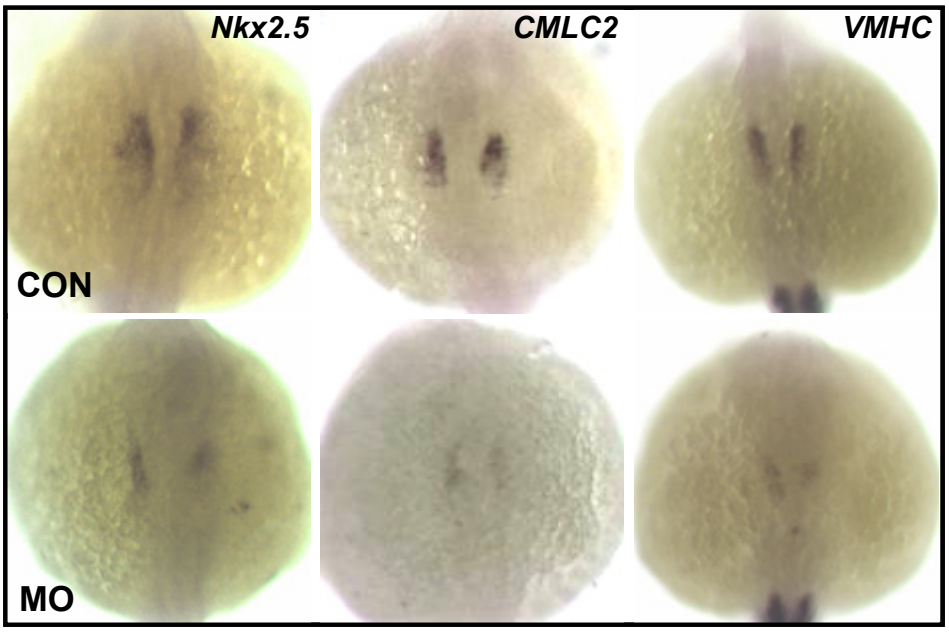

Figure 3.22: Cardiac gene expression domains are reduced in the differentiating cardiac primordia of morphant embryos at 16 somites. Differentiating bilateral cardiac primordia were stained for expression of the early cardiac transcription factor *nkx2.5* and for genes encoding components of the myocardial sarcomere. *cmlc2* = cardiac myosin light chain2; *vmhc* = ventricular myosin heavy chain. Expression of all three genes was reduced following knockdown of $zNa_v1.5b$.

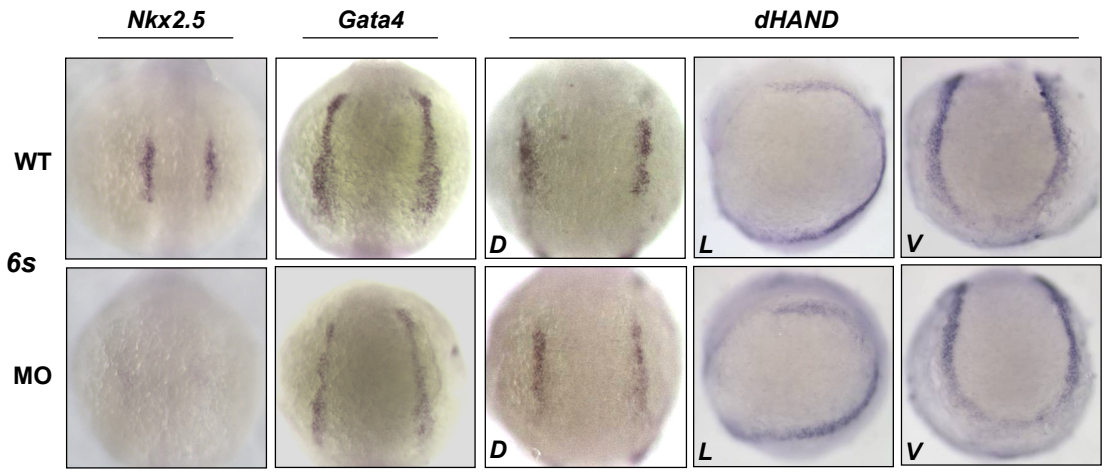

Figure 3.23: Knockdown of zNa$_v$1.5b perturbed the specification of cardiac mesoderm without affecting lateral mesoderm formation. Early cardiogenic fields (6 somites) were stained for expression of the transcription factors *nkx2.5, gata4, and dHand (Hand2)*. In morphants, expression of *nkx2.5* was absent and *gata4* was reduced. *dHand* expression was unaffected. D = dorsal, L = lateral, V = ventral; all three views are shown to highlight the complete expression domain of *dHand* in lateral mesoderm.

observed no qualitative difference in the number of cells labeled by AO in the lateral mesoderm of morphants versus controls (Figure 3.24). Moreover, we observed no change in the expression of *dHand*, indicating that defects in the formation or migration of anterior lateral mesoderm did not underlie the observed changes in expression of cardiac transcription factors (Figure 3.23). Taken together, these data demonstrated that cardiac-type voltage-gated sodium channels are required for the specification of cardiac mesoderm in the zebrafish embryo. Moreover, the timing of the patterning defects induced by knockdown of $zNa_v1.5b$ suggested that voltage-gated sodium channels may have important functions prior to the differentiation of excitable tissues. Consistent with this data, we readily detected transcripts of *zscn5Lab* in the early blastula and during gastrulation (prior to the onset of *nkx2.5*) with expression diminishing by 10 somites (Figure 3.25). As transcripts of *zscn5Lab* were undetectable on multiple occasions by conventional *in situ* hybridization techniques, however, we do not have data addressing the spatial localization of *zscn5Lab* expression during gastrulation or in early somitogenesis.

Excitability in cardiac lineage specification

Voltage-gated sodium channels depolarize membranes by permitting the rapid influx of Na+ ions into the cytosol (2). Our findings thus suggested the possibility that $zNa_v1.5b$ produces an electrical signal during gastrulation or in early somitogenesis that is required for the expression of cardiogenic transcription factors in mesoderm. To test the hypothesis that membrane depolarization mediated by $zNa_v1.5b$ is required for early cardiogenesis, we used two approaches. Since sodium current requires extracellular sodium, we reasoned that rearing fertilized embryos in sodium-free media starting from the 1 cell stage would dramatically perturb heart development. However, embryos reared in sodium-free media displayed no distinguishable defects in cardiac morphogenesis at day 1 or day 2. In a second approach, we reared dechorionated embryos starting at the 16 cell stage in solutions of modulators of sodium channel function or injected high concentrations of these compounds into the yoke sack of 1 cell stage embryos. Delivery of TTX, ATX II, veratridine, flecainide, and lidocaine by any means did not perturb cardiogenesis, despite

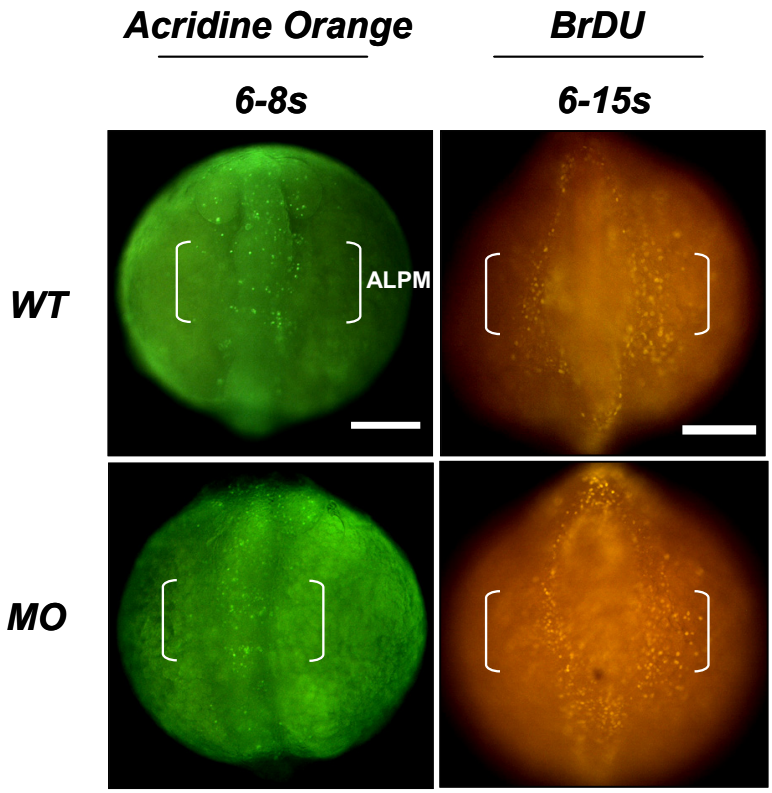

Figure 3.24: The morphant phenotype did not appear to be caused by loss of early progenitor cell viability or defects in the proliferation of cells within lateral mesoderm. Live embryos were stained at 6 somites with the vital dye acridine orange to label dying cells. Embryos were also incubated with BrDU between 6 and 15 somites to label all proliferating progenitors in lateral mesoderm. No differences were appreciated in either assay upon qualitative inspection. Brackets mark the anterior lateral plate mesoderm (ALPM).

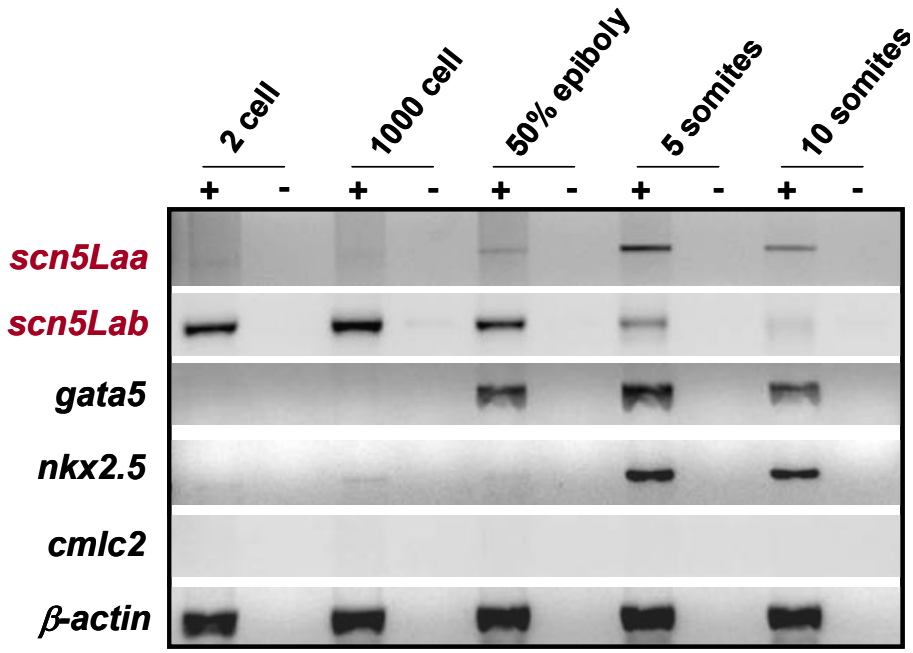

Figure 3.25: RT-PCR detected complementary expression of both *scn5Laa* ($zNa_v1.5a$) and *scn5Lab* ($zNa_v1.5b$) during zebrafish gastrulation. See methods for details.

clear physiological evidence at days 1 and 2 that non-cardiac sodium channels were either profoundly blocked or activated (total paralysis, hyperkinetic movements) (Figure 3.26). To determine whether other known channels that contribute to cardiac action potential generation play a role in early cardiac development, we similarly reared embryos from 16 cells onwards in micromolar concentrations of the L-type calcium channel blocker nisoldipine, the L-type/T-type calcium channel blocker mibefradil, and the HERG blocker E-4031. In every instance, embryos reared in solutions of these compounds displayed profound perturbations of heart beat in the absence of any defects in heart formation. Moreover, we used high concentrations of an antisense morpholino targeting ZERG to knockdown expression of this channel (296), and similarly, no abnormalities of heart development were observed. Taken together, these results strongly suggest that ion channel block (by toxins or by altering extracellular solution) generates abnormal heart beating but does not result in developmental abnormalities. These data thus point to the concept that voltage-gated sodium channels play a heretofore-undescribed, non-electrogenic role in cardiogenesis.

Follow-up studies of the function of zNa$_v$1.5Lb (zscn5Lab)

Cloning of the full-length cDNA sequence of *zscn5Lab* permitted the design of additional morpholino oligonucleotides to confirm our initial findings. An antisense morpholino generated against the E6/I6 splice junction also clearly perturbed splicing of *zscn5Lab* but produced a milder heart development defect that manifested that was most obvious between days 3 and 4. An E6/I6 5-mismatch control morpholino injected at the same dose did not produce any abnormal phenotype. To test whether the zNa$_v$1.5b protein (and not the mRNA) is required for heart development, we generated a morpholino targeting the translation initiation site. Again, knockdown of zNa$_v$1.5b was observed to cause defects in heart development (reduced chamber size, absence of looping) with subsequent embryonic lethality, the severity of which was comparable to the E6I6 splice-site morpholino. In summary, all three active morpholinos used in this study produced a similar spectrum of defects in heart development with the following order of severity: E24/I24 (1-2ng/embryo) > E6/I6 (3-4ng/embryo) = ATG (5-6ng/embryo).

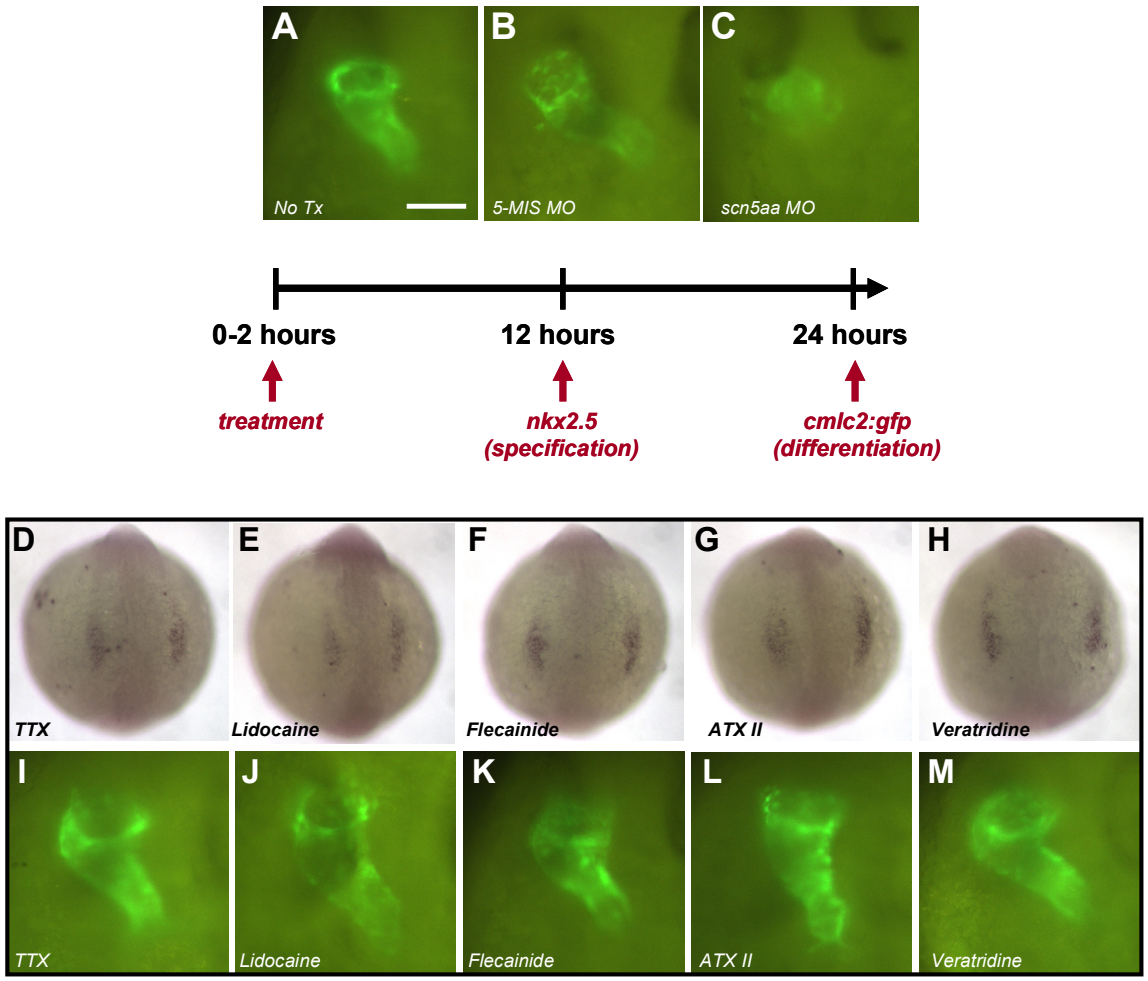

Figure 3.26: Regulation of the cardiac cell fate by zNa$_v$1.5b is independent of its activity as a sodium channel. Early embryos (0-2 hours) were either injected with sodium channel modulators or dechorionated and immersed in drug-containing solutions. **(D-H)** Specification was assayed by expression of *nkx2.5* at 6 somites. **(I-M)** Differentiation was assayed by visualizing heart tube formation in live *cmlc2*:*GFP* embryos. **A-C** shows the effect of morpholino.

Function of zNa$_v$1.5La (zscn5Laa) in zebrafish embryos

Low doses of morpholinos directed against the translation start site (4ng/embryo) and against the E3I3 splice junction (2ng/embryo) each produced defects of cardiac morphogenesis, in addition to reduced head size and body length (Figure 3.27). Five-mismatch control morpholinos directed against each of these sites, however, did not produce any noticeable defects (Figure 3.27). Wheras wild-type and control morpholino-injected clutchmates displayed normal development of atrial and ventricular chambers and initiated looping by 36 hours post-fertilization (hpf), zNa$_v$1.5La morphants retained tube-like hearts and failed to form normal cardiac chambers even at 60-72hpf (Figure 3.27). These results lend further strong support to the idea that cardiac-type sodium channels play important roles in heart development.

Since each morpholino directed against zNa$_v$1.5La consistently produced a severe phenotype, we characterized the cardiac defects in these morphants in more detail using similar approaches to zNa$_v$1.5Lb. Atrial and ventricular myocytes arise from distinct populations of progenitor cells that exhibit genetic differences from their earliest stages of differentiation (297;298). At 54-60 hpf, after chamber formation, atrial and ventricular myocytes exhibited striking differences in cellular appearance and patterning as imaged in wild type *cmlc2*:*GFP* transgenic embryos. While atrial cells displayed less *cmlc2* promoter activity and were irregular in shape and loosely-packed, ventricular myocytes displayed greater *cmlc2* promoter activity, were generally more elliptical in shape, and densely-packed within the chamber wall (Figure 3.28). These early-appearing cellular differences, which likely reflect the future functions of the atrium as a receptacle of low pressure venous blood and the ventricle as a high-pressure pump that maintains systemic circulation, are preserved in morphant hearts and suggest normal atrial and ventricular patterning (Figure 3.28). At the genetic level, this was confirmed by double immunostaining with S46 and MF20 antibodies. Although morphant chambers were patterned normally on day 2, these hearts appeared to be dramatically reduced in cell number (Figure 3.28). Similar reductions were observed qualitatively by imaging both control and morphant hearts on day 4 of development, when the ventricular chamber has entered a phase of concentric growth.

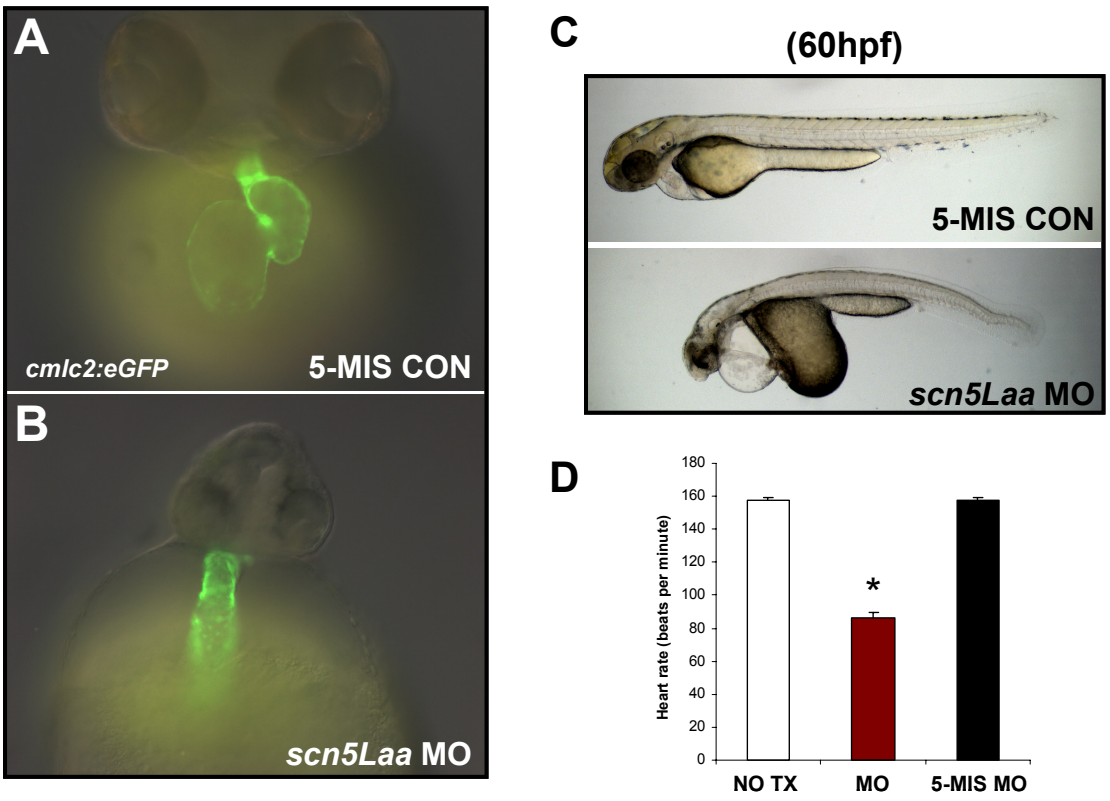

Figure 3.27: Knockdown of zNa$_v$1.5a (*scn5Laa*) resulted in severe defects in heart development and function as shown on day 2. (A, B) Morphant embryos have reduced heart and head size and aberrant looping. **(C, D)** Morphant embryos are also smaller in total body size and exhibit bradycardia compared to control embryos.

Confocal analysis revealed that whereas wild-type embryonic hearts added cells to the ventricular wall on the interior to produce a chamber that is multiple cell layers thick, morphant hearts maintained the single cell layer of earlier stages (Figure 3.29). To quantify these differences in embryonic heart cell number, we imaged morphants in a different transgenic line, *cmlc2:dsRed-nuclear*, in which the nuclear label facilitated accurate quantification of total cardiac cell number in embryos in their native condition (Figure 3.30). This analysis revealed an average of 45% less cells in morphant hearts compared to control morpholino-injected hearts on day 3.

To determine whether reduced expression of $zNa_v1.5La$ affected the production of cardiac progenitor cells, we imaged and quantified the total number of newly differentiated myocytes in *cmlc2*:*GFP* transgenic embryos. As shown in Figure 3.31, knockdown of $zNa_v1.5La$ resulted in a significant decrease in the number of progenitors. These defects in cell number were correlated with the reduced expression of markers of differentiation (*cmlc2*, *vmhc*), and the loss of expression of *nkx2.5* at 6 somites by both *in situ* hybridization and quantitative PCR (Figure 3.32). Despite strong evidence supporting a *gata5-nkx2.5* signaling axis in early zebrafish cardiogenesis (299;300), we found the expression of *gata5* to be normal in morphant embryos (Figure 3.32). These data suggested that $zNa_v1.5La$ either acts downstream of *gata5* in this signaling axis, or regulates the expression *nkx2.5* by a *gata5* independent mechanism, similar to *Fgf8* (see Chapter 5).

Cell-autonomous role for $zNa_v1.5La$ in cardiac fate specification

By morpholino knockdown, our data demonstrated that $zNa_v1.5La$ plays a critical role in the patterning of pre-cardiac mesoderm. Since earlier data suggested that sodium channels act via a non-electrogenic mechanisms to regulate specification of early cardiac cells, we transplanted late-stage blastomeres between the margins of embryos at 30% epiboly, to determine whether morphant cells more readily adopt the cardiac cell fate in a wild-type background. As shown in Figure 3.33, labeled wild-type cells transplanted into a wild-type host embryo adopted cardiac cell fates in nearly 26% of embryos. Even when placed in a wild-type

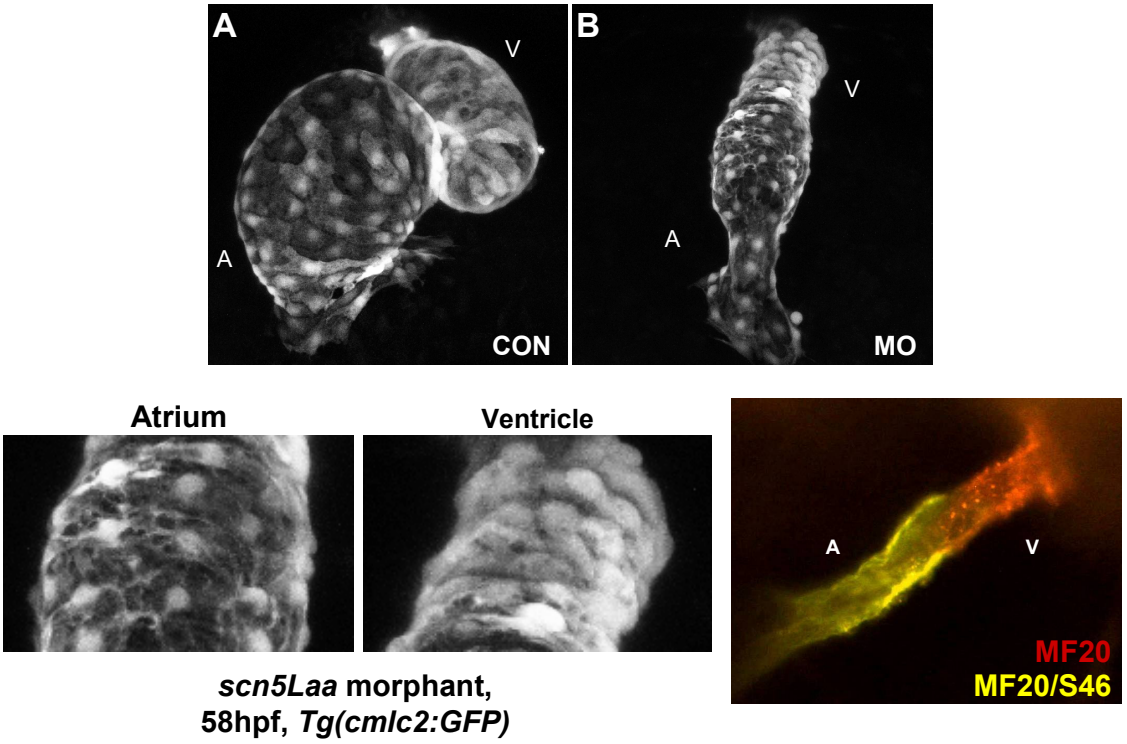

Figure 3.28: zNa$_v$1.5a (*scn5Laa*) morphants retained normal chamber-specific cellular morphology and differentiation as observed by confocal microscopy and double immunostaining. (A, B) Morphant embryo hearts are smaller and unlooped compared to control embryo hearts. A = atrium, V = ventricle, CON = control, and MO = morpholino-injected. **(C, D)** Higher magnification of the morphant atrium and ventricle revealed normal chamber-specific differences in cellular morphology. **(E)** Double immunostaining with MF20 and S46 antibodies confirm that morphant hearts have normal chamber-specific differentiation.

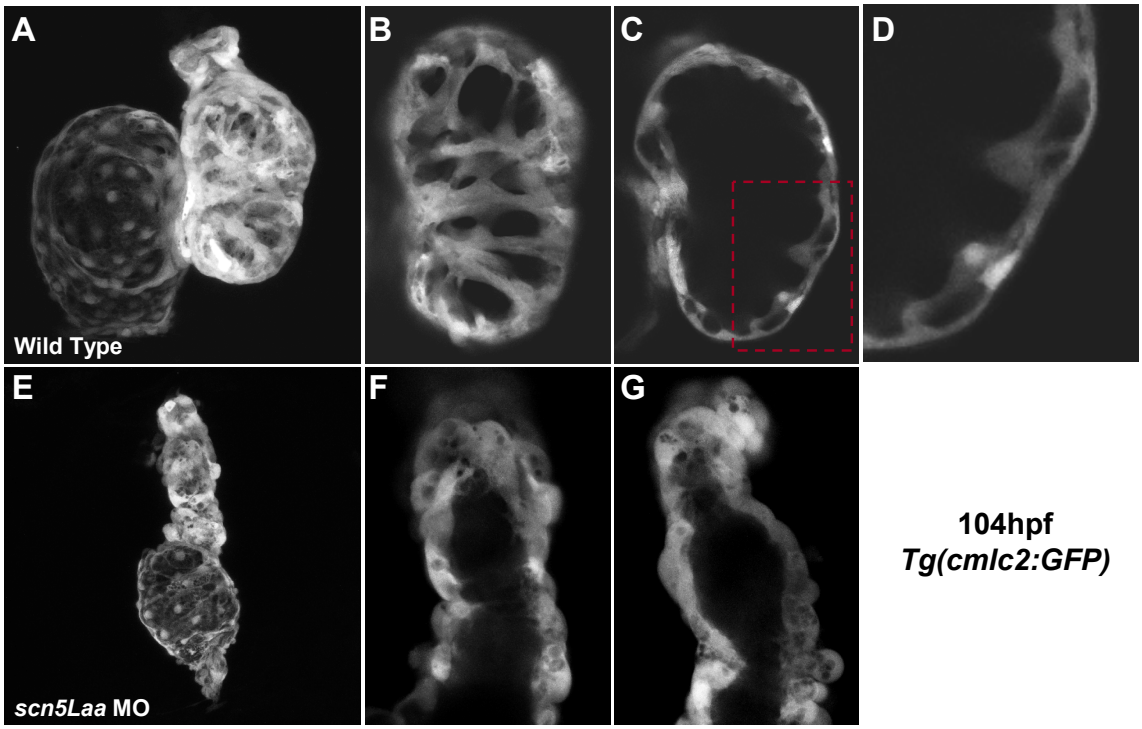

Figure 3.29: zNa$_v$1.5a (*scn5Laa*) morphant ventricles did not develop multiple cell layers through day 4. Confocal imaging was used to optically section through the ventricular chamber of both wild type and *scn5Laa* morphant hearts. **(A)** Confocal reconstruction of wild type embryo heart at 104 hours post-fertilization. **(B)** Optical sectioning throught the wild type ventricle revealed new cardiomyocytes being added to the interior of the chamber to thicken the wall. **(C)** Wild type ventricles have two layers of cardiomyocytes at this timepoint. **(D)** Higher magnification of red box from figure C. **(E)** Confocal reconstruction of morphant embryo heart at 104 hours post fertilization. **(F, G)** *scn5Laa* morphant ventricles have only one cell layer. F and G represent ventricles of two different morphant embryos.

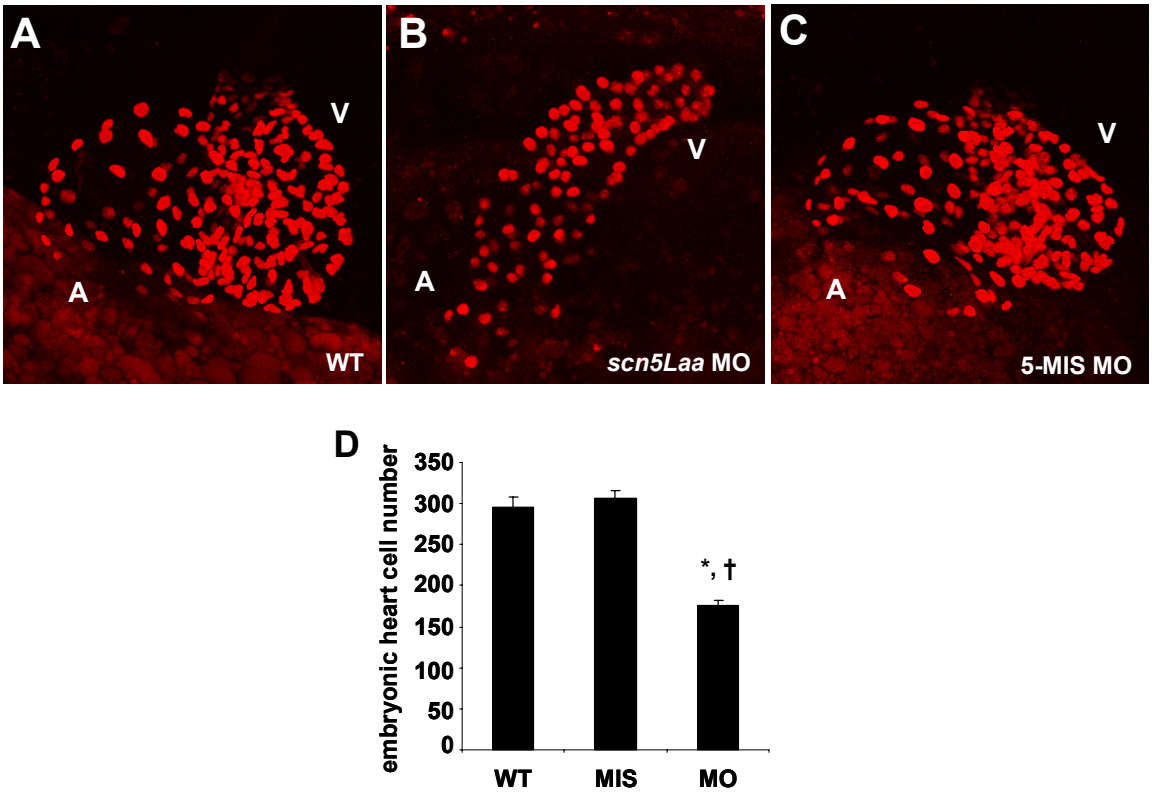

Figure 3.30: zNa$_v$1.5a (*scn5Laa*) morphant embryos displayed 45% less cardiomyocytes in the transgenic *cmlc2*:*dsRed-nuclear* background. (A-C) Confocal reconstructions of the embryonic heart in *Tg(cmlc2:DsRed2-nuclear)* embryos at 78 hours post-fertilization. *Scn5Laa* is required for normal embryonic heart cell number. A and V indicate the atrium and ventricle, respectively. **(D)** At 60-62 h.p.f., *scn5Laa* morphant hearts (MO1, n=8) have significantly fewer embryonic cardiomyocytes compared to the hearts of wild type (WT, n=4) and MIS1-injected (MIS1, n=5) clutchmates. Results are mean ± s.e.m; n=number of embryos analyzed. *, $P<0.001$ versus wild-type and †, $P<0.001$ versus MIS1-injected, ANOVA.

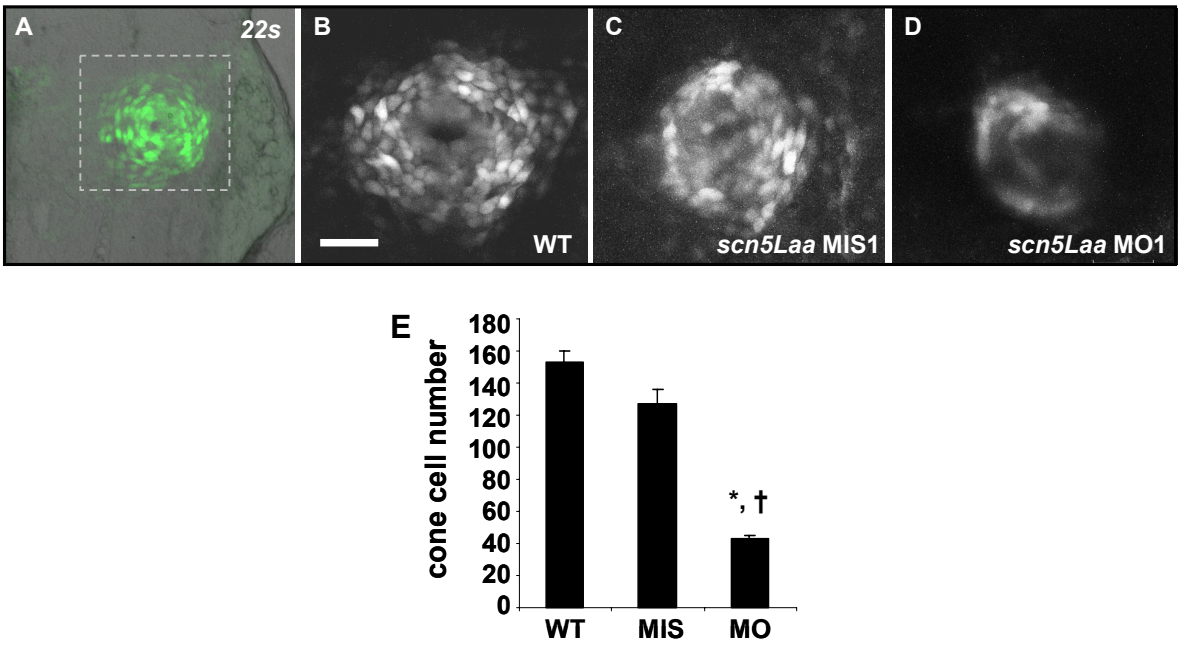

Figure 3.31: zNa$_v$1.5a is required for the differentiation of appropriate numbers of cardiac progenitors. (A-D) Confocal reconstructions of the developing heart cone in *Tg(cmlc2:GFP)* embryos at the 22 somite stage. B-D are higher magnification images of the box shown in A. *Scn5Laa* is required for the normal number of newly differentiated embryonic cardiomyocytes. Scale bar = 50μm. **(E)** *Scn5Laa* morphant heart cones (MO1, n=4) have significantly fewer differentiating cardiomyocytes compared to the heart cones of wild-type (WT, n=6) and MIS1-injected (n=3) clutchmates. Results are mean ± s.e.m; n=number of embryos analyzed. *, P<0.001 versus wild-type and †, P<0.001 versus MIS1-injected, ANOVA.

background, however, morphant blastomeres were significantly less likely to become cardiomyocytes, as indicated by a lower percentage of embryos with donor cells in the heart (approximately 14%) (Figure 3.33). Morphant cells, however, contributed successfully to a number of other mesoderm-derived lineages including blood and muscle (Figure 3.33). These data suggested that cardiac sodium channels are likely to act cell-autonomously. Reciprocal experiments are in progress to determine the frequency with which wild-type cells adopt cardiac cell fates in morphant embryo backgrounds.

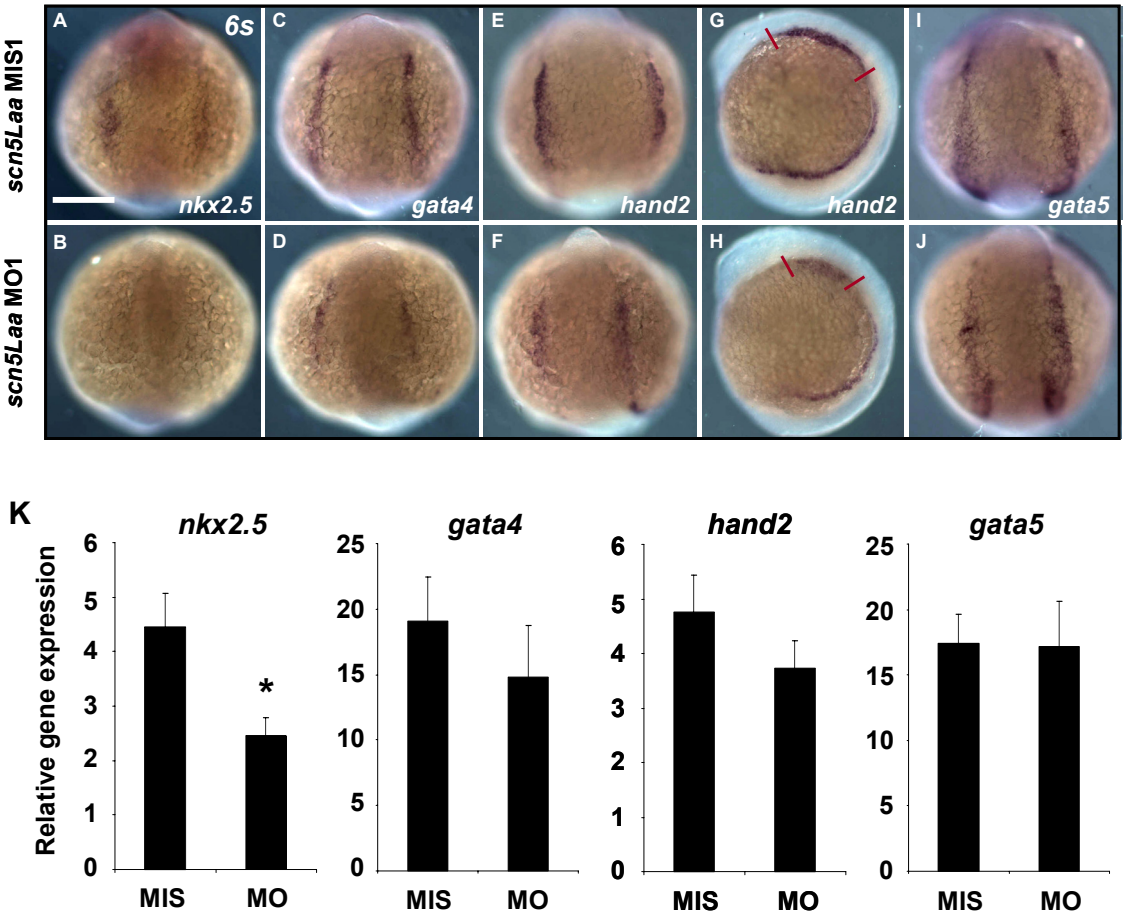

Figure 3.32: Formation of the pre-cardiac mesoderm is perturbed in zNa$_v$1.5a (*scn5Laa*) morphants. (A-J) Analysis of gene expression in the early heart-forming region of anterior lateral plate mesoderm at the 6-somite stage by *in situ* hybridization. Embryos injected with *scn5Laa* translation inhibitor morpholino (MO1) (B, D, F, H) had reduced expression of *nkx2.5*, *gata4*, and *hand2* but no change in *gata5* expression (J) compared to embryos injected with 5-mismatch control morpholino (MIS1) (A, C, E, G, I). All embryos shown are from the same injected clutch. Scale bar = 200μm. **(K)** Real-time quantitative RT-PCR performed using independent clutches of embryos also revealed significantly reduced *nkx2.5* expression but no change in *gata5* expression following injection of MO1 compared to injection of MIS1 control morpholino. Results are mean ± s.e.m for three independent experiments performed in triplicate. *P*<0.05 for *nkx2.5*, T-test. Overall expression levels of *gata4* and *hand2* were reduced by real time PCR, but differences were not statistically significant.

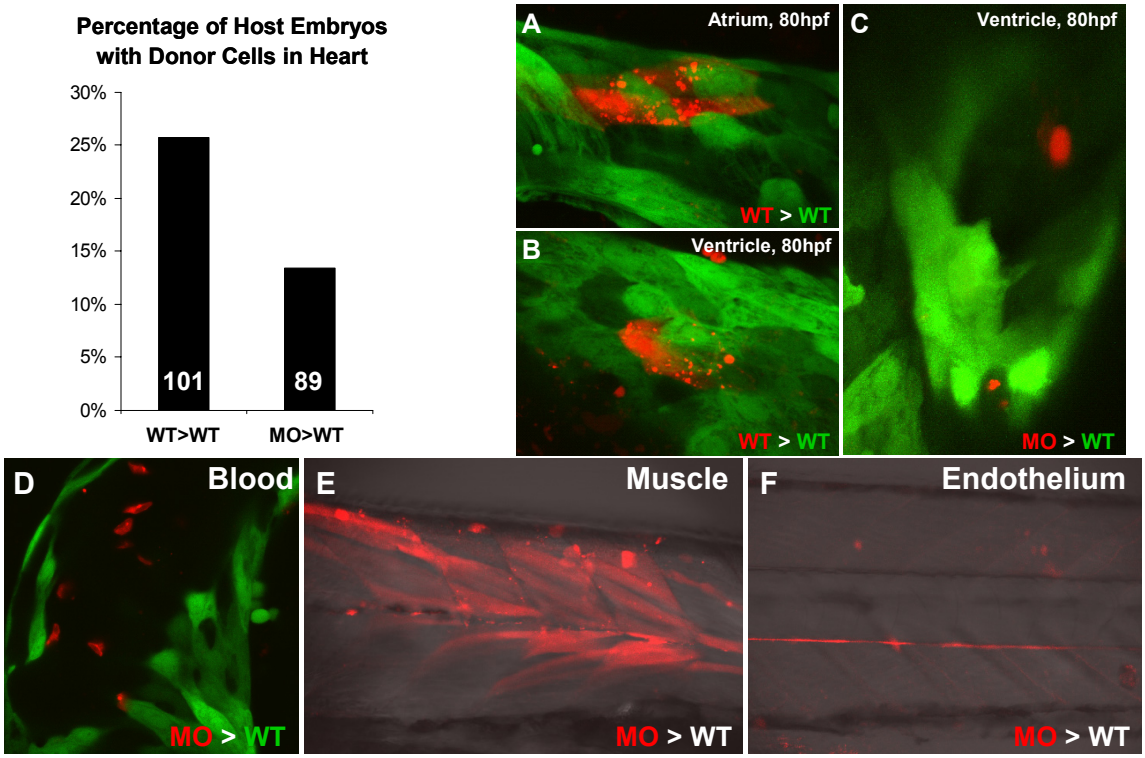

Figure 3.33: zNa$_v$1.5a sodium channels may act cell-autonomously in mesoderm to promote the cardiac cell fate. Labeled morphant blastomeres transplanted to the margin of the wild type blastula displayed reduced probability of entering the cardiac lineage than wild type control cells. **(A, B)** Multiple wild type cells were typically seen in the atrium and ventricle of individual host embryos. **(C)** Conversely, morphant cells were infrequently observed in host hearts despite differentating into other mesoderm-derived lineages **(D-F)**.

Discussion

Na_v1 voltage-gated sodium channels underlie the upstroke of the action potential and are thus the principal determinants of membrane excitability in the nervous system, skeletal muscle, heart, and other tissues. Using zebrafish as a model system, we have identified a critical role for cardiac-type sodium channels at the earliest stages of organ formation, well in advance of their role in mediating excitability in the beating heart. By use of antisense-mediated gene knockdown, we found that reduced expression of either $Na_v1.5La$ or $Na_v1.5Lb$ in the zebrafish embryo disrupted the patterning of early cardiogenic mesoderm, therein compromising the production of sufficient numbers of progenitor cells for cardiac morphogenesis. By independently evaluating the phenotypic consequences of reduced sodium channel expression and perturbed sodium channel-mediated excitability, we found that cardiac-type sodium channels act via a previously-unappreciated, non-electrogenic mechanism to regulate early cardiac development. Moreover, cellular transplantation studies revealed that sodium channels are likely to be cell-autonomously required for specification of pre-cardiac mesoderm. Our results thus suggest that sodium channels, which are among the most phylogenetically recent channels in the ion channel superfamily (4;301), have been recruited in vertebrates for two mechanistically-distinct roles: 1. in the mature heart, cardiac-type sodium channels depolarize the membrane to initiate action potentials; 2. during development, the same sodium channels act by a non-electrogenic mechanism to regulate organ formation. Moreover, our results describe the earliest-known function of any vertebrate voltage-gated sodium channel during development.

Limitations

One primary limitation of this study was the use of morpholino antisense oligonucleotides, which in zebrafish have been demonstrated to have off-target effects (302). Although the targeting of *scn5Laa* by both translation and splice morpholinos produced consistent developmental abnormalities, morpholinos directed against *scn5Lab* (ATG, E6/I6, and E24/I24) resulted in defects that were variable in severity. Without antibodies against these proteins, we cannot predict whether the variability in phenotype resulted from differences in the efficiency of

knockdown at the protein level or from alternative mechanisms. Notably, studies of *scn5a* in mice revealed important gene-dose effects in cardiac development: whereas mice homozygous null for *scn5a* (-/-) displayed defects in early cardiac morphogenesis, heterozygous mice (+/-) were born with structurally normal hearts. Interestingly, morpholinos directed against E24/I24 of *scn5Lab* required the lowest dose but elicited the strongest effects. Since the aberrant mRNA splice products induced by E24/I24 appeared to be stable (Figure 3.7), it is possible that the predicted truncated zNa_v1.5b protein (1458 amino acids) persisted and acted in a dominant negative fashion to repress unperturbed channels (zNa_v1.5a or zNa_v1.5b) or other proteins. Although a single α subunit polypeptide is required to form the sodium channel pore, some evidence suggests, for example, that sodium channel proteins may interact before they reach the membrane (303). Another limitation of our studies is the lack of direct evidence of sodium channel protein during gastrulation, the period of development when our morpholinos appear to be exerting their effects. However, the combination of expression data (RT-PCR) and the use of morpholinos directed against the translation initiation site of zNa_v1.5a together suggest that the observed phenotypes are mediated by perturbations of sodium channel protein.

Molecular basis of heart rhythm in the zebrafish embryo

The first large-scale forward genetic screens in zebrafish uncovered a number of mutants displaying complex arrhythmias, demonstrating that the simple two-chambered heart of a young fish embryo could manifest physiologically-meaningful rhythm phenotypes and would be a useful model to study the molecular determinants of cardiac impulse propagation (172;173). Moreover, electrophysiological studies of dissociated and cultured embryonic zebrafish cardiomyocytes revealed currents typical of multiple families of cardiac ion channels well-studied in other species (174). The initial objective of our studies was thus to apply a reverse genetics approach to establish a loss of functional model for cardiac sodium channel function in zebrafish embryos, with the larger goal of establishing an experimental platform for clarifying the role of channel-associated proteins in the regulation of heart rhythm. Our identification of a relatively late functional requirement for sodium channels in the developing zebrafish heart (commencing

between days 4 and 5) was unanticipated given that multiple, well-characterized determinants of excitability and calcium homeostasis in the mature myocardium have also been demonstrated to be critical to early heart beating in this model (262;270;296;304-308). In two independent studies, for example, reduced function of the repolarizing K^+ channel encoded by *kcnh2/zerg* by mutation or pharmacological blockade resulted in bradycardia and AV block in the early beating heart (262;296). Additional *kcnh2* mutant lines displayed ventricular standstill, delayed repolarization, and prolonged action potentials characteristic of the hereditary long QT syndrome in humans (307). In the zebrafish *tremblor* mutant, reduced function of the cardiac Na^+/Ca^{2+} exchanger (NCX) resulted in atrial fibrillation and ventricular standstill from the very outset of cardiac function on day 1 (304;305). The *island beat* mutant, which was found to harbor a nonsense mutation in a cardiac-specific L-type voltage-gated calcium channel, similarly presented with atrial fibrillation and a silent, non-contractile ventricle. Finally, reduced function of the Na^+-K^+ ATPase by mutation or pharmacological blockade resulted in significant slowing of the embryonic heart rate (306). As we observed for cardiac sodium channels, many of these determinants of nascent excitability were found to play different roles in the atrium and the ventricle. These data demonstrate that the functional determinants of both excitability and calcium homeostasis, well-appreciated to be distinct in different chambers of the mature heart, are established in chamber-specific processes from very earliest stages of heart development.

The role of sodium channels in embryonic heart rhythm

To assay for the role of sodium channels in the embryonic heart, we employed three well-characterized toxins that have distinct binding sites and mechanisms of action: the sodium channel "blocker" tetrodotoxin (TTX) and the channel "activators" anemone toxin II (ATX II) and veratridine (284;285). The arrhythmias elicited by TTX were consistent with impaired ventricular conduction due to reduced sodium channel availability (133). The tonic contraction and arrhythmias induced by ATX II on day 3 may have resulted from a loss of the sodium gradient across the membrane through persistently open sodium channels. Obliteration of the sodium gradient likely inhibited the function of one of the primary mechanisms of calcium extrusion from

the cytosol of embryonic myocytes after systole, the Na^+-Ca^{2+} exchanger (304;305), possibly leading to calcium overload during diastole and tonic contraction.

Our observation of a late requirement for voltage-gated sodium channels in zebrafish embryonic heart function (between days 4 and 5) is consistent with the findings of previous studies conducted in mouse and chick embryos and murine cell lines. Although the murine heart tube starts to beat at approximately E8.5, cultured myocytes isolated from E11-E13 mouse hearts displayed only small sodium currents with a pattern of functional expression that was suggested to be inconsistent with sodium channels being the primary mechanism of depolarization in the early mammalian heart (309). In cardiomyocytes differentiated *in vitro* from murine embryonic stem (ES) cells, Na^+ currents were absent from early beating cells and were detectable only 3-4 days after the appearance of outwardly-rectifying K^+ currents and inward Ca^{2+} currents (310). Similarly, studies of differentiating P19 embryonic carcinoma (EC) cells indicated that sodium currents played no role in the electrical activity of early, differentiating cardiomyocytes (311-313). Similar observations were made by a number of laboratories studying the molecular determinants of early cardiac excitability in chick embryos over two decades ago, who found that TTX produced limited effects on early excitability but more profoundly inhibited action potentials at later developmental stages (286;314-324). These studies also revealed that the appearance of sodium channel-dependent action potentials coincided with a dramatic increase in the number of available channels and hyperpolarization of the resting membrane potential (sodium channels are inactivated at depolarized membrane potentials) (286;314). Similarly, the results of our studies using both channel toxins and immunohistochemistry support the concept that these sodium channels are dramatically upregulated during the course of heart development. Taken together, multiple lines of evidence from different model systems thus suggest that voltage-gated sodium channels are essential for cardiac excitation only after the earliest steps of cardiac morphogenesis have been completed. A dynamic developmental program for electrophysiology characterized by changes in the expression and function of ion channel genes appears to accompany early morphogenesis of the vertebrate heart.

Our delivery of sodium channel toxins into the systemic circulation of early embryos at day 1 revealed pronounced effects on movement and sensation that were consistent functional expression of sodium channel proteins in muscle and nerve tissue prior to heart. On day 3, we similarly observed dense sodium channel staining in skeletal muscle, spinal cord, and brain but minimal staining in heart, using antibodies that recognize a conserved epitope present in all sodium channel isoforms. In evolutionary terms, this may suggest that voltage-gated sodium channels, which are thought to have evolved as an adaptation that permitted high-frequency action potentials in the evolving nervous systems of early vertebrates, are a relatively recent innovation in the heart (1;325). Since slow conduction is arrhythmogenic in the mammalian heart (133), we speculate that mechanisms permitting increased conduction velocity may have become adaptive as early vertebrate hearts grew in size and elaborated chambers with thick myocardial layers. This possibility is supported by the finding that sodium channels play no functional role in simpler, invertebrate heart structures including the contractile dorsal vessel in *Drosophila* and the contractile pharynx in *C. elegans*, despite evidence of expression of an array of other ion channel proteins in these tissues. Evidence to test this hypothesis could be derived from studying the mechanisms that underlie cardiac excitability in the simple, tubular hearts of invertebrate chordates such as ascidians or amphioxus (288).

Role of heart function in heart development

Given the late role for sodium channels in regulating heart rhythm in fish, mice, and chick embryos, our finding that reduced expression of $Na_v1.5$-like voltage-gated sodium channels resulted in severe defects in cardiac chamber formation suggests that the primary function of sodium channels in early embryos is to support organ development, not organ function. Notably, loss-of-function models of the cardiac L-type calcium channel, the Na^+-Ca^{2+} exchanger, and the Na^+-K^+ ATPase proteins all displayed variable defects of cardiac morphogenesis in zebrafish (270;304;306;308). Although these data would initially seem to support the hypothesis that early cardiac function is required for the development of normal cardiac form, zebrafish *silent heart* mutants which have mutations in a cardiac troponin gene that rendered their hearts completely

non-contractile displayed normal chamber formation, patterning, and looping through day 2 (326). These findings strongly suggested that early heart development is driven by an intrinsic genetic program that is not significantly influenced by function. However, because *silent heart* mutants displayed normal excitability and calcium cycling, we initially hypothesized that excitation (the well-established function of sodium channels) might be required for cardiac morphogenesis independent of contraction. In addition to being required for contraction, for example, Ca^{2+} is an integral second messenger that acts through numerous proteins including calcium-calmodulin-dependent kinases, the calcium-activated phosphatase calcineurin, and calcium-modulated transcription factors such as CREB, NFAT, and Elk-1 to connect membrane excitability to changes in gene expression (327-331). Moreover, the results of numerous prior studies had demonstrated that sodium channel-mediated action potentials are required for the normal development of other excitable tissues such as the nervous system (332-336). Despite these previous findings, our use of the L-type calcium channel blocker nisoldipine to inhibit calcium entry and silence the heart from the very outset of beating did not produce any early defects in cardiac morphogenesis.

Although other membrane proteins that regulate excitability and/or calcium homeostasis have been shown be required for normal zebrafish heart development, the mechanisms by which they act in cardiac morphogenesis are not well understood. In the *small heart* and *heart and mind* mutants, loss of function of the zebrafish cardiac Na^+/K^+ ATPase resulted in diminished heart size because of an early defect in heart tube elongation (306;308). However, mutation of a related transporter, the cardiac Na^+/Ca^{2+} exchanger (*NCX*), did not affect heart tube formation despite being strongly expressed in this early structure (304;305). Similarly, although blocking calcium entry into nascent myocytes with nisoldipine did not affect early heart development, loss of function of a cardiac-specific, L-type voltage-gated calcium channel (the *island beat* mutant) resulted in striking defects ventricular size attributed to perturbation of the growth and proliferation of embryonic myocytes (270). The discrepancies between these findings suggests that like sodium channels, calcium channels may have effects in the developing heart that are independent of calcium entry, as was recently demonstrated in neurons (337).

Scn5a in the mouse heart

In this study, we found an unexpected role for cardiac sodium channels in patterning the pre-cardiac mesoderm early in somitogenesis. Because of the novelty of the findings, future studies should aim to verify our results in mammalian models. Mice lacking *scn5a* (-/-) were embryo-lethal at E10 and displayed severe abnormalities of development of the ventricular myocardium, with a sparing of other developing heart structures including the endocardial cushions, the common atrial chamber, and the truncus arteriosus. The early lethality of these mice and the severity of the defects were reminiscent to some degree of the phenotypes of loss-of-function mouse models early cardiac transcription factors (289;338-340). However, the timepoint at which *scn5a* is first required for cardiac development is unknown. It is similarly not known when and where *scn5a* is expressed prior E9.5, when our data demonstrated its expression in the atrial and ventricular myocardium, and whether expression of *scn5a* will be detected in the heart tube (E8.25-8.5) or early heart fields of the cardiac crescent (E7.75). Loss of function mouse models of early cardiogenic transcription factors also typically die on E10, but often display perturbed development at much earlier timepoints, consistent with their early expression patterns. Mice null for the T-box transcription factor *Tbx5*, for example, died on E10 with hypoplastic sinoatrial structures and left ventricles (341). The expression of *Tbx5*, however, was detected in the cardiac crescent on E7.75, and then was subsequently found in a graded fashion in the developing heart tube before b;eing selectively expressed in the atria and left ventricle but not the right ventricle or outflow tract of the maturing heart (342). Moreover, close examination of *Tbx5*$^{-/-}$ embryos at timepoints prior to lethality revealed developmental defects that first manifest at E8.5 with aberrant heart tube formation. Analogously, the embryonic lethality of *scn5a*$^{-/-}$ mice on E10 is likely to reflect an early expression pattern for *scn5a* and an important functional role for $Na_v1.5$ in cardiogenesis prior to chamber formation.

A non-electrogenic role for cardiac sodium channels

The tractability of externally-fertilized zebrafish embryos permitted us to directly test whether sodium channels influence cardiac development by electrogenesis or alternative

mechanisms. Neither removal of sodium from the media in which early embryos were reared, nor prolonged exposure of embryos to modulators of sodium channel function including TTX, ATX II, veratridine, lidocaine, and flecainide, adversely affected cardiac development. These data thus strongly suggest that sodium current is not required for cardiac specification and that cardiac-type sodium channels are likely to act via a previously-unappreciated, non-electrogenic mechanism in undifferentiated tissues to regulate cardiac cell fate specification. Interestingly, studies of murine P19 EC cells and ES cells displayed clear evidence of *scn5a* expression in undifferentiated and early differentiating cells in the absence of any detectable sodium currents by patch-clamp electrophysiology (312;343). Although transcripts for both *zscn5Laa* and *zscn5Lab* were readily detected during gastrulation, we do not yet have direct evidence that sodium channel protein is expressed in undifferentiated tissues of the early zebrafish embryo.

The proposed non-electrogenic role of sodium channels in early development may involve one of a number of possible mechanisms. Sodium channel complexes have previously-described roles in cell adhesion that are mediated by their ancillary β subunits (162). These small, single membrane-spanning proteins with extracellular immunoglobulin domains are integral members of sodium channel complexes that have been shown in multiple studies to interact with other cell adhesion molecules and extracellular matrix proteins (162;344-346). Intracellularly, β subunits can also interact with components of the cytoskeleton through their cytoplasmic, C-terminal tails (14;347-349). Although the role of sodium channel β subunits in development is unknown, studies of the protein N-cadherin have demonstrated that cell-adhesion is an important requirement for normal early heart development in chicks an mice (350-352;352). Alternatively, sodium channel proteins may act as scaffolds for other signaling molecules that are essential for early development. It is increasingly well-appreciated, for example, that sodium channels interact with a diverse array of proteins through discreet domains on the channel protein (141). We also cannot discount that $zNa_v1.5La$ and $zNa_v1.5Lb$ play important roles inside cells or on the membranes of subcellular organelles, as was recently shown for $Na_v1.5$ in macrophages (353). Finally, we hypothesize that the pore-forming α subunit may possess an uncharacterized, non-electrogenic signaling mechanism that is intrinsic to the channel protein. As was recently

demonstrated for L-type calcium channels, for example, sodium channel proteins may have specific domains that are cleaved and translocate from the membrane to the nucleus to regulate gene expression (337). Notably, cardiac sodium channel expression has been detected in non-excitable tissues where they may act in any of the proposed capacities (354-357).

In addition to informing development, further investigation into these putative mechanisms may also provide insight into the etiology of unanticipated disease phenotypes that have recently been associated with reduced function or expression of cardiac-type sodium channels. Although mutations in *SCN5A* have most commonly been associated with heritable disorders of heart rhythm, for example, recent studies of human patients and mouse models have implicated $Na_v1.5$ dysfunction and/or haploinsufficiency in dilated cardiomyopathy, cardiac fibrosis, and ventricular non-compaction, with mechanisms that are not well understood (272;275;276;358;359). Although defects in excitability or ion homeostasis and subsequent cardiac remodeling have been hypothesized as potential mechanisms underlying these phenotypes, it remains to be understood why other disorders resulting from significant dysfunction of cardiac sodium channels do not also generate structural heart phenotypes. Based on the results of our study, we hypothesize that at least some component of sodium channel-associated structural heart disease may be attributable to non-electrogenic mechanisms (e.g. specific derangements of channel structure) that are required for the maintenance or integrity of the myocardium. In this context, it is of interest that cardiac sodium channels have been demonstrated to directly interact with cytoskeletal proteins such as ankyrin as well as components of the dystrophin complex (360;361), and that derangements of protein components of the cytoskeleton or sarcomere represent the most common underlying mechanism underlying heritable cardiomyopathies (362).

Although a sizeable literature has demonstrated that Na_v1 channel isoforms play important roles in development, no prior studies have directly attributed any biological phenotype to the non-electrogenic functions of a sodium channel protein. Previous studies dating back over a century used sensory deprivation, TTX, and other tools to demonstrate that excitability is an important contributor to the development of the nervous system, both *in vitro* and *in vivo* (332-

335;363-369). The results of our studies, however, directly implicate non-electrogenic roles for $zNa_v1.5a$ and $zNa_v1.5b$ that could only be revealed by reducing levels of sodium channel protein, as would be achieved in knockout models. Interestingly, *scn2a*$^{-/-}$ mice died within two days of birth from severe hypoxia, suggesting a specific, non-redundant role for *scn2a* in the brainstem (82). Despite the absence of gross anatomical or histological abnormalities in the brains of *scn2a*$^{-/-}$ mice, assays for cell death revealed significantly increased neuronal apoptosis in both the brainstem and neocortex (82). In zebrafish, knockdown of $Na_v1.6a$ (*scn8aa*) resulted in developmental defects in selective types of motoneurons that were both cell-autonomous and non-cell-autonomous (370). It was not directly tested in either study whether the observed effects were mediated by excitability or by alternative mechanisms. Because of our findings, future studies of zebrafish Na_v1 channels will benefit from the direct comparison of phenotypes that result from reduced protein expression to those that result from the prolonged inhibition or modulation of sodium influx. The striking early phenotype reported here is not only of developmental interest, but may serve as a valuable *in vivo* platform for future structure-function analysis of the non-electrogenic functions of voltage-gated sodium channels.

CHAPTER IV

MOLECULAR CLONING AND ANALYSIS OF ZEBRAFISH VOLTAGE-GATED SODIUM CHANNEL BETA SUBUNIT GENES - IMPLICATIONS FOR THE EVOLUTION OF ELECTRICAL SIGNALING IN VERTEBRATES

Overview

In the previous chapter, we presented data that suggested critical non-electrogenic functions for zebrafish cardiac sodium channels in early development. Moreover, we hypothesized that these functions may derive from a putative role of the sodium channel complex as a large scaffold for other signaling molecules that may be required for cell fate determination in the gastrulating embryo. One of the most unique features of sodium channels compared to other ion channel complexes is their association with accessory proteins termed "β subunits," which are characterized by extracellular immunoglobulin domains most commonly found in cell adhesion molecules and cell-surface receptors of the immunoglobulin superfamily. Although they have important effects in modulating the function and cell-surface expression of pore-forming sodium channel α subunits, β subunits may also play non-electrogenic roles through their IG domains. The efforts of several laboratories have revealed that through protein-protein interactions, sodium channel β subunits act as transmembrane bridges linking the extracellular matrix and the intracellular cytoskeleton, conferring to cells the properties of adhesion and adhesion-mediated intracellular cell signaling. Such functions could be essential to the non-electrogenic developmental functions of a sodium channel complex, given the previously recognized role for cell adhesion molecules in cardiac development (see Chapter 5). As a critical first step towards investigating this putative mechanism, we have initiated studies of sodium channel-interacting proteins and here describe the cloning, evolution, and characterization of voltage-gated sodium channel β subunits in zebrafish. These efforts have been described in the context of the canonical role of β subunits in modulating sodium channel function and membrane excitability,

which are their most widely-recognized functions and for which a rich database of prior studies exists in the literature.

Abstract

In mammals, sodium channels exist as macromolecular complexes that include a pore-forming alpha subunit and 1 or more modulatory beta subunits. Although alpha subunit genes have been cloned from diverse metazoans including flies, jellyfish, and humans, beta subunits have not previously been identified in any non-mammalian species. To gain further insight into the evolution of electrical signaling in vertebrates, we investigated beta subunit genes in the teleost *Danio rerio* (zebrafish). We identified and cloned single zebrafish gene homologs for beta1-beta3 (*zbeta1-zbeta3*) and duplicate genes for beta4 (*zbeta4.1, zbeta4.2*). Sodium channel beta subunit loci are similarly organized in fish and mammalian genomes. Unlike their mammalian counterparts, *zbeta1* and *zbeta2* subunit genes display extensive alternative splicing. Zebrafish beta subunit genes and their splice variants are differentially-expressed in excitable tissues, indicating tissue-specific regulation of *zbeta1-4* expression and splicing. Co-expression of the genes encoding zbeta1 and the zebrafish sodium channel alpha subunit $Na_v1.5$ in Chinese Hamster Ovary cells increased sodium current and altered channel gating, demonstrating functional interactions between zebrafish alpha and beta subunits. Analysis of the synteny and phylogeny of mammalian, teleost, amphibian, and avian beta subunit and related genes indicated that all extant vertebrate beta subunits are orthologous, that beta2/beta4 and beta1/beta3 share common ancestry, and that beta subunits are closely related to other proteins sharing the V-type immunoglobulin domain structure. Vertebrate sodium channel beta subunit genes were not identified in the genomes of invertebrate chordates and are unrelated to known subunits of the *para* sodium channel in *Drosophila*. The identification of conserved orthologs to all 4 voltage-gated sodium channel beta subunit genes in zebrafish and the lack of evidence for beta subunit genes in invertebrate chordates together indicate that this gene family emerged early in vertebrate evolution, prior to the divergence of teleosts and tetrapods. The evolutionary history of sodium channel beta subunits suggests that these genes may have played a key role in the diversification and specialization of electrical signaling in early vertebrates.

Introduction

In mammals, voltage-gated sodium channels are multi-protein complexes that include a pore-forming α subunit and 1 or more modulatory β subunits (5-9). While sodium channel α subunits are large proteins with 24 membrane-spanning domains, β subunits are smaller proteins with a single transmembrane domain and an extracellular V-type immunoglobulin-like domain (10-14). While heterologous expression of α subunit genes alone can reconstitute key properties of voltage-gated sodium channels observed in native tissues, co-expression with β subunit genes modifies channel gating and increases channel cell surface expression (10-13). Studies of mice with targeted ablation of either β1 or β2 genes corroborated these roles for β subunits *in vivo* and revealed an additional function for β subunits in α subunit localization (17;18). Moreover, the unique expression profiles of each β subunit gene and their variable effects on α subunit function, expression, and localization suggest that different subunit combinations in heart, brain, and muscle may contribute to diversity and specialization in electrical signaling (19;371).

The physiological importance of sodium channel β subunits is reinforced by their role in human disease. β1 subunit gene mutations are a cause of generalized epilepsy with febrile seizures plus (GEFS+), and variants in sodium channel α subunits that disrupt their interaction with β subunits may be pathological in the heart (76-79). More recently, a mutation in the β4 subunit gene was implicated as a cause of the long QT syndrome, a congenital arrhythmia (372).

The unique electrophysiological properties, expression patterns, and physiological roles of mammalian sodium channel α subunits suggest that the duplication of these genes may have been an adaptation that permitted the diversification and functional specialization of electrical signaling in vertebrates (1;175;176). The physical interaction of α subunits with auxiliary proteins such as β subunits that modify their expression or function may have been similarly adaptive (97;98). Although sodium channel β subunits have not previously been identified in non-mammalian species, we hypothesize that a sodium channel macromolecular complex comprised of α subunits and auxiliary β subunits is an evolutionarily-conserved structural entity. Evidence for the emergence of sodium channel β subunit genes early in vertebrate evolution would be

consistent with the idea that these genes may have played a role in diversifying and fine-tuning electrical signaling not only in mammals but in all vertebrates.

Here we report the identification and molecular cloning of conserved orthologs of all 4 mammalian β subunit genes in *Danio rerio* (zebrafish), a teleost vertebrate and a popular developmental and physiological model system. By direct sequence analysis and alignment, we assessed whether zebrafish β subunits possess the structural hallmarks of their mammalian counterparts. We provide evidence for extensive splicing of zebrafish beta subunit genes and demonstrate their expression in excitable tissues. To determine whether zebrafish sodium channel α and β subunits functionally interact, we studied sodium currents generated by the co-expression of the genes encoding zNa_v1.5 (α subunit) and zβ1 in a heterologous cell system. Finally, we assessed the synteny and phylogeny of β subunits and a group of closely-related genes with IG domains in several vertebrate species. Our findings strongly suggest that all 4 voltage-gated sodium channel β subunit genes emerged early in vertebrate evolution, and support the concept that the voltage-gated sodium channel α-β subunit macromolecular complex is a conserved and functionally-important vertebrate innovation.

Methods

Identification and cloning of zSCN1B-4B genes and splice variants

Mammalian *SCN1B-4B* gene sequences were used in BLASTN queries of the draft zebrafish genome (Ensembl Zv2-5) to identify DNA contigs containing putative zebrafish orthologs. Primers directed against predicted exons were then used to amplify partial β subunit gene sequences using the Titan RT-PCR enzyme system (Roche) and total day 2 embryonic zebrafish RNA as template. RNA was isolated using Trizol (GIBCO), digested with RQ1 DNase (Promega), and purified with the RNeasy Mini Kit (Qiagen). 5' and 3' ends and alternatively-spliced forms of each gene were identified using 5' and 3' RNA ligase mediated rapid amplification of cDNA ends (RLM-RACE) PCR (Ambion). Additional splice variants were identified by RT-PCR while examining tissue-specific expression. All amplicons were subcloned directly into the pGEM-TEasy vector (Promega) and sequenced in their entirety. Consensus sequences for each gene were established after comparing the forward and reverse sequences of a minimum of 5 clones.

Sequence data and annotation

Eleven novel zebrafish gene sequences were deposited in the NCBI GenBank database: zβ1A [Genbank:DQ489722], zβ1B [Genbank:DQ489723], zβ1C [Genbank:DQ489724], zβ1D [Genbank:DQ489725], zβ2A [Genbank:DQ489726], zβ2B [Genbank:DQ489727], zβ2C [Genbank:DQ489728], zβ2D [Genbank:DQ489729], zβ3 [Genbank:DQ489730], zβ4 locus 1 [Genbank:DQ489731], zβ4 locus 2 [Genbank:DQ489732]. Intron-exon boundaries for each gene and splice variant were determined by comparing cDNA and genomic sequences. Sequences for zebrafish β1-β4 were annotated by alignment with their mammalian orthologs using the AlignX function of Vector NTI v9.1 (Invitrogen) and by use of the following informatics resources: signal peptide (SMART) (373), IG-like domain (SMART (373), NCBI conserved domain database, CDD, v2.06 (374), and REF (14)), transmembrane (TMpred (375) and REF (376)), disulfide bridge (Prosite) (377), and putative N-linked glycosylation sites (NetNGlyc 1.0 server) (378).

Gene expression

Tissues were dissected from wild type adult zebrafish (strain TuAB, 12-16 months old) and flash frozen on dry ice in ethanol. Tissue-specific total RNA was isolated and purified as described above. First strand cDNA synthesis was performed using 1µg of RNA from each tissue, random hexamer primers, and Transcriptor reverse transcriptase enzyme (Roche). 2µl of first strand cDNA was used in 25µl PCR reactions with Expand High Fidelity DNA polymerase (Roche). Amplicons were analyzed on a 1-2% agarose gel made with 1x Tris-Acetate-EDTA (TAE) buffer. Primer pairs used to amplify each individual gene and splice variant are listed in Table 5. All amplicons were subcloned directly into the pGEM-TEasy vector (Promega) and sequenced in their entirety in both sense and antisense directions.

Identification of β subunit-like genes

Human sodium channel β subunit nucleotide and amino acid sequences were used in BLAST searches of the human genome to identify β subunit-like genes. Four human genes sharing the greatest homology as well as similar genomic organization and/or synteny with known sodium channel β subunit genes were included for further analysis: myelin protein zero (MPZ) [Genbank:NP_000521], myelin protein zero-like gene, isoform A (MPZL1 isoform A) [Genbank:NP_003944], epithelial V-like antigen (EVA) [Genbank:NP_005788], and epithelial V-like antigen-like gene (hypothetical protein LOC196264 or EVA1-like gene) [Genbank:NP_938016].

Analysis of synteny

Synteny between vertebrate β subunits and related genes was assessed by chromosomal walking and reciprocal BLAST searches of genes adjacent to β subunit loci in human, zebrafish, *Rattus norvegicus*, *Xenopus tropicalis*, and *Gallus gallus* genome databases (Ensembl).

Analysis of phylogeny

To estimate phylogeny, additional β subunit and β subunit-like gene sequences were identified in *Rattus norvegicus*, *Xenopus tropicalis*, and *Gallus gallus* genome databases (Ensembl). Predicted amino acid sequences were aligned with cloned zebrafish sequences using CLUSTALX (v1.83). Phylogenetic trees were reconstructed using the neighbor-joining method of Saitou and Nei (Ref (232)) and viewed with NJplot software. Alignment gaps were excluded in the analysis, and the Kimura correction was made for multiple substitutions (379). The robustness of each node in the phylogenetic tree was analyzed with bootstrap analysis (n=1000). Trees were unrooted due to limited evidence for β subunit-like genes in non-vertebrate species.

Genome databases

All genome resources utilized for this study were accessed through the Ensembl gateway (380) with the exception of the sea urchin genome, which is available for BLAST searches by the National Human Genome Sequencing Center at Baylor College of Medicine (381).

Expression vectors

The full-length zebrafish β1D splice variant was amplified in one step from total D2 embryonic RNA template using the Titan one-tube RT-PCR system (Roche) and the following primers: Fwd: *Spe I* - GACTCTGAAAACAAAGCCTG, Rev: *Sac II* – AGAGCTTCAAGCTTTTGGCT. The 733 base pair product was sublconed directly into the pGEM-TEasy vector. Multiple clones were purified, sequenced, and screened against the consensus sequence determined during the cloning of the zβ1 gene. Insert was digested out of a single zβ1D consensus clone and subcloned into the pGFP-IRES vector (Clontech) using *Spe I* and *Sac II* restriction sites. We have used similar methods to identify, clone and assemble a full-length *zscn5a* expression construct (pBK-CMV-*zscn5a*) which encodes zebrafish $Na_v1.5$. These methods are described elsewhere (manuscript in preparation).

Transient transfection and electrophysiology

Cultured Chinese Hamster Ovary (CHO) cells were transiently transfected with pBK-CMV-*zscn5a* and pGFP-IRES-*zβ1D* constructs using FuGENE6 (Roche). Cells were grown for 48 hours after transfection before electrophysiologic study. Whole-cell voltage clamp was performed at room temperature with 2-MΩ patch microelectrodes and an Axopatch 200A amplifier. To minimize the capacitive transients, we compensated for approximately 70% to 80% of the cell capacitance and series resistance (233). Cells exhibiting very large currents (>6 nA) were also excluded from further analysis. Cells were also excluded if voltage control was compromised. The extracellular bath solution contained (in mmol/L) NaCl 145, KCl 4.0, $MgCl_2$ 1.0, $CaCl_2$ 1.8, glucose 10, and HEPES 10; the pH was 7.4, adjusted with NaOH. The pipette (intracellular) solution contained (in mmol/L) NaF 10, CsF 110, CsCl 20, EGTA 10, and HEPES 10; the pH was 7.4, adjusted with CsOH. Cells were held at -120 mV, and activating currents were elicited with depolarizing pulses from -100 to +50 mV in 10 mV increments. Specific clamp protocols are indicated with the data. Data were acquired by pClamp8.0 (Axon Instruments Inc), sampled at 50 kHz, and low-pass filtered at 5 kHz. All currents were normalized to the cell capacitance calculated by Membrane Test (OUT O) in pClamp8.0.

Results

Identification and cloning of zebrafish sodium channel β subunit genes

We identified 5 distinct zebrafish β subunit gene loci by mining the draft zebrafish genome sequence (ensembl Zv2-4) for genes homologous to the human and mouse β1- β4 genes. *In silico* prediction of coding sequence on the relevant genomic DNA contigs enabled us to amplify partial β subunit gene sequences for each locus by RT-PCR and subsequently complete the full-length zebrafish β subunit clones by rapid amplification of cDNA ends (RACE)-PCR. Analysis of putative open reading frames within each cDNA sequence predicted proteins ranging from 220-232 amino acids in length. Deduced translation and alignment of the five zebrafish amino acid sequences with each mammalian β subunit protein sequence suggested the identities of these genes (Figures 4.1A-4.4A). While single homologs were identified for the genes encoding β1-β3 (*zβ1-zβ3*), zebrafish express two distinct but closely-related β4 genes (*zβ4.1, zβ4.2*). Alignment of the amino acid sequences of zebrafish β1, β2, β3, β4.1, and β4.2 with their human homologs indicated that these proteins share 53.4%, 49.6%, 51.1%, 43.2%, and 40.8% identity, respectively.

Conserved features of zebrafish sodium channel β subunits

Mammalian sodium channel β subunits possess a single transmembrane domain, a short intracellular carboxyl C-terminal tail, a cleavable amine (N)-terminal signal peptide, and a conserved V-type extracellular IG domain that most closely resembles the type found in cell-adhesion molecules (14;382). Hydropathy analysis of zebrafish β subunit amino acid sequences using TMpred software revealed that all 5 proteins are likely to possess cleavable N-terminal signal peptides and single transmembrane domains (Figure 4.10). To assess the presence of an extracellular V-type IG domain, we first analyzed each zebrafish beta subunit amino acid sequence with the NCBI conserved domain database. By this method, all 5 zebrafish β subunit genes are predicted to possess V-type extracellular IG domains (Figure 4.11). To more rigorously analyze these predictions, we manually examined the amino acid sequence of each zebrafish β

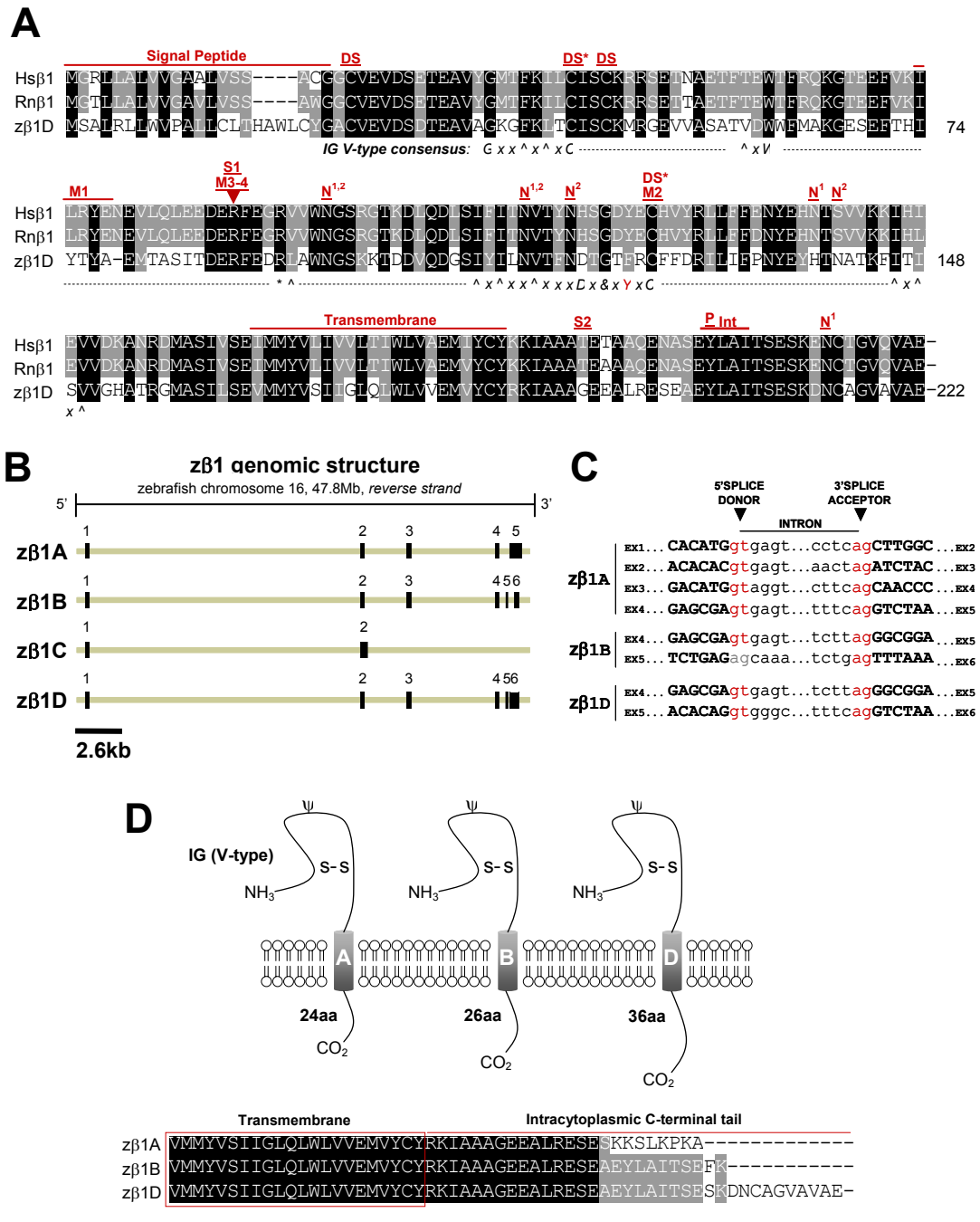

Figure 4.1: Analysis of the cloned zebrafish β1 subunit gene and novel splice variants. (A) Alignment of cloned human, rat, and zebrafish β1 amino acid sequences. Black = identical in all three species; grey = identical in 2/3 species or conserved substitution. Shown for zebrafish is the most conserved β1 splice form (variant D). Hs = *Homo sapiens*, Rn = *Rattus norvegicus*, z = zebrafish; DS* = cysteine residue predicted to participate in a disulfide bridge, based on the myelin P0 protein crystal structure; DS = predicted second disulfide bridge; N = predicted N-linked glycosylation site (N1 = human/rat, N2 = zebrafish); M1 = site of epilepsy-causing deletion (I70_E74del) in Hsβ1; M2 = site of second epilepsy-causing mutation (C121W) in Hsβ1; M3/4 =

site of third and fourth epilepsy-causing mutations (R85C, R85H); S1 = nonsynonymous Hsβ1 single nucleotide polymorphism (SNP, G/A > R85H); S2 = nonsynonymous Hsβ1 SNP (C/T > T189M); P = phosphorylation site (tyrosine Y181) that regulates ankyrin recruitment (NOTE: Y200 = Y181 following cleavage of 19 amino acid signal peptide); IN = putative internalization sequence. Consensus sequence for V-type IG domain is depicted beneath the alignment: G = glycine, x = any residue, ^ = hydrophobic residues, C = cysteine, - = gap in alignment with consensus sequence, W = tryptophan, * = basic residue, L = leucine, D = aspartic acid, & = glycine, alanine, or aspartate, and Y = tyrosine. Red indicates zebrafish residues that deviate from the consensus sequence. See Results for references supporting sequence annotation. **(B)** 5' and 3' RLM-RACE PCR and RT-PCR identified four distinct splice variants expressed from zβ1 locus on zebrafish chromosome 16 (*Ensembl*). **(C)** Splice donor and acceptor sites of zebrafish β1 splice variants, derived from comparing cloned cDNA against genomic DNA sequences (*Ensembl*). Consensus GT-AG splice sites are labeled in red. A splice-site deviating from the consensus appears in grey. **(D)** Schematic diagram of β1 splice variants A, B, and D, whose predicted proteins differ only in the length of their intracytoplasmic C-terminal tail. S-S = disulfide bridge. NH3 = 5' amino terminus, CO2 = 3' carboxyl terminus, β = putative N-linked glyosylation site. Alignment of C-terminal tail of variants zβ1A, zβ1B, and zβ1D (below). zβ1C is not shown as it is predicted to lack both extracellular IG and transmembrane domains.

subunit for the V-type IG domain consensus sequence (annotated beneath alignments, Figures 4.1A-4.4A). With the exception of a conservative tyrosine to phenylalanine (Y>F) substitution in zβ1 and a non-polar methionine to basic lysine residue substitution (M>K) in zβ3 (illustrated in red text in Figures 4.1A and 4.3A), all 5 zebrafish β subunits exhibit 100% conservation of the consensus sequence for V-type IG domains (14;382). Typical of this domain is the linkage of 2 cysteine residues in a disulfide bridge (DS*, Figures 4.1A-4.4A), the structural importance of which was revealed by a mutation that results in familial epilepsy (76). A second putative disulfide bridge that may further stabilize the extracellular IG domain in β1 and β3 is suggested of the crystal structure of myelin protein zero (MPZ), the primary structural protein of peripheral nerve myelin, whose IG domain closely resembles that found in sodium channel β subunits (12;382;383). The cysteine residues that contribute to proposed second bridge are conserved in zβ1 and zβ3 (DS, Figures 4.1A, 4.3A). Similar to mammalian β2 and β4, zβ2 and zβ4 proteins do not possess this second disulfide bridge but have an unpaired cysteine residue that may underlie covalent interactions with partnering sodium channel α subunits (S-, Figures 4.2A, 4.4A) (5;11;13).

In addition to V-type IG domains, our sequence analysis indicated that other functional and/or structural domains are conserved in zebrafish β subunits (Figures 4.1A-4.4A). These include a tyrosine in β1 that is phosphorylated and regulates interactions with ankyrin G (Y181 or Y200 with signal peptide intact) (348), the C-terminal tyrosine-leucine-alanine-isoleucine (Y-L-A-I) internalization motif in β1 and β3 which may be recognized by clathrin-coated pits (12), and a juxtatransmembrane gamma-secretase cleavage site in β2 that may play a role in cell adhesion or the movement of cells expressing this subunit (384). Zebrafish β subunits are also likely to exhibit post-translational modification by amide nitrogen (N)-linked glycosylation, a key feature of all 4 mammalian β subunits (10-13). The zβ1 protein possesses 2 of 4 predicted N-linked glycosylation sites found in human or rat β1 in addition to exhibiting two unique sites (Figure 4.1A). Similarly, zβ2 conserves 3 of 4 sites, zβ3 conserves 1 of 3 sites and displays 2 novel sites, zβ4.1 conserves 4 sites and displays 1 novel site, and zβ4.2 conserves 3 of four sites and displays 3 novel sites (Figures 4.2A-4.4A).

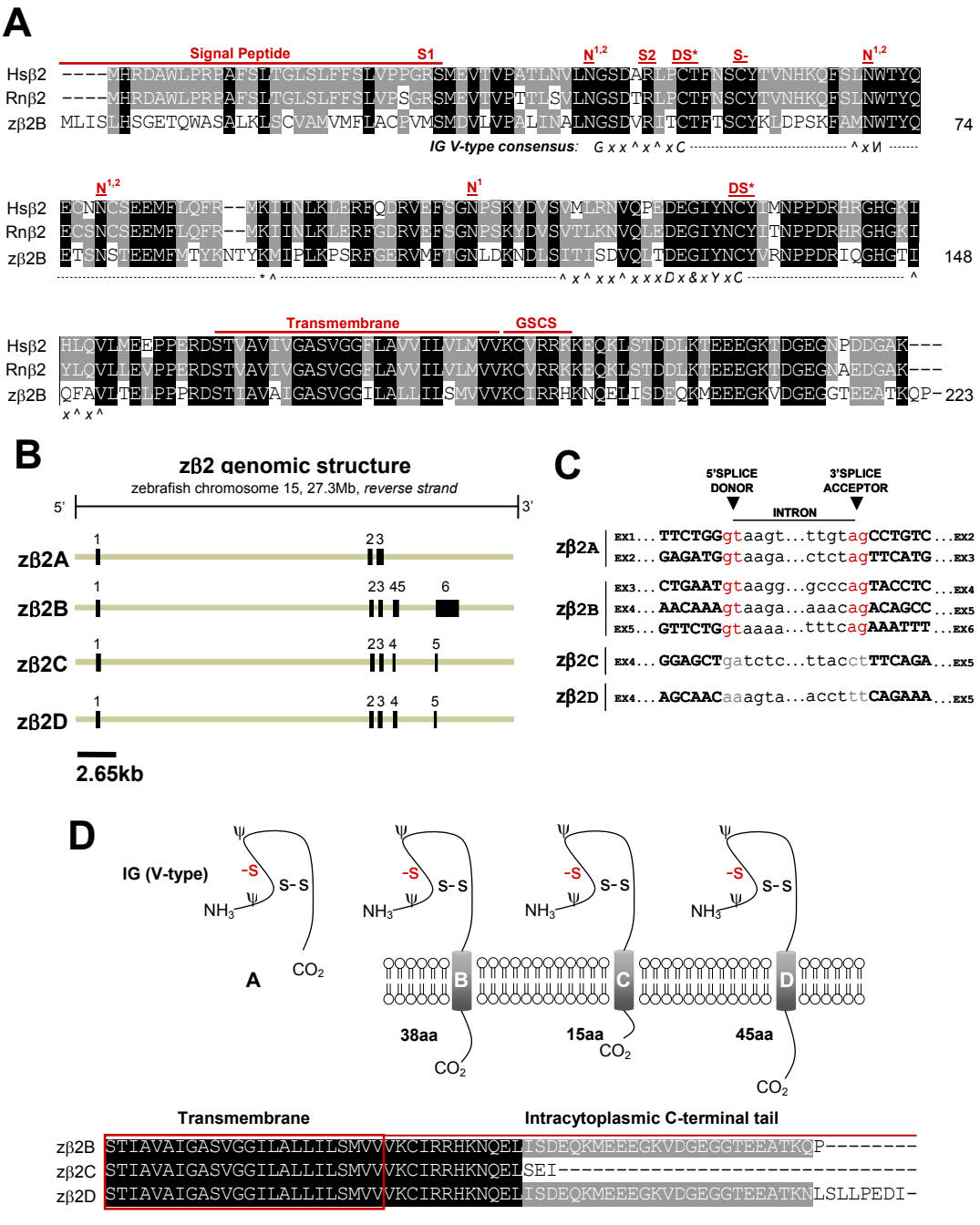

Figure 4.2: Analysis of the cloned zebrafish β2 subunit gene and novel splice variants. Presentation and labeling as in Figure 1. **(A)** Alignment of cloned human, rat, and zebrafish β2 amino acid sequences. Shown for zebrafish is the most conserved β2 splice form (*variant B*). S- = conserved cysteine in β2 that is a putative site of covalent linkage with a partner α subunit; S1 = nonsynonymous Hsβ2 single nucleotide polymorphism (SNP, C/T > R28W) (NCBI dbSNP, PharmGKB); S2 = nonsynonymous Hsβ2 SNP (G/A > R47H) (NCBI dbSNP, PharmGKB); GSCS = γ-secretase cleavage site. **(B)** 5' and 3' RLM-RACE PCR and RT-PCR identified four distinct splice variants expressed from the zβ2 locus on zebrafish chromosome 15 (*Ensembl*). **(C)** Splice

donor and acceptor sites of zebrafish β2 splice variants. Zβ2 variants C and D both differ from the consensus sequences at the exon 4-intron 4 and intron 4-exon 5 splice junctions. **(D)** Schematic diagram of β2 splice variants A-D. With the exception of variant A, the predicted proteins of zβ2 variants B-D differ only in the length of their intracytoplasmic C-terminal tail. Alignment of C-terminal tail of variants zβ2B, zβ2C, and zβ2D (below).

Comparative genomics of β subunit gene variants

The conservation of amino acid residues between homologous genes in distantly-related species may uncover previously unappreciated regions of functional importance and facilitate the evaluation of novel human mutations and polymorphisms. To determine whether previously identified mutations and polymorphisms are conserved in zebrafish β subunit genes, we mapped these variants onto the alignments of mammalian and zebrafish β subunit amino acid sequences. Four mutations in the human β1 gene have been linked to the heritable epilepsy syndrome GEFS+, the first resulting in a 5 amino acid deletion from isoleucine at position 70 to glutamic acid at position 74 (I70_E74del), the second in substitution of a cysteine residue that participates in a disulfide bridge (C121W), and the third and fourth resulting in substitution of an arginine at position 85 for either a cysteine or a histidine, respectively (R85C, R85H) (76;148;149). All of these mutations are expected to destabilize the extracellular IG domain of β1 and result in loss of function. In zβ1, 2 of 5 amino acids in the deleted segment (isoleucine, tyrosine), C121, and R85 are all conserved (M1, M2, M3/4, Figure 4.1A). R85H was also previously reported as a non-synonymous SNP in NCBI and PharmGKB SNP databases (S1, Figure 4.1A). A second reported SNP in human β1 results in a threonine to methionine substitution at position 189 (T189M), but T189 is not conserved in the amino acid sequence of zβ1 (S2, Figure 4.1A).

Although disease-causing mutations are not currently associated with either *SCN2B* or *SCN3B*, nonsynonymous SNPs have been reported for *SCN2B* that result in an arginine to tryptophan substitution at position 28 (R28W) and an arginine to histidine substitution at position 47 (R47H). R47 but not R28 is conserved in the amino acid sequence of zebrafish β2 (S1, S2, Figure 4.2A). A mutation in *SCN4B* resulting in a leucine to phenylalanine substitution at position 179 (L179F) was recently implicated as a putative cause of the congenital long QT syndrome (385). Although this leucine is conserved in zebrafish β4.1, rat β4 and zebrafish β4.2 display a cysteine (C) and threonine (T) at this position, respectively (M1, Figure 4.4A). A nonsynonymous *SCN4B* polymorphism has also been reported, resulting in an asparagine to histidine substitution at position 210 (N210H). N210 is conserved in the sequences of both zβ4.1 and zβ4.2 (S1, Fig 4A).

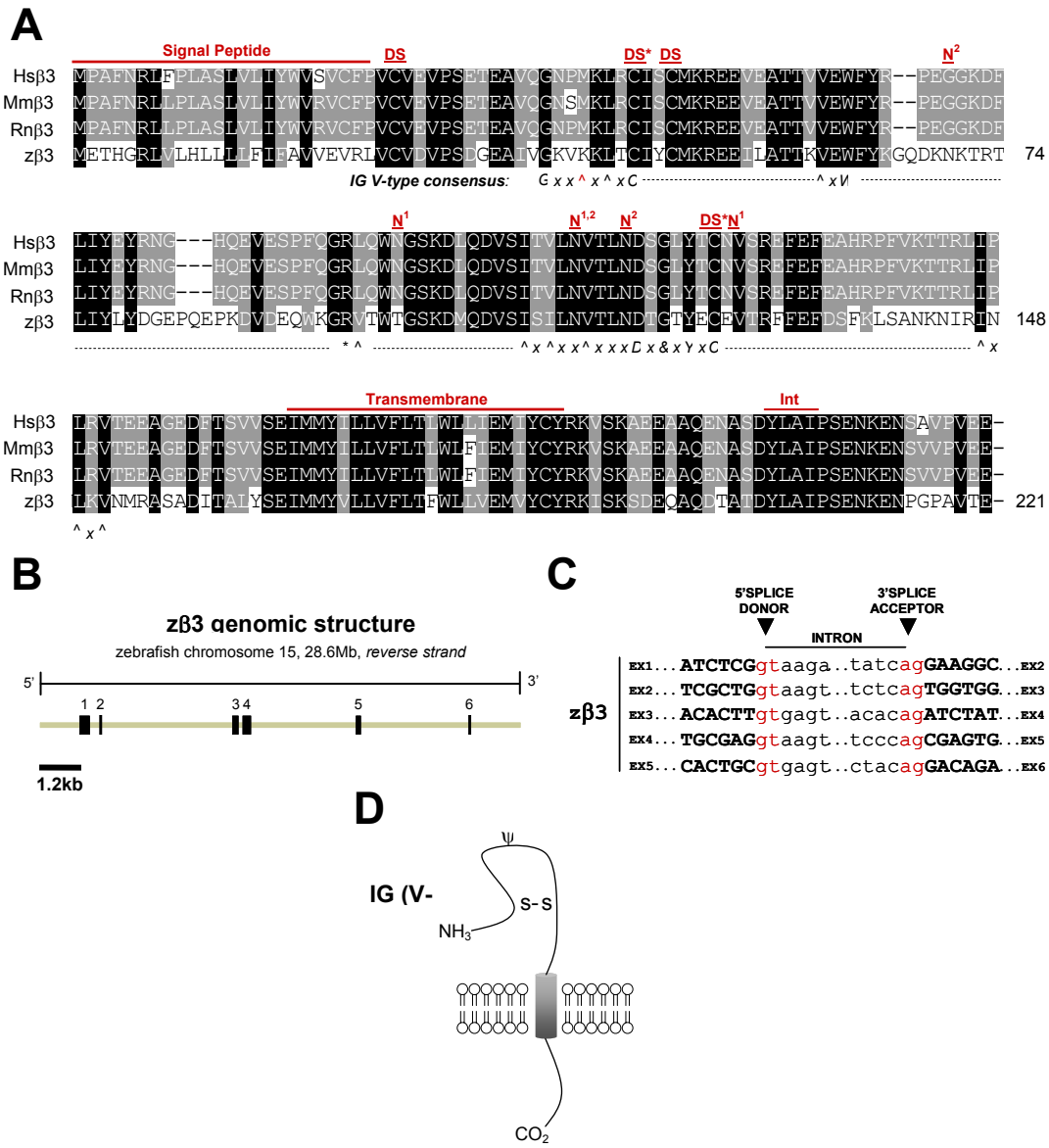

Figure 4.3: Analysis of the cloned zebrafish β3 subunit gene. Presentation and labeling as in Figure 1. **(A)** Alignment of cloned human, mouse, rat, and zebrafish β3 amino acid sequences. INT = putative internalization sequence. **(B)** 5' and 3' RLM-RACE PCR and RT-PCR identified a single transcript expressed from the zβ3 locus on zebrafish chromosome 15 (*Ensembl*). zβ3 has six exons. **(C)** All zβ3 splice sites adhere to GT-AG consensus sequences. **(D)** Schematic diagram of the β3 protein.

Alternative splicing of zebrafish β subunit genes

The mammalian β1 subunit gene is alternatively-spliced in both rats (β1A) and humans (β1B), with retention of intron 3 being the primary event in both species that dramatically alters the transmembrane domain and intracellular C-terminus of the β1 subunit protein (386;387). An alternative splice-variant of β1 that retains intron 5 and adds 86 nucleotides to the 3' untranslated region (UTR) of β1 mRNA transcripts has also been reported (388;389). In zebrafish, we detected 4 alternatively-spliced variants of the β1 gene, designated here as *A-D*. Comparisons between complementary DNA and genomic DNA revealed that zβ1A transcripts have 5 exons whereas zβ1B and zβ1D each have 6 exons and zβ1C has only 2 (Figure 4.1B, Table 1). Transcripts of zβ1A, zβ1B, and zβ1D all share exons 1 through 4 but not exons 5 and 6; and all splice junctions except exon 5-intron 5 of zβ1B display canonical GT-AG splice donor-acceptor sites (Figures 4.1B, 4.1C; Table 1). The zβ1 splice variant that shares the most identity with human β1 at the amino acid level (zβ1D) also shares nearly identical genomic organization (Table 1). With the exception of differences in exons 5 and 6, zβ1A and zβ1B variants also share this conserved genomic architecture (Table 1).

Similar to splice variants of the mammalian β1 gene, splice variants of zβ1 are all predicted to encode proteins with variable C-termini. Unlike the mammalian variants, however, zβ1A, zβ1B, and zβ1D are predicted to possess identical transmembrane domains and differ only in their distal C-termini (Figure 4.1D). As a result of alternative-splicing, zβ1A lacks the conserved tyrosine residue (Y200, Figure 4.1A) that was found to regulate recruitment of ankyrin G by mammalian β1, as well as the putative internalization sequence (Y-L-A-I) discussed above (Figures 4.1A, 4.1D) (12;348;349). These alterations may affect interactions between zβ1A and zebrafish ankyrin, as well as influence the cycling of the mature zβ1A protein from its membrane compartment. The zβ1C splice variant, which results from retention of intron 2 and has an open reading frame of only 105 amino acids, is predicted to lack both an extracellular IG domain and a membrane-spanning segment.

Although alternative splicing of the β2 gene has not previously been identified in mammals, we identified 4 unique β2 transcripts in zebrafish. While zβ2A and zβ2B are spliced at

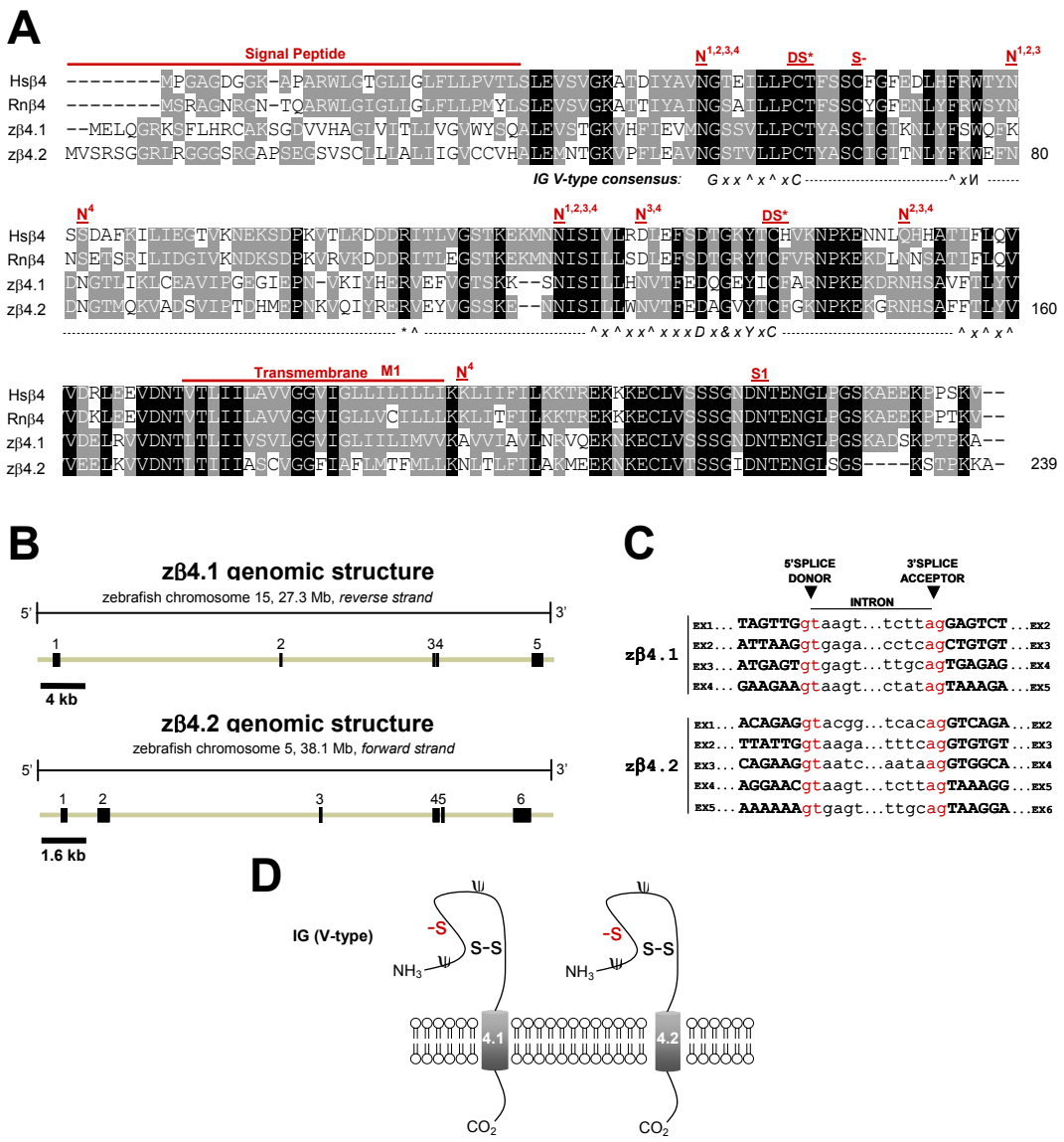

Figure 4.4: Analysis of cloned zebrafish β4.1 and β4.2 subunit genes. Presentation and labeling as in Figure 1. **(A)** Alignment of cloned human, rat, and zebrafish β4 amino acid sequences. S- = conserved cysteine in β4 that is a putative site of covalent linkage with a partner α subunit; N = predicted N-linked glycosylation site (N1 = human, N2 = rat, N3 = zebrafish β4.1, N4 = zebrafish β4.2); M = site of putative Long QT syndrome-causing mutation L179F; S1 = nonsynonymous Hsβ4 SNP (A/C > N210H). **(B)** Genomic organization of zβ4.1 and zβ4.2 derived from comparing cloned cDNA sequences with genomic sequences of zebrafish chromosomes 15 and 5, respectively. zβ4.1 has five exons and zβ4.2 has six exons. **(C)** All zβ4.1 and zβ4.2 splice sites exhibit consensus GT-AG donor/acceptor sequences. **(D)** Schematic diagram of zβ4.1 and zβ4.2 proteins.

canonical splice donor and acceptor sites, variants zβ2C and zβ2D are assembled by splicing at non-canonical exon 4-intron 4 and intron 4-exon 5 splice donor and acceptor sites. zβ2A is assembled from only 3 exons, zβ2B from 6 exons, and zβ2C and zβ2D from 5 exons each (Figure 4.2B). Mammalian and zebrafish β2 genes all share a second exon that is 167 nucleotides in length and encodes the initial segment of the subunit's extracellular IG domain. Otherwise, the genomic organization of zβ2 splice variants diverges from that of human, mouse, and rat β2 genes which all have 4 coding exons (Table 2). Nevertheless, exons 1 and 3 are similar in length in all species, as is the coding segment of exon 4 in the mammalian β2 genes and the zβ2B and zβ2D splice variants (Table 2). zβ2B, zβ2C, and zβ2D are unique in possessing a fifth exon that contributes to the gene's open reading frame. Similar to mouse β2, the most conserved zebrafish β2 splice variant at the amino acid level (zβ2B) has a lengthy terminal exon that is entirely non-coding.

As observed for zβ1, the conceptual translation of zβ2 splice variants predict zβ2 proteins that are of variable length and amino acid sequence at their intracellular C-terminal tail (Figure 4.2D). The variant zβ2A results from retention of intron 3 and is predicted to result in a 160 amino acid protein that has an intact extracellular IG domain but no transmembrane domain (Figure 4.2D). zβ2A is thus unlikely to display canonical beta subunit activities such as modulation of the trafficking and/or function of voltage-gated sodium channels α subunits, or mediation of cell-adhesion between cells expressing this protein and other cells or the extracellular matrix, which all depend on integration in the cell membrane. Transcripts for variants zβ2B-D result from alternative splicing of exons 4-6 and are expected to produce proteins of 223, 201, and 231 amino acids, respectively (Figure 4.2D, Table 2). Since the function of the intracellular C-terminal tail of zβ2 is not well-characterized, the predicted impact of these splice variants on zβ2 function cannot be readily predicted.

Unlike the zβ1 and zβ2 genes, alternatively-spliced transcripts of zβ3, zβ4.1, and zβ4.2 genes were not detected. For each of these three genes, the genomic organization is well-conserved compared to that of its respective mammalian homolog (Tables 3, 4). The open reading frame of *SCN3B* in humans, mice, rats, and zebrafish is derived from 5 exons (exons 2-6),

with a non-coding initial exon found in all 4 species and a non-coding terminal exon found only in the mammalian β3 gene (Table 3). Splicing of zebrafish β3 is determined by canonical GT-AG splice donor and acceptor sites, producing a putative protein whose secondary structure is similar to the β3 subunit found in mammals (Figures 4.3C, 4.3D). z*β4.1* and *zβ4.2* transcripts are comprised of 5 and 6 exons, respectively, all of which are assembled from splicing at canonical GT-AG splice donor and acceptor sites (Figure 4.4B, C). *zβ4.2* is unique among β4 genes in possessing a non-coding exon 1 (Table 4). The predicted secondary structures of zβ4.1 and zβ4.2 are both similar to the β4 subunit found in mammals (Figure 4.4D).

Tissue-specific regulation of zebrafish β subunit gene expression and splicing

Mammalian sodium channel β subunit genes are expressed primarily in excitable tissues such as the heart, brain, and skeletal muscle. By RT-PCR, we observed that zebrafish β subunit genes are also expressed in excitable tissues where they may act to regulate the expression or function of sodium channel α subunits (Figure 4.5, Table 5). Moreover, we detected distinct expression patterns for zβ1-4, suggesting that the functional importance of each β subunit likely varies by tissue type. Transcripts of zβ2 or zβ3 are absent from skeletal muscle whereas zβ1 and zβ4.2 are expressed only at low levels in the heart. As might be expected for non-excitable tissues, few β subunit transcripts were detected in the zebrafish liver and only zβ1 and zβ2 are expressed in the gill.

By designing splice variant-specific primers, we also found evidence for tissue-specific regulation of splicing of zebrafish β subunit genes (Figure 4.5). While zβ1 variants B and D are expressed primarily in the brain and eye (including the optic nerve), zβ1A is expressed in the atrium, ventricle, skeletal muscle and gill. Similarly, whereas zβ2 variant B is primarily expressed in the brain and eye, zβ2 variants A, C, and D are also expressed in the atrium, ventricle, brain, eye, and variant D is additionally expressed in the gill. Interestingly, zβ3 may be alternatively-spliced in the brain and eye but not in the atrium or ventricle. We were unable to recover the shorter variant because of its apparent low level of expression. Although zβ1 variant C was identified by RACE-PCR using total embryonic RNA as template, we were unable to detect

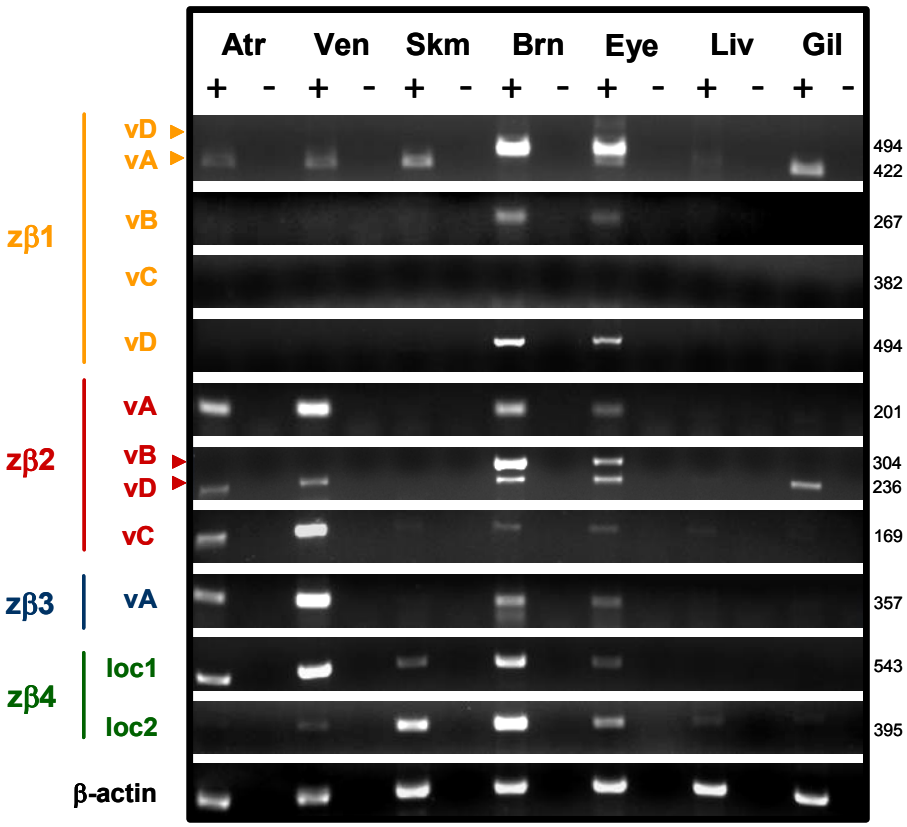

Figure 4.5: Zebrafish sodium channel β1-4 subunit genes and novel splice variants are differentially expressed in excitable tissues. Total RNA was isolated from wild-type adult zebrafish tissues. RT-PCR with gene and splice variant-specific primers was used to detect expression (see Table 5 for primer sequences and amplicon details). Atr = atrium, Ven = ventricle, Skm = skeletal muscle, Brn = Brain, Eye = eye/optic nerve, Liv = liver, Gil = gill. + = enzyme added to reverse transcription step, - = no reverse transcriptase enzyme (negative control). Zebrafish β-actin was amplified from each template as a positive control.

expression of this short splice variant in the adult tissues analyzed for this study. This suggests that zβ1 variant C may be developmentally regulated, expressed in other tissues, unstable, or is the result of an infrequent alternative splicing event.

Zebrafish β1 functionally modifies sodium channel expression, function in vitro

As the first sodium channel auxiliary subunit to be identified, β1 is the most widely-studied of the four known mammalian β subunit proteins. To evaluate whether functional α and β subunit interactions are likely to occur in zebrafish, we heterologously co-expressed the most conserved variant of *zβ1 (variant D)* with the gene encoding the zebrafish pore-forming sodium channel α subunit $zNa_v1.5$, whose expression we detected in the adult zebrafish brain and heart (unpublished observations). Prior studies suggest that the mammalian β1 subunit may influence the current amplitude and possibly the gating of mammalian $Na_v1.5$ *in vitro* (154-157). Co-expression of *zβ1* with *zscn5a* in Chinese Hamster Ovary (CHO) cells increased peak sodium current by 68% at a -30 mV depolarizing pulse (n=5, $p<0.001$) compared to *zscn5a* alone (n=8) (Figure 4.6A-C, table 6). Co-expression of *zβ1* with *zscn5a* also resulted in small but significant changes in the gating of the $zNa_v1.5$ channel protein. zβ1 induced hyperpolarizing shifts in both the voltage-dependence of activation and inactivation of $zNa_v1.5$, without altering recovery from inactivation (Figure 4.6D-F, table 6). These data suggest that the canonical modulatory effects of mammalian sodium channel β subunits on α subunit function and expression are likely to be conserved in teleosts and other non-mammalian vertebrates.

Evolutionary relationships of vertebrate β subunit genes

Although β subunit genes appear to be related both structurally and functionally to each other and to cell adhesion molecules with V-type IG domains such as myelin protein zero and contactin (11;12), the evolutionary relationships among these genes have not previously been formally studied. To investigate these relationships, we first identified an extended group of human genes that display sequence homology to β subunits. BLAST searches of the human

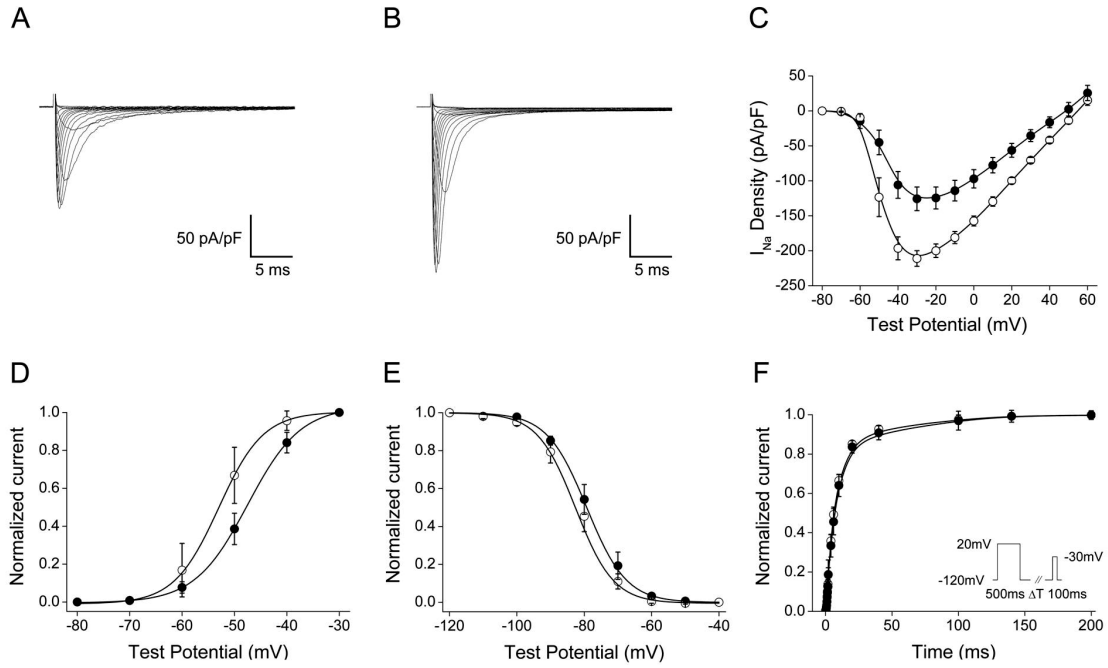

Figure 4.6. The zebrafish β1 subunit modulates the biophysical properties of the zebrafish sodium channel α subunit zNa$_v$1.5 in CHO cells. **(A)** Typical whole-cell sodium current trace of zNav1.5 following expression of the pBK-CMV-*zscn5a* expression vector in CHO cells (n=8). **(B)** Typical whole-cell sodium current trace of zNa$_v$1.5 + zβ1 (variant D) following co-expression of pBK-CMV-*zscn5a* and pGFP-IRES-*zβ1D*. zβ1 significantly increased the peak amplitude of sodium current by 68% (p=0.005) at a -30 millivolt (mV) depolarizing pulse (n=5). **(C)** Current-voltage relationship demonstrating an increase in sodium current at every test potential between -50 and +50mV. Filled circles = zNa$_v$1.5 alone; open circles = zNa$_v$1.5 + zβ1. **(D)** Voltage dependence of activation (zNa$_v$1.5 alone, n=8; zNa$_v$1.5 + zβ1, n=5). **(E)** Voltage-dependence of inactivation. (zNa$_v$1.5 alone, n=5; zNa$_v$1.5 + zβ1, n=6). **(F)** Recovery from inactivation (zNa$_v$1.5 alone, n=4; zNa$_v$1.5 + zβ1, n=6). Pulse protocol in inset. Summary data is reported in table 6.

genome with human β subunit nucleotide and amino acid sequences most frequently-identified the genes *myelin protein zero*, *myelin protein zero-like 1, isoform A* (*MPZL1 iso A*), *epithelial V-like antigen* (*EVA1*), and hypothetical protein LOC196264 which we named "*EVA1-like gene*" (*EVA1L*) for its similarity to *EVA1* and the proximity of these two genes in the human genome. Analysis of the amino acid sequence of each gene using the NCBI conserved domain database and TMpred software revealed that all 4 proteins likely possess single V-type IG domains and transmembrane segments, respectively, similar to sodium channel β subunits (Figure 4.7A). Moreover, comparison of the complementary DNA sequences of these genes against their respective genomic loci indicated that all 4 genes also possess genomic organization similar to sodium channel β subunits (Figure 4.7B). We therefore included these genes in our analysis of the synteny and phylogeny of the extended family of vertebrate β subunit genes. To analyze synteny, we first identified all β subunit-like genes in human, rat, zebrafish, frog (*Xenopus tropicalis*) and bird (*Gallus gallus*) genomes (Table 7). Notably, whereas humans and rats each have 4 and zebrafish have 5 β subunit genes, only 3 β subunit genes were identified in frogs and birds (β1 was not found in either genome). Next, we used reciprocal BLAST searches and *in silico* chromosome walking to assess physical relationships among β-subunit like genes (Figure 4.8). Strikingly, *scn2b*, *scn4b*, and *EVA1/EVA1L* genes map to common locations in every vertebrate genome analyzed (human chromosome 11, rat chromosome 8, zebrafish chromosome 5/15, frog scaffold_39, and chicken chromosome 24), suggestive of a close evolutionary relationship that may have resulted from gene duplication. Although physically more distant, *scn3b* is also syntenic with this group of genes in 4/5 genomes analyzed. Of the 4 sodium channel β subunits, only *scn1b* falls outside this syntenic block. The common ancestry of human, rat, and zebrafish *scn1b* is supported, however, by the proximity of the genes encoding the 26S protease regulatory subunit 6B (*PSMC4*) and fibrillarin (*FBL*) to the *scn1b* locus in all three species (human chromosome 19, rat chromosome 1, zebrafish chromosome 16). The synteny of β subunit genes in mammalian, fish, amphibian, and avian lineages thus supports the hypothesis that extant vertebrate β subunits are orthologous. Moreover, these findings strongly suggest that the evolution of at least several members of this extended gene family (*scn2b*, *scn4b*, *EVA1*,

EVA1L) may have arisen from duplication events that predated the divergence of teleosts and tetrapods.

To further analyze the evolution of vertebrate β subunit-like genes, we reconstructed the phylogeny of this gene family (Figure 4.9). Neighbor-joining phylogenetic analysis of amino acid sequences demonstrated that all-identified sodium channel β subunits fall on one of four branches corresponding to β1, β2, β3, or β4, supporting the preliminary identity assigned to each cloned zebrafish β subunit gene (including the duplicated zebrafish β4 genes) by alignment with each individual mammalian subunit (Figures 4.1A-4.4A). Despite synteny among *scn2b*, *scn3b*, and *scn4b*, phylogenetic analysis revealed that β3 is more closely related to β1 than to either β2 or β4. Moreover, our phylogenetic model incorporating β subunit-like genes additionally indicated that β2 and β4 are more closely-related to each other and to β subunit-like genes than to either β1 or β3. Our analysis thus supports an evolutionary model where β2/β4/β subunit-like genes and β1/β3 arose following duplications of 2 distinct precursor genes. The timing of such duplications cannot be gleaned from this model. The presence of gene orthologs to all 4 β subunits in divergent vertebrates (mammals and teleosts) strongly suggests, however, that the early vertebrate common ancestor to these lineages already had four distinct β subunit genes. Duplication events that occurred in this gene family – aside from that which produced two zebrafish β4 genes – thus occurred earlier in vertebrate evolution or prior to the emergence of the vertebrates altogether.

Absence of β subunit genes in invertebrates

The sequenced genomes of the ascidians *Ciona intestinalis* and *Ciona savignyi* provide an opportunity to identify putative precursors to vertebrate β subunits genes in invertebrate chordates (390;391). Although both ascidian genomes contain several loci encoding Na_v1 voltage-gated sodium channel α subunits, BLAST searches using the nucleotide and protein sequences of zebrafish and mammalian sodium channel β subunits and related proteins (MPZ, EVA1) did not identify any homologous genes. The absence of β subunit-like genes in sequenced *Ciona* genomes does not preclude the presence of numerous other genes with V-type and other

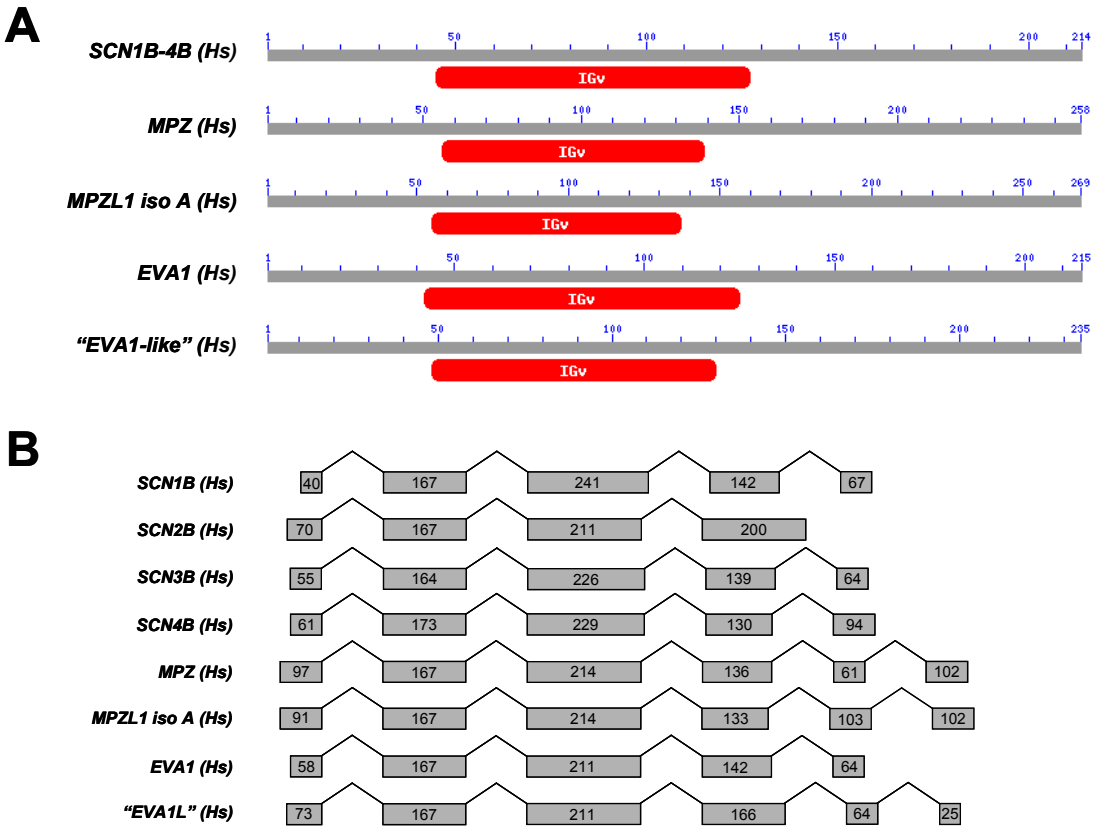

Figure 4.7. Four additional human genes share homology with β subunits in sequence and genomic organization. **(A)** BLASTP searches of the human genome using sodium channel β subunit amino acid sequences identified significant homology to myelin P0 protein (*MPZ*), myelin P0 protein-like protein isoform A (*MPZL1 isoform A)*, epithelial V-like antigen 1 (*EVA1*), and epithelial V-like antigen 1-like gene (*EVA1L*), all of which are single transmembrane proteins with extracellular V-type immunoglobulin domains and intracellular C-terminal tails as predicted by NCBI *conserved domain database v2.09 and TMPred* (see Methods for further details). **(B)** This group of genes additionally shares similar genomic organization. Numbers in grey boxes refer to exon size (nucleotides) with untranslated sequence excluded for clarity.

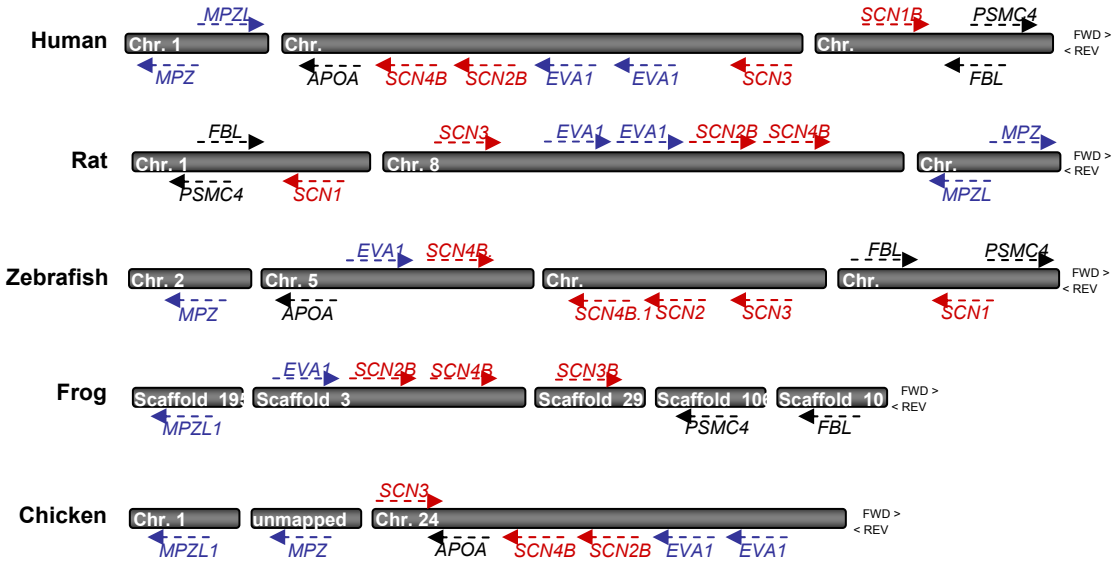

Figure 4.8: *SCN2B*, *SCN3B*, and *SCN4B* are syntenic with each other and with *EVA1*, *EVA-1L*, and *APOA-1* in multiple vertebrate genomes, whereas *SCN1B* is syntenic with *FBL* and *PSMC4* in humans, rats, and zebrafish. To analyze synteny, β subunits and subunit-like genes were identified in human, rat, zebrafish, frog and bird genomes (see Table 7 for gene IDs and physical locations). While humans and rats have four and zebrafish have five β subunit genes, only three β subunit genes were identified in frogs and birds (β1 was not found in either genome). Reciprocal blast searches and *in silico* chromosome walking were used to assess physical relationships among vertebrate β subunit-like genes. HUGO gene nomenclature symbol IDs: *PSMC4* = 26S protease regulatory subunit 6B; *FBL* = fibrillarin; *APOA1* = apolipoprotein A-1; *MPZ* = myelin protein zero; *MPZL1* = myelin protein zero-like gene, isoform A; *EVA1* = epithelial V-like antigen 1; *EVA1L* = unannotated gene similar to EVA1. Red = β subunit genes, Blue = β subunit-like genes, Black = unrelated genes that are syntenic with β subunits.

IG-like domains ((392;393) and unpublished observations). These findings strongly suggest that sodium channel β subunit genes are an innovation of vertebrates. As predicted, searches of the genome of the echinoderm *Strongylocentrotus purpuratus* (sea urchin) (394), a non-chordate deuterostome, also did not reveal any sodium channel β subunits genes.

Despite the lack of evidence for β subunits genes outside of vertebrates, studies conducted in *Drosophila melanogaster* demonstrate that invertebrate sodium channels require additional subunits for normal function. Mutations in the *Drosophila tip-E (temperature-induced paralysis)* gene, which encodes a sodium channel auxiliary subunit, disrupt nerve conduction by perturbing the expression and function of the *para* voltage-gated sodium channel (395-399). Moreover, 4 recently-identified *tip-E* related genes (*TEH1-4* or *tip-E* homologs 1-4) were found to modulate the density and kinetics of sodium currents of heterologously-expressed *para* sodium channels (400). Based on these findings, we sought to assess whether vertebrate and invertebrate sodium channel auxiliary subunits share common structural elements or functional domains. Use of TMPred software and the NCBI conserved domain database demonstrated, however, that *Drosophila* tip-E and tip-E homologous genes (*TEH1-4*) each possess two predicted membrane-spanning segments (not one) and lack the canonical V-type IG domain found in vertebrate β subunits. Additionally, alignment of the amino acid sequences of cloned zebrafish and human sodium channel β subunit genes with the sequences of *Drosophila* tip-E and tip-E homologous genes also revealed only minimal homology (<15% amino acid identity). BLAST searches of the *Drosophila* genome did not uncover any additional genes sharing homology with vertebrate β subunits, despite the presence of numerous genes encoding proteins with immunoglobulin domains ((401) and unpublished observations). These results indicate that vertebrate and invertebrate sodium channel auxiliary subunits are dissimilar in structure and unrelated.

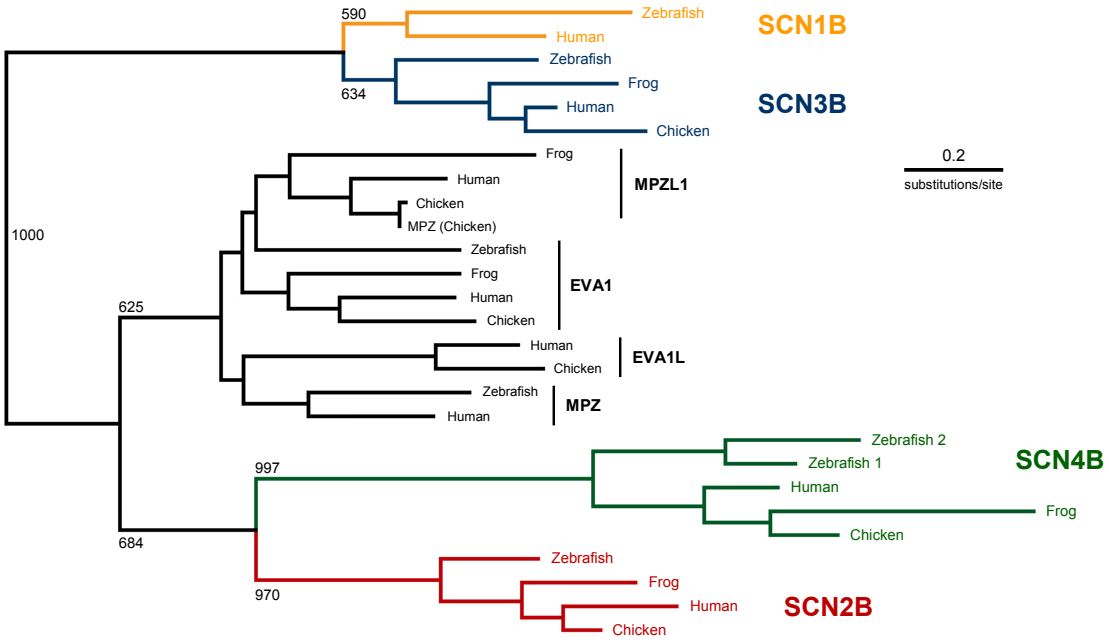

Figure 4.9: Phylogenetic analysis demonstrates that vertebrate sodium channel β1-4 subunit genes are orthologous, that β1/β3 and β2/β4 are closely related, and that zβ4.1 and zβ4.2 resulted from a recent gene duplication in fish. Actual (human, zebrafish) and predicted (chicken, frog) amino acid sequences of β subunit and related genes were aligned using CLUSTALX (v1.83). Phylogenetic trees were reconstructed using the neighbor-joining method of Saitou and Nei and viewed with NJPlot software. Alignment gaps were excluded and the Kimura correction was made for multiple substitutions. Bootstrapping (n=1000) was applied to test the robustness of each node. Tree is unrooted due to the lack of evidence for β subunit-like genes in invertebrate species. HUGO gene nomenclature symbol IDs: *MPZ* = myelin protein zero; *MPZL1* = myelin protein zero-like gene isoform A; *EVA1* = epithelial V-like antigen 1; *EVA1L* = unannotated gene similar to *EVA1*.

Discussion

Numerous studies of mammalian voltage-gated sodium channel β subunits have demonstrated that these small, single membrane-spanning proteins are integral components of sodium channel complexes in excitable tissues, modulators of the expression and function of pore-forming sodium channel α subunits, and candidate genes for clinical disorders linked to perturbed membrane excitability such as arrhythmia and epilepsy (19;402). Despite the early origins of the Na_v1 family of sodium channel α subunits and their cloning from diverse metazoans including eels, jellyfish, flies, and humans, the evolutionary history of sodium channel β subunits has remained obscure. The primary objective of this study was thus to investigate β subunit genes in *Danio rerio* (zebrafish), a pivotal vertebrate species whose teleost ancestors diverged from mammals over 400 million years ago, in order to gain further insight into the origin and regulation of the voltage-gated sodium channel macromolecular complex.

Using a combination of bioinformatics, molecular cloning, and phylogenetic analysis, we identified conserved orthologs of all 4 mammalian β subunit genes and 8 novel β1 and β2 splice variants in zebrafish. Using our cloned zebrafish sequences, we subsequently identified β subunit genes in other non-mammalian vertebrates including *Xenopus tropicalis* (Western clawed frog) and *Gallus gallus* (Red jungle fowl). The existence of conserved mammalian, teleost, amphibian, and avian sodium channel β subunit loci indicates that this gene family is likely to be found in most if not all vertebrate genomes. Moreover, our detection of zebrafish β subunit gene expression in tissues including the heart, muscle, and the brain suggests that the voltage-gated sodium channel α-β subunit macromolecular complex is likely to be a common structural feature of excitable membranes.

Sodium channel complexes in non-mammalian vertebrates: An emerging concept

Our data are the first to support the existence of voltage-gated sodium channel α-β subunit macromolecular complexes in non-mammalian vertebrates. Data from prior studies, however, suggest that sodium channels form α-β subunit complexes in mammals but not in other vertebrate lineages (5-7;142-145;403-407). While sodium channels biochemically purified from rat

neuronal membranes and rat and rabbit skeletal muscle membranes were found to be comprised of 1 α subunit and 1 or more auxiliary β subunits, for example, α subunits purified from the electroplax (electric organ) of the South American eel *Electrophorus electricus* and from chick cardiac muscle were unaccompanied by β subunits (5-7;142-145;403-407). Further investigation into the existence of sodium channel α-β macromolecular complexes in non-mammalian vertebrates is thus needed to reconcile our current findings with the results of previous studies.

There are several possible reasons for the discord between biochemical and molecular genetic approaches. First, it is possible that some but not all voltage-gated sodium channel isoforms within a particular species form complexes by associating with auxiliary β subunits, or that pore-forming α subunits form complexes only in specific tissues. Evidence suggests that even in mammals, for example, the subunit composition of voltage-gated sodium channels significantly varies both by α subunit isoform and by tissue (9;143). Second, at least for the eel electroplax, the function of this organ may depend on sodium channel α subunits that have evolved unique properties which may preclude association with auxiliary subunits (408). Third, it is possible that sodium channel α subunit isoforms in certain tissues form complexes not with canonical β subunits but with yet unidentified proteins. In mammals, the interaction of sodium channel α subunits with a number of additional components and modulators in macromolecular complexes suggest that β subunits may not always serve as obligatory functional partners (for review, see refs (19;168)). Our detection of conserved β subunit mRNA expression in excitable organs such as heart, brain, and skeletal muscle, however, suggests the strong possibility of α-β subunit complexes in these zebrafish tissues. Moreover, co-expression of zebrafish α and β subunit genes in CHO cells demonstrated meaningful functional interactions between the two subunits, with significant differences observed in sodium current amplitude and channel gating when both subunit genes are expressed together versus when the α subunit gene is expressed alone. Despite these findings, however, we cannot completely rule out the possibility that sodium channel β subunit genes play different *in vivo* functional roles in mammals than in non-mammalian vertebrates.

Evolution of sodium channel β subunits and related genes

Our analysis of the synteny and phylogeny of vertebrate sodium channel β subunit genes suggests a different evolutionary history for α and β subunits. For sodium channel α subunits, prevailing evolutionary models posit that the 10 mammalian isoforms arose from the tandem duplication of at least 2 of 4 ancestral sodium channel genes, which in turn had duplicated from 1 or 2 precursor chordate Na_v1 sodium channel genes by polyploidization (97;98;175;180). As would be predicted by this model, the total number of Na_v1 sodium channel genes varies between teleosts and mammals despite the phylogenetic clustering of all of these genes into 4 groups derived from ancestral vertebrate sodium channel genes (180;230). Sodium channel β subunits, which are fewer in number, do not appear to have undergone tandem duplication in either mammals or in non-mammalian vertebrates. This is supported by our finding that 4 distinct vertebrate lineages (mammals, ray-finned fishes, amphibians and birds) all appear to share distinct orthologs to 3 or 4 β subunit genes. Thus, it is likely that the common ancestor to teleosts and tetrapods over 400 million years ago also possessed 4 distinct ancestral β subunit genes (β1-4). The presence of 2 β4 orthologs on different zebrafish chromosomes is likely to be the remnant of an additional polyploidization event known to have occurred in teleost vertebrates but not in mammals (227). It is difficult to determine why duplicate genes for β1-3 have not been retained in zebrafish; it is possible that >5 β subunit genes did not offer teleosts any evolutionary advantage (176).

The close phylogenetic relationship of *SCN1B* and *SCN3B* and the physical proximity of *SCN2B* and *SCN4B* to each other and to genes (e.g. *EVA1*) that are β subunit-like in sequence and genomic organization is strong evidence that duplication events gave rise to the β subunit gene family during the postulated large-scale expansion of the early vertebrate genome. Although we cannot accurately predict the early evolutionary history of sodium channel β subunit genes prior to the divergence of teleosts from other vertebrate lineages, the results of our phylogenetic analysis support the existence of 2 ancestral β subunit genes (β1/β3 and β2/β4) in early vertebrates. Somewhat surprisingly (but in agreement with a previous report (177)), BLASTN and BLASTP searches of available urochordate (*Ciona intestinalis*, *Ciona savignyi*) genomes did not

identify any sodium channel β subunit-like genes, despite the clear existence of genes encoding proteins with immunoglobulin domains similar to those found in β subunits (392;393). Moreover, we and others also found limited homology between vertebrate β subunit genes and the *tip-E*/*TEH* subunits of the *para* sodium channel in *Drosophila* (178;397). These findings strongly suggest that sodium channel β subunits are a unique vertebrate innovation.

The similarity of vertebrate sodium channel β subunits to members of a more ancient family of IG domain-containing proteins suggests that β subunit genes may have arisen *de novo* in early vertebrates from genes encoding cell-adhesion molecules, membrane receptors, or components of the innate immunity. The property of modulation of the expression and function of sodium channel β subunits may thus represent a more evolutionarily recent function for this gene family. These findings support the idea that molecular mechanisms enhancing functional diversity and specialization in electrical signaling – either through α subunit gene duplication, editing or alternative splicing of α subunit RNA transcripts, or the emergence of auxiliary proteins that associate with α subunits to modulate their expression and/or function – may have been adaptive and underwent selection in the evolving nervous system of early vertebrates and subsequently, in the increasingly complex excitable tissues of diverse vertebrate lineages including mammals. Despite the lack of common ancestry among invertebrate *tip-E/TEH* subunits and vertebrate IG-like β subunits, the apparent independent evolution of Na_v1 sodium channel-interacting proteins in distantly-related species demonstrates that the formation of sodium channel macromolecular complexes is an evolutionary advantageous and conserved mechanism for fine-tuning the properties of excitable membranes.

Functional implications of alternative splicing of zebrafish β subunit genes

The evidence we present for the extensive C-terminal alternative splicing of zebrafish β subunit genes is intriguing because it may represent another conserved molecular mechanism for modulating electrical signaling in vertebrates. Alternative splicing has been reported for both mammalian sodium channel α and β subunits and invertebrate α subunits, often with important functional consequences (386;387;409-415). The intronic retention events that produce both the

rat β1A and human β1B variants each result in a protein with a novel transmembrane domain and intracellular C-terminal tail. When stably expressed in Chinese Hamster Lung (CHL) fibroblasts, rat β1 and β1A differentially modulate the function of the rat sodium channel α subunit $Na_v1.2$ (*scn2a*) (386). Similarly, the human β1 and β1B subunits differentially modulate the function of human $Na_v1.2$ in *Xenopus* oocytes (387). These studies suggest that the transmembrane domain and C-terminus of the human and rat β1 subunits contribute to the functional modulation of sodium channel α subunits. In a subsequent study, the β1 intracellular C-terminal tail in particular was found to be required for both efficient physical association with $Na_v1.2$ and for the modulation of sodium channel function in both mammalian cells and *Xenopus* oocytes (416). This raises the possibility that the zebrafish β1 and β2 subunit splice variants identified in this study may also differentially influence the function of sodium channel α subunits. Our identification of distinctive expression patterns for different splice variants of the same gene underscores the complexity of this putative sodium channel regulatory mechanism.

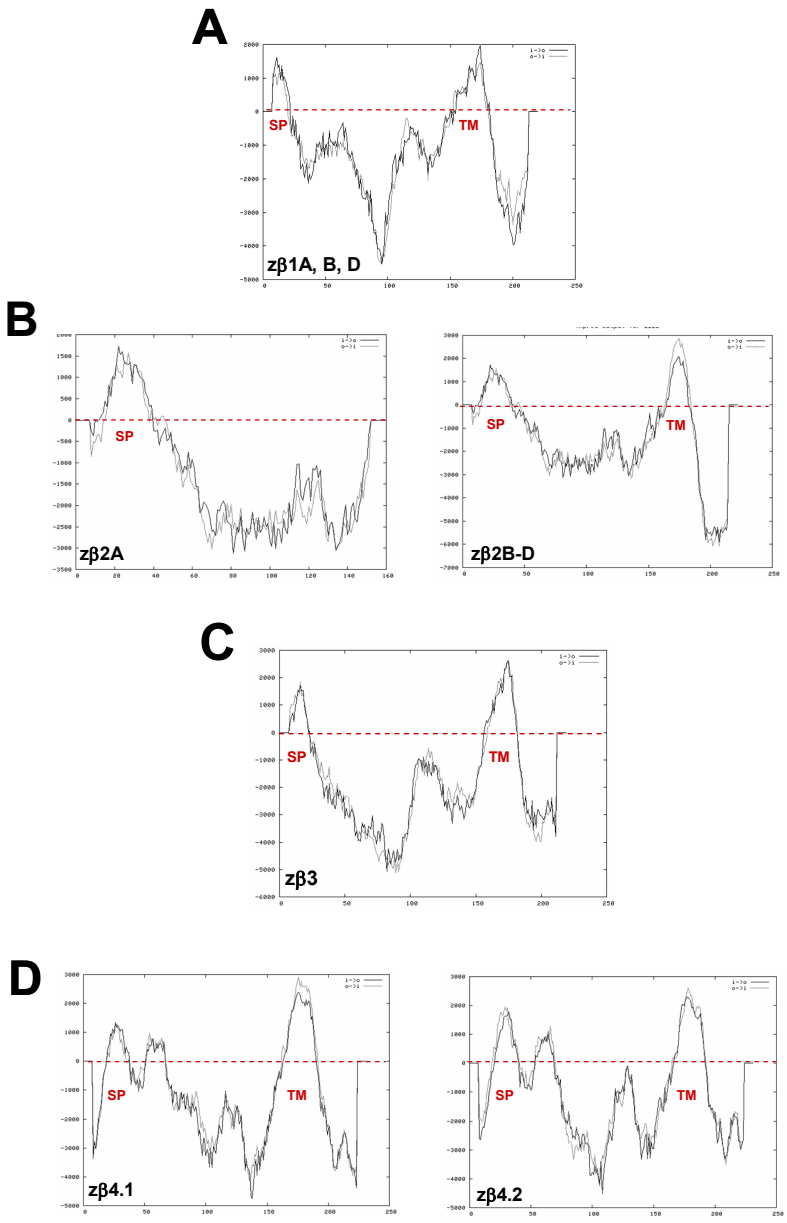

Figure 4.10: Hydropathy analysis of zebrafish β subunit amino acid sequences reveals conserved protein secondary structure. TMPred hyropathy plot based on the method of Kyte and Doolittle. Dotted red line drawn at 0 (neutral). SP = signal peptide and TM = transmembrane domain. Dotted line plot (black) indicates outside>inside orientation relative to membrane, while solid line plot (black) indicates inside>outside orientation. **(A)** Hydropathy plots for zβ1 variants A, B, and D are nearly identical (zβ1D shown). **(B)** zβ2A and zβ2B-D. **(C)** zβ3. **(D)** zβ4.1 and zβ4.2.

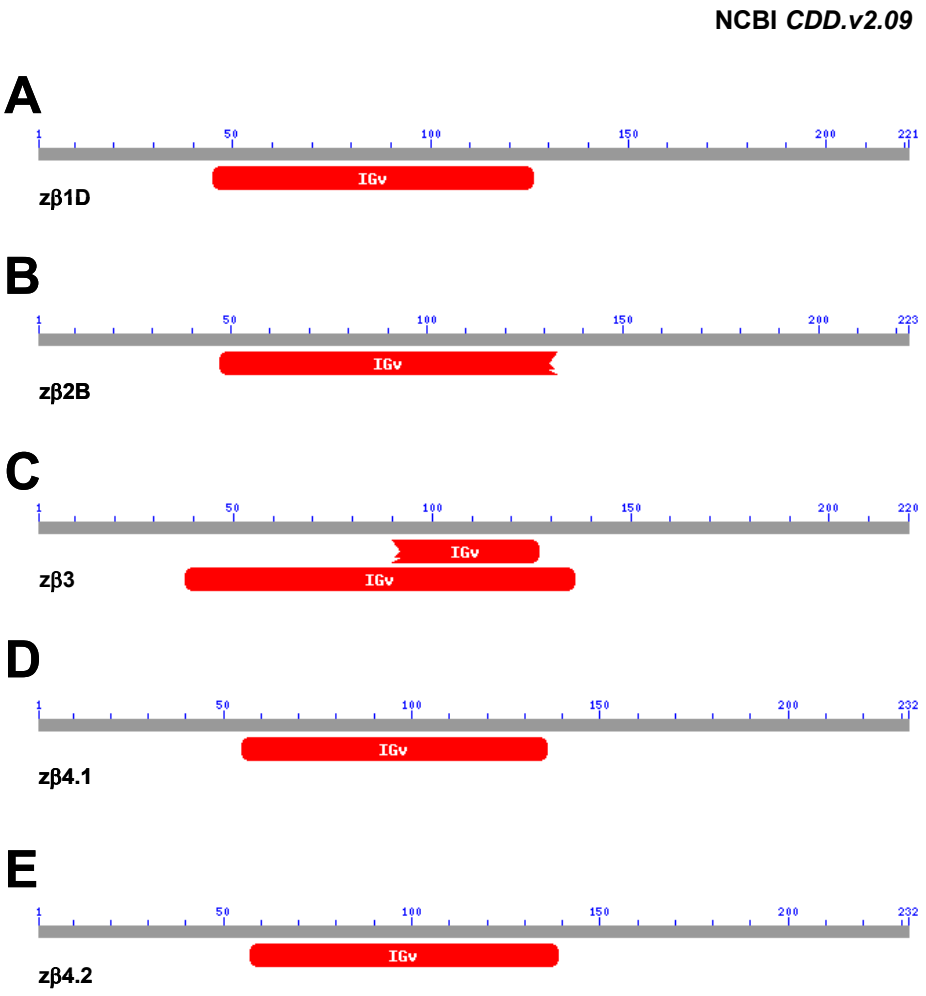

Figure 4.11: Prediction of conserved extracellular V-type IG domains in the amino acid sequences of the most highly-conserved splice variants of zβ1-4, NCBI Conserved Domain Database (CDD *v2.09*). Predicted V-type IG domain is shown in red, and the scale denotes the length of the full-length protein. **(A)** zβ1D. **(B)** zβ2B. **(C)** zβ3. **(D)** zβ4.1. **(E)** zβ4.2.

Table 4.1: Comparative genomics of the sodium channel β1 gene in zebrafish and mammals.

gene	Genbank accession number	gene location	cDNA	exon 1	exon 2	exon 3	exon 4	exon 5	exon 6	protein	%ID (%SIM)	topology
zβ1A	DQ489722	Chr 16	1411	219 (52)	167	238	142	645 (31)	—	209	47.5% (57.0%)	IG(V): 37-149 TM: 164-185
zβ1B	DQ489723	Chr 16	1054	219 (52)	167	238	142	28	260 (9)	211	49.8% (59.6%)	IG(V): 37-149 TM: 164-185
zβ1C	DQ489724	Chr 16	574	219 (52)	355 (266)	—	—	—	—	105	13.0% (17.5%)	IG(V): none TM: none
zβ1D	DQ489725	Chr 16	1320	219 (52)	167	238	142	72 (67)	482 (0)	221	53.4% (63.7%)	IG(V): 37-149 TM: 164-185
hβ1	NM_001037	Chr 19	1521	231 (40)	167	241	142	72 (67)	668 (0)	218	100% (100%)	IG(V): 33-146 TM: 161-182
rβ1A	AF182949	Chr 1	850	40	167	643 (615)	—	—	—	273	55.1% (59.1%)	IG(V): 33-146 TM: 216-234
hβ1B	NM_199037	Chr 19	1170	231 (40)	167	772 (600)	—	—	—	268	58.0% (60.2%)	IG(V): 33-146 TM: 244-263

Gene: z = zebrafish, h = human, r = rat, and letters A-D refer to different splice variants. Accession numbers are identifiers for nucleotide sequences in NCBI GenBank. Values for cDNA and exons represent number of nucleotides. (Parentheses) indicate nucleotides within the open reading frame (difference = untranslated sequence or UTR). Protein values represent amino acid number with signal peptide intact. %ID (%SIM) refers to percentage identity and similarity with the human β1 protein sequence as determined by alignment. Zebrafish β subunit topology was determined as described in Methods. IG(V) = V-type immunoglobulin domain and TM = transmembrane domain. Numbering refers to β1 protein sequence with signal peptide intact. IG(V) domain and transmembrane regions for human β1 and human/rat splice variants were annotated based on previous reports (10;14;382;386;387).

Table 4.2: Comparative genomics of the sodium channel β2 gene in zebrafish and mammals.

gene	Genbank accession number	gene location	cDNA	exon 1	exon 2	exon 3	exon 4	exon 5	exon 6	protein	%ID (%SIM)	topology
zβ2A	DQ489726	Chr 15	821	243 (82)	167	411 (234)	—	—	—	160	32.6% (42.5%)	IG(V): 47-152 TM: none
zβ2B	DQ489727	Chr 15	2449	243 (82)	167	217	196	68 (10)	1558 (0)	223	49.6% (64.7%)	IG(V): 47-152 TM: 162-186
zβ2C	DQ489728	Chr 15	851	243 (82)	167	217	124	100 (13)	—	201	45.2% (58.4%)	IG(V): 47-152 TM: 162-186
zβ2D	DQ489729	Chr 15	918	243 (82)	167	217	193	98 (34)	—	231	48.1% (62.8%)	IG(V): 47-152 TM: 162-186
Hsβ2	NM_004588	Chr 11	4939	260 (70)	167	211	4301 (200)	—	—	215	100% (100%)	IG(V): 43-146 TM: 156-180
Mmβ2	NM_001014761	Chr 9	3980	213 (70)	167	211	618 (200)	2771 (0)	—	215	92.1% (94.4%)	IG(V): 43-146 TM: 156-180
Rnβ2	NM_012877	Chr 8	873	236 (70)	167	211	259 (200)	—		215	93.0% (94.9%)	IG(V): 43-146 TM: 156-180

Presentation and labeling as in Table 1. %ID (%SIM) refers to percentage identity and similarity with the human β2 protein sequence as determined by alignment. Zebrafish β2 subunit topology was determined as described in Methods. Numbering refers to β2 protein sequence with signal peptide intact. IG(V) domain and transmembrane regions for human β2 and human/mouse/rat splice variants were annotated based on previous reports (11;14;382;417).

Table 4.3: Comparative genomics of the sodium channel β3 gene in zebrafish and mammals.

gene	Genbank accession number	gene loc.	cDNA	exon 1	exon 2	exon 3	exon 4	exon 5	exon 6	exon 7	protein	%ID (%SIM)	topology
zβ3	DQ489730	Chr 15	1006	294 (0)	103 (55)	170	235	139	65 (64)	__	220	51.1% (65.2%)	IG(V): 38-150 TM: 165-186
Hsβ3	NM_018400	Chr 11	4052	778 (0)	80 (55)	164	226	139	86 (64)	2579 (0)	215	100% (100%)	IG(V): 38-145 TM: 160-181
Mmβ3	NM_178227	Chr 9	3549	206 (0)	80 (55)	164	226	139	80 (64)	2654 (0)	215	97.7% (97.7%)	IG(V): 38-145 TM: 160-181
Rnβ3	NM_139097	Chr 8	3910	350 (0)	82 (55)	164	226	139	80 (64)	2837 (0)	215	98.1% (98.1%)	IG(V): 38-145 TM: 160-181

Presentation and labeling as in Table 1. %ID (%SIM) refers to percentage identity and similarity with the human β3 protein sequence as determined by alignment. Zebrafish β3 subunit topology was determined as described in Methods. Numbering refers to β3 protein sequence with signal peptide intact. IG(V) domain and transmembrane regions for human β3 and human/mouse/rat splice variants were annotated based on previous reports (12;14).

Table 4.4: Comparative genomics of the sodium channel β4 gene in zebrafish and mammals.

gene	Genbank accession number	gene loc.	cDNA	exon -1	exon 1	exon 2	exon 3	exon 4	exon 5	protein	%ID (%SIM)	topology
zβ4.1	DQ489731	Chr 22	2072	__	597 (91)	164	220	130	961 (94)	232	43.2% (59.3%)	IG(V): 53-155 TM: 165-187
zβ4.2	DQ489732	Chr 5	1490	233 (0)	410 (97)	164	223	130	330 (85)	232	40.8% (56.7%)	IG(V): 55-158 TM: 168-190
Hsβ4	NM_174934	Chr 11	4489	__	214 (61)	173	229	130	3743 (94)	228	100% (100%)	IG(V): 46-151 TM: 162-183
Mmβ4	NM_001013390	Chr 9	4244	__	61	173	229	130	3651 (94)	228	79.4% (88.2%)	IG(V): 46-151 TM: 162-183
Rnβ4	NM_001008880	Chr 8	4272	__	61	173	229	130	3679 (94)	228	80.3% (88.6%)	IG(V): 46-151 TM: 162-183

Presentation and labeling as in Table 1. %ID (%SIM) refers to percentage identity and similarity with the human β4 protein sequence as determined by alignment. Zebrafish β4 subunit topology was determined as described in Methods. Numbering refers to β4 protein sequence with signal peptide intact. IG(V) domain and transmembrane regions for human β4 and human/mouse/rat splice variants were annotated based on previous reports (13;14).

Table 4.5: Primers used to detect expression of zebrafish β subunit genes and splice variants in different tissues of the adult zebrafish.

Forward Primer (5'-3')	*Reverse Primer (5'-3')*	*Gene*	*Variant*	*Amplicon Size (bp)*
CTACACTTATGCAGAAATGACAGCCAGC	GATGGACAGAGCTTCAAGCTTTTGGCT	zβ1	A	422
		zβ1	D	494
GACAGAATCCTCATCTTCCCCAACTATG	CTGCATTCTTCATTTAAACTCAGAGGT	zβ1	B	267
		zβ1	D	534
GTCCCTGCGCTGTTGTGTTTAACACAT	GGGTGAACAATCCCTTTAAGCTGCACT	zβ1	C	382
CAGCTGACAGACGAGGGCATCTACAACT	CAACACCTGCAGTGAGAAAACCCCATT	zβ2	A	201
CATCCTTGCTCTGCTCATTCTGTCCAT	TCGCTACACGATAATACCAGGGAGTGT	zβ2	B	304
		zβ2	C	169
		zβ2	D	236
CTGGTGTGTGTGGATGTGCCATCA	CTTGTTGGCGGAAAGCTTGAATGA	zβ3	—	357
AGGTGAGCACAGGGAAGGTCCATT	GGAGGCCATTTTCTGTGTTGTCGT	zβ4	loc1	543
TGTGTTGTGTTCATGCTTTG	GACCACCTTTAGTTCCTCTA	zβ4	loc2	395

Note: several primer pairs detected multiple splice variants, as indicated above and displayed in Figure 4.5. BP= base pairs or nucleotide number.

Table 4.6: Biophysical properties of $zNa_v1.5$ and $zNa_v1.5$ plus zβ1 (variant D) in CHO cells.

	Peak amplitude (pA)*	Activation $V_{1/2}$ (mV)	Inactivation $V_{1/2}$ (mV)	Recovery from inactivation, Tau (ms)
$zNa_v1.5$ alone	-125.7 ± 16.9 pA/pF (n=8)	-47.5 ± 1.6mV (n=8)	-79.3 ± 1.0mV (n=5)	127.9 ± 8.1ms (n=4)
$zNa_v1.5$ + zβ1	-211.1 ± 11.2 pA/pF† (n=5)	-53.0 ± 2.5mV† (n=5)	-82.6 ± 1.1mV† (n=6)	125.7 ± 4.1ms (n=6)

All values are mean ± standard error of the mean (SEM). * at a -30 mV depolarizing pulse. † $p<0.001$ vs. $zNa_v1.5$ alone, Student's T-Test. pA = picoamperes; mV = millivolts; ms = milliseconds; pF = picofahrads; $V_{1/2}$ = half maximal voltage.

Table 4.7: List of cloned and predicted genes utilized for analysis of synteny and phylogeny of the extended β subunit gene family in vertebrates.

		Analysis of Synteny		Analysis of Phylogeny
Gene	**Species**	**Accession No. (Gene)**	**Physical Location**	**Accession No. (Protein)**
SCN1B	*Homo sapiens*	ENSG00000105711	chr. 19 (FWD, 40.21-40.22Mb)	ENSP00000262631
	Rattus norvegicus	ENSRNOG00000021102	chr. 1 (REV, 86.16-86.17Mb)	n/a
	Danio rerio	ENSDARG00000060222	chr. 16 (REV, 47.82-47.83Mb)	ABF47239
SCN2B	*Homo sapiens*	ENSG00000149575	chr. 11 (REV, 117.54-117.55Mb)	ENSP00000278947
	Rattus norvegicus	ENSRNOG00000016221	chr. 8 (FWD, 48.07-48.08Mb)	n/a
	Danio rerio	ENSDARG00000041176	chr. 15 (REV, 27.32Mb)	ABF47241.
	Xenopus tropicalis	ENSXETESTG00000009930	*scaffold_39 (FWD, 0.58-0.59Mb)	ENSXETESTP00000016971
	Gallus gallus	ENSGALG00000021272	chr. 24 (REV, 5.10-5.11Mb)	ENSGALP00000033652
SCN3B	*Homo sapiens*	ENSG00000166257	chr. 11 (REV, 123.01-123.03Mb)	ENSP00000299333
	Rattus norvegicus	ENSRNOG00000006937	chr. 8 (FWD, 43.23-43.25Mb)	n/a
	Danio rerio	ENSDARESTG00000011553	chr. 15 (REV, 28.62-28.64Mb)	ABF47244
	Xenopus tropicalis	ENSXETESTG00000002589	*scaffold_298 (FWD, 0.94-0.96Mb)	ENSXETESTP00000004357
	Gallus gallus	ENSGALESTG00000012587	chr. 24 (FWD, 2.82-2.83Mb)	ENSGALESTP00000019882
SCN4B.1	*Homo sapiens*	ENSG00000177098	chr. 11 (REV, 117.51-117.53Mb)	ENSP00000322460
	Rattus norvegicus	ENSRNOG00000026679	chr. 8 (FWD, 48.09-48.11Mb)	n/a
	Danio rerio	ENSDARESTG00000010162	chr. 15 (REV, 27.26-27.29Mb)	ABF47245
	Xenopus tropicalis	ENSXETESTG00000009931	*scaffold_39 (FWD, 0.61-0.63Mb)	ENSXETESTP00000016972
	Gallus gallus	ENSGALG00000007409	chr. 24 (REV, 5.10Mb)	ENSGALP00000011971
SCN4B.2	*Danio rerio*	ENSDARESTG00000000878	chr. 5 (FWD, 38.08-38.10Mb)	ABF47246
MPZ	*Homo sapiens*	ENSG00000158887	chr. 1 (REV, 159.54-159.55Mb)	ENSP00000289928
	Rattus norvegicus	ENSRNOESTG00000011377	chr. 13 (FWD, 87.04-87.05Mb)	n/a
	Danio rerio	ENSDARG00000038609	chr. 2 (REV, 46.60-46.62Mb)	ENSDARP00000056371
	Gallus gallus	ENSGALESTG00000015635	*chr. Un (REV, 60.79-60.80Mb)	ENSGALP00000008810
MPZL1 isoA	*Homo sapiens*	ENSG00000197965	chr. 1 (FWD, 165.96-166.03Mb)	ENSP00000352513
	Rattus norvegicus	ENSRNOG00000003248	chr. 13 (REV, 81.32-81.36Mb)	n/a
	Xenopus tropicalis	ENSXETG00000023014	*scaffold_195 (REV, 1.78-1.79Mb)	ENSXETP00000049765
	Gallus gallus	ENSGALG00000015438	chr. 1 (REV, 85.41-85.44Mb)	ENSGALP00000024855
EVA1	*Homo sapiens*	ENSG00000149573	chr. 11 (REV, 117.63-117.64Mb)	ENSP00000278937
	Rattus norvegicus	ENSRNOG00000016085	chr. 8 (FWD, 47.99-48.00Mb)	n/a
	Danio rerio	ENSDARG00000027345	chr. 5 (FWD, 38.05-38.07Mb)	ENSDARP00000032601
	Xenopus tropicalis	ENSXETESTG00000008504	*scaffold_39 (FWD, 0.51-0.54Mb)	ENSXETESTP00000014524
	Gallus gallus	ENSGALG00000007412	chr. 24 (REV, 5.12-5.13Mb)	ENSGALP00000011976
"EVA1-like"	*Homo sapiens*	ENSG00000160588	chr. 11 (REV, 117.60-117.63Mb)	ENSP00000278949
	Rattus norvegicus	ENSRNOG00000026753	chr. 8 (FWD, 48.00-48.01Mb)	n/a
	Gallus gallus	ENSGALG00000021271	chr. 24 (REV, 5.11-5.12Mb)	ENSGALP00000033649

PSMC4	*Homo sapiens*	ENSG00000013275	chr. 19 (FWD, 45.17-45.18Mb)	n/a
	Rattus norvegicus	ENSRNOG00000018994	chr. 1 (REV, 83.15-83.16Mb)	n/a
	Danio rerio	ENSDARG00000027099	chr. 16 (FWD, 47.99-5-48.00Mb)	n/a
	Xenopus tropicalis	ENSXETG00000014266	*scaffold_1060 (REV, 0.17Mb)	n/a
FBL	*Homo sapiens*	ENSG00000105202	chr. 19 (REV, 45.02-45.03Mb)	n/a
	Rattus norvegicus	ENSRNOG00000019229	chr. 1 (FWD, 83.27-83.28Mb)	n/a
	Danio rerio	ENSDARG00000053912	chr. 16 (FWD, 47.49-47.50Mb)	n/a
	Xenopus tropicalis	ENSXETG00000017830	*scaffold_1073 (REV, 0.14Mb)	n/a
APOA1	*Homo sapiens*	ENSG00000118137	chr. 11 (REV, 116.21Mb)	n/a
	Danio rerio	ENSDARG00000012076	chr. 5 (REV, 38.04Mb)	n/a
	Gallus gallus	ENSGALG00000007114	chr. 24 (REV, 4.79-4.80Mb)	n/a

All genes and proteins are identified by Ensembl accession numbers, except for cloned zebrafish beta subunit protein sequences (which begin with ABF and represent accession numbers assigned by GenBank). * = unmapped scaffolds in Ensembl database. FWD = forward and REV = reverse and refers to gene orientation. n/a = not applicable (e.g. proteins for this species were not included in phylogenetic analysis).

CHAPTER V

A DISCUSSION OF FUTURE STUDIES

Introduction

By initiating action potentials in excitable tissues, voltage-gated sodium channels underlie each human thought, movement, and heartbeat. *In vitro* and *in vivo* models have recently begun to divulge how perturbations of the expression or function of sodium channels within single cells may underlie paroxysmal disorders of excitability including epilepsy, myotonia, and arrhythmia (257). However, our nascent understanding of the functional importance of voltage-gated sodium channels is continually challenged by evidence that implicates these proteins in the genesis of multiple unexpected phenotypes. In the adult heart, recent reports suggest that that mutations in the cardiac sodium channel gene *SCN5A* underlie a form of structural heart disease known as dilated cardiomyopathy (275;359;418;419). In a deceased child who was heterozygous for 2 distinct *SCN5A* mutations, post-mortem analysis of the myocardium revealed dilated cardiomyopathy accompanied by myocardial fibrosis and severe degenerative changes of the conduction system (420). In a study of 18 patients with the Brugada syndrome, myocardial tissue of carriers of *SCN5A* mutations displayed cellular hypertrophy and degenerative changes including fibrofatty infiltration, vacuolization, and apoptosis, as revealed by biventricular endomyocardial biopsy (421). Similarly, evaluation of the explanted heart of a patient with the Brugada syndrome demonstrated hypertrophy, fibrosis and fatty infiltration of the right ventricular myocardium (422). In an emerging story, cardiac sodium channel mutations have been linked to a second form of cardiomyopathy known as left ventricular non-compaction, a disease of the myocardium that is thought to result from an arrest of myocardial development *in utero* (272;423).

Mouse models of *scn5a* loss of function also display structural myocardial defects. Mice heterozygous for *scn5a* (+/-), which are considered a model for Lenègre Disease (progressive cardiac conduction disorder), developed significant age-related myocardial fibrosis accompanied

by disorganized expression of gap junction proteins, elevated expression of the hypertrophic markers β-myosin heavy and skeletal α-actin, and upregulation of the transcription factors *Atf3* and *Egr1* (424-426). Mice overexpressing the transcriptional repressor *Snail* under the control of the MHC-α gene promoter (active shortly after birth) developed dilated cardiomyopathy that was strongly correlated with decreased sodium channel expression and function (427). Finally, of particular interest to us, mice homozygous null for *scn5a* (-/-) were found to be embryo-lethal on E10 with severe defects in ventricular morphogenesis.

The mechanisms underlying these structural myocardial phenotypes are not well understood and are likely to be complex. Royer et al. hypothesized that the structural abnormalities observed in *scn5a*$^{+/-}$ mice resulted from the protracted effects of decreased sodium current and asynchronous ventricular excitation, which may have altered cardiac load and induced myocardial remodeling (424). McNair et al. argued that sodium channel-associated dilated cardiomyopathy may have resulted from changes in ion homeostasis (359). Both Olson et al. and Frustaci et al. elaborated on this concept, suggesting that *SCN5A* mutations may perturb intracellular sodium homeostasis, which in turn could trigger increased activity of membrane transporters such as the Na^+-Ca^{2+} exchanger and Na^+-H^+ exchanger, whose function depends on sodium gradients (421;428). In the long-term, altered function of such transporters could lead to deleterious changes in intracellular calcium levels and pH. Having observed an increased level of apoptosis in the hearts of 4 patients with *SCN5A*-associated Brugada syndrome, Frustaci et al. additionally hypothesized that cardiac structural abnormalities may have resulted from a previously-undefined role for sodium current in myocyte viability (421). Although compelling, support for any of these models has been hampered by a lack of direct, empirical evidence from animal models or *in vitro* cellular assays. Moreover, it remains to be explained in each model why patients with certain loss-of-function sodium channel mutations display only perturbations of heart rhythm, whereas patients with other mutations predicted to similarly compromise sodium channel function additionally develop structural abnormalities of the myocardium.

Given the results of our recent studies and evidence from the literature, perturbations of electrical activation or ion homeostasis also do not readily explain the impressive role of *scn5a* in

murine cardiac morphogenesis. Cultured myocytes isolated from E11-E13 mouse hearts displayed only small sodium currents, and in a pattern that was inconsistent with sodium channels being the primary mechanism of depolarization in the early mammalian heart (309). Similarly, studies conducted over two decades ago using chick embryos demonstrated that early action potentials were insensitive to high concentrations of tetrodotoxin and thus unlikely to be mediated by voltage-gated sodium channels (286;314). In zebrafish, we found no role for voltage-gated sodium channels in cardiac rhythm until between days 4 and 5, well after the cardiac chambers had formed and looped (Chapter 3). Moreover, our data suggested that cardiac-type sodium channels can function via a non-electrogenic mechanism to regulate the patterning of early cardiogenic mesoderm (Chapter 3). Finally, a child who was compound heterozygous for mutations in *SCN5A* that were predicted to reduce sodium current by 90-95% died at 1 year of age but did not display congenital defects in cardiac chamber formation (420).

In light of these findings, it is notable that a significant literature has emerged regarding the voltage-gated sodium channel "complex" that may guide future investigation into the proposed non-electrogenic roles of these proteins in development. It is increasingly well-appreciated that sodium channel pore-forming α subunits do not exist alone at the membrane but recruit a number of functionally diverse proteins (429). The canonical ancillary components of this complex are termed β subunits (*SCN1B-4B*) and are small, single membrane-spanning proteins with extracellular immunoglobulin domains and short intracellular C-terminal tails (5;8;143;430). In addition to their well-known effects modulating the expression and function of pore-forming α subunits, β subunits have been shown to act as bidirectional signaling molecules at the membrane. The β subunit IG domain, for example, can act as a cell-adhesion molecule by mediating interactions between the sodium channel complex and proteins in the extracellular matrix (345;346;348;349;431). Intracellularly, the β subunit C-terminal tail has been shown to interact with the cytoskeletal protein ankyrin (348;349). In addition to β subunits, more recent studies indicate that cardiac-type sodium channels also interact with a functionally-diverse array of additional proteins including 14-3-3, Nedd-4 type ubiquitinases, calmodulin, ankyrin G, syntrophins, and fibroblast growth factor homologous factors, among others

(235;236;241;243;432-435). Many of these interactions are mediated by discreet domains within the sodium channel protein. With some minor exceptions, however, studies investigating the roles of sodium channel-interacting proteins have focused exclusively on the ability to modulate sodium current conveyed by the pore forming α subunits. The idea that the pore-forming α subunit itself could act as a scaffold that facilitates the non-electrogenic functions of channel-associated proteins has never been formally tested. Given the demonstrated interaction of sodium channels with both ankyrin and components of the dystrophin complex, for example, it is notable that a phenotype recently associated with *SCN5A* mutations (heritable dilated cardiomyopathy) has most often been previously linked to mutations in the genes encoding components of the sarcomere or cytoskeleton (235;243;423). It is unknown whether interactions with large membrane proteins such as voltage-gated sodium channels are important to the normal function and/or localization of structural components of myocytes, but such studies could be readily performed mice that lack one or more alleles of *scn5a*.

It is also worth considering that particular regions of the voltage-gated sodium channel α subunit may act as signaling molecules independent of the channel protein. The remarkable recent observation that the C-terminus of the L-type calcium channel is cleaved from the α subunit and subsequently travels to the nucleus to act as a transcriptional regulator lends further support to the concept that ion channel proteins may act via unanticipated, non-electrogenic mechanisms (337). The close phylogenetic relationship between voltage-gated ion channels that convey sodium and calcium suggest an additional avenue for investigation into the mechanisms by which $Na_v1.5$ regulates cardiac development.

Future studies may test the hypothesis that voltage-gated sodium channels can influence both cardiac form and function by mechanisms that are independent of their role in generating action potentials. Our studies in zebrafish were the first to explicitly uncouple sodium channel-mediated excitability from the expression of sodium channel protein and therein identified a putative non-electrogenic role for a Na_v1 voltage-gated sodium channel in development. Like mice, fish with reduced sodium channel expression developed significant defects in cardiac morphogenesis that are associated with a reduced number of embryonic

myocytes. Our results indicated that these defects are likely to have arisen from changes in the expression of early cardiogenic transcription factors that are required for the production of appropriate numbers of cardiac progenitor cells. The absence of early expression of *nkx2.5* in sodium channel morphant zebrafish is not only of biological and developmental interest, but represents a discreet phenotype that can be now be exploited *in vivo* to test particular mechanistic hypotheses regarding the non-electrogenic functions of voltage-gated sodium channels. Future studies may thus be performed to clarify the role of cardiac-type sodium channels in early development and to identify putative non-electrogenic mechanisms that govern this role. These endeavors would be motivated by the following 2 key questions:

1. **Which signaling pathways underlying cardiac lineage specification are regulated by cardiac-type voltage-gated sodium channels?**
2. **By what structural and/or functional mechanisms do sodium channels act to influence development?**

As described below in the following 4 proposed future studies, both animal models (zebrafish, mice) as well as *in vitro* approaches may be employed to investigate these questions.

Future Study I

To identify the pro-cardiogenic signaling pathways perturbed by reduced sodium channel expression in the gastrulating zebrafish embryo. Recent fate mapping studies in zebrafish have revealed that presumptive cardiac progenitor cells are organized at the margin of the blastula between 60º and 140º bilaterally from the dorsal aspect (279). During gastrulation, these cells involute and subsequently begin to express markers of the cardiac lineage including the homeobox transcription factors *nkx2.7* (1 somite) and *nkx2.5* (6 somites) in bilateral stripes of anterior lateral mesoderm (291;436). The loss of expression of *nkx2.5* at 6 somites following knockdown of $zNa_v1.5a$ or $zNa_v1.5b$ suggested the disruption of critical molecular mechanisms that normally act to specify the cardiac cell fate during gastrulation. In zebrafish, a number of conserved molecules are required for cardiac fate specification including components of the bone morphogenetic protein (BMP), TGF-β/nodal, Wnt/β-catenin, retinoic acid, and fibroblast growth

factor (FGF) signaling pathways (290;300;437-441). We hypothesize that one or more of these pathways are disrupted by reduced cardiac-type sodium channel expression in the gastrulating embryo.

The proposed hypothesis may be tested using whole-mount *in situ* hybridization, transcriptional profiling, and analysis of epistasis in embryos with reduced expression of cardiac-type sodium channels. By conventional RT-PCR, we found that transcripts of both *zscn5Laa* and *zscn5Lab* are expressed during gastrulation. As morpholino antisense oligonucleotides directed against *zscn5Laa* more consistently induced defects in the expression of *nkx2.5*, studies of this gene may be pursued in greater detail. First, it is important to determine whether the loss of *nkx2.5* can alone sufficiently account for the defects in cardiac morphogenesis and reduced myocyte number. Although loss of expression of *nkx2.5* in *Drosophila* leads to complete absence of a contractile dorsal vessel, *nkx2.5* does not act alone to specify the cardiac cell fate in murine embryos (442;443). These data indicate that unlike invertebrates, vertebrates are likely to have evolved additional genes that act in concert to specify the cardiac cell fate. To determine whether the loss of *nkx2.5* expression alone is sufficient to account for the cardiac development defects observed in *zscn5Laa* morphants, wild-type *nkx2.5* may be overexpressed in the morphant background to look for rescue of heart tube morphogenesis and embryonic heart cell number in transgenic *cmlc2*:*GFP* and *cmlc2*:*dsRed-nuclear* embryos.

Second, it is important to identify additional pro-cardiogenic signals that are adversely affected by the loss of cardiac-type voltage-gated sodium channel expression. Initially, a candidate gene approach and whole mount *in situ* hybridization may be used to assay for changes in the expression of known genes that contribute to cardiac fate specification in zebrafish including *BMP2b*, *Fgf8*, and *Oep* (300;437;438;440;444). A more unbiased, genome-wide approach using microarray technology may also be employed to identify other signaling pathways that are disrupted by reduced sodium channel expression (445-447). Zebrafish gene-chips may be used to assay for significant changes in gene expression that occur in the late blastula (40% epiboly) and during gastrulation (90% epiboly) following injection of active or control morpholinos directed against transcripts encoding zNa_v1.5La. Quantitative real-time PCR

and/or *in situ* hybridization may be used to confirm changes in the expression specific genes of interest that show the greatest changes in expression. These studies are directed at identifying known or previously unappreciated factors that contribute to early cardiogenesis in zebrafish, and the signaling pathways by which *zscn5Laa* influences cardiogenesis.

Finally, epistatic interactions between early cardiogenic-promoting pathways may be studied to clarify where the sodium channel acts within the hierarchy of signaling events that contribute to cardiac lineage specification in zebrafish. Prior gain/loss of function studies in zebrafish demonstrated that *gata5* is a potent positive regulator of *nkx2.5* expression, potentially analogous to the role played by *gata4* or *gata6* in mammals (299;448-450). Moreover, significant defects in the expression of *gata5* were observed in embryos harboring mutations in components of the BMP and TGF-β/Nodal signaling pathways that result in a loss of early expression of *nkx2.5* (299). Despite the evidence supporting a *gata5*-*nkx2.5* signaling axis for cardiogenesis, our results demonstrated that *zscn5Laa* regulates *nkx2.5* expression without affecting levels of *gata5*, analogous to *fgf8* signaling (300;440). These findings suggest that *zscn5Laa* acts downstream of *gata5* or *fgf8*, or in a parallel, previously-undefined pathway to regulate cardiogenesis. To distinguish between these possibilities, *zscn5Laa*'s position relative to *gata5* in cardiogenesis may be assessed by both overexpression and knockdown of *gata5* and *fgf8*, followed by direct measurement of transcript levels of *zscn5Laa* by real-time, quantitative PCR.

Although retinoic acid (RA, vitamin A) signaling plays multiple, time-dependent roles in heart development, it was recently demonstrated that RA signaling normally restricts the number of cells that adopt the cardiac cell fate during gastrulation (439;451). Attenuation of RA signaling by mutation of an enzyme in the RA synthesis pathway (*neckless*) or by pharmacological treatment with RA receptor antagonists expanded the field of cells expressing *nkx2.5* at 6 somites via mechanisms that independently required intact *gata5* and *fgf8* signals (439). The *neckless* mutant and pharmacological tools may be employed to investigate the hypothesis that *zscn5Laa* regulates *nkx2.5* by a previously undefined pathway. If inhibition of RA signaling rescues the early expression of *nkx2.5* in *zscn5Laa* morphants, for example, these data will provide further evidence that *gata5* and *fgf8* pathways are both intact despite the loss of *zscn5Laa*. If inhibition

of RA signaling cannot rescue *nkx2.5* expression in *zscn5Laa* morphants, however, this would suggest that RA acid either signals through *zscn5aa* or that *zscn5aa* is an integral component of *gata5* or *fgf8* signaling pathways. Such findings would be interpreted within the context of *in vivo* data addressing the regulation of *zscn5Laa* expression by *gata5* and *fgf8*, as described above.

Finally, recent findings regarding the role of Wnt/β-catenin signals during cardiogenesis may be exploited to determine the potential interaction of *zscn5Laa* with this pathway. A number of studies have suggested that similar to RA signaling, Wnt signals play both supportive and antagonistic roles in cardiogenesis depending on the timing of the signal (441;452-455). In zebrafish, inhibition of Wnt signals at the onset of gastrulation (6hpf) by conditional overexpression of an inhibitor of canonical Wnt signaling (Dickkopf-1, Dkk-1) resulted in a dramatic expansion of the field of cells that express *nkx2.5* at 6 somites (441). We will use a transgenic line of zebrafish that expresses Dkk-1 under the control of heat shock promoter (*hsDkk1*:GFP) to determine whether inhibition of canonical Wnt signaling during gastrulation can rescue expression of *nkx2.5* in *zscn5Laa* morphants (441;456). This study will provide insight into whether *zscn5Laa* is downstream or parallel to Wnt signaling pathways during cardiac lineage specification.

Future Study II

To test the hypothesis that the zebrafish $Na_v1.5La$ channel regulates the expression of early cardiogenic signaling pathways via a non-electrogenic, structural mechanism. Our preliminary data using multiple morpholino antisense oligonucleotides in zebrafish suggests that the channel $Na_v1.5La$ is required for normal expression of the early cardiogenic transcription factor *nkx2.5* following gastrulation and thus for the production of normal numbers of cardiac progenitor cells. Since prolonged exposure of early embryos to a number of mechanistically-distinct modulators of known sodium channel function failed to reproduce the profound developmental phenotype resulting from channel knockdown, we hypothesize that $Na_v1.5La$ acts via a previously undefined, non-electrogenic mechanism to regulate cardiac

development. An important corollary of this hypothesis is that specific domains of the $Na_v1.5La$ protein are required for early heart development.

In vivo mRNA rescue and detailed structure-function analysis are two effective methods for directly testing mechanisms of non-electrogenic sodium channel function. These methods would first require the assembly of a full-length expression vector for the zebrafish $Na_v1.5La$ (*zscn5Laa*) channel and characterization of its biophysical properties in mammalian cells, as we have successfully performed for $Na_v1.5Lb$ (*scn5Lab*). Given the provocative preliminary findings regarding the role of this channel in early development, the key question driving this effort will be whether $Na_v1.5La$ is capable of acting as a typical sodium channel or has evolved entirely novel functions (e.g. analogous to the gene product of *SCN7A/scn6a,* which encodes the atypical sodium channel Na_x in humans and mice, respectively). We have recently independently cloned and sequenced zebrafish *scn5Laa* and our detailed analysis of the deduced amino acid sequence of this channel suggests it will function as a typical Na_v1 channel. For example, $zNa_v1.5La$ displays conservation of residues in many of the important structural determinants of voltage-gated sodium channel function including the S4 voltage sensors, pore loop selectivity filters, the inactivation gate, and C-terminus. In addition to assessing the function of the *scn5Laa* gene product, successful functional expression of an epitope-tagged channel in CHO or other mammalian cells may provide a convenient *in vitro* assay for testing the effects of various mutations on the function and expression of this channel, as discussed below.

Following the assembly and functional expression of $zNa_v1.5La$, *zscn5Laa* mRNA may be synthesized from our full-length construct for attempted rescue of the early expression of *nkx2.5*, which is significantly diminished in morphant embryos by both *in situ* hybridization and quantitative PCR. As the sodium channel is encoded by a long mRNA (>6kb), this experiment will be performed with epitope-tagged channels to ensure that translation is successful *in vivo*. If co-injection of wild-type *zscn5Laa* mRNA and splice-site directed morpholino antisense oligonucleotides results in normalization of the early expression of *nkx2.5*, a valuable *in vivo* experimental platform will have been established for structure-function analysis of $zNa_v1.5La$ in the developing zebrafish embryo.

Initial experiments in this system may be directed towards further tests of the hypothesis that zNa_v1.5A acts in a non-electrogenic manner to regulate early cardiogenic pathways. To accomplish this, mutations may be engineered based on the rich database of information previously assembled from studies of human patients with mutations in *SCN5A* and from structure-function studies of mammalian sodium channels by site-directed mutagenesis. Based on the literature, we predict that single mutations in the zebrafish *scn5Laa* cDNA may result in a loss of sodium conductance without changes in the functional expression of the channel at the membrane (457). Conversely, other mutations may be identified that perturb channel inactivation and result in persistent sodium current. Mutations in the regions of *SCN5A* encoding the inactivation gate (DIII-IV linker) or an acidic region of the proximal C-terminus, for example, have already been shown to underlie the long QT syndrome, type 3, by encoding for channels that do not properly close during repolarization (458-460). The biophysical effects of both "loss of function" and "gain of function" mutations in the zebrafish Na_v1.5a channel may first be studied in CHO cells, prior to overexpression of mutant *scn5Laa* mRNAs *in vivo* in zebrafish embryos for assessment of phenotype rescue.

Using similar strategies of site-directed mutagenesis, *in vitro* analysis, and *in vivo* phenotype rescue, subsequent experiments may address additional questions regarding the putative structural requirements for the zNa_v1.5a in early cardiac development. For example, our system may enable one to test whether expression of zNa_v1.5a at the cell-surface is required for development, or whether the channel acts intracellularly as was recently reported in macrophages (353). Guidance for engineering mutant channels with these properties may be found in the literature describing *SCN5A* mutations that underlie the Brugada syndrome, as the trafficking of Na_v1.5 to the cell surface may be affected in this disease (461-464). Moreover, as detailed in Chapter 2, a number of demonstrated sites of functional protein-protein interactions have been observed in mammalian cardiac sodium channels, including domains required for interaction with ankyrins, calmodulin, 14-3-3 proteins, protein ubiquitinases, syntrophins, and fibroblast growth factor homologous factors (141;236;243;360). As prior studies have focused primarily on assaying sodium current through Na_v1.5, it may now be of interest to test whether

sites of protein-protein interaction in the sodium channel protein are required for non-electrogenic functions (e.g. cardiac development).

The C-terminus of the cardiac sodium channel is of interest because of two predicted Ca2+ binding EF hand structures (242;465). Moreover, a close phylogenetic relative of Na_v1 channels, the L-type calcium channel, was recently demonstrated to have a C-terminus that is cleaved and acts as a transcription factor in a manner regulated by calcium (337). Although it is unknown whether the C-terminus of Na_v1 sodium channels is similarly cleaved or has function independent of the main channel protein, identification and mutation of conserved protease cleavage sites may also be readily tested in rescue experiments.

Future Study III

To test the hypothesis that the function of voltage-gated sodium channels in early cardiogenesis is mediated by one or more associated components in a channel complex. This study would more directly assess the role of known sodium channel-interacting proteins in early cardiac development, with an emphasis on those proteins that interact with sodium channel α subunits indirectly or by less discreet functional domains. Previously unappreciated proteins that function in this context may also be identified. At the outset of these studies, it would be important to determine whether sodium channel accessory β subunits, significant for extracellular immunoglobulin domains that mediate cell-adhesion, are requisite components of a sodium channel complex that functions in early zebrafish cardiogenesis. Additional studies may employ mass spectrometry-based technique termed “direct analysis of large protein complexes” (DALPC) to characterize the complex of proteins associating with the sodium channel α subunit by immunoprecipitation of an epitope-tagged $zNa_v1.5a$ channel expressed from sense RNA in the zebrafish embryo. To identify sodium channel partners that may be required for early cardiogenesis, proteins associated with the channel in the gastrulating embryo may be directly compared to those associating with the channel in the embryonic heart.

Unlike the accessory subunits of other ion channel complexes, sodium channel β subunits possess extracellular IG domains that enable them to interact with each other,

extracellular matrix proteins, and other proteins that mediate cell adhesion (162). Although the role sodium channel of β subunits in cardiogenesis is unknown, a number of other cell adhesion molecules including N-cadherin, neural cell adhesion molecule (NCAM), fibronectin, tenascin, and *fas* (*Drosophila*) are all expressed in developing heart structures and/or have been shown to be required for normal cardiogenesis (350;466-470). Among these proteins, the vast majority of available evidence supports a role for N-cadherin in heart development (468). In the chick embryo, antibodies interfering with N-cadherin function disrupted early heart development *in vivo* and blocked the differentiation of presumptive cardiomyocytes *in vitro* (350;351;467). In zebrafish, N-cadherin is expressed in the developing heart and its loss of function by morpholino antisense or mutation, respectively, resulted in defects in cardiac morphogenesis (471). In mice, expression of N-cadherin was observed in early mesoderm, in precardiac mesoderm, and in the heart tube between E7.5 and E9.0 (352). Mice lacking N-cadherin died on E10 with significant defects in cardiac morphogenesis, among other tissues (352). We hypothesize that in early cardiac development, sodium channel complexes comprised of α and β subunits may play similar roles in cell-adhesion.

To test this hypothesis, the expression and function of β subunits may be studied in early zebrafish embryos. Prior studies have established that sodium channel β subunits interact homophilically via their extracellular IG domains, and subsequently recruit ankyrin to points of cell-cell contact via their short cytoplasmic domains (349). Other studies have demonstrated that β subunits also interact heterophilically with proteins in the extracellular matrix including tenascin-C and tenascin-R, as well as with other cell adhesion molecules including neurofascin, contactin, and NrCAM (346;349;431;472-474). Moreover, the phosphorylated β1 subunit was shown to directly interact with N-cadherin, even in the absence of sodium channel α subunits (475). Our previous studies indicate that zebrafish possess five distinct β subunit genes that represent single orthologs to mammalian β1- β3 and duplicate genes of β4 (476). RT-PCR may be used to determine which, if any, of the zebrafish sodium channel beta subunits are expressed during gastrulation and in early somitogenesis, prior to the onset of expression of *nkx2.5* at 6 somites. Those β subunit genes demonstrating early expression by RT-PCR may be further studied by *in*

situ hybridization, and the relevant genes subsequently knocked down using alone or in combination with morpholino antisense oligonucleotides directed against both translation initiation sites of mRNAs and intron-exon splice junctions of pre-mRNAs. Effects on heart development may be assayed in *cmlc2*:*GFP* transgenic embryos on days 2 and 3. Expression of *nkx2.5* may be assayed by *in situ* hybridization at 6 somites and *cmlc2* may be assayed at 16 somites to determine the effects of loss of beta subunit function on the specification and differentiation of cardiac progenitor cells, respectively. For those β subunits whose loss of function results in a developmental phenotype, rescue experiments may be performed by co-injecting splice site-directed morpholinos with sense RNA. To determine whether the extracellular IG domain or the intracellular C-terminus is required for the observed phenotype, experiments may be repeated with sense RNA harboring mutations in either of those regions.

To identify novel channel partners in cardiogenesis, sense RNA encoding an epitope-tagged $zNa_v1.5a$ may be injected into zebrafish embryos followed by immunoprecipitation of the channel protein complex. If this experiment is performed during gastrulation and again after the embryonic heart has formed, the DALPC application of mass spectrometry may be employed to characterize the identity of proteins associating $zNa_v1.5a$ at different developmental stages (477-480). Proteins that are differentially associated with the sodium channel in the gastrulating embryo versus the embryonic heart may represent novel sodium channel partners required for early cardiogenesis.

Future Study IV

To investigate the expression and function of *scn5a* in the developing mouse heart. In this study, our findings in zebrafish may be pursued in greater detail within the context of a mammalian model system. In five parts, a detailed investigation may be performed into the role of *scn5a* in murine heart development. Although *scn5a*$^{-/-}$ mice displayed defects in cardiac morphogenesis and are embryo-lethal at E10, the expression pattern of *scn5a* during early development has not previously been investigated. To address this question, our laboratory has knocked-in a bicistronic lacZ-GFP cassette into exon 2 of *scn5a* such that both markers will be

expressed by native regulatory elements within the murine sodium channel locus. Second, the time course and etiology of cardiac defects resulting from the loss of *scn5a* expression may be characterized by performing anatomical and histological studies of the developing heart between E7.5 and E11 in homozygous *scn5a* lacZ-GFP (*scn5a*$^{-/-}$) mice. Third, flow cytometry and microarray technology may be used to compare the gene expression profiles of GFP+ cells isolated from both homozygous and heterozygous *scn5a* lacZ-GFP mice (*scn5a*$^{-/-}$ and *scn5a*$^{+/-}$), in order to identify early cardiogenic signaling pathways that are autonomously disrupted in early murine cardiac progenitor cells that lack *scn5a*. Fourth, in order to clarify whether the morphogenesis defects and early lethality of *scn5a*$^{-/-}$ mice are likely to have resulted from perturbed excitability or other, non-electrogenic mechanisms, action potentials may be recorded from the ventricular chamber of wild-type mice from E9-E12 to determine the precise timepoint at which sodium channels become required for cardiac excitability. Finally, one may examine the morphogenesis of the developing heart in homozygous *scn5a* ΔKPQ transgenic mice, which were reported to be embryo-lethal at E10.5 by unexplained mechanisms.

The propsed studies are made feasible by the successful application of Cre-Recombinase-Mediated Cassette Exchange (RMCE) technology to engineer murine ES cells with a bicistronic lacZ-GFP cassette in place of exon 2 in the murine *scn5a* locus (481). Exon 2 was targeted because it contains the translation initiation site and because prior targeting of this exon abolished sodium channel expression (482). Using these engineered ES cells, transgenic mice may be generated where the expression of both lacZ and GFP will be driven by endogenous regulatory elements in the murine *scn5a* locus. Since heterozygous (*scn5a*$^{+/-}$) mice develop normally (482), *scn5a*$^{+/-}$ lacZ-GFP transgenic mice may first be used to characterize the expression of *scn5a* in embryonic mice by conventional lacZ staining at various developmental timepoints. The expression of *scn5a* may first be examined in gastrulating mouse embryos, followed by a detailed examination of expression of this gene in the developing heart. As the embryonic heart is derived from two distinct heart fields, *scn5a* expression may be examined in either the 1º or 2º heart field of the cardiac crescent between E7.5 and E7.75, and subsequently, in the developing heart tube at E8.25 and in the embryonic heart during looping and chamber

morphogenesis between E9.5 and E10.5 (287;289;483). Our preliminary results from conventional RT-PCR analysis suggested that *scn5a* is expressed at least as early as E8.5 in the mouse embryo (Chapter 3). Moreover, we detected transcripts of *scn5a* specifically in the developing atrial and ventricular myocardium, the forebrain, and somites between E9.5 and E10.5 by isotopic *in situ* hybridization, suggesting a cell-autonomous role for *scn5a* in the developing heart (Chapter 3).

In order to study the time course and etiology of cardiac defects resulting from the complete loss of *scn5a* expression, heterozygote transgenic mice may be interbred to obtain homozygous *scn5a* lacZ-GFP (*scn5a*$^{-/-}$) mice. We predict that these mice will recapitulate the reported cardiac developmental phenotype observed in *scn5a*$^{-/-}$ mice, which would permit the detailed anatomical and histological studies of the developing heart between E7.75 and E12. These studies may be guided by the timing and localization of *scn5a* expression as revealed by approaches taken in the first part of this specific aim. Next, cells may be isolated from early mouse hearts (E7.75-9.5) by digestion and FACS used to isolate pure populations of GFP+ cardiac progenitors and/or embryonic myocytes from both homozygous and heterozygous *scn5a* lacZ-GFP mice (*scn5a*$^{-/-}$ and *scn5a*$^{+/-}$). Using total RNA isolated from these two cell populations, microarray technology may be used to compare the gene expression profiles in developing cells that harbor 0 or 1 wild-type alleles of *scn5a*, in order to identify early cardiogenic signaling pathways that are autonomously disrupted in progenitor cells lacking $Na_v1.5$. As before, the developmental timepoint at which these studies are performed would be dictated by the cardiac expression of murine *scn5a*. The value of utilizing transgenic mice, flow cytometry, and transcriptome analysis to identify pathways driving early cardiogenesis has recently been demonstrated (484;485). In these studies, mice expressing GFP under the direction of a cardiac-specific enhancer of the transcription factor *nkx2.5* were successfully generated and used to profile the molecular program driving cardiogenesis at different stages of heart development (484;485).

Finally, the role of sodium channels in generating action potentials in the early murine heart may be studied in order to determine whether the defects in ventricular morphogenesis

observed in *scn5a*$^{-/-}$ mice are likely to be caused by perturbations of nascent excitability or by other mechanisms. Although our findings in the zebrafish model strongly suggest that excitability (whether mediated by sodium or calcium channels) is not required for heart development, transgenic mice expressing two alleles of the long QT syndrome mutation ΔKPQ that cause persistent sodium current and action potential prolongation were reported to die at E10.5 of unknown causes (256). To determine the cause of death in these mice, and to assess whether significant perturbations of sodium channel-mediated excitability result in defects in cardiac morphogenesis, *scn5a* ΔKPQ transgenic mice may be obtained from the Carmeliet lab for further study. In order to clarify the role of sodium channels in mediating excitation in the developing mouse heart, action potentials may be recorded from the ventricular chamber of wild-type mice from E9-E14 to determine the precise timepoint at which sodium channels become required for cardiac excitation.

Additional projects

1. Novel molecular basis for tetrodotoxin resistance in a zebrafish cardiac sodium channel.

Prior to understanding the developmental regulation of sodium channels in the zebrafish heart, we hypothesized that the resistance of the early embryonic heart to high concentrations of TTX was due to the intrinsic resistance of the molecular target of the toxin. Mammalian cardiac sodium channels, for example, are prototypical TTX "resistant" channels because they have evolved a single mutation in the domain I pore loop that confers resistance to the nanomolar quantities of TTX that readily block neuronal and skeletal muscle-type sodium channels (246). Although we discovered that sodium channels become necessary for zebrafish heart function between days 4 and 5 of development, we noted that micromolar not nanomolar doses of TTX were required to perturb cardiac function at these and subsequent timepoints up to day 7. These data conflicted with our prior findings that adult zebrafish ventricular action potentials were readily suppressed by nanomolar concentrations of toxin, and suggested the differential expression of TTX-sensitive and TTX-resistant sodium channel isoforms in the adult versus larval heart. Surprisingly, a survey of the domain I pore loop sequences of all 8 zebrafish Na_v1 channels predicted that all of these proteins are sensitive to nanomolar TTX. However, we identified novel pore loop mutations in both domains I and IV of the sodium channel encoded by the gene *zscn5Laa* that were not found in any other zebrafish sodium channel gene. We hypothesized that these mutations conferred the property of TTX-resistance upon this channel, thus providing a rational explanation for the observed TTX resistance of the larval heart (days 5-7). The results of our experiments are described in the abstract below.

Background: Tetrodotoxin (TTX) is a naturally-occurring poison that occludes the sodium channel pore and has been instrumental in the cloning, characterization, and classification of Na_v1 voltage-gated sodium channels. Unlike most sodium channels, the cardiac isoform $Na_v1.5$ (*SCN5A*) has evolved a cysteine substitution of an aromatic residue (Y or F) in a highly conserved domain I pore loop sequence that confers TTX-resistance (C373). Two other TTX-resistant sodium channel isoforms, $Na_v1.8$ (*SCN10A*) and $Na_v1.9$ (*SCN11A*), have evolved serine substitutions at analogous positions (S357 and S360, respectively), further supporting the

prevailing concept that this aromatic residue in the domain I pore loop is critical for TTX-channel interactions.

Methods and Results: We have identified a novel molecular mechanism underlying TTX-resistance in a zebrafish cardiac sodium channel. While 1μM TTX solution microinjected into the systemic circulation rapidly impaired mobility and responsiveness in >95% of day 7 larvae, no effect was observed on cardiac function (n=22). The resistance of the zebrafish heart to TTX was confirmed by pericardial delivery of 1μM TTX, which elicited arrhythmia in only 28% of larvae (n=25). The zebrafish genome encodes two *SCN5A* orthologs (*scn5Laa*, *scn5Lab*), both of which are expressed in the early heart. Unexpectedly, the cloned sequences of *scn5Laa* and *scn5Lab* each predict the canonical, domain I aromatic residue required for high-affinity TTX binding. However, alignment of the pore loop sequences of all 8 zebrafish sodium channels revealed novel substitutions in domains I (N378S) and IV (D1634N) of *scn5Laa*. Heterologous expression of the full-length *scn5Lab* cDNA in CHO cells produced typical sodium current that was highly sensitive to TTX (IC_{50} 9.6nM, n=5 cells). Introduction of N378S and D1634N in *scn5Lab* by site-directed mutagenesis resulted in a nearly 100-fold reduction in TTX sensitivity (IC_{50} 910nM, n=5 cells), conferring the property of TTX-resistance on a TTX-sensitive channel.

Conclusions: Mammals and zebrafish have independently evolved TTX-resistant cardiac sodium channels through unique mutations. Our findings support a structural model of the sodium channel pore where residues in the domain IV pore loop may be required for high-affinity TTX blockade.

2. The role of calcium in embryonic heart development. Calcium is a ubiquitous second messenger that regulates numerous processes ranging from the contraction of muscle to the release of synaptic vesicles. Calcium signals also regulate gene expression in by modulating the function of key transcription factors. In the developing zebrafish heart, nonsense mutation of the cardiac L-type calcium channel (*cacna1c*) in the *island beat* mutant resulted in atrial fibrillation and a silent, non-contractile ventricle that displayed severe defects in morphogenesis and reduced myocyte number. Although these findings suggested that calcium cycling in the early

embryonic heart is required for both for development of cardiac form and function, prolonged treatment of embryos with the L-type calcium channel blocker nisoldipine produced neither atrial fibrillation nor ventricular hypoplasia. Rather, incubation in this pharmacological agent resulted in embryonic hearts that never beat but appear to form normally through day 2. The primary defect observed in nisoldipine-treated embryos was a significant decrease in the intensity of GFP expression, suggesting reduced activity at the *cmlc2* promoter. Analogous to our observations with sodium channels, these results suggest that L-type calcium channels may regulate cardiac development independent of their role in facilitate calcium entry into myocytes. The recent report that the C-terminus of an L-type calcium channel isoform is cleaved in neurons and acts as a transcription factor provides an avenue for further study of these provocative findings (337).

3. The role of voltage-gated sodium channels in other mesoderm-derived tissues such as skeletal muscle. Evidence from zebrafish and mice suggest that two isoforms of the voltage-gated sodium channel (*scn5a*) and (*scn4a*) are expressed in developing skeletal muscle at different timepoints (209;486). As delivery of high doses of TTX to the zebrafish embryo resulted in paralysis but not in defects of muscle development, we propose to knockdown both isoforms alone and in combination to determine whether sodium channel proteins but not excitability are required for the development of muscle. Interestingly, the results of our transplantation experiments indicated that morphant mesodermal cells lacking *scn5a* infrequently produced cardiomyocytes but frequently produced skeletal myocytes, suggesting distinct early sodium channel signaling mechanisms for the development of heart and muscle (Chapter 3).

REFERENCES

(1) Hille B. Ion channels of excitable membranes. 3rd ed. Sunderland, MA: Sinauer Associates, 2001.

(2) Yu FH, Catterall WA. Overview of the voltage-gated sodium channel family. *Genome Biol* 2003; 4(3):207.

(3) Goldin AL. Resurgence of sodium channel research. *Annu Rev Physiol* 2001; 63:871-894.

(4) Anderson PA, Greenberg RM. Phylogeny of ion channels: clues to structure and function. *Comp Biochem Physiol B Biochem Mol Biol* 2001; 129(1):17-28.

(5) Hartshorne RP, Messner DJ, Coppersmith JC, Catterall WA. The saxitoxin receptor of the sodium channel from rat brain. Evidence for two nonidentical beta subunits. *J Biol Chem* 1982; 257(23):13888-13891.

(6) Barchi RL. Protein components of the purified sodium channel from rat skeletal muscle sarcolemma. *J Neurochem* 1983; 40(5):1377-1385.

(7) Roberts RH, Barchi RL. The voltage-sensitive sodium channel from rabbit skeletal muscle. Chemical characterization of subunits. *J Biol Chem* 1987; 262(5):2298-2303.

(8) Isom LL, De Jongh KS, Catterall WA. Auxiliary subunits of voltage-gated ion channels. *Neuron* 1994; 12(6):1183-1194.

(9) Maier SK, Westenbroek RE, McCormick KA, Curtis R, Scheuer T, Catterall WA. Distinct subcellular localization of different sodium channel alpha and beta subunits in single ventricular myocytes from mouse heart. *Circulation* 2004; 109(11):1421-1427.

(10) Isom LL, De Jongh KS, Patton DE et al. Primary structure and functional expression of the beta 1 subunit of the rat brain sodium channel. *Science* 1992; 256(5058):839-842.

(11) Isom LL, Ragsdale DS, De Jongh KS et al. Structure and function of the beta 2 subunit of brain sodium channels, a transmembrane glycoprotein with a CAM motif. *Cell* 1995; 83(3):433-442.

(12) Morgan K, Stevens EB, Shah B et al. Beta 3: an additional auxiliary subunit of the voltage-sensitive sodium channel that modulates channel gating with distinct kinetics. *Proc Natl Acad Sci (USA)* 2000; 97(5):2308-2313.

(13) Yu FH, Westenbroek RE, Silos-Santiago I et al. Sodium channel beta4, a new disulfide-linked auxiliary subunit with similarity to beta2. *J Neurosci* 2003; 23(20):7577-7585.

(14) Isom LL, Catterall WA. Na+ channel subunits and Ig domains. *Nature* 1996; 383(6598):307-308.

(15) Catterall WA, Goldin AL, Waxman SG. International Union of Pharmacology. XLVII. Nomenclature and structure-function relationships of voltage-gated sodium channels. *Pharmacol Rev* 2005; 57(4):397-409.

(16) Goldin AL, Snutch T, Lubbert H et al. Messenger RNA coding for only the alpha subunit of the rat brain Na channel is sufficient for expression of functional channels in Xenopus oocytes. *Proc Natl Acad Sci (USA)* 1986; 83(19):7503-7507.

(17) Chen C, Westenbroek RE, Xu X et al. Mice lacking sodium channel beta1 subunits display defects in neuronal excitability, sodium channel expression, and nodal architecture. *J Neurosci* 2004; 24(16):4030-4042.

(18) Chen C, Bharucha V, Chen Y et al. Reduced sodium channel density, altered voltage dependence of inactivation, and increased susceptibility to seizures in mice lacking sodium channel beta 2-subunits. *Proc Natl Acad Sci (USA)* 2002; 99(26):17072-17077.

(19) Meadows LS, Isom LL. Sodium channels as macromolecular complexes: implications for inherited arrhythmia syndromes. *Cardiovasc Res* 2005; 67(3):448-458.

(20) Isom LL. Sodium channel beta subunits: anything but auxiliary. *Neuroscientist* 2001; 7(1):42-54.

(21) Seyfarth EA. Julius Bernstein (1839-1917): pioneer neurobiologist and biophysicist. *Biol Cybern* 2006; 94(1):2-8.

(22) Schuetze S. The discovery of the action potential. *Trends Neurosci* 1983; 6:164-168.

(23) Nilius B. Pflugers Archiv and the advent of modern electrophysiology. From the first action potential to patch clamp. *Pflugers Arch* 2003; 447(3):267-271.

(24) Ringer S, Murrell W. The Action of Chloride of Potassium on the Nervous System of Frogs. *J Anat Physiol* 1877; Oct 12(Pt 1):54-57.

(25) Ringer S, Morshead EA. The Influence on the Afferent Nerves of the Frog's Leg from the Local Application of the Chlorides, Bromides, and Iodides of Potassium, Ammonium, and Sodium. *J Anat Physiol* 1877; Oct 12(Pt 1):58-72.

(26) Ringer S, Morshead EA. The Effect of the Chlorides, Bromides, and Iodides of Potassium and Sodium on Frogs. *J Anat Physiol* 1877; Oct 12(Pt 1):73-84.

(27) Ringer S. Regarding the Action of Hydrate of Soda, Hydrate of Ammonia, and Hydrate of Potash on the Ventricle of the Frog's Heart. *J Physiol* 1882; Jan 3(3-4):195-202.

(28) Ringer S. A further Contribution regarding the influence of the different Constituents of the Blood on the Contraction of the Heart. *J Physiol* 1883; Jan 4(1):29-42.

(29) Ringer S. Concerning the Influence exerted by each of the Constituents of the Blood on the Contraction of the Ventricle. *J Physiol* 1882; Aug 3(5-6):380-393.

(30) Ringer S. A third contribution regarding the Influence of the Inorganic Constituents of the Blood on the Ventricular Contraction. *J Physiol* 1883; Aug 4(2-3):222-225.

(31) Bernstein J. Untersuchungen zur Thermodynamik der bioelektrischen Ströme. *Pflugers Arch* 1902; 92:521-562.

(32) Seyfarth EAPL. A hundred years ago: Julius Bernstein (1839-1917) formulates his "membrane theory". *Neuroforum* 2002; 274-276.

(33) Hodgkin AL. Nobel Lectures, Physiology or Medicine 1963-1970. Amsterdam: Elsevier Publishing Company, 1972.

(34) Huxley AF. Nobel Lectures, Physiology or Medicine 1963-1970. Amsterdam: Elsevier Publishing Company, 1972.

(35) De WP. A century of thinking about cell membranes. *Annu Rev Physiol* 2000; 62:919-26:919-926.

(36) Neuroscience. second ed. Sunderland, MA: Sinauer Associates, Inc., 2001.

(37) Keynes R. John Zachary Young (18 March 1907-4 July 1997). *Proc Amer Philosoph Soc.* 1999;143[4]:728-732.

(38) Hodgkin AL, Huxley AF. Action potentials recorded from inside a nerve fiber. *Nature* 1939; 144:710-711.

(39) Hodgkin AL, Huxley AF. Potassium leakage from an active nerve fibre. *J Physiol* 1947; 106(3):341-367.

(40) Hodgkin AL, KATZ B. The effect of sodium ions on the electrical activity of the giant axon of the squid. *J Physiol* 1949; 108(1):37-77.

(41) Cole KS. Dynamic electrical characteristics of the squid axon membrane. *Arch Sci Physiol*. 1949; 3:253-258.

(42) Marmont G. Studies on the axon membrane; a new method. *J Cell Physiol* 1949; 34(3):351-382.

(43) Hodgkin AL, Huxley AF. A quantitative description of membrane current and its application to conduction and excitation in nerve. *J Physiol* 1952; 117(4):500-544.

(44) Neher E, Sakmann B. Single-channel currents recorded from membrane of denervated frog muscle fibres. *Nature* 1976; 260(5554):799-802.

(45) Sigworth FJ, Neher E. Single Na+ channel currents observed in cultured rat muscle cells. *Nature* 1980; 287(5781):447-449.

(46) Hamill OP, Marty A, Neher E, Sakmann B, Sigworth FJ. Improved patch-clamp techniques for high-resolution current recording from cells and cell-free membrane patches. *Pflugers Arch* 1981; 391(2):85-100.

(47) Ackerman MJ, Clapham DE. Ion channels--basic science and clinical disease. *N Engl J Med* 1997; 336(22):1575-1586.

(48) Hodgkin AL, Huxley AF. The components of membrane conductance in the giant axon of Loligo. *J Physiol* 1952; 116(4):473-496.

(49) Marban E, Yamagishi T, Tomaselli GF. Structure and function of voltage-gated sodium channels. *J Physiol* 1998; 508(Pt 3):647-657.

(50) George AL, Jr. Inherited disorders of voltage-gated sodium channels. *J Clin Invest* 2005; 115(8):1990-1999.

(51) Roden DM, Balser JR, George AL, Jr., Anderson ME. Cardiac ion channels. *Annu Rev Physiol* 2002; 64:431-75.:431-475.

(52) Koopmann TT, Bezzina CR, Wilde AA. Voltage-gated sodium channels: action players with many faces. *Ann Med* 2006; 38(7):472-482.

(53) Escayg A, MacDonald BT, Meisler MH et al. Mutations of SCN1A, encoding a neuronal sodium channel, in two families with GEFS+2. *Nat Genet* 2000; 24(4):343-345.

(54) Sugawara T, Tsurubuchi Y, Agarwala KL et al. A missense mutation of the Na+ channel alpha II subunit gene Na(v)1.2 in a patient with febrile and afebrile seizures causes channel dysfunction. *Proc Natl Acad Sci (USA)* 2001; 98(11):6384-6389.

(55) Weiss LA, Escayg A, Kearney JA et al. Sodium channels SCN1A, SCN2A and SCN3A in familial autism. *Mol Psychiatry* 2003; 8(2):186-194.

(56) Ptacek LJ, George AL, Jr., Griggs RC et al. Identification of a mutation in the gene causing hyperkalemic periodic paralysis. *Cell* 1991; 67(5):1021-1027.

(57) Wang Q, Shen J, Splawski I et al. SCN5A mutations associated with an inherited cardiac arrhythmia, long QT syndrome. *Cell* 1995; 80(5):805-811.

(58) Trudeau MM, Dalton JC, Day JW, Ranum LP, Meisler MH. Heterozygosity for a protein truncation mutation of sodium channel SCN8A in a patient with cerebellar atrophy, ataxia, and mental retardation. *J Med Genet* 2006; 43(6):527-530.

(59) Yang Y, Wang Y, Li S et al. Mutations in SCN9A, encoding a sodium channel alpha subunit, in patients with primary erythermalgia. *J Med Genet* 2004; 41(3):171-174.

(60) Lossin C, Wang DW, Rhodes TH, Vanoye CG, George AL, Jr. Molecular basis of an inherited epilepsy. *Neuron* 2002; 34(6):877-884.

(61) Dichgans M, Freilinger T, Eckstein G et al. Mutation in the neuronal voltage-gated sodium channel SCN1A in familial hemiplegic migraine. *Lancet* 2005; 366(9483):371-377.

(62) Claes L, Del-Favero J, Ceulemans B, Lagae L, Van BC, De JP. De novo mutations in the sodium-channel gene SCN1A cause severe myoclonic epilepsy of infancy. *Am J Hum Genet* 2001; 68(6):1327-1332.

(63) Sugawara T, Mazaki-Miyazaki E, Fukushima K et al. Frequent mutations of SCN1A in severe myoclonic epilepsy in infancy. *Neurology* 2002; 58(7):1122-1124.

(64) Fujiwara T, Sugawara T, Mazaki-Miyazaki E et al. Mutations of sodium channel alpha subunit type 1 (SCN1A) in intractable childhood epilepsies with frequent generalized tonic-clonic seizures. *Brain* 2003; 126(Pt 3):531-546.

(65) Mantegazza M, Gambardella A, Rusconi R et al. Identification of an Nav1.1 sodium channel (SCN1A) loss-of-function mutation associated with familial simple febrile seizures. *Proc Natl Acad Sci (USA)* 2005; 102(50):18177-18182.

(66) Heron SE, Crossland KM, Andermann E et al. Sodium-channel defects in benign familial neonatal-infantile seizures. *Lancet* 2002; 360(9336):851-852.

(67) Berkovic SF, Heron SE, Giordano L et al. Benign familial neonatal-infantile seizures: characterization of a new sodium channelopathy. *Ann Neurol* 2004; 55(4):550-557.

(68) Feero WG, Wang J, Barany F et al. Hyperkalemic periodic paralysis: rapid molecular diagnosis and relationship of genotype to phenotype in 12 families. *Neurology* 1993; 43(4):668-673.

(69) McClatchey AI, Van den BP, Pericak-Vance MA et al. Temperature-sensitive mutations in the III-IV cytoplasmic loop region of the skeletal muscle sodium channel gene in paramyotonia congenita. *Cell* 1992; 68(4):769-774.

(70) McClatchey AI, Kenna-Yasek D, Cros D et al. Novel mutations in families with unusual and variable disorders of the skeletal muscle sodium channel. *Nat Genet* 1992; 2(2):148-152.

(71) Orrell RW, Jurkat-Rott K, Lehmann-Horn F, Lane RJ. Familial cramp due to potassium-aggravated myotonia. *J Neurol Neurosurg Psychiatry* 1998; 65(4):569-572.

(72) Bulman DE, Scoggan KA, van O et al. A novel sodium channel mutation in a family with hypokalemic periodic paralysis. *Neurology* 1999; 53(9):1932-1936.

(73) Sokolov S, Scheuer T, Catterall WA. Gating pore current in an inherited ion channelopathy. *Nature* 2007; 446(7131):76-78.

(74) Cox JJ, Reimann F, Nicholas AK et al. An SCN9A channelopathy causes congenital inability to experience pain. *Nature* 2006; 444(7121):894-898.

(75) Fertleman CR, Baker MD, Parker KA et al. SCN9A mutations in paroxysmal extreme pain disorder: allelic variants underlie distinct channel defects and phenotypes. *Neuron* 2006; 52(5):767-774.

(76) Wallace RH, Wang DW, Singh R et al. Febrile seizures and generalized epilepsy associated with a mutation in the Na+-channel beta1 subunit gene SCN1B. *Nat Genet* 1998; 19(4):366-370.

(77) Spampanato J, Kearney JA, de HG et al. A novel epilepsy mutation in the sodium channel SCN1A identifies a cytoplasmic domain for beta subunit interaction. *J Neurosci* 2004; 24(44):10022-10034.

(78) An RH, Wang XL, Kerem B et al. Novel LQT-3 mutation affects Na+ channel activity through interactions between alpha- and beta1-subunits. *Circ Res* 1998; 83(2):141-146.

(79) Wan X, Wang Q, Kirsch GE. Functional suppression of sodium channels by beta(1)-subunits as a molecular mechanism of idiopathic ventricular fibrillation. *J Mol Cell Cardiol* 2000; 32(10):1873-1884.

(80) Makita N, Shirai N, Wang DW et al. Cardiac Na(+) channel dysfunction in Brugada syndrome is aggravated by beta(1)-subunit. *Circulation* 2000; 101(1):54-60.

(81) Medeiros-Domingo A, Kaku T, Tester DJ et al. SCN4B-Encoded Sodium Channel {beta}4 Subunit in Congenital Long-QT Syndrome. *Circulation* 2007; 116:134-142.

(82) Planells-Cases R, Caprini M, Zhang J et al. Neuronal death and perinatal lethality in voltage-gated sodium channel alpha(II)-deficient mice. *Biophys J* 2000; 78(6):2878-2891.

(83) Watanabe E, Fujikawa A, Matsunaga H et al. Nav2/NaG channel is involved in control of salt-intake behavior in the CNS. *J Neurosci* 2000; 20(20):7743-7751.

(84) Burgess DL, Kohrman DC, Galt J et al. Mutation of a new sodium channel gene, Scn8a, in the mouse mutant 'motor endplate disease'. *Nat Genet* 1995; 10(4):461-465.

(85) Buchner DA, Seburn KL, Frankel WN, Meisler MH. Three ENU-induced neurological mutations in the pore loop of sodium channel Scn8a (Na(v)1.6) and a genetically linked retinal mutation, rd13. *Mamm Genome* 2004; 15(5):344-351.

(86) Nassar MA, Stirling LC, Forlani G et al. Nociceptor-specific gene deletion reveals a major role for Nav1.7 (PN1) in acute and inflammatory pain. *Proc Natl Acad Sci (USA)* 2004; 101(34):12706-12711.

(87) Akopian AN, Sivilotti L, Wood JN. A tetrodotoxin-resistant voltage-gated sodium channel expressed by sensory neurons. *Nature* 1996; 379(6562):257-262.

(88) Zimmermann K, Leffler A, Babes A et al. Sensory neuron sodium channel Nav1.8 is essential for pain at low temperatures. *Nature* 2007; 447(7146):855-858.

(89) Roden DM, Balser JR, George AL, Jr., Anderson ME. Cardiac ion channels. *Annu Rev Physiol* 2002; 64:431-75.:431-475.

(90) Marban E. Cardiac channelopathies. *Nature* 2002; 415(6868):213-218.

(91) Wehrens XH, Lehnart SE, Marks AR. Intracellular calcium release and cardiac disease. *Annu Rev Physiol* 2005; 67:69-98.:69-98.

(92) Wehrens XH, Marks AR. Novel therapeutic approaches for heart failure by normalizing calcium cycling. *Nat Rev Drug Discov* 2004; 3(7):565-573.

(93) Ter Keurs HE, Boyden PA. Calcium and arrhythmogenesis. *Physiol Rev* 2007; 87(2):457-506.

(94) Dulhunty AF. Excitation-contraction coupling from the 1950s into the new millennium. *Clin Exp Pharmacol Physiol* 2006; 33(9):763-772.

(95) Wang Q, Li Z, Shen J, Keating MT. Genomic organization of the human SCN5A gene encoding the cardiac sodium channel. *Genomics* 1996; 34(1):9-16.

(96) George AL, Jr., Varkony TA, Drabkin HA et al. Assignment of the human heart tetrodotoxin-resistant voltage-gated Na+ channel alpha-subunit gene (SCN5A) to band 3p21. *Cytogenet Cell Genet* 1995; 68(1-2):67-70.

(97) Plummer NW, Meisler MH. Evolution and diversity of mammalian sodium channel genes. *Genomics* 1999; 57(2):323-331.

(98) Goldin AL. Evolution of voltage-gated Na(+) channels. *J Exp Biol* 2002; 205(Pt 5):575-584.

(99) Maier SK, Westenbroek RE, Schenkman KA, Feigl EO, Scheuer T, Catterall WA. An unexpected role for brain-type sodium channels in coupling of cell surface depolarization to contraction in the heart. *Proc Natl Acad Sci (USA)* 2002; 99(6):4073-4078.

(100) Maier SK, Westenbroek RE, McCormick KA, Curtis R, Scheuer T, Catterall WA. Distinct subcellular localization of different sodium channel alpha and beta subunits in single ventricular myocytes from mouse heart. *Circulation* 2004; 109(11):1421-1427.

(101) Lei M, Jones SA, Liu J et al. Requirement of neuronal- and cardiac-type sodium channels for murine sinoatrial node pacemaking. *J Physiol* 2004; 559(Pt 3):835-848.

(102) Maier SK, Westenbroek RE, Yamanushi TT et al. An unexpected requirement for brain-type sodium channels for control of heart rate in the mouse sinoatrial node. *Proc Natl Acad Sci (USA)* 2003; 100(6):3507-3512.

(103) Zimmer T, Bollensdorff C, Haufe V, Birch-Hirschfeld E, Benndorf K. Mouse heart Na+ channels: primary structure and function of two isoforms and alternatively spliced variants. *Am J Physiol Heart Circ Physiol* 2002; 282(3):H1007-H1017.

(104) Pereon Y, Lande G, Demolombe S et al. Paramyotonia congenita with an SCN4A mutation affecting cardiac repolarization. *Neurology* 2003; 60(2):340-342.

(105) George AL, Jr., Knittle TJ, Tamkun MM. Molecular cloning of an atypical voltage-gated sodium channel expressed in human heart and uterus: evidence for a distinct gene family. *Proc Natl Acad Sci (USA)* 1992; 89(11):4893-4897.

(106) Felipe A, Knittle TJ, Doyle KL, Tamkun MM. Primary structure and differential expression during development and pregnancy of a novel voltage-gated sodium channel in the mouse. *J Biol Chem* 1994; 269(48):30125-30131.

(107) Zipes DP, Wellens HJ. Sudden cardiac death. *Circulation* 1998; 98(21):2334-2351.

(108) Vincent GM. The molecular genetics of the long QT syndrome: genes causing fainting and sudden death. *Annu Rev Med* 1998; 49:263-74.:263-274.

(109) Roden DM, Anderson ME. Proarrhythmia. *Handb Exp Pharmacol* 2006;(171):73-97.

(110) Priori SG, Barhanin J, Hauer RN et al. Genetic and molecular basis of cardiac arrhythmias; impact on clinical management. Study group on molecular basis of arrhythmias of the working group on arrhythmias of the european society of cardiology. *Eur Heart J* 1999; 20(3):174-195.

(111) Kusmirek SL, Gold MR. Sudden cardiac death: the role of risk stratification. *Am Heart J* 2007; 153(4 Suppl):25-33.

(112) Anderson ME, Al-Khatib SM, Roden DM, Califf RM. Cardiac repolarization: current knowledge, critical gaps, and new approaches to drug development and patient management. *Am Heart J* 2002; 144(5):769-781.

(113) Somberg JC. Arrhythmia therapy. *Am J Ther* 2002; 9(6):537-542.

(114) Elming H, Brendorp B, Pehrson S, Pedersen OD, Kober L, Torp-Petersen C. A benefit-risk assessment of class III antiarrhythmic agents. *Expert Opin Drug Saf* 2004; 3(6):559-577.

(115) Prystowsky EN. Primary and secondary prevention of sudden cardiac death: the role of the implantable cardioverter defibrillator. *Rev Cardiovasc Med* 2001; 2(4):197-205.

(116) Grant AO. Molecular biology of sodium channels and their role in cardiac arrhythmias. *Am J Med* 2001; 110(4):296-305.

(117) Viswanathan PC, Balser JR. Inherited sodium channelopathies: a continuum of channel dysfunction. *Trends Cardiovasc Med* 2004; 14(1):28-35.

(118) Brugada P, Brugada J. Right bundle branch block, persistent ST segment elevation and sudden cardiac death: a distinct clinical and electrocardiographic syndrome. A multicenter report. *J Am Coll Cardiol* 1992; 20(6):1391-1396.

(119) Wang DW, Makita N, Kitabatake A, Balser JR, George AL, Jr. Enhanced Na(+) channel intermediate inactivation in Brugada syndrome. *Circ Res* 2000; 87(8):E37-E43.

(120) Balser JR. Sodium "channelopathies" and sudden death: must you be so sensitive? *Circ Res* 1999; 85(9):872-874.

(121) Valdivia CR, Tester DJ, Rok BA et al. A trafficking defective, Brugada syndrome-causing SCN5A mutation rescued by drugs. *Cardiovasc Res* 2004; 62(1):53-62.

(122) Herfst LJ, Rook MB, Jongsma HJ. Trafficking and functional expression of cardiac Na+ channels. *J Mol Cell Cardiol* 2004; 36(2):185-193.

(123) Moss AJ. Long QT Syndrome. *JAMA* 2003; 289(16):2041-2044.

(124) Splawski I, Shen J, Timothy KW et al. Spectrum of mutations in long-QT syndrome genes. KVLQT1, HERG, SCN5A, KCNE1, and KCNE2. *Circulation* 2000; 102(10):1178-1185.

(125) Roden DM. The problem, challenge and opportunity of genetic heterogeneity in monogenic diseases predisposing to sudden death. *J Am Coll Cardiol* 2002; 40(2):357-359.

(126) Mohler PJ, Schott JJ, Gramolini AO et al. Ankyrin-B mutation causes type 4 long-QT cardiac arrhythmia and sudden cardiac death. *Nature* 2003; 421(6923):634-639.

(127) Vatta M, Ackerman MJ, Ye B et al. Mutant caveolin-3 induces persistent late sodium current and is associated with long-QT syndrome. *Circulation* 2006; 114(20):2104-2112.

(128) Wang DW, Yazawa K, George AL, Jr., Bennett PB. Characterization of human cardiac Na+ channel mutations in the congenital long QT syndrome. *Proc Natl Acad Sci (USA)* 1996; 93(23):13200-13205.

(129) Keating MT. The long QT syndrome. A review of recent molecular genetic and physiologic discoveries. *Medicine (Baltimore)* 1996; 75(1):1-5.

(130) Dumaine R, Wang Q, Keating MT et al. Multiple mechanisms of Na+ channel--linked long-QT syndrome. *Circ Res* 1996; 78(5):916-924.

(131) Antzelevitch C, Brugada P, Brugada J et al. Brugada syndrome: a decade of progress. *Circ Res* 2002; 91(12):1114-1118.

(132) Nuyens D, Stengl M, Dugarmaa S et al. Abrupt rate accelerations or premature beats cause life-threatening arrhythmias in mice with long-QT3 syndrome. *Nat Med* 2001; 7(9):1021-1027.

(133) Papadatos GA, Wallerstein PM, Head CE et al. Slowed conduction and ventricular tachycardia after targeted disruption of the cardiac sodium channel gene Scn5a. *Proc Natl Acad Sci (USA)* 2002; 99(9):6210-6215.

(134) Lei M, Goddard C, Liu J et al. Sinus node dysfunction following targeted disruption of the murine cardiac sodium channel gene Scn5a. *J Physiol* 2005; 567(Pt 2):387-400.

(135) Echt DS, Liebson PR, Mitchell LB et al. Mortality and morbidity in patients receiving encainide, flecainide, or placebo. The Cardiac Arrhythmia Suppression Trial. *N Engl J Med* 1991; 324(12):781-788.

(136) Pu J, Balser JR, Boyden PA. Lidocaine action on Na+ currents in ventricular myocytes from the epicardial border zone of the infarcted heart. *Circ Res* 1998; 83(4):431-440.

(137) Liu H, Tateyama M, Clancy CE, Abriel H, Kass RS. Channel openings are necessary but not sufficient for use-dependent block of cardiac Na(+) channels by flecainide: evidence from the analysis of disease-linked mutations. *J Gen Physiol* 2002; 120(1):39-51.

(138) Balser JR. Inherited sodium channelopathies: novel therapeutic and proarrhythmic molecular mechanisms. *Trends Cardiovasc Med* 2001; 11(6):229-237.

(139) Viswanathan PC, Bezzina CR, George AL, Jr., Roden DM, Wilde AA, Balser JR. Gating-dependent mechanisms for flecainide action in SCN5A-linked arrhythmia syndromes. *Circulation* 2001; 104(10):1200-1205.

(140) Shimizu W, Antzelevitch C, Suyama K et al. Effect of sodium channel blockers on ST segment, QRS duration, and corrected QT interval in patients with Brugada syndrome. *J Cardiovasc Electrophysiol* 2000; 11(12):1320-1329.

(141) Abriel H, Kass RS. Regulation of the voltage-gated cardiac sodium channel Nav1.5 by interacting proteins. *Trends Cardiovasc Med* 2005; 15(1):35-40.

(142) Hartshorne RP, Catterall WA. Purification of the saxitoxin receptor of the sodium channel from rat brain. *Proc Natl Acad Sci (USA)* 1981; 78(7):4620-4624.

(143) Hartshorne RP, Catterall WA. The sodium channel from rat brain. Purification and subunit composition. *J Biol Chem* 1984; 259(3):1667-1675.

(144) Hartshorne RP, Keller BU, Talvenheimo JA, Catterall WA, Montal M. Functional reconstitution of the purified brain sodium channel in planar lipid bilayers. *Proc Natl Acad Sci (USA)* 1985; 82(1):240-244.

(145) Casadei JM, Gordon RD, Barchi RL. Immunoaffinity isolation of Na+ channels from rat skeletal muscle. Analysis of subunits. *J Biol Chem* 1986; 261(9):4318-4323.

(146) Isom LL. Sodium channel beta subunits: anything but auxiliary. *Neuroscientist* 2001; 7(1):42-54.

(147) Medeiros-Domingo A, Kaku T, Tester DJ et al. SCN4B-Encoded Sodium Channel {beta}4 Subunit in Congenital Long-QT Syndrome. *Circulation* 2007; 116:134-142.

(148) Scheffer IE, Harkin LA, Grinton BE et al. Temporal lobe epilepsy and GEFS+ phenotypes associated with SCN1B mutations. *Brain* 2007; 130(Pt.1):100-109.

(149) Audenaert D, Claes L, Ceulemans B, Lofgren A, Van BC, De JP. A deletion in SCN1B is associated with febrile seizures and early-onset absence epilepsy. *Neurology* 2003; 61(6):854-856.

(150) Wallace RH, Scheffer IE, Parasivam G et al. Generalized epilepsy with febrile seizures plus: mutation of the sodium channel subunit SCN1B. *Neurology* 2002; 58(9):1426-1429.

(151) Hanlon MR, Wallace BA. Structure and function of voltage-dependent ion channel regulatory beta subunits. *Biochemistry* 2002; 41(9):2886-2894.

(152) McClatchey AI, Cannon SC, Slaugenhaupt SA, Gusella JF. The cloning and expression of a sodium channel beta 1-subunit cDNA from human brain. *Hum Mol Genet* 1993; 2(6):745-749.

(153) Wallner M, Weigl L, Meera P, Lotan I. Modulation of the skeletal muscle sodium channel alpha-subunit by the beta 1-subunit. *FEBS Lett* 1993; 336(3):535-539.

(154) Makita N, Bennett PB, Jr., George AL, Jr. Voltage-gated Na+ channel beta 1 subunit mRNA expressed in adult human skeletal muscle, heart, and brain is encoded by a single gene. *J Biol Chem* 1994; 269(10):7571-7578.

(155) Qu Y, Isom LL, Westenbroek RE et al. Modulation of cardiac Na+ channel expression in Xenopus oocytes by beta 1 subunits. *J Biol Chem* 1995; 270(43):25696-25701.

(156) Nuss HB, Chiamvimonvat N, Perez-Garcia MT, Tomaselli GF, Marban E. Functional association of the beta 1 subunit with human cardiac (hH1) and rat skeletal muscle (mu 1) sodium channel alpha subunits expressed in Xenopus oocytes. *J Gen Physiol* 1995; 106(6):1171-1191.

(157) Xiao YF, Wright SN, Wang GK, Morgan JP, Leaf A. Coexpression with beta(1)-subunit modifies the kinetics and fatty acid block of hH1(alpha) Na(+) channels. *Am J Physiol* Heart Circ Physiol 2000; 279(1):H35-H46.

(158) Makita N, Shirai N, Wang DW et al. Cardiac Na(+) channel dysfunction in Brugada syndrome is aggravated by beta(1)-subunit. *Circulation* 2000; 101(1):54-60.

(159) Makielski JC. The heart sodium channel phenotype for inactivation and lidocaine block. *Jpn Heart J* 1996; 37(5):733-739.

(160) Makielski JC, Limberis J, Fan Z, Kyle JW. Intrinsic lidocaine affinity for Na channels expressed in Xenopus oocytes depends on alpha (hH1 vs. rSkM1) and beta 1 subunits. *Cardiovasc Res* 1999; 42(2):503-509.

(161) Malhotra JD, Chen C, Rivolta I et al. Characterization of sodium channel alpha- and beta-subunits in rat and mouse cardiac myocytes. *Circulation* 2001; 103(9):1303-1310.

(162) Isom LL. The role of sodium channels in cell adhesion. *Front Biosci* 2002; 7:12-23.

(163) Stevens EB, Cox PJ, Shah BS et al. Tissue distribution and functional expression of the human voltage-gated sodium channel beta3 subunit. *Pflugers Arch* 2001; 441(4):481-488.

(164) Fahmi AI, Patel M, Stevens EB et al. The sodium channel beta-subunit SCN3b modulates the kinetics of SCN5a and is expressed heterogeneously in sheep heart. *J Physiol* 2001; 537(Pt 3):693-700.

(165) Medeiros-Domingo A, Kaku T, Tester DJ et al. SCN4B-Encoded Sodium Channel {beta}4 Subunit in Congenital Long-QT Syndrome. *Circulation* 2007; 116:134-142.

(166) Medeiros-Domingo A, Kaku T, Tester DJ et al. SCN4B-Encoded Sodium Channel {beta}4 Subunit in Congenital Long-QT Syndrome. *Circulation* 2007; 116:134-142.

(167) Ko SH, Lenkowski PW, Lee HC, Mounsey JP, Patel MK. Modulation of Na(v)1.5 by beta1-- and beta3-subunit co-expression in mammalian cells. *Pflugers Arch* 2005; 449(4):403-412.

(168) Abriel H, Kass RS. Regulation of the voltage-gated cardiac sodium channel Nav1.5 by interacting proteins. *Trends Cardiovasc Med* 2005; 15(1):35-40.

(169) Messner DJ, Catterall WA. The sodium channel from rat brain. Separation and characterization of subunits. *J Biol Chem* 1985; 260(19):10597-10604.

(170) Stainier DY, Fouquet B, Chen JN et al. Mutations affecting the formation and function of the cardiovascular system in the zebrafish embryo. *Development* 1996; 123:285-92.:285-292.

(171) Chen JN, Haffter P, Odenthal J et al. Mutations affecting the cardiovascular system and other internal organs in zebrafish. *Development* 1996; 123:293-302.:293-302.

(172) Stainier DY, Fouquet B, Chen JN et al. Mutations affecting the formation and function of the cardiovascular system in the zebrafish embryo. *Development* 1996; 123:285-92.:285-292.

(173) Chen JN, Haffter P, Odenthal J et al. Mutations affecting the cardiovascular system and other internal organs in zebrafish. *Development* 1996; 123:293-302.:293-302.

(174) Baker K, Warren KS, Yellen G, Fishman MC. Defective "pacemaker" current (Ih) in a zebrafish mutant with a slow heart rate. *Proc Natl Acad Sci (USA)* 1997; 94(9):4554-4559.

(175) Piontkivska H, Hughes AL. Evolution of vertebrate voltage-gated ion channel alpha chains by sequential gene duplication. *J Mol Evol* 2003; 56(3):277-285.

(176) Hughes AL. The evolution of functionally novel proteins after gene duplication. *Proc Biol Sci* 1994; 256(1346):119-124.

(177) Okamura Y, Nishino A, Murata Y et al. Comprehensive analysis of the ascidian genome reveals novel insights into the molecular evolution of ion channel genes. *Physiol Genomics* 2005; 22(3):269-282.

(178) Littleton JT, Ganetzky B. Ion channels and synaptic organization: analysis of the Drosophila genome. *Neuron* 2000; 26(1):35-43.

(179) Blackshaw SE, Henderson LP, Malek J et al. Single-cell analysis reveals cell-specific patterns of expression of a family of putative voltage-gated sodium channel genes in the leech. *J Neurobiol* 2003; 55(3):355-371.

(180) Lopreato GF, Lu Y, Southwell A et al. Evolution and divergence of sodium channel genes in vertebrates. *Proc Natl Acad Sci (USA)* 2001; 98(13):7588-7592.

(181) Long M, Betran E, Thornton K, Wang W. The origin of new genes: glimpses from the young and old. *Nat Rev Genet* 2003; 4(11):865-875.

(182) Hughes AL. Gene duplication and the origin of novel proteins. *Proc Natl Acad Sci (USA)* 2005; 102(25):8791-8792.

(183) Taylor JS, Raes J. Duplication and divergence: the evolution of new genes and old ideas. *Annu Rev Genet* 2004; 38:615-43.:615-643.

(184) Ohta T. Evolution by gene duplication revisited: differentiation of regulatory elements versus proteins. *Genetica* 2003; 118(2-3):209-216.

(185) Li WH, Yang J, Gu X. Expression divergence between duplicate genes. *Trends Genet* 2005; 21(11):602-607.

(186) Gibert JM. The evolution of engrailed genes after duplication and speciation events. *Dev Genes Evol* 2002; 212(7):307-318.

(187) Ono S. Ancient linkage groups and frozen accidents. *Nature* 1973; 244(5414):259-262.

(188) Byun-McKay SA, Geeta R. Protein subcellular relocalization: a new perspective on the origin of novel genes. *Trends Ecol Evol* 2007; 22(7):338-344.

(189) Force A, Lynch M, Pickett FB, Amores A, Yan YL, Postlethwait J. Preservation of duplicate genes by complementary, degenerative mutations. *Genetics* 1999; 151(4):1531-1545.

(190) Lynch M, Force A. The probability of duplicate gene preservation by subfunctionalization. *Genetics* 2000; 154(1):459-473.

(191) Chiu CH, Amemiya C, Dewar K, Kim CB, Ruddle FH, Wagner GP. Molecular evolution of the HoxA cluster in the three major gnathostome lineages. *Proc Natl Acad Sci (USA)* 2002; 99(8):5492-5497.

(192) Lynch VJ, Roth JJ, Wagner GP. Adaptive evolution of Hox-gene homeodomains after cluster duplications. *BMC Evol Biol* 2006; 6:86.:86.

(193) Rodin SN, Parkhomchuk DV, Rodin AS, Holmquist GP, Riggs AD. Repositioning-dependent fate of duplicate genes. *DNA Cell Biol* 2005; 24(9):529-542.

(194) Katju V, Lynch M. On the formation of novel genes by duplication in the Caenorhabditis elegans genome. *Mol Biol Evol* 2006; 23(5):1056-1067.

(195) Sangameswaran L, Fish LM, Koch BD et al. A novel tetrodotoxin-sensitive, voltage-gated sodium channel expressed in rat and human dorsal root ganglia. *J Biol Chem* 1997; 272(23):14805-14809.

(196) Lu CM, Han J, Rado TA, Brown GB. Differential expression of two sodium channel subtypes in human brain. *FEBS Lett* 1992; 303(1):53-58.

(197) Noda M, Ikeda T, Kayano T et al. Existence of distinct sodium channel messenger RNAs in rat brain. *Nature* 1986; 320(6058):188-192.

(198) Klugbauer N, Lacinova L, Flockerzi V, Hofmann F. Structure and functional expression of a new member of the tetrodotoxin-sensitive voltage-activated sodium channel family from human neuroendocrine cells. *EMBO J* 1995; 14(6):1084-1090.

(199) Ahmed CM, Ware DH, Lee SC et al. Primary structure, chromosomal localization, and functional expression of a voltage-gated sodium channel from human brain. *Proc Natl Acad Sci (USA)* 1992; 89(17):8220-8224.

(200) Chen YH, Dale TJ, Romanos MA, Whitaker WR, Xie XM, Clare JJ. Cloning, distribution and functional analysis of the type III sodium channel from human brain. *Eur J Neurosci* 2000; 12(12):4281-4289.

(201) Whitaker WR, Clare JJ, Powell AJ, Chen YH, Faull RL, Emson PC. Distribution of voltage-gated sodium channel alpha-subunit and beta-subunit mRNAs in human hippocampal formation, cortex, and cerebellum. *J Comp Neurol* 2000;422(1):123-139.

(202) Whitaker WR, Faull RL, Waldvogel HJ, Plumpton CJ, Emson PC, Clare JJ. Comparative distribution of voltage-gated sodium channel proteins in human brain. *Brain Res Mol Brain Res* 2001; 88(1-2):37-53.

(203) Suzuki H, Beckh S, Kubo H et al. Functional expression of cloned cDNA encoding sodium channel III. *FEBS Lett* 1988; 228(1):195-200.

(204) Gordon D, Merrick D, Auld V et al. Tissue-specific expression of the RI and RII sodium channel subtypes. *Proc Natl Acad Sci (USA)* 1987; 84(23):8682-8686.

(205) Felipe A, Knittle TJ, Doyle KL, Tamkun MM. Primary structure and differential expression during development and pregnancy of a novel voltage-gated sodium channel in the mouse. *J Biol Chem* 1994; 269(48):30125-30131.

(206) George AL, Jr., Knittle TJ, Tamkun MM. Molecular cloning of an atypical voltage-gated sodium channel expressed in human heart and uterus: evidence for a distinct gene family. *Proc Natl Acad Sci (USA)* 1992; 89(11):4893-4897.

(207) Rogart RB, Cribbs LL, Muglia LK, Kephart DD, Kaiser MW. Molecular cloning of a putative tetrodotoxin-resistant rat heart Na+ channel isoform. *Proc Natl Acad Sci (USA)* 1989; 86(20):8170-8174.

(208) Gellens ME, George AL, Jr., Chen LQ et al. Primary structure and functional expression of the human cardiac tetrodotoxin-insensitive voltage-dependent sodium channel. *Proc Natl Acad Sci (USA)* 1992; 89(2):554-558.

(209) Kallen RG, Sheng ZH, Yang J, Chen LQ, Rogart RB, Barchi RL. Primary structure and expression of a sodium channel characteristic of denervated and immature rat skeletal muscle. *Neuron* 1990; 4(2):233-242.

(210) White MM, Chen LQ, Kleinfield R, Kallen RG, Barchi RL. SkM2, a Na+ channel cDNA clone from denervated skeletal muscle, encodes a tetrodotoxin-insensitive Na+ channel. *Mol Pharmacol* 1991; 39(5):604-608.

(211) Sangameswaran L, Delgado SG, Fish LM et al. Structure and function of a novel voltage-gated, tetrodotoxin-resistant sodium channel specific to sensory neurons. *J Biol Chem* 1996; 271(11):5953-5956.

(212) Rabert DK, Koch BD, Ilnicka M et al. A tetrodotoxin-resistant voltage-gated sodium channel from human dorsal root ganglia, hPN3/SCN10A. *Pain* 1998; 78(2):107-114.

(213) Dib-Hajj SD, Tyrrell L, Black JA, Waxman SG. NaN, a novel voltage-gated Na channel, is expressed preferentially in peripheral sensory neurons and down-regulated after axotomy. *Proc Natl Acad Sci (USA)* 1998; 95(15):8963-8968.

(214) Jeong SY, Goto J, Hashida H et al. Identification of a novel human voltage-gated sodium channel alpha subunit gene, SCN12A. *Biochem Biophys Res Commun* 2000; 267(1):262-270.

(215) Whitaker W, Faull R, Waldvogel H et al. Localization of the type VI voltage-gated sodium channel protein in human CNS. *Neuroreport* 1999; 10(17):3703-3709.

(216) Krzemien DM, Schaller KL, Levinson SR, Caldwell JH. Immunolocalization of sodium channel isoform NaCh6 in the nervous system. *J Comp Neurol* 2000; 420(1):70-83.

(217) Caldwell JH, Schaller KL, Lasher RS, Peles E, Levinson SR. Sodium channel Na(v)1.6 is localized at nodes of ranvier, dendrites, and synapses. *Proc Natl Acad Sci (USA)* 2000; 97(10):5616-5620.

(218) George AL, Jr., Komisarof J, Kallen RG, Barchi RL. Primary structure of the adult human skeletal muscle voltage-dependent sodium channel. *Ann Neurol* 1992; 31(2):131-137.

(219) Wang JZ, Rojas CV, Zhou JH, Schwartz LS, Nicholas H, Hoffman EP. Sequence and genomic structure of the human adult skeletal muscle sodium channel alpha subunit gene on 17q. *Biochem Biophys Res Commun* 1992; 182(2):794-801.

(220) Trimmer JS, Cooperman SS, Tomiko SA et al. Primary structure and functional expression of a mammalian skeletal muscle sodium channel. *Neuron* 1989; 3(1):33-49.

(221) Dhar MJ, Chen C, Rivolta I et al. Characterization of sodium channel alpha- and beta-subunits in rat and mouse cardiac myocytes. *Circulation* 2001; 103(9):1303-1310.

(222) Ahmad S, Dahllund L, Eriksson AB et al. A stop codon mutation in SCN9A causes lack of pain sensation. *Hum Mol Genet* 2007; 16(17):2114-21.

(223) Goldberg YP, MacFarlane J, MacDonald ML et al. Loss-of-function mutations in the Nav1.7 gene underlie congenital indifference to pain in multiple human populations. *Clin Genet* 2007; 71(4):311-319.

(224) Ribera AB, Nusslein-Volhard C. Zebrafish touch-insensitive mutants reveal an essential role for the developmental regulation of sodium current. *J Neurosci* 1998; 18(22):9181-9191.

(225) Tsai CW, Tseng JJ, Lin SC et al. Primary structure and developmental expression of zebrafish sodium channel Na(v)1.6 during neurogenesis. *DNA Cell Biol* 2001; 20(5):249-255.

(226) Warren KS, Baker K, Fishman MC. The slow mo mutation reduces pacemaker current and heart rate in adult zebrafish. *Am J Physiol Heart Circ Physiol* 2001; 281(4):H1711-H1719.

(227) Amores A, Force A, Yan YL et al. Zebrafish hox clusters and vertebrate genome evolution. *Science* 1998; 282(5394):1711-1714.

(228) Postlethwait JH, Yan YL, Gates MA et al. Vertebrate genome evolution and the zebrafish gene map. *Nat Genet* 1998; 18(4):345-349.

(229) Novak AE, Taylor AD, Pineda RH, Lasda EL, Wright MA, Ribera AB. Embryonic and larval expression of zebrafish voltage-gated sodium channel alpha-subunit genes. *Dev Dyn* 2006; 235(7):1962-1973.

(230) Novak AE, Jost MC, Lu Y, Taylor AD, Zakon HH, Ribera AB. Gene duplications and evolution of vertebrate voltage-gated sodium channels. *J Mol Evol* 2006; 63(2):208-221.

(231) Venkatesh B, Lu SQ, Dandona N, See SL, Brenner S, Soong TW. Genetic basis of tetrodotoxin resistance in pufferfishes. *Curr Biol* 2005; 15(22):2069-2072.

(232) Saitou N, Nei M. The neighbor-joining method: a new method for reconstructing phylogenetic trees. *Mol Biol Evol* 1987; 4(4):406-425.

(233) Darbar D, Yang T, Churchwell K, Wilde AA, Roden DM. Unmasking of brugada syndrome by lithium. *Circulation* 2005; 112(11):1527-1531.

(234) LeMaillet G, Walker B, Lambert S. Identification of a conserved ankyrin-binding motif in the family of sodium channel alpha subunits. *J Biol Chem* 2003; 278(30):27333-27339.

(235) Mohler PJ, Rivolta I, Napolitano C et al. Nav1.5 E1053K mutation causing Brugada syndrome blocks binding to ankyrin-G and expression of Nav1.5 on the surface of cardiomyocytes. *Proc Natl Acad Sci (USA)* 2004; 101(50):17533-17538.

(236) Liu CJ, Dib-Hajj SD, Renganathan M, Cummins TR, Waxman SG. Modulation of the cardiac sodium channel Nav1.5 by fibroblast growth factor homologous factor 1B. *J Biol Chem* 2003; 278(2):1029-1036.

(237) Deschenes I, Neyroud N, DiSilvestre D, Marban E, Yue DT, Tomaselli GF. Isoform-specific modulation of voltage-gated Na(+) channels by calmodulin. *Circ Res* 2002; 90(4):E49-E57.

(238) Tan HL, Kupershmidt S, Zhang R et al. A calcium sensor in the sodium channel modulates cardiac excitability. *Nature* 2002; 415(6870):442-447.

(239) Young KA, Caldwell JH. Modulation of skeletal and cardiac voltage-gated sodium channels by calmodulin. *J Physiol* 2005; 565(Pt 2):349-370.

(240) Shah VN, Wingo TL, Weiss KL, Williams CK, Balser JR, Chazin WJ. Calcium-dependent regulation of the voltage-gated sodium channel hH1: intrinsic and extrinsic sensors use a common molecular switch. *Proc Natl Acad Sci (USA)* 2006; 103(10):3592-3597.

(241) van Bemmelen MX, Rougier JS, Gavillet B et al. Cardiac voltage-gated sodium channel Nav1.5 is regulated by Nedd4-2 mediated ubiquitination. *Circ Res* 2004; 95(3):284-291.

(242) Wingo TL, Shah VN, Anderson ME, Lybrand TP, Chazin WJ, Balser JR. An EF-hand in the sodium channel couples intracellular calcium to cardiac excitability. *Nat Struct Mol Biol* 2004; 11(3):219-225.

(243) Ou Y, Strege P, Miller SM et al. Syntrophin gamma 2 regulates SCN5A gating by a PDZ domain-mediated interaction. *J Biol Chem* 2003; 278(3):1915-1923.

(244) Zhou J, Yi J, Hu N, George AL, Jr., Murray KT. Activation of protein kinase A modulates trafficking of the human cardiac sodium channel in Xenopus oocytes. *Circ Res* 2000; 87(1):33-38.

(245) Zhou J, Shin HG, Yi J, Shen W, Williams CP, Murray KT. Phosphorylation and putative ER retention signals are required for protein kinase A-mediated potentiation of cardiac sodium current. *Circ Res* 2002;91(6):540-546.

(246) Satin J, Kyle JW, Chen M et al. A mutant of TTX-resistant cardiac sodium channels with TTX-sensitive properties. *Science* 1992; 256(5060):1202-1205.

(247) Pineda RH, Heiser RA, Ribera AB. Developmental, molecular, and genetic dissection of INa in vivo in embryonic zebrafish sensory neurons. *J Neurophysiol* 2005; 93(6):3582-3593.

(248) Black JA, Dib-Hajj S, Cohen S, Hinson AW, Waxman SG. Glial cells have heart: rH1 Na+ channel mRNA and protein in spinal cord astrocytes. *Glia* 1998; 23(3):200-208.

(249) Hartmann HA, Colom LV, Sutherland ML, Noebels JL. Selective localization of cardiac SCN5A sodium channels in limbic regions of rat brain. *Nat Neurosci* 1999; 2(7):593-595.

(250) Donahue LM, Coates PW, Lee VH, Ippensen DC, Arze SE, Poduslo SE. The cardiac sodium channel mRNA is expressed in the developing and adult rat and human brain. *Brain Res* 2000; 887(2):335-343.

(251) Renganathan M, Dib-Hajj S, Waxman SG. Na(v)1.5 underlies the 'third TTX-R sodium current' in rat small DRG neurons. *Brain Res Mol Brain Res* 2002; 106(1-2):70-82.

(252) Wu L, Nishiyama K, Hollyfield JG, Wang Q. Localization of Nav1.5 sodium channel protein in the mouse brain. *Neuroreport* 2002; 13(18):2547-2551.

(253) Ou Y, Gibbons SJ, Miller SM et al. SCN5A is expressed in human jejunal circular smooth muscle cells. *Neurogastroenterol Motil* 2002; 14(5):477-486.

(254) Tate S, Benn S, Hick C et al. Two sodium channels contribute to the TTX-R sodium current in primary sensory neurons. *Nat Neurosci* 1998; 1(8):653-655.

(255) Keating MT, Sanguinetti MC. Molecular and cellular mechanisms of cardiac arrhythmias. *Cell* 2001; 104(4):569-580.

(256) Nuyens D, Stengl M, Dugarmaa S et al. Abrupt rate accelerations or premature beats cause life-threatening arrhythmias in mice with long-QT3 syndrome. *Nat Med* 2001; 7(9):1021-1027.

(257) George AL, Jr. Inherited disorders of voltage-gated sodium channels. *J Clin Invest* 2005; 115(8):1990-1999.

(258) Echt DS, Liebson PR, Mitchell LB et al. Mortality and morbidity in patients receiving encainide, flecainide, or placebo. The Cardiac Arrhythmia Suppression Trial. *N Engl J Med* 1991; 324(12):781-788.

(259) Burns CG, Milan DJ, Grande EJ, Rottbauer W, Macrae CA, Fishman MC. High-throughput assay for small molecules that modulate zebrafish embryonic heart rate. *Nat Chem Biol* 2005; 1(5):263-264.

(260) Mably JD, Mohideen MA, Burns CG, Chen JN, Fishman MC. heart of glass regulates the concentric growth of the heart in zebrafish. *Curr Biol* 2003; 13(24):2138-2147.

(261) Milan DJ, Giokas AC, Serluca FC, Peterson RT, Macrae CA. Notch1b and neuregulin are required for specification of central cardiac conduction tissue. *Development* 2006; 133(6):1125-1132.

(262) Milan DJ, Peterson TA, Ruskin JN, Peterson RT, Macrae CA. Drugs that induce repolarization abnormalities cause bradycardia in zebrafish. *Circulation* 2003; 107(10):1355-1358.

(263) Desai SP, Marsh JD, Allen PD. Contractility effects of local anesthetics in the presence of sodium channel blockade. *Reg Anesth* 1989; 14(2):58-62.

(264) Sakura S, Bollen AW, Ciriales R, Drasner K. Local anesthetic neurotoxicity does not result from blockade of voltage-gated sodium channels. *Anesth Analg* 1995; 81(2):338-346.

(265) Josephson I, Sperelakis N. Local anesthetic blockade of Ca2+ -mediated action potentials in cardiac muscle. *Eur J Pharmacol* 1976; 40(2):201-208.

(266) Josephson IR. Lidocaine blocks Na, Ca and K currents of chick ventricular myocytes. *J Mol Cell Cardiol* 1988; 20(7):593-604.

(267) Campbell TJ, Wyse KR, Pallandi R. Differential effects on action potential duration of class IA, B and C antiarrhythmic drugs: modulation by stimulation rate and extracellular K+ concentration. *Clin Exp Pharmacol Physiol* 1991; 18(8):533-541.

(268) Follmer CH, Cullinan CA, Colatsky TJ. Differential block of cardiac delayed rectifier current by class Ic antiarrhythmic drugs: evidence for open channel block and unblock. *Cardiovasc Res* 1992; 26(11):1121-1130.

(269) Nasevicius A, Ekker SC. Effective targeted gene 'knockdown' in zebrafish. *Nat Genet* 2000; 26(2):216-220.

(270) Rottbauer W, Baker K, Wo ZG, Mohideen MA, Cantiello HF, Fishman MC. Growth and function of the embryonic heart depend upon the cardiac-specific L-type calcium channel alpha1 subunit. *Dev Cell* 2001; 1(2):265-275.

(271) Royer A, van Veen TA, Le BS et al. Mouse model of SCN5A-linked hereditary Lenegre's disease: age-related conduction slowing and myocardial fibrosis. *Circulation* 2005; 111(14):1738-1746.

(272) Makita N, Sasaki K, Yokoshiki H, Yamada S, Tsutsui H. Left ventricular noncompaction assocated with mutations in cardiac sodium channel gene *SCN5A*. American Heart Association Scientific Sessions, Abstract, 2006.

(273) McNair WP, Ku L, Taylor MR et al. SCN5A mutation associated with dilated cardiomyopathy, conduction disorder, and arrhythmia. *Circulation* 2004; 110(15):2163-2167.

(274) Adler E, Fuster V. SCN5A--a mechanistic link between inherited cardiomyopathies and a predisposition to arrhythmias? *JAMA* 2005; 293(4):491-493.

(275) Olson TM, Michels VV, Ballew JD et al. Sodium channel mutations and susceptibility to heart failure and atrial fibrillation. *JAMA* 2005; 293(4):447-454.

(276) van Veen TA, Stein M, Royer A et al. Impaired impulse propagation in Scn5a-knockout mice: combined contribution of excitability, connexin expression, and tissue architecture in relation to aging. *Circulation* 2005; 112(13):1927-1935.

(277) Garrity DM, Childs S, Fishman MC. The heartstrings mutation in zebrafish causes heart/fin Tbx5 deficiency syndrome. *Development* 2002; 129(19):4635-4645.

(278) Yelon D, Horne SA, Stainier DY. Restricted expression of cardiac myosin genes reveals regulated aspects of heart tube assembly in zebrafish. *Dev Biol* 1999; 214(1):23-37.

(279) Keegan BR, Meyer D, Yelon D. Organization of cardiac chamber progenitors in the zebrafish blastula. *Development* 2004; 131(13):3081-3091.

(280) Rottbauer W, Saurin AJ, Lickert H et al. Reptin and pontin antagonistically regulate heart growth in zebrafish embryos. *Cell* 2002; 111(5):661-672.

(281) Jia H, King IN, Chopra SS et al. Vertebrate heart growth is regulated by functional antagonism between Gridlock and Gata5. *Proc Natl Acad Sci (USA)*. in press. 2007.

(282) Kupperman E, An S, Osborne N, Waldron S, Stainier DY. A sphingosine-1-phosphate receptor regulates cell migration during vertebrate heart development. *Nature* 2000; 406(6792):192-195.

(283) Mably JD, Mohideen MA, Burns CG, Chen JN, Fishman MC. heart of glass regulates the concentric growth of the heart in zebrafish. *Curr Biol* 2003; 13(24):2138-2147.

(284) Cestele S, Catterall WA. Molecular mechanisms of neurotoxin action on voltage-gated sodium channels. *Biochimie* 2000; 82(9-10):883-892.

(285) Catterall WA, Cestele S, Yarov-Yarovoy V, Yu FH, Konoki K, Scheuer T. Voltage-gated ion channels and gating modifier toxins. *Toxicon* 2007; 49(2):124-141.

(286) Renaud JF, Romey G, Lombet A, Lazdunski M. Differentiation of the fast Na+ channel in embryonic heart cells: interaction of the channel with neurotoxins. *Proc Natl Acad Sci (USA)* 1981; 78(9):5348-5352.

(287) Garry DJ, Olson EN. A common progenitor at the heart of development. *Cell* 2006; 127(6):1101-1104.

(288) Olson EN. Gene regulatory networks in the evolution and development of the heart. *Science* 2006; 313(5795):1922-1927.

(289) Srivastava D. Making or breaking the heart: from lineage determination to morphogenesis. *Cell* 2006; 126(6):1037-1048.

(290) Olson EN, Schneider MD. Sizing up the heart: development redux in disease. *Genes Dev* 2003; 17(16):1937-1956.

(291) Chen JN, Fishman MC. Zebrafish tinman homolog demarcates the heart field and initiates myocardial differentiation. *Development* 1996; 122(12):3809-3816.

(292) Holtzinger A, Evans T. Gata4 regulates the formation of multiple organs. *Development* 2005; 132(17):4005-4014.

(293) Heicklen-Klein A, McReynolds LJ, Evans T. Using the zebrafish model to study GATA transcription factors. *Semin Cell Dev Biol* 2005; 16(1):95-106.

(294) Yelon D, Ticho B, Halpern ME et al. The bHLH transcription factor hand2 plays parallel roles in zebrafish heart and pectoral fin development. *Development* 2000; 127(12):2573-2582.

(295) Angelo S, Lohr J, Lee KH et al. Conservation of sequence and expression of Xenopus and zebrafish dHAND during cardiac, branchial arch and lateral mesoderm development. *Mech Dev* 2000; 95(1-2):231-237.

(296) Langheinrich U, Vacun G, Wagner T. Zebrafish embryos express an orthologue of HERG and are sensitive toward a range of QT-prolonging drugs inducing severe arrhythmia. *Toxicol Appl Pharmacol* 2003; 193(3):370-382.

(297) Keegan BR, Meyer D, Yelon D. Organization of cardiac chamber progenitors in the zebrafish blastula. *Development* 2004; 131(13):3081-3091.

(298) Yelon D, Horne SA, Stainier DY. Restricted expression of cardiac myosin genes reveals regulated aspects of heart tube assembly in zebrafish. *Dev Biol* 1999; 214(1):23-37.

(299) Reiter JF, Alexander J, Rodaway A et al. Gata5 is required for the development of the heart and endoderm in zebrafish. *Genes Dev* 1999; 13(22):2983-2995.

(300) Reiter JF, Verkade H, Stainier DY. Bmp2b and Oep promote early myocardial differentiation through their regulation of gata5. *Dev Biol* 2001; 234(2):330-338.

(301) Yu FH, Yarov-Yarovoy V, Gutman GA, Catterall WA. Overview of molecular relationships in the voltage-gated ion channel superfamily. *Pharmacol Rev* 2005; 57(4):387-395.

(302) Robu ME, Larson JD, Nasevicius A et al. p53 activation by knockdown technologies. *PLoS Genet* 2007; 3(5):e78.

(303) Poelzing S, Forleo C, Samodell M et al. SCN5A polymorphism restores trafficking of a Brugada syndrome mutation on a separate gene. *Circulation* 2006; 114(5):368-376.

(304) Ebert AM, Hume GL, Warren KS et al. Calcium extrusion is critical for cardiac morphogenesis and rhythm in embryonic zebrafish hearts. *Proc Natl Acad Sci (USA)* 2005; 102(49):17705-17710.

(305) Langenbacher AD, Dong Y, Shu X et al. Mutation in sodium-calcium exchanger 1 (NCX1) causes cardiac fibrillation in zebrafish. *Proc Natl Acad Sci (USA)* 2005; 102(49):17699-17704.

(306) Shu X, Cheng K, Patel N et al. Na,K-ATPase is essential for embryonic heart development in the zebrafish. *Development* 2003; 130(25):6165-6173.

(307) Arnaout R, Ferrer T, Huisken J et al. Zebrafish model for human long QT syndrome. *Proc Natl Acad Sci (USA)* 2007; 104(27):11316-11321.

(308) Yuan S, Joseph EM. The small heart mutation reveals novel roles of Na+/K+-ATPase in maintaining ventricular cardiomyocyte morphology and viability in zebrafish. *Circ Res* 2004; 95(6):595-603.

(309) Davies MP, An RH, Doevendans P, Kubalak S, Chien KR, Kass RS. Developmental changes in ionic channel activity in the embryonic murine heart. *Circ Res* 1996; 78(1):15-25.

(310) Maltsev VA, Wobus AM, Rohwedel J, Bader M, Hescheler J. Cardiomyocytes differentiated in vitro from embryonic stem cells developmentally express cardiac-specific genes and ionic currents. *Circ Res* 1994; 75(2):233-244.

(311) van der Heyden MA, Defize LH. Twenty one years of P19 cells: what an embryonal carcinoma cell line taught us about cardiomyocyte differentiation. *Cardiovasc Res* 2003; 58(2):292-302.

(312) van der Heyden MA, van Kempen MJ, Tsuji Y, Rook MB, Jongsma HJ, Opthof T. P19 embryonal carcinoma cells: a suitable model system for cardiac electrophysiological differentiation at the molecular and functional level. *Cardiovasc Res* 2003; 58(2):410-422.

(313) Wobus AM, Kleppisch T, Maltsev V, Hescheler J. Cardiomyocyte-like cells differentiated in vitro from embryonic carcinoma cells P19 are characterized by functional expression of adrenoceptors and Ca2+ channels. *In Vitro Cell Dev Biol Anim* 1994; 30A(7):425-434.

(314) Sperelakis N, Pappano AJ. Physiology and pharmacology of developing heart cells. *Pharmacol Ther* 1983; 22(1):1-39.

(315) Shigenobu K, Sperelakis N. Development of sensitivity to tetrodotoxin of chick embryonic hearts with age. *J Mol Cell Cardiol* 1971; 3(3):271-286.

(316) McDonald TF, Sachs HG. Electrical activity in embryonic heart cell aggregates. Developmental aspects. *Pflugers Arch* 1975; 354(2):151-164.

(317) Pappano AJ. Action potentials in chick atria. Increased susceptibility to blockade by tetrodotoxin during embryonic development. *Circ Res* 1972; 31(3):379-388.

(318) Sperelakis N, Shigenobu K. Changes in membrane properties of chick embryonic hearts during development. *J Gen Physiol* 1972; 60(4):430-453.

(319) McDonald TF, Sachs HG, DeHaan RL. Development of sensitivity to tetrodotoxin in beating chick embryo hearts, single cells, and aggregates. *Science* 1972; 176(40):1248-1250.

(320) Nathan RD, DeHaan RL. In vitro differentiation of a fast Na+ conductance in embryonic heart cell aggregates. *Proc Natl Acad Sci (USA)* 1978; 75(6):2776-2780.

(321) Galper JB, Catterall WA. Developmental changes in the sensitivity of embryonic heart cells to tetrodotoxin and D600. *Dev Biol* 1978; 65(1):216-227.

(322) Iijima T, Pappano AJ. Ontogenetic increase of the maximal rate of rise of the chick embryonic heart action potential. Relationship to voltage, time, and tetrodotoxin. *Circ Res* 1979; 44(3):358-367.

(323) Fujii S, Hirota A, Kamino K. Optical signals from early embryonic chick heart stained with potential sensitive dyes: evidence for electrical activity. *J Physiol* 1980; 304:503-18.:503-518.

(324) Marcus NC, Fozzard H. Tetrodotoxin sensitivity in the developing and adult chick heart. *J Mol Cell Cardiol* 1981; 13(3):335-340.

(325) Fishman MC, Chien KR. Fashioning the vertebrate heart: earliest embryonic decisions. *Development* 1997; 124(11):2099-2117.

(326) Sehnert AJ, Huq A, Weinstein BM, Walker C, Fishman M, Stainier DY. Cardiac troponin T is essential in sarcomere assembly and cardiac contractility. *Nat Genet* 2002; 31(1):106-110.

(327) Anderson ME. Connections count: excitation-contraction meets excitation-transcription coupling. *Circ Res* 2000; 86(7):717-719.

(328) Barlow CA, Rose P, Pulver-Kaste RA, Lounsbury KM. Excitation-transcription coupling in smooth muscle. *J Physiol* 2006; 570(Pt 1):59-64.

(329) Bers DM, Guo T. Calcium signaling in cardiac ventricular myocytes. *Ann N Y Acad Sci* 2005; 1047:86-98.:86-98.

(330) Dolmetsch R. Excitation-transcription coupling: signaling by ion channels to the nucleus. *Sci STKE* 2003; 2003(166):E4.

(331) Crabtree GR, Olson EN. NFAT signaling: choreographing the social lives of cells. *Cell* 2002; 109 Suppl:S67-79.:S67-S79.

(332) Kalil RE. The influence of action potentials on the development of the central visual pathway in mammals. *J Exp Biol* 1990; 153:261-76.:261-276.

(333) Shatz CJ. Emergence of order in visual system development. *Proc Natl Acad Sci (USA)* 1996; 93(2):602-608.

(334) Katz LC, Shatz CJ. Synaptic activity and the construction of cortical circuits. *Science* 1996; 274(5290):1133-1138.

(335) Bergey GK, Fitzgerald SC, Schrier BK, Nelson PG. Neuronal maturation in mammalian cell culture is dependent on spontaneous electrical activity. *Brain Res* 1981; 207(1):49-58.

(336) Jackson MB, Lecar H, Brenneman DE, Fitzgerald S, Nelson PG. Electrical development in spinal cord cell culture. *J Neurosci* 1982; 2(8):1052-1061.

(337) Gomez-Ospina N, Tsuruta F, Barreto-Chang O, Hu L, Dolmetsch R. The C terminus of the L-type voltage-gated calcium channel Ca(V)1.2 encodes a transcription factor. *Cell* 2006; 127(3):591-606.

(338) Srivastava D, Gottlieb PD, Olson EN. Molecular mechanisms of ventricular hypoplasia. *Cold Spring Harb Symp Quant Biol* 2002; 67:121-5.

(339) Olson EN. A genetic blueprint for growth and development of the heart. *Harvey Lect* 2002; 98:41-64.

(340) Bruneau BG. Transcriptional regulation of vertebrate cardiac morphogenesis. *Circ Res* 2002; 90(5):509-519.

(341) Bruneau BG, Nemer G, Schmitt JP et al. A murine model of Holt-Oram syndrome defines roles of the T-box transcription factor Tbx5 in cardiogenesis and disease. *Cell* 2001; 106(6):709-721.

(342) Bruneau BG, Logan M, Davis N et al. Chamber-specific cardiac expression of Tbx5 and heart defects in Holt-Oram syndrome. *Dev Biol* 1999; 211(1):100-108.

(343) van KM, van GA, de G, I et al. Expression of the electrophysiological system during murine embryonic stem cell cardiac differentiation. *Cell Physiol Biochem* 2003; 13(5):263-270.

(344) McEwen DP, Meadows LS, Chen C, Thyagarajan V, Isom LL. Sodium channel beta1 subunit-mediated modulation of Nav1.2 currents and cell surface density is dependent on interactions with contactin and ankyrin. *J Biol Chem* 2004; 279(16):16044-16049.

(345) Isom LL. Sodium channel beta subunits: anything but auxiliary. *Neuroscientist* 2001; 7(1):42-54.

(346) Xiao ZC, Ragsdale DS, Malhotra JD et al. Tenascin-R is a functional modulator of sodium channel beta subunits. *J Biol Chem* 1999; 274(37):26511-26517.

(347) Malhotra JD, Thyagarajan V, Chen C, Isom LL. Tyrosine-phosphorylated and nonphosphorylated sodium channel beta1 subunits are differentially localized in cardiac myocytes. *J Biol Chem* 2004; 279(39):40748-40754.

(348) Malhotra JD, Koopmann MC, Kazen-Gillespie KA, Fettman N, Hortsch M, Isom LL. Structural requirements for interaction of sodium channel beta 1 subunits with ankyrin. *J Biol Chem* 2002; 277(29):26681-26688.

(349) Malhotra JD, Kazen-Gillespie K, Hortsch M, Isom LL. Sodium channel beta subunits mediate homophilic cell adhesion and recruit ankyrin to points of cell-cell contact. *J Biol Chem* 2000; 275(15):11383-11388.

(350) Linask KK, Knudsen KA, Gui YH. N-cadherin-catenin interaction: necessary component of cardiac cell compartmentalization during early vertebrate heart development. *Dev Biol* 1997; 185(2):148-164.

(351) Nakagawa S, Takeichi M. N-cadherin is crucial for heart formation in the chick embryo. *Dev Growth Differ* 1997; 39(4):451-455.

(352) Radice GL, Rayburn H, Matsunami H, Knudsen KA, Takeichi M, Hynes RO. Developmental defects in mouse embryos lacking N-cadherin. *Dev Biol* 1997; 181(1):64-78.

(353) Carrithers MD, Dib-Hajj S, Carrithers LM et al. Expression of the voltage-gated sodium channel NaV1.5 in the macrophage late endosome regulates endosomal acidification. *J Immunol* 2007; 178(12):7822-7832.

(354) Ritchie JM. Voltage-gated ion channels in Schwann cells and glia. *Trends Neurosci* 1992; 15(9):345-351.

(355) Sontheimer H, Waxman SG. Expression of voltage-activated ion channels by astrocytes and oligodendrocytes in the hippocampal slice. *J Neurophysiol* 1993; 70(5):1863-1873.

(356) Sontheimer H. Voltage-dependent ion channels in glial cells. *Glia* 1994; 11(2):156-172.

(357) Sontheimer H, Black JA, Waxman SG. Voltage-gated Na+ channels in glia: properties and possible functions. *Trends Neurosci* 1996; 19(8):325-331.

(358) Royer A, van Veen TA, Le BS et al. Mouse model of SCN5A-linked hereditary Lenegre's disease: age-related conduction slowing and myocardial fibrosis. *Circulation* 2005; 111(14):1738-1746.

(359) McNair WP, Ku L, Taylor MR et al. SCN5A mutation associated with dilated cardiomyopathy, conduction disorder, and arrhythmia. *Circulation* 2004; 110(15):2163-2167.

(360) Mohler PJ, Rivolta I, Napolitano C et al. Nav1.5 E1053K mutation causing Brugada syndrome blocks binding to ankyrin-G and expression of Nav1.5 on the surface of cardiomyocytes. *Proc Natl Acad Sci (USA)* 2004; 101(50):17533-17538.

(361) Ou Y, Strege P, Miller SM et al. Syntrophin gamma 2 regulates SCN5A gating by a PDZ domain-mediated interaction. *J Biol Chem* 2003; 278(3):1915-1923.

(362) Morita H, Seidman J, Seidman CE. Genetic causes of human heart failure. *J Clin Invest* 2005; 115(3):518-526.

(363) Shatz CJ, Stryker MP. Prenatal tetrodotoxin infusion blocks segregation of retinogeniculate afferents. *Science* 1988; 242(4875):87-89.

(364) Gyllensten L, Malmfors T, Norrlin ML. Effect of visual deprivation on the optic centers of growing and adult mice. *J Comp Neurol* 1965; 124:149-60.

(365) Wiesel TN, Hubel DH. Single-cell responses in striate cortex of kittens deprived of vision in one eye. *J Neurophysiol* 1963; 26:1003-17.

(366) Wiesel TN, Hubel DH. Effects of visual deprivation on morphology and physiology of cells in the cats lateral geniculate body. *J Neurophysiol* 1963; 26:978-93.

(367) Cragg BG. The effects of vision and dark-rearing on the size and density of synapses in the lateral geniculate nucleus measured by electron microscopy. *Brain Res* 1969; 13(1):53-67.

(368) Godfrey EW, Nelson PG, Schrier BK, Breuer AC, Ransom BR. Neurons from fetal rat brain in a new cell culture system: a multidisciplinary analysis. *Brain Res* 1975; 90(1):1-21.

(369) Kalil RE, Dubin MW, Scott G, Stark LA. Elimination of action potentials blocks the structural development of retinogeniculate synapses. *Nature* 1986; 323(6084):156-158.

(370) Pineda RH, Svoboda KR, Wright MA et al. Knockdown of Nav1.6a Na+ channels affects zebrafish motoneuron development. *Development* 2006; 133(19):3827-3836.

(371) Isom LL. Sodium channel beta subunits: anything but auxiliary. *Neuroscientist* 2001; 7(1):42-54.

(372) Medeiros-Domingo A, Kaku T, Tester DJ et al. SCN4B-Encoded Sodium Channel {beta}4 Subunit in Congenital Long-QT Syndrome. *Circulation* 2007; 116:134-142.

(373) Simple Modular Architecture Research Tool (SMART) [http://smart.embl-heidelberg.de/]. 2007.

(374) Conserved Domain Database, NCBI [http://www.ncbi.nlm.nih.gov/Structure/cdd/wrpsb.cgi]. 2007.

(375) TM Pred [http://www.ch.embnet.org/]. 2007.

(376) Kyte J, Doolittle RF. A simple method for displaying the hydropathic character of a protein. *J Mol Biol* 1982; 157(1):105-132.

(377) Prosite [http://ca.expasy.org/]. 2007.

(378) NetNGlyc [http://www.cbs.dtu.dk/services/]. 2007.

(379) Kimura M. The Neutral Theory of Molecular Evolution. Cambridge: Cambridge University Press, 1983.

(380) Ensembl genome browser [www.ensembl.org]. 2007.

(381) National Human Genome Sequencing Center, Baylor College of Medicine [http://www.hgsc.bcm.tmc.edu/projects/seaurchin/]. 2007.

(382) McCormick KA, Isom LL, Ragsdale D, Smith D, Scheuer T, Catterall WA. Molecular determinants of Na+ channel function in the extracellular domain of the beta1 subunit. *J Biol Chem* 1998; 273(7):3954-3962.

(383) Shapiro L, Doyle JP, Hensley P, Colman DR, Hendrickson WA. Crystal structure of the extracellular domain from P0, the major structural protein of peripheral nerve myelin. *Neuron* 1996; 17(3):435-449.

(384) Kim DY, Ingano LA, Carey BW, Pettingell WH, Kovacs DM. Presenilin/gamma-secretase-mediated cleavage of the voltage-gated sodium channel beta2-subunit regulates cell adhesion and migration. *J Biol Chem* 2005; 280(24):23251-23261.

(385) Medeiros-Domingo A, Kaku T, Tester DJ et al. SCN4B-Encoded Sodium Channel {beta}4 Subunit in Congenital Long-QT Syndrome. *Circulation* 2007; 116:134-142.

(386) Kazen-Gillespie KA, Ragsdale DS, D'Andrea MR, Mattei LN, Rogers KE, Isom LL. Cloning, localization, and functional expression of sodium channel beta1A subunits. *J Biol Chem* 2000; 275(2):1079-1088.

(387) Qin N, D'Andrea MR, Lubin ML, Shafaee N, Codd EE, Correa AM. Molecular cloning and functional expression of the human sodium channel beta1B subunit, a novel splicing variant of the beta1 subunit. *Eur J Biochem* 2003; 270(23):4762-4770.

(388) Oh Y, Waxman SG. The beta 1 subunit mRNA of the rat brain Na+ channel is expressed in glial cells. *Proc Natl Acad Sci (USA)* 1994; 91(21):9985-9989.

(389) Dib-Hajj SD, Waxman SG. Genes encoding the beta 1 subunit of voltage-dependent Na+ channel in rat, mouse and human contain conserved introns. *FEBS Lett* 1995; 377(3):485-488.

(390) Dehal P, Satou Y, Campbell RK et al. The draft genome of Ciona intestinalis: insights into chordate and vertebrate origins. *Science* 2002; 298(5601):2157-2167.

(391) Canestro C, Bassham S, Postlethwait JH. Seeing chordate evolution through the Ciona genome sequence. *Genome Biol* 2003; 4(3):208.

(392) Azumi K, De SR, De TA et al. Genomic analysis of immunity in a Urochordate and the emergence of the vertebrate immune system: "waiting for Godot". *Immunogenetics* 2003; 55(8):570-581.

(393) Du PL, Zucchetti I, De SR. Immunoglobulin superfamily receptors in protochordates: before RAG time. *Immunol Rev* 2004; 198:233-248.

(394) Sodergren E, Weinstock GM, Davidson EH et al. The genome of the sea urchin Strongylocentrotus purpuratus. *Science* 2006; 314(5801):941-952.

(395) Jackson FR, Wilson SD, Hall LM. The tip-E mutation of Drosophila decreases saxitoxin binding and interacts with other mutations affecting nerve membrane excitability. J *Neurogenet* 1986; 3(1):1-17.

(396) O'Dowd DK, Aldrich RW. Voltage-clamp analysis of sodium channels in wild-type and mutant Drosophila neurons. *J Neurosci* 1988; 8(10):3633-3643.

(397) Feng G, Deak P, Chopra M, Hall LM. Cloning and functional analysis of TipE, a novel membrane protein that enhances Drosophila para sodium channel function. *Cell* 1995; 82(6):1001-1011.

(398) Warmke JW, Reenan RA, Wang P et al. Functional expression of Drosophila para sodium channels. Modulation by the membrane protein TipE and toxin pharmacology. *J Gen Physiol* 1997; 110(2):119-133.

(399) Hodges DD, Lee D, Preston CF, Boswell K, Hall LM, O'Dowd DK. tipE regulates Na+-dependent repetitive firing in Drosophila neurons. *Mol Cell Neurosci* 2002; 19(3):402-416.

(400) Derst C, Walther C, Veh RW, Wicher D, Heinemann SH. Four novel sequences in Drosophila melanogaster homologous to the auxiliary Para sodium channel subunit TipE. *Biochem Biophys Res Commun* 2006; 339(3):939-948.

(401) Hobert O, Hutter H, Hynes RO. The immunoglobulin superfamily in Caenorhabditis elegans and Drosophila melanogaster. *Development* 2004; 131(10):2237-2238.

(402) Isom LL. Sodium channel beta subunits: anything but auxiliary. *Neuroscientist* 2001; 7(1):42-54.

(403) Agnew WS, Levinson SR, Brabson JS, Raftery MA. Purification of the tetrodotoxin-binding component associated with the voltage-sensitive sodium channel from Electrophorus electricus electroplax membranes. *Proc Natl Acad Sci (USA)* 1978; 75(6):2606-2610.

(404) Miller JA, Agnew WS, Levinson SR. Principal glycopeptide of the tetrodotoxin/saxitoxin binding protein from Electrophorus electricus: isolation and partial chemical and physical characterization. *Biochemistry* 1983; 22(2):462-470.

(405) Rosenberg RL, Tomiko SA, Agnew WS. Single-channel properties of the reconstituted voltage-regulated Na channel isolated from the electroplax of Electrophorus electricus. *Proc Natl Acad Sci (USA)* 1984; 81(17):5594-5598.

(406) Recio-Pinto E, Duch DS, Levinson SR, Urban BW. Purified and unpurified sodium channels from eel electroplax in planar lipid bilayers. *J Gen Physiol* 1987; 90(3):375-395.

(407) Lombet A, Lazdunski M. Characterization, solubilization, affinity labeling and purification of the cardiac Na+ channel using Tityus toxin gamma. *Eur J Biochem* 1984; 141(3):651-660.

(408) Zakon HH, Lu Y, Zwickl DJ, Hillis DM. Sodium channel genes and the evolution of diversity in communication signals of electric fishes: Convergent molecular evolution. *Proc Natl Acad Sci (USA)* 2006; 103(10):3675-3680.

(409) Camacho JA, Hensellek S, Rougier JS et al. Modulation of Nav1.5 channel function by an alternatively spliced sequence in the DII/DIII linker region. *J Biol Chem* 2006; 281(14):9498-9506.

(410) Thimmapaya R, Neelands T, Niforatos W et al. Distribution and functional characterization of human Nav1.3 splice variants. *Eur J Neurosci* 2005; 22(1):1-9.

(411) Tan BH, Valdivia CR, Rok BA et al. Common human SCN5A polymorphisms have altered electrophysiology when expressed in Q1077 splice variants. *Heart Rhythm* 2005; 2(7):741-747.

(412) Makielski JC, Ye B, Valdivia CR et al. A ubiquitous splice variant and a common polymorphism affect heterologous expression of recombinant human SCN5A heart sodium channels. *Circ Res* 2003; 93(9):821-828.

(413) Zimmer T, Bollensdorff C, Haufe V, Birch-Hirschfeld E, Benndorf K. Mouse heart Na+ channels: primary structure and function of two isoforms and alternatively spliced variants. *Am J Physiol Heart Circ Physiol* 2002; 282(3):H1007-H1017.

(414) Dietrich PS, McGivern JG, Delgado SG et al. Functional analysis of a voltage-gated sodium channel and its splice variant from rat dorsal root ganglia. *J Neurochem* 1998; 70(6):2262-2272.

(415) O'Dowd DK, Gee JR, Smith MA. Sodium current density correlates with expression of specific alternatively spliced sodium channel mRNAs in single neurons. *J Neurosci* 1995; 15(5 Pt 2):4005-4012.

(416) Meadows L, Malhotra JD, Stetzer A, Isom LL, Ragsdale DS. The intracellular segment of the sodium channel beta 1 subunit is required for its efficient association with the channel alpha subunit. *J Neurochem* 2001; 76(6):1871-1878.

(417) Eubanks J, Srinivasan J, Dinulos MB, Disteche CM, Catterall WA. Structure and chromosomal localization of the beta2 subunit of the human brain sodium channel. *Neuroreport* 1997; 8(12):2775-2779.

(418) Adler E, Fuster V. SCN5A--a mechanistic link between inherited cardiomyopathies and a predisposition to arrhythmias? *JAMA* 2005; 293(4):491-493.

(419) Chen S, Chung MK, Martin D, Rozich R, Tchou PJ, Wang Q. SNP S1103Y in the cardiac sodium channel gene SCN5A is associated with cardiac arrhythmias and sudden death in a white family. *J Med Genet* 2002; 39(12):913-915.

(420) Bezzina CR, Rook MB, Groenewegen WA et al. Compound heterozygosity for mutations (W156X and R225W) in SCN5A associated with severe cardiac conduction disturbances and degenerative changes in the conduction system. *Circ Res* 2003; 92(2):159-168.

(421) Frustaci A, Priori SG, Pieroni M et al. Cardiac histological substrate in patients with clinical phenotype of Brugada syndrome. *Circulation* 2005; 112(24):3680-3687.

(422) Coronel R, Casini S, Koopmann TT et al. Right ventricular fibrosis and conduction delay in a patient with clinical signs of Brugada syndrome: a combined electrophysiological, genetic, histopathologic, and computational study. *Circulation* 2005; 112(18):2769-2777.

(423) Towbin JA, Bowles NE. The failing heart. *Nature* 2002; 415(6868):227-233.

(424) Royer A, van Veen TA, Le BS et al. Mouse model of SCN5A-linked hereditary Lenegre's disease: age-related conduction slowing and myocardial fibrosis. *Circulation* 2005; 111(14):1738-1746.

(425) van Veen TA, Stein M, Royer A et al. Impaired impulse propagation in Scn5a-knockout mice: combined contribution of excitability, connexin expression, and tissue architecture in relation to aging. *Circulation* 2005; 112(13):1927-1935.

(426) Probst V, Kyndt F, Potet F et al. Haploinsufficiency in combination with aging causes SCN5A-linked hereditary Lenegre disease. *J Am Coll Cardiol* 2003;41(4):643-652.

(427) Hesse M, Kondo CS, Clark RB et al. Dilated cardiomyopathy is associated with reduced expression of the cardiac sodium channel Scn5a. *Cardiovasc Res* 2007; 75(3):498-509.

(428) Olson TM, Michels VV, Ballew JD et al. Sodium channel mutations and susceptibility to heart failure and atrial fibrillation. *JAMA* 2005; 293(4):447-454.

(429) Abriel H, Kass RS. Regulation of the voltage-gated cardiac sodium channel Nav1.5 by interacting proteins. *Trends Cardiovasc Med* 2005; 15(1):35-40.

(430) Isom LL, De Jongh KS, Patton DE et al. Primary structure and functional expression of the beta 1 subunit of the rat brain sodium channel. *Science* 1992; 256(5058):839-842.

(431) Kazarinova-Noyes K, Malhotra JD, McEwen DP et al. Contactin associates with Na+ channels and increases their functional expression. *J Neurosci* 2001; 21(19):7517-7525.

(432) Allouis M, Le BF, Wilders R et al. 14-3-3 is a regulator of the cardiac voltage-gated sodium channel Nav1.5. *Circ Res* 2006; 98(12):1538-1546.

(433) Shah VN, Wingo TL, Weiss KL, Williams CK, Balser JR, Chazin WJ. Calcium-dependent regulation of the voltage-gated sodium channel hH1: intrinsic and extrinsic sensors use a common molecular switch. *Proc Natl Acad Sci (USA)* 2006; 103(10):3592-3597.

(434) Young KA, Caldwell JH. Modulation of skeletal and cardiac voltage-gated sodium channels by calmodulin. *J Physiol* 2005; 565(Pt 2):349-370.

(435) Kim J, Ghosh S, Liu H, Tateyama M, Kass RS, Pitt GS. Calmodulin mediates Ca2+ sensitivity of sodium channels. *J Biol Chem* 2004; 279(43):45004-45012.

(436) Lee KH, Xu Q, Breitbart RE. A new tinman-related gene, nkx2.7, anticipates the expression of nkx2.5 and nkx2.3 in zebrafish heart and pharyngeal endoderm. *Dev Biol* 1996; 180(2):722-731.

(437) Kishimoto Y, Lee KH, Zon L, Hammerschmidt M, Schulte-Merker S. The molecular nature of zebrafish swirl: BMP2 function is essential during early dorsoventral patterning. *Development* 1997; 124(22):4457-4466.

(438) Griffin KJ, Kimelman D. One-Eyed Pinhead and Spadetail are essential for heart and somite formation. *Nat Cell Biol* 2002; 4(10):821-825.

(439) Keegan BR, Feldman JL, Begemann G, Ingham PW, Yelon D. Retinoic acid signaling restricts the cardiac progenitor pool. *Science* 2005; 307(5707):247-249.

(440) Reifers F, Walsh EC, Leger S, Stainier DY, Brand M. Induction and differentiation of the zebrafish heart requires fibroblast growth factor 8 (fgf8/acerebellar). *Development* 2000; 127(2):225-235.

(441) Ueno S, Weidinger G, Osugi T et al. Biphasic role for Wnt/beta-catenin signaling in cardiac specification in zebrafish and embryonic stem cells. *Proc Natl Acad Sci (USA)* 2007; 104(23):9685-9690.

(442) Bodmer R. The gene tinman is required for specification of the heart and visceral muscles in Drosophila. *Development* 1993; 118(3):719-729.

(443) Harvey RP. NK-2 homeobox genes and heart development. *Dev Biol* 1996; 178(2):203-216.

(444) Gritsman K, Zhang J, Cheng S, Heckscher E, Talbot WS, Schier AF. The EGF-CFC protein one-eyed pinhead is essential for nodal signaling. *Cell* 1999; 97(1):121-132.

(445) Xu J, Srinivas BP, Tay SY et al. Genomewide expression profiling in the zebrafish embryo identifies target genes regulated by Hedgehog signaling during vertebrate development. *Genetics* 2006; 174(2):735-752.

(446) Rohrschneider MR, Elsen GE, Prince VE. Zebrafish Hoxb1a regulates multiple downstream genes including prickle1b. *Dev Biol* 2007;309(2):358-72.

(447) Douglas SE. Microarray studies of gene expression in fish. *OMICS* 2006; 10(4):474-489.

(448) Brewer AC, Alexandrovich A, Mjaatvedt CH, Shah AM, Patient RK, Pizzey JA. GATA factors lie upstream of Nkx 2.5 in the transcriptional regulatory cascade that effects cardiogenesis. *Stem Cells Dev* 2005; 14(4):425-439.

(449) Brown CO, III, Chi X, Garcia-Gras E, Shirai M, Feng XH, Schwartz RJ. The cardiac determination factor, Nkx2-5, is activated by mutual cofactors GATA-4 and Smad1/4 via a novel upstream enhancer. *J Biol Chem* 2004; 279(11):10659-10669.

(450) Peterkin T, Gibson A, Loose M, Patient R. The roles of GATA-4, -5 and -6 in vertebrate heart development. *Semin Cell Dev Biol* 2005; 16(1):83-94.

(451) Pan J, Baker KM. Retinoic Acid and the heart. *Vitam Horm* 2007; 75:257-83.:257-283.

(452) Kwon C, Arnold J, Hsiao EC, Taketo MM, Conklin BR, Srivastava D. Canonical Wnt signaling is a positive regulator of mammalian cardiac progenitors. *Proc Natl Acad Sci (USA)* 2007; 104(26):10894-10899.

(453) Naito AT, Shiojima I, Akazawa H et al. Developmental stage-specific biphasic roles of Wnt/beta-catenin signaling in cardiomyogenesis and hematopoiesis. *Proc Natl Acad Sci (USA)* 2006; 103(52):19812-19817.

(454) Tzahor E. Wnt/beta-catenin signaling and cardiogenesis: timing does matter. *Dev Cell* 2007; 13(1):10-13.

(455) Eisenberg LM, Eisenberg CA. Wnt signal transduction and the formation of the myocardium. *Dev Biol* 2006; 293(2):305-315.

(456) Stoick-Cooper CL, Weidinger G, Riehle KJ et al. Distinct Wnt signaling pathways have opposing roles in appendage regeneration. *Development* 2007; 134(3):479-489.

(457) McNulty MM, Edgerton GB, Shah RD, Hanck DA, Fozzard HA, Lipkind GM. Charge at the lidocaine binding site residue Phe-1759 affects permeation in human cardiac voltage-gated sodium channels. *J Physiol* 2007; 581(Pt 2):741-755.

(458) Bennett PB, Yazawa K, Makita N, George AL, Jr. Molecular mechanism for an inherited cardiac arrhythmia. *Nature* 1995; 376(6542):683-685.

(459) Wei J, Wang DW, Alings M et al. Congenital long-QT syndrome caused by a novel mutation in a conserved acidic domain of the cardiac Na+ channel. *Circulation* 1999; 99(24):3165-3171.

(460) Viswanathan PC, Balser JR. Inherited sodium channelopathies: a continuum of channel dysfunction. *Trends Cardiovasc Med* 2004; 14(1):28-35.

(461) Liu K, Yang T, Viswanathan PC, Roden DM. New mechanism contributing to drug-induced arrhythmia: rescue of a misprocessed LQT3 mutant. *Circulation* 2005; 112(21):3239-3246.

(462) Pfahnl AE, Viswanathan PC, Weiss R et al. A sodium channel pore mutation causing Brugada syndrome. *Heart Rhythm* 2007; 4(1):46-53.

(463) Valdivia CR, Tester DJ, Rok BA et al. A trafficking defective, Brugada syndrome-causing SCN5A mutation rescued by drugs. *Cardiovasc Res* 2004; 62(1):53-62.

(464) Herfst LJ, Rook MB, Jongsma HJ. Trafficking and functional expression of cardiac Na+ channels. *J Mol Cell Cardiol* 2004; 36(2):185-193.

(465) Shah VN, Wingo TL, Weiss KL, Williams CK, Balser JR, Chazin WJ. Calcium-dependent regulation of the voltage-gated sodium channel hH1: intrinsic and extrinsic sensors use a common molecular switch. *Proc Natl Acad Sci (USA)* 2006; 103(10):3592-3597.

(466) Crossin KL, Hoffman S. Expression of adhesion molecules during the formation and differentiation of the avian endocardial cushion tissue. *Dev Biol* 1991; 145(2):277-286.

(467) Imanaka-Yoshida K, Knudsen KA, Linask KK. N-cadherin is required for the differentiation and initial myofibrillogenesis of chick cardiomyocytes. *Cell Motil Cytoskeleton* 1998; 39(1):52-62.

(468) Linask KK, Manisastry S, Han M. Cross talk between cell-cell and cell-matrix adhesion signaling pathways during heart organogenesis: implications for cardiac birth defects. *Microsc Microanal* 2005; 11(3):200-208.

(469) Imanaka-Yoshida K, Matsumoto K, Hara M, Sakakura T, Yoshida T. The dynamic expression of tenascin-C and tenascin-X during early heart development in the mouse. *Differentiation* 2003; 71(4-5):291-298.

(470) Burroughs CL, Watanabe M, Morse DE. Distribution of the neural cell adhesion molecule (NCAM) during heart development. *J Mol Cell Cardiol* 1991; 23(12):1411-1422.

(471) Bagatto B, Francl J, Liu B, Liu Q. Cadherin2 (N-cadherin) plays an essential role in zebrafish cardiovascular development. *BMC Dev Biol* 2006; 6:23.:23.

(472) Srinivasan J, Schachner M, Catterall WA. Interaction of voltage-gated sodium channels with the extracellular matrix molecules tenascin-C and tenascin-R. *Proc Natl Acad Sci (USA)* 1998; 95(26):15753-15757.

(473) Ratcliffe CF, Westenbroek RE, Curtis R, Catterall WA. Sodium channel beta1 and beta3 subunits associate with neurofascin through their extracellular immunoglobulin-like domain. *J Cell Biol* 2001; 154(2):427-434.

(474) McEwen DP, Isom LL. Heterophilic interactions of sodium channel beta1 subunits with axonal and glial cell adhesion molecules. *J Biol Chem* 2004; 279(50):52744-52752.

(475) Malhotra JD, Thyagarajan V, Chen C, Isom LL. Tyrosine-phosphorylated and nonphosphorylated sodium channel beta1 subunits are differentially localized in cardiac myocytes. *J Biol Chem* 2004; 279(39):40748-40754.

(476) Chopra SS, Watanabe H, Zhong TP, Roden DM. Molecular cloning and analysis of zebrafish voltage-gated sodium channel beta subunit genes: Implications for the evolution of electrical signaling in vertebrates. *BMC Evol Bio*l 2007; 7(1):113.

(477) Link AJ, Eng J, Schieltz DM et al. Direct analysis of protein complexes using mass spectrometry. *Nat Biotechnol* 1999; 17(7):676-682.

(478) Gould KL, Ren L, Feoktistova AS, Jennings JL, Link AJ. Tandem affinity purification and identification of protein complex components. *Methods* 2004; 33(3):239-244.

(479) Link AJ, Fleischer TC, Weaver CM, Gerbasi VR, Jennings JL. Purifying protein complexes for mass spectrometry: applications to protein translation. *Methods* 2005; 35(3):274-290.

(480) Fleischer TC, Weaver CM, McAfee KJ, Jennings JL, Link AJ. Systematic identification and functional screens of uncharacterized proteins associated with eukaryotic ribosomal complexes. *Genes Dev* 2006; 20(10):1294-1307.

(481) Liu K, Hipkens S, Yang T et al. Recombinase-mediated cassette exchange to rapidly and efficiently generate mice with human cardiac sodium channels. *Genesis* 2006; 44(11):556-564.

(482) Papadatos GA, Wallerstein PM, Head CE et al. Slowed conduction and ventricular tachycardia after targeted disruption of the cardiac sodium channel gene Scn5a. *Proc Natl Acad Sci (USA)* 2002; 99(9):6210-6215.

(483) Buckingham M, Meilhac S, Zaffran S. Building the mammalian heart from two sources of myocardial cells. *Nat Rev Genet* 2005; 6(11):826-835.

(484) Latif S, Masino A, Garry DJ. Transcriptional pathways direct cardiac development and regeneration. *Trends Cardiovasc Med* 2006; 16(7):234-240.

(485) Masino AM, Gallardo TD, Wilcox CA, Olson EN, Williams RS, Garry DJ. Transcriptional regulation of cardiac progenitor cell populations. *Circ Res* 2004; 95(4):389-397.

(486) Novak AE, Taylor AD, Pineda RH, Lasda EL, Wright MA, Ribera AB. Embryonic and larval expression of zebrafish voltage-gated sodium channel alpha-subunit genes. *Dev Dyn* 2006; 235(7):1962-1973.